ISBN: 978-3-95450-201-1 doi:10.18429/JACoW-IBIC2018-MOOA02

NOISE IN RADIO/OPTICAL COMMUNICATIONS

M. Vidmar†, University of Ljubljana, FE, Tržaška 25, 1000 Ljubljana, Slovenia

Abstract

Noise is a random signal that affects the performance of all electronic and/or optical devices. Although the sources of different kinds of noise have their backgrounds in physics, engineers dealing with noise use different methods and units to specify noise. The intention of this tutorial is to describe the main effects of noise in electronics up to optical frequencies while providing links between the physics and engineering worlds. In particular, noise is considered harmful while degrading the signal-to-noise ratio or broadening the spectrum of signal sources. On the other hand, noise can be itself a useful signal. Finally, artificially generated signals that exhibit many properties of random natural noise are sometimes required.

NATURAL NOISE

Noise is a broadband signal. Therefore it makes sense to describe its intensity by the noise spectral density N_0 or amount of noise power per unit bandwidth (see Fig. 1). In electronics the most important type of noise is thermal noise. Thermal noise adds to any signal. In optics the most important type of noise is shot noise. Shot noise is a property of any signal made from a discrete number of photons.

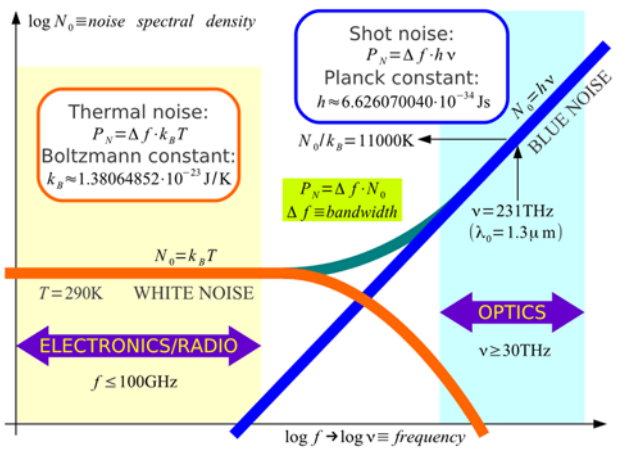

Figure 1: Noise spectral density.

Since the photon energy increases proportional with frequency, the higher the frequency the larger the shot noise spectral density. Such a noise is also called blue noise. Shot noise is unimportant in the radio-frequency range at room temperatures. Shot noise can only be observed at the highest end of the radio-frequency range at cryogenic temperatures.

Thermal noise is caused by thermal radiation. The Planck law (see Fig. 2) describes the spectral brightness B_f or radiated power per unit bandwidth, unit area and unit solid angle of a black body. A black body with zero reflectivity Γ=0 is the most efficient thermal radiator while a perfect mirror |Γ|=1 does not radiate at all.

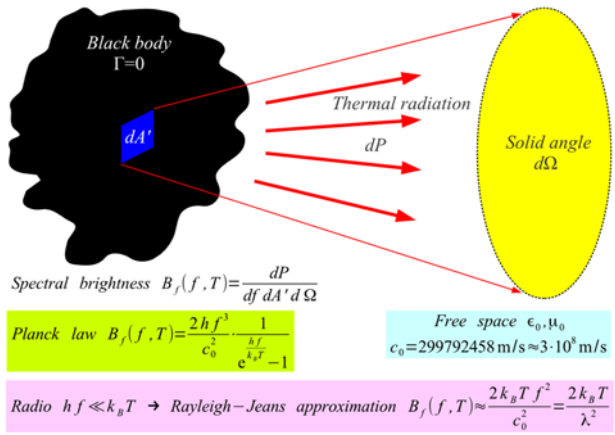

Figure 2: Black-body thermal radiation.

In the radio-frequency range it makes sense to use the Rayleigh-Jeans approximation of the Planck law to calculate the noise power collected by a lossless antenna. An antenna with an electrical connector (see Fig. 3) only collects half of the incident noise power on its effective area A_{eff}, the remaining half being orthogonally polarized.

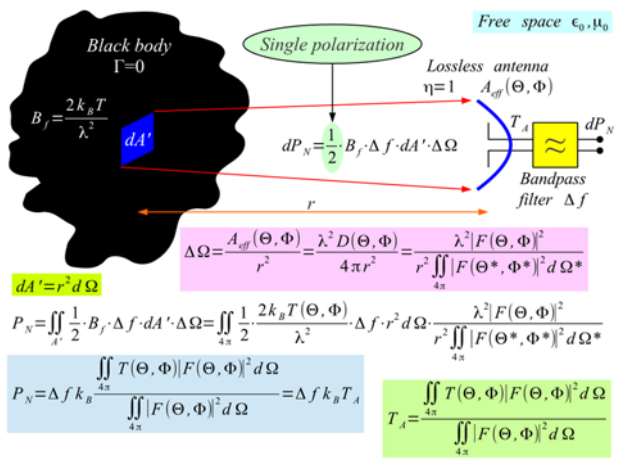

Figure 3: Received thermal-noise power.

In the radio-frequency range the noise spectral density is frequency independent. Thermal noise therefore behaves as white noise. Thermal noise spectral density is simply described by the black-body temperature T_A as observed by the radiation pattern $F(\Theta,\Phi)$ of a lossless antenna (η=1).

Above a certain frequency the thermal noise power begins decreasing when the complete Planck law applies. However, the sum of both noise spectral densities, thermal noise and shot noise, remains a monotonic function of

† email address: matjaz.vidmar@fe.uni-lj.si

Content from this work may be used under the terms of the CC BY 3.0 licence (© 2018). Any distribution of this work must maintain attribution to the author(s), title of the work, publisher, and DOI.

ISBN: 978-3-95450-201-1 doi:10.18429/JACoW-IBIC2018-MOOB01

BEAM COMMISSIONING OF SuperKEKB RINGS AT PHASE-2

M. Tobiyama*, M. Arinaga, J. W. Flanagan, H. Fukuma, H. Ikeda, S. Iwabuchi, H. Ishii, G. Mistuka, K. Mori, E. Mulyani and M. Tejima, KEK Accelerator. Laboratory, 1-1 Oho, Tsukuba 305-0801, Japan and also SOKENDAI, Japan
G.S. Varner, U. Hawaii, Dept. Physics and Astronomy, 2505 Correa Rd., Honolulu HI 96822, USA
G. Bonvicini, Wayne State U., 135 Physics Bldg., Detroit MI 4820, USA.

Abstract

The Phase 2 commissioning of SuperKEKB rings with Belle II detector began in Feb. 2018. Staring the commissioning of positron damping ring (DR), the injection and storage of the main rings (HER and LER) smoothly continued in Apr. 2018. The first collision has been achieved on 26th Apr. with the detuned optics (200 mm x 8 mm). Performance of beam instrumentation systems and the difficulties encountered during commissioning time will be shown.

INTRODUCTION

The KEKB collider has been upgraded to the SuperKEKB collider with a final target of 40 times higher luminosity than that of KEKB. It consists of a 7 GeV high energy ring (HER, electrons) and a 4 GeV low energy ring (LER, positrons). About 2500 bunches per ring will be stored at total beam currents of 2.6 A (HER) and 3.6 A (LER) in the final design goal. After the first stage of commissioning (Phase 1) without the Belle-II detector, which started in Feb. 2016 and continued until the end of June [1, 2], we have installed the superconducting final quadrupoles (QCS) and the Belle-II detector, without innermost detectors vertex detectors such as Pixel detectors nor Silicon Vertex Detectors (VXD).

The primary target of the Phase-2 operation in accelerator side was to verify the large crossing angle, nano-beam collision scheme by squeezing the βy^* smaller than the bunch length and to achieve high luminosity consistent to βy^*. There also required to achieve the following conditions to proceed to the phase-3 operation by the Belle II group:

- Achieve a machine luminosity of O(10^{34}/cm^2/s) and see a clear path to further improvement.
- Examine the VXD background to verify that we can install the VXD at the start of phase 3 and then operate it for the initial first few years of phase 3.

The Phase-2 operation has started in Feb. 2018 with the commissioning of the positron damping ring (DR). The commissioning of HER and LER has started in late Mar. with detuned (non-collision) optics. After establishing the beam storage, we have jumped to the collision optics on 11th. Apr. The first collision has been observed on 26th. Apr with the IP parameter of (βx^*, βy^* = 200 mm, 8 mm) [3, 4].

The beam instrumentation has played a very important role at each step of commissioning, such as establishing the circulating orbit, finding the beam-beam kick, accumulating large beam currents, and so on.

In this paper we describe the results of the beam commissioning of phase 2 operation of SuperKEKB rings with the obtained performance of the beam instrumentations. The main parameters of the phase 2 operation of SuperKEKB HER/LER/DR and the types and number of main beam instrumentations are shown in Table 1.

Table 1: Main Parameters of SuperKEKB HER/LER/DR in Phase 2 Operation

	HER	LER	DR
Energy (GeV)	7	4	1.1
Circumference(m)	3016		135
Max. current (mA)	800	860	12
Bunch length (mm)	5	6	6.6
RF frequency (MHz)	508.887		
Harmonic number (h)	5120		230
Betatron tune(H/V)	44.54/ 46.56	45.54/ 43.56	8.24/ 7.17
Synchrotron tune	0.02	0.018	0.025
T. rad. damp time (ms)	58	43	12
x-y coupling (%)	0.27	0.28	10
Emittance (nm)	3.2	4.6	29
Peak luminosity	5.5x10^{33}/cm^2/s		
Beam position monitor	486	444	83
Turn by turn monitor	69	70	83
Trans. FB system	2	2	1
Visible SR monitor	1	1	1
X-ray size monitor	1	1	0
Beta. tune monitor	1	1	1
DCCT	1	1	1
Bunch current mon.	1	1	1
Beam loss monitor	105(IC)/101(PIN)		34

* email address makoto.tobiyama@kek.jp

Content from this work may be used under the terms of the CC BY 3.0 licence (© 2018). Any distribution of this work must maintain attribution to the author(s), title of the work, publisher, and DOI.

ISBN: 978-3-95450-201-1 doi:10.18429/JACoW-IBIC2018-MOOB03

UPGRADE AND STATUS OF STANDARD DIAGNOSTIC-SYSTEMS AT FLASH AND FLASHFORWARD

N. Baboi*, H.-T. Duhme, O. Hensler, G. Kube, T. Lensch, D. Lipka, B. Lorbeer, R. Neumann, P. Smirnov, T. Wamsat, M. Werner, DESY, 22607 Hamburg, Germany

Abstract

Electron beam diagnostics plays a crucial role in the precise and reliable generation of ultra-short high brilliance XUV and soft X-ray beams at the Free Electron Laser in Hamburg (FLASH). Most diagnostic systems monitor each of up to typically 600 bunches per beam, with a frequency of up to 1 MHz, a typical charge between 0.1 and 1 nC and an energy of 350 to 1250 MeV.

The diagnostic monitors have recently undergone a major upgrade. This process started several years ago with the development of monitors fulfilling the requirements of the European XFEL and of the FLASH2 undulator beamline and it continued with their installation and commissioning. Later they have been further improved and an upgrade was made in the old part of the linac. Also the FLASHForward plasma-wakefield acceleration experiment has been installed in the third beamline.

This paper will give an overview of the upgrade of the BPM, Toroid and BLM systems, pointing out to their improved performance. Other systems underwent a partial upgrade, mainly by having their VME-based ADCs replaced with MTCA type. The overall status of the diagnostic will be reviewed.

INTRODUCTION

FLASH [1] is self-amplified spontaneous-emission free electron laser (SASE-FEL) user facility. It generates high brilliance ultra-short XUV and soft X-ray pulses. It is also a test facility for various studies.

Figure 1 shows a schematic drawing of the facility. Seven TESLA accelerating modules accelerate the beam to an energy of 350 to 1250 MeV. Within each bunch train with a length of typically 400-600 µs different lasers generate the sub-trains destined to the various beamlines. These can have different bunch frequency, up to 1 MHz, and bunch charge, typically between 0.1 and 1 nC. The train repetition rate is 10 Hz. During machine setup or special bunches may have a reduced rate of 1 Hz.

While the first 2 beamlines, FLASH1 and FLASH2, generate intense photon pulses for users, a plasma experiment, FLASHForward, was recently installed in the third beamline [2].

The FEL requires a precise control of the beam. The diagnostics system is essential for this, and therefore has to follow the increasing requirements over time.

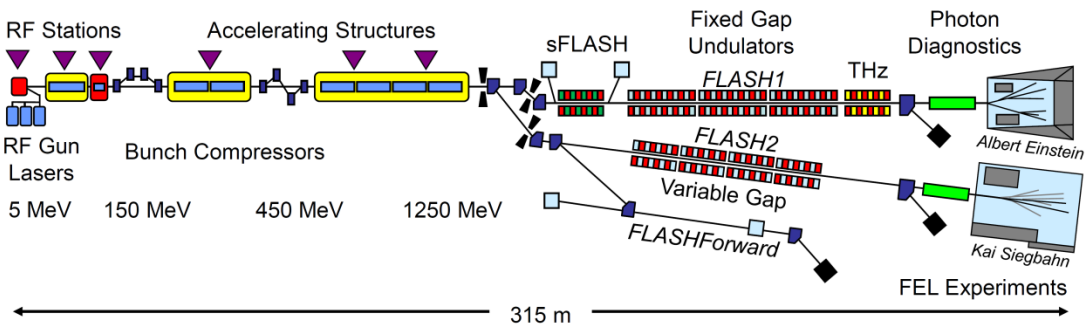

Figure 1: Schematic view of the FLASH facility [1].

This paper describes the recent upgrades that the various diagnostics systems underwent. After an overview of the diagnostics, the monitor types which underwent main upgrades are described, followed by the smaller work. The paper ends with a summary.

Standard Diagnostics at FLASH

Many different kinds of diagnostics have been installed along the years in FLASH: toroids to monitor the individual bunch charge, beam position monitors (BPM) of various kinds, beam loss monitors (BLM), beam size monitors, mainly OTR stations and wire scanners, dark current monitor etc. So-called special diagnostics has been developed mainly for longitudinal diagnostics, and is not the topic of this paper. Many of the systems deliver bunch-by-bunch information, and have to deal with the different bunch charge and pulse structure of the sub-trains for the various beamlines.

In recent years, many diagnostics systems have been developed for and installed in the European XFEL [3] and FLASH2 [4], which fulfil new requirements. The MTCA.4 standard [5] has been introduced for several systems. Besides the diagnostics, also LLRF and the timing system are based on this standard. Different systems

* nicoleta.baboi@desy.de.

Content from this work may be used under the terms of the CC BY 3.0 licence (© 2018). Any distribution of this work must maintain attribution to the author(s), title of the work, publisher, and DOI.

ISBN: 978-3-95450-201-1 doi:10.18429/JACoW-IBIC2018-MOOB04

UPGRADE OF THE MACHINE PROTECTION SYSTEM TOWARD 1.3 MW OPERATION OF THE J-PARC NEUTRINO BEAMLINE

K. Sakashita*, M.Friend, K.Nakayoshi, High Energy Accelerator Research Organization (KEK), Tsukuba, Japan
S. Yamasu, Y. Koshio, Okayama University, Okayama, Japan

Abstract

The machine protection system (MPS) is one of the essential components to realize safe operation of the J-PARC neutrino beamline, where a high intensity neutrino beam for the T2K long baseline neutrino oscillation experiment is generated by striking 30 GeV protons on a graphite target. The proton beam is extracted from the J-PARC main ring proton synchrotron (MR) into the primary beamline. The beamline is currently operated with 485 kW MR beam power. The MR beam power is planned to be upgraded to 1.3 MW. The neutrino production target could be damaged if the high intensity beam hits off-centered on the target, due to non-uniform thermal stress. Therefore, in order to protect the target, it is important to immediately stop the beam when the beam orbit is shifted. A new FPGA-based interlock module, with which the beam profile is calculated in real time, was recently developed and commissioned. This module reads out signals from a titanium-strip-based secondary emission profile monitor (SSEM) which is placed in the primary beamline. An overview of the upgrade plan of the MPS system and the results of an initial evaluation test of the new interlock module will be discussed.

INTRODUCTION

T2K(Tokai-to-Kamioka) is a long-baseline neutrino oscillation experiment. One of the main physics motivations is a search for CP (Charge-Parity symmetry) violation in neutrino oscillation. If CP is not conserved in neutrino oscillations, it may indicate a significant hint for the origin of our matter dominate universe. T2K can measure the CP asymmetry by comparing the oscillation probabilities between $\nu_\mu \rightarrow \nu_e$ and $\overline{\nu}_\mu \rightarrow \overline{\nu}_e$. Since those probabilities are small, a high intensity neutrino beam is essential to measure the CP asymmetry. A high intensity muon neutrino beam is produced at the Japan Proton Accelerator Research Complex (J-PARC) at Tokai village, Ibaraki, Japan. The muon neutrino (anti-neutrino) beam is then directed to the Super-Kamiokande detector located 295 km away from J-PARC.

Recently, T2K operated stably with 485 kW of MR beam power. Figure 1 shows the accumulated protons on target (POT) and the beam power since 2010. T2K collected 3.16×10^{21} POT up to the end of May 2018. Based on the data collected until December 2017, T2K made a preliminary report that the CP conserving phase values $(0,\pm\pi)$ are outside of 2σ region [1]. This result indicates a hint of neutrino CP violation, although the significance is still low.

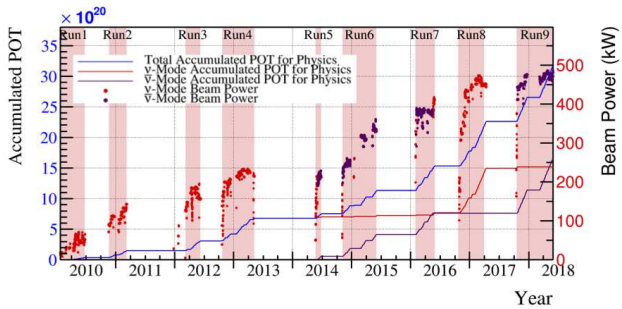

Figure 1: T2K accumulated protons on target (POT) and the beam power as a function of year.

In order to confirm the measurement of CP violation, T2K plans to collect more data up to 2×10^{22} POT by 2026 (T2K extension proposal, J-PARC E65 [2]). The expected sensitivity to CP violation with the exposure of 2×10^{22} POT is 3σ assuming certain values of the oscillation parameters. In the T2K extension proposal, three upgrades are planned; (1) upgrade of the J-PARC MR beam power up to 1.3 MW, (2) increase of signal statistics by both hardware and analysis improvements, and (3) improvement of systematic uncertainties by upgrade of the T2K near detector.

The MR beam power will be upgraded up to 1.3 MW by both shortening the repetition time from 2.48 s to 1.16 s, and increasing the number of protons per pulse up to 3.2×10^{14} [3]. Table 1 shows the achieved and target values. For the shortened repetition time, the MR main magnet power supplies will be upgraded. Intensive development work on the new power supply design has been performed. Installation of these new power supplies will be completed by 2021. For the increase of the number of protons per pulse, intensive MR beam studies are in progress. So far, 520 kW with 2.7×10^{14} protons per pulse and 2.48 s repetition has been successfully performed. The total beam loss in the MR was estimated to be $\sim$ 1 kW. Although further beam loss reduction is necessary, this demonstrates that the MR has the capability of achieving $\sim$ 1MW beam operation with 1.3 s of the repetition time.

Table 1: MR Operation Parameters for the Achieved and Target Beam Power. N_p represents the number of protons per pulse.

	Achieved	**Target**
Beam Power [MW]	0.49	1.3
N_p	2.5×10^{14}	3.2×10^{14}
Repetition Time [s]	2.48	1.16

* kensh@post.kek.jp

Content from this work may be used under the terms of the CC BY 3.0 licence (© 2018). Any distribution of this work must maintain attribution to the author(s), title of the work, publisher, and DOI.

ISBN: 978-3-95450-201-1 doi:10.18429/JACoW-IBIC2018-MOOC03

THE REMOVAL OF INTERFERENCE NOISE OF ICT USING PCA METHOD*

J. Chen[1], Y.B. Leng†, N. Zhang, L.Y. Yu
Shanghai Institute of Applied Physics, Chinese Academy of Science, 201204 Shanghai, China
[1]also at University of the Chinese Academy of Science, 100049 Beijing, China

Abstract

The measurement of beam charge is a fundamental requirement to all particle accelerators facility. Shanghai soft X-ray free-electron laser (SXFEL) started construction in 2015 and is now in the commission phase. Although integrated current transformer (ICT) were installed in the entire FEL for the measurement of the absolute beam charge, the accurate measurement becomes difficult in the injector and the main accelerator section due to the noise interference from external factors such as klystron modulator. The evaluation of the source of noise signals and the procession of noise reduction using the principal component analysis (PCA) are proposed in this paper. Experiment results show that PCA method combing with polynomial fitting method can effectively remove the interference noise from the klystron modulator and it can also improve the resolution of the ICT system. Detailed experiment results and data analysis will be mentioned as well.

INTRODUCTION

Beam charge is a fundamental parameter for the particle accelerator facility; therefore, the beam current detector is a very important diagnostic means. Beam charge measurement methods including intercepting measurements such as Faraday cup which often used for LINAC, transfer line and storage ring. Another brunch is the Non-intercepting measurements, DCCT often be used to measure the DC current and the beam lifetime in the booster and storage ring. But for the ultra-fast short pulse charge, since ICT has a time response of the order of ps to ns, it is widely used in LINAC and transfer line for the measurement of bunch charge.

For the ICT, typical usage is the use of Bergoz's ICT probe and BCM-IHR-E processor which can be seen in Fig. 1.

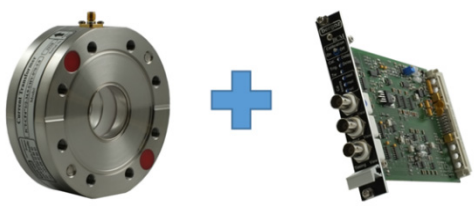

Figure 1: ICT and BCM processor.

The secondary coil of the transformer coupling electron pulse signal and then be widened through the shaping network, and the integral area of the output pulse is proportional to the amount of charge. The diagram of Bergoz ICT is shown in Fig. 2.

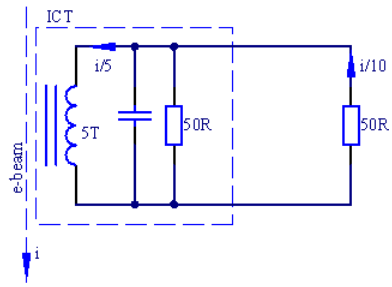

Figure 2: Diagram of Bergoz ICT.

If the input impedance of the external signal processing circuit is also 50 ohms, the Eq.(1) and Eq.(2)are satisfied between the beam charge Q, the bunch current i, and the voltage signal u_0 detected by the signal processing circuit:

$$u_0 = \frac{i}{5} * \frac{1}{2} * 50\Omega . \qquad (1)$$

$$Q = \int idt = \int \frac{5*2*u}{50\Omega} dt \qquad (2)$$

Therefore, it is only necessary to measure the integral value of the output voltage pulse signal, the original beam charge can be calculated by combining the probe calibration coefficient. Typical signal processing method like BCM-IHR is to use an analog pulse integrator integrates the output pulse signal of ICT and a level signal which proportional to the integral value can be sampled and quantified by a slow ADC to calculate the beam charge.

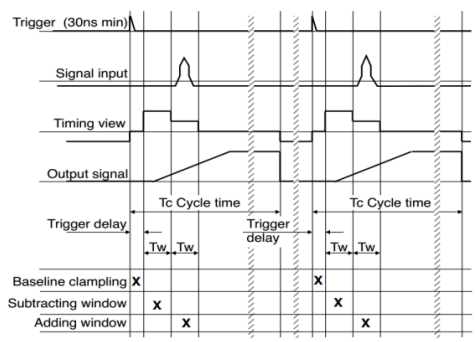

Figure 3: Timing of the BCM-IHR.

Figure 3 show the timing of the BCM-IHR processor. The signal processing is initiated by the external positive-going trigger pulse, then the timer creates three successive time windows: a trigger delay window and two integra-

*Work supported by The National Key Research and Development Program of China (Grant No. 2016YFA0401903, 2016YFA0401900)
†lengyongbin@sinap.ac.cn

Content from this work may be used under the terms of the CC BY 3.0 licence (© 2018). Any distribution of this work must maintain attribution to the author(s), title of the work, publisher, and DOI.

ISBN: 978-3-95450-201-1 doi:10.18429/JACoW-IBIC2018-MOPA01

STATUS OVERVIEW OF THE HESR BEAM INSTRUMENTATION

C. Böhme, A. Halama, V. Kamerdzhiev, F. Klehr, B. Klimczok, M. Maubach, S. Merzliakov, D. Prasuhn, R. Tölle, Forschungszentrum Jülich, Germany

Abstract

The High Energy Storage Ring (HESR), within the Facility for Antiproton and Ion Research (FAIR), will provide proton and anti-proton beams for PANDA (Proton Antiproton Annihilation at Darmstadt) and heavy ion beams for SPARC (Stored Particles Atomic Physics Research Collaboration. With the beam instrumentation devices envisaged in larger quantities, e.g. BPM and BLM being in production, other BI instruments like Viewer, Scraper, or Ionization Beam Profile Monitor are in the mechanical design phase. An overview of the status is presented.

INTRODUCTION

The HESR, part of the FAIR project in Darmstadt, Germany, is dedicated to the field of antiproton and heavy ion physics. The envisaged momentum range is 1.5 GeV/c to 15 GeV/c. The ring will be 574 m long in a racetrack shape. The planned beam instrumentation within the modularized start version is:

76	Diagonally Cut Beam Position Monitors (BPM)
118	Beam Loss Monitors (BLM)
2	Beam Current Transformers (BCT)
2	Ionization Beam Profile Monitor(IPM)
1	Wall Current Monitor (WCM)
1	Schottky Pick-up
1	Dynamical Tune-meter
1	Transverse Feedback System
5	Viewer
2	Scraper
73	Ion Clearing Chambers

BPM SYSTEM

The pick-up design is based upon the COSY BPMs [1]. The length and diameter is shrunk by a common factor in order to keep the length to diameter ratio. Each BPM units consist of two diagonally cut pick-ups rotated by 90° around the beam axis in respect to each other. The setup is shown in Figure 1. The inner diameter of the pick-ups is 89 mm and the length 78 mm with a gap of 3 mm between the electrodes using an angle of 55.5°. The expected signal levels are depending on the capacitance of the pick-ups, the ion charge, the amount of ions, and the bunch length and can be calculated. The capacitance was calculated by means of COMSOL Multiphysics 5 simulations. This calculation resulted in a capacity to ground of 19 pF after optimization. For the lowest case, the first injection of antiprotons with 10^8 particles in the ring, the signal level was calculated to 0.5 mV. For the highest intensity case, with 10^{11} antiprotons stored, the signal level is 390 mV.

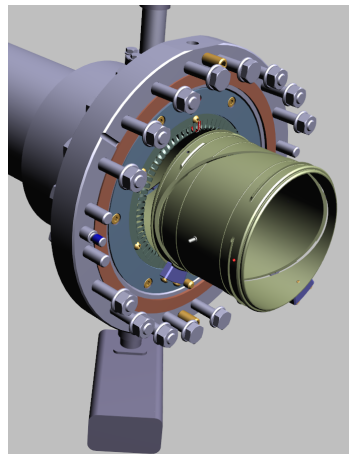

Figure 1: Schematic view on the BPM pick-up. Some parts of the assembly are not shown for better view on the pick-up.

Signal Amplification

Fixed Gain Head Amplifiers

Due to low amplitudes the HESR BPM signals require additional boosting prior to transmission over cables in order to achieve a better signal to noise ratio active head amplifiers with a high impedance low noise input were developed. At HESR the expected radiations levels are at a level an active solution could be taken into consideration. The amplifier itself is shown in Figure 2.

The specification of this amplifier is:

Amplification:	20 dB
Noise:	6 µV at 50 pF input capacitance and 10 MHz bandwidth
Bandwidth:	10 MHz default, configurable up to 70 MHz
Input Impedance:	500 kΩ
Power supply:	+8 V and -8 V
Output range:	± 1.5 V at 50 Ω

Hadron Pre-Amplifier (HPA)

Within the FAIR project the decision was made early that a common amplifier solution should be found for all machines. Therefore the HPA was developed [2] in cooperation of the Gesellschaft für Schwerionenforschung (GSI) and Instrumentation Technologies, Slovenia.

The HPA amplifier has a gain range of +60 dB do -60 dB and is equipped with an overload protection which has been seen necessarry especially for the SIS100. The HPA is equipped with a 50 Ω input.

For the above listed arguments the HESR deviated from this concept by introducing active head amplifiers instead of the passive impedance transformer. Still the HPA remains part of the signal chain, as the head amplifier will have a fixed

Content from this work may be used under the terms of the CC BY 3.0 licence (© 2018). Any distribution of this work must maintain attribution to the author(s), title of the work, publisher, and DOI.

ISBN: 978-3-95450-201-1 doi:10.18429/JACoW-IBIC2018-MOPA02

BEAM DIAGNOSTICS FOR SuperKEKB DAMPING RING IN PHASE-II OPERATION

H. Ikeda*, A),B), M. Arinaga[A)], H. Ishii[A)], S. Iwabuchi[A)], M. Tejima[A)], M. Tobiyama[A),B)], H. Fukuma[A)], J. W. Flanagan[A),B)], G. Mitsuka[A)], K. Mori[A)],
[A)] High Energy Accelerator Research Organization (KEK) Ibaraki 305-0801, Japan
[B)] The Graduate University for Advanced Science (SOKENDAI)

Abstract

The SuperKEKB damping ring (DR) commissioning started in February 2018, before main ring (MR) Phase-II operation. We constructed the DR in order to deliver a low-emittance positron beam. The design luminosity of SuperKEKB is 40 times larger than that of KEKB with high current and low emittance. A turn-by-turn beam position monitor (BPM), transverse feedback system, synchrotron radiation monitor (SRM), DCCT, loss monitor (LM) using ion chambers, bunch current monitor and tune meter have been installed for beam diagnostics at the DR. An overview of the instrumentation and its status will be presented.

INTRODUCTION

SuperKEKB [1] is an electron-positron collider and started construction towards 40 times luminosity as large as KEKB in 2011. The beam energies are 4GeV and 7GeV for positron rings (LER) and electronic ring (HER). Phase-I was the test operation of the main ring (MR) for confirmation that there was no problem in accelerator from February 2016 through June [2]. We installed the Belle-II detector and remodeled injection region of an accelerator for Phase-II operation. The beam commissioning was from March 2018 to July [3,4]. It is necessary to squeeze the vertical beam size to nm level at the collision point to achieve design luminosity. We build the damping ring (DR) in order to achieve a low-emittance positron beam [5,6]. The present parameters of DR are shown in Table 1. DR tuning was started prior to MR commissioning at the beginning of February 2018. We performed the tuning of injection from the injection line (LTR) to DR and DR to extraction line (RTL) in approximately one month [7]. The DR monitor system adjustment including timing system and feedback system was smoothly advanced.

The monitor system of DR follows a system of the MR as shown in Table 2 [8]. Two button electrodes of BPM are attached to the top and down of the ante-chamber of 24mm height in 83 quadrupole magnets. The visible light from a bending magnet downstream of the extraction line is used for a synchrotron radiation monitor. The ion chambers are attached on the wall to cover all the tunnels to monitor beam loss. We installed a monitor chamber and a kicker chamber for bunch feedback, and a DCCT chamber for beam current monitors just upstream of the injection point of DR.

Table 1: Damping Ring Parameters

Parameter		unit
Energy	1.1	GeV
No. of bunch trains/ bunches per train	2/2	
Circumference	135.5	m
Maximum stored current	12	mA
Damping time (h/v/z)	11.5/11.7/5.8	ms
Emittance(h/v)	29.2/1.5	nm
Energy spread	0.055	%
Bunch length	6.6	mm
Mom. compaction factor	0.01	
Cavity voltage	1.0	MV
RF frequency	509	MHz

Table 2: Beam Monitors in DR

System	Quantity
Beam position monitor	83
Synchrotron radiation monitor	1
Beam loss monitor	34
Transverse bunch by bunch feedback	1
DCCT	1
Bunch current monitor	1

BEAM POSITION MONITOR

A button electrode with a diameter of 6 mm has been developed for the beam position monitor (BPM). Two button electrodes are attached in one flange due to narrow space for their installation as shown in Fig. 1. The detection circuit is VME 18K11 L/R which incorporates a logarithm amplifier. The signals of BPM are sent to four control racks which accommodate VME racks near cable holes on the ground to reduce a cable loss. 20 or 21 signals are sent to one rack and the converted signals are sent to the central control room through network.

* email address: hitomi.ikeda@kek.jp

Content from this work may be used under the terms of the CC BY 3.0 licence (© 2018). Any distribution of this work must maintain attribution to the author(s), title of the work, publisher, and DOI.

ISBN: 978-3-95450-201-1 doi:10.18429/JACoW-IBIC2018-MOPA04

THE BEAM INSTRUMENTS FOR HIMM@IMP

T. C. Zhao†, R. S. Mao, X. C. Kang, M. Li, Y. C. Feng, Y. C. Chen, J. M. Dong, Z. L. Zhao, Z. G. Xu, K. Song, Y. Yan, W. N. Ma, Y. M. Wang, H. H. Song, W. L. Li, S. P. Li, K. Wei
Insitute of Modern Physics, Lanzhou, China

Abstract

The beam diagnositics(BD) devices for HIMM（Heavy Ion Medical Machine） are designed and produced by IMP BD department .An overview of the integrated devices is presented, and the common beam parameters in the different parts of the accelerator facility are reviewed including intensity measurement, beam profile, emmittance, energy, beam loss and so on with the related detectors such as the View Screen, Faraday Cup, Radial Detector, Multi-wires, Phase Probe, Wire Scanner, DCCT, ICT, BPM, Schottky, Slit, Beam Stopper, Beam Halo Monitor, Multi-channel Ionization Chamber. Additionally, the RF-KO for beam extraction, the strip foil with automatic control system as well as the detectors for terminal therapy are described.

INTRODUCTION

HIMM is a synchrotron based accelerator for cancer therapy in Wuwei city, China. It is composed of 2 ion sources, LEBT, cyclotron, MEBT, a synchrotron, HEBT and therapy terminals. The commissioning of HIMM is completed. The layout of the machine is shown in Fig. 1. At present, electrical safety, electromagnetic compatibility and performance testing of medical devices have been passed, and now enters the clinical tests phase.

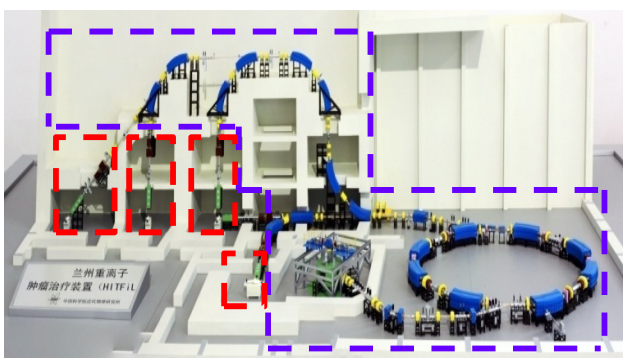

Figure 1: Layout of HIMM.

RADIAL PROBE

HIMM selects a cyclotron as its primary accelerator. Two radial probes have been installed to measure the beam intensity in the central area of the cyclotron. The target includes integrating and differential figures shown in Fig.2 and the beam turn measurement is displayed in Fig.3. What's more, in order to obtain the intensity distribution of different radius, it is necessary to synchronize motion control and data acquisition.

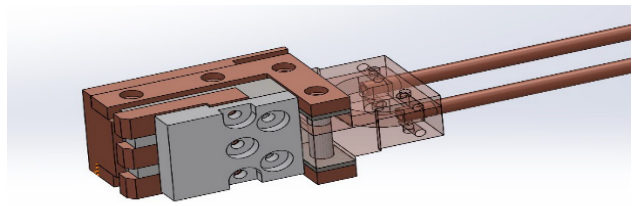

Figure 2: Target of radial probe.

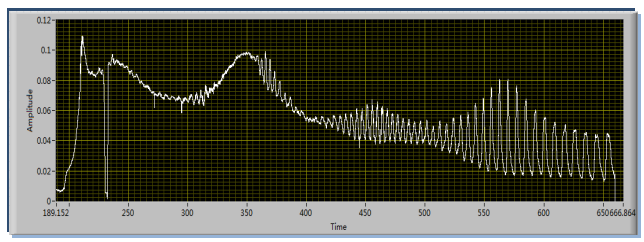

Figure 3: Intensity distribution of different radius.

VIEW SCREENS

View Screen (VS) is a commonly used profile detector, especially in the early stage of the commissioning. 13 VS are installed in the MEBT, Synchrotron and MEBT. In order to measure the beam profile at different tracks, the servo motor is used, and the repeatability of positioning accuracy is better than 0.1mm comparing its mechanical installation precision which is less than 0.5mm. The signals from CCD are read in two ways, one is the release video transmitted on the internet after video compression, and the other is to use video capture card. After digitalization, the FWHM and the centre position of the beam are obtained through software analysis. The captured photos and its analysed profile information is displayed in Fig. 4.

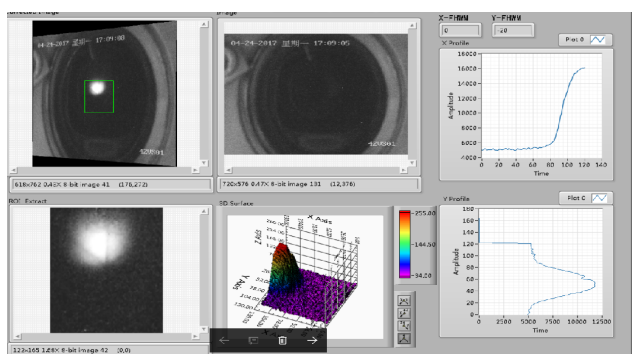

Figure 4: Beam profile and digital results.

Content from this work may be used under the terms of the CC BY 3.0 licence (© 2018). Any distribution of this work must maintain attribution to the author(s), title of the work, publisher, and DOI.

ISBN: 978-3-95450-201-1 doi:10.18429/JACoW-IBIC2018-MOPA06

RECENT ADVANCES IN BEAM MONITORING DURING SEE TESTING ON ISDE&JINR HEAVY ION FACILITIES

V. S. Anashin†, P. A. Chubunov, Branch of JSC United Rocket and Space Corporation - Institute of Space Device Engineering, Moscow, Russia
S.V. Mitrofanov, A. T. Isatov, Joint Institute for Nuclear Research, Dubna, Russia

Abstract

SEE testing of candidate electronic components for space applications is essential part of a spacecraft radiation hardness assurance process in terms of its operability in the harsh space radiation environment. The unique in Russia SEE test facilities have been created to provide SEE testing [1]. The existing facilities, including ion beam monitoring system have been presented at IBIC 2017[2]. However, this system has a number of shortcomings related to the lack of reliable online ion fluence measurement on the DUT, and inability to measure energies of the high-energy (15-60 MeV/nucleon) long-range (10-2000 μm) ions on the DUT. The paper presents the latest developments and their test results of the ISDE and JINR collaboration in the field of real-time flux monitoring (including, on the DUT) during tests using scintillation detectors, and ion energy measurement by total absorption method. The modernization of the standard beam monitoring procedure during testing is proposed.

WIDE-ANGLE COMPLETE-OVERLAP ION BEAM PROFILE MONITORING SYSTEM

This system is designed to monitor the stability and non-uniformity of the ion beams during heavy-ion testing on the low-energy test facilities. The system is based on an array of scintillation detectors consisting of 64 (8x8) sensors and designed for measuring such ion beam parameters as flux and integral fluence in real-time during heavy-ion testing, as well as non-uniformity. An important advantage of the system is the ability to obtain data without stopping the irradiation, i.e. in real time during testing, through the use of vacuum actuator installed in close proximity to the DUT.

Table 1 shows the technical features of the system, and Figures 1 and 2 show the appearance of the system after assembly and already mounted at the test facility.

Table 1: Technical features of the wide-angle complete-overlap ion beam profile monitoring system

Feature	Value	Unit
Ion species	Ne to Bi	
Energy range	3-6	MeV/nucleon
Fluxes	1-10^5	$cm^{-2}*s^{-1}$
Area	200x200	mm
Number of detectors	8x8	
Visualization system	Yes	
Input/output to/from the beam	In real-time	
Measurement and data output time	1	min
Ion flux determination error	Less than 10	%
Non-uniformity indication	Yes	

Figure 1: Wide-angle complete-overlap ion beam profile monitoring system (ready-assembled, before installation).

† npk1@niikp.org

Content from this work may be used under the terms of the CC BY 3.0 licence (© 2018). Any distribution of this work must maintain attribution to the author(s), title of the work, publisher, and DOI.

ISBN: 978-3-95450-201-1 doi:10.18429/JACoW-IBIC2018-MOPA07

BEAM DIAGNOSTICS AND INSTRUMENTATION FOR PROTON IRRADIATION FACILITY AT INR RAS LINAC

S. Gavrilov†[1,2], A. Melnikov[1,2], A. Titov[1,2]
[1]Institute for Nuclear Research of the Russian Academy of Sciences, Troitsk, Moscow, Russia
[2]Moscow Institute of Physics and Technology (State University), Moscow, Russia

Abstract

A new proton irradiation facility to study radiation effects in electronics and other materials has been built in INR RAS linac. The range of the specified current from 10^7 to 10^{12} protons per beam pulse is covered with three beam diagnostic instruments: current transformer, phosphor screen and multianode gas counter. Peculiarities of the joint use of the three instruments are described. Experimental results of beam parameters observations and adjustments are presented.

INTRODUCTION

A proton irradiation facility (PIF) at INR RAS linac is intended to research on proton irradiation induced effects in different electronics, devices and materials. PIF is installed at the outlet of the linac, where bending magnet is used to deflect a beam for in air irradiation of targets. Beam energy at the PIF is adjusted in 20÷210 MeV range. Beam flux is defined by a combination of three parameters: pulse duration, pulse repetition rate and pulse current, which can be controlled in the range of 10^7÷10^{12} p/pulse by two collimators at the linac injection channel.

A general PIF layout is shown in Fig. 1. The main parts are: bending magnet with vacuum beam pipe, beam dump, target positioning system with energy degrader and beam diagnostic instrumentation.

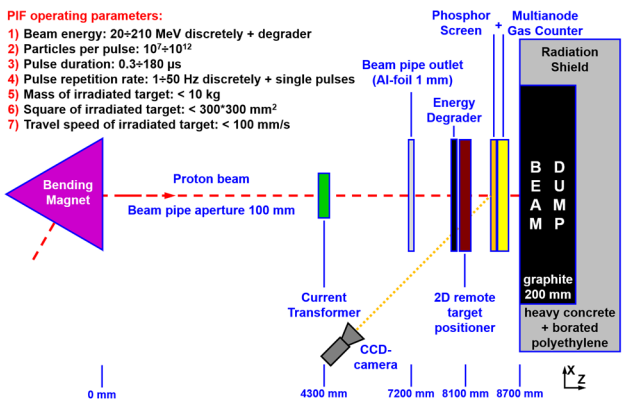

Figure 1: PIF layout.

The beam current transformer (BCT) is installed in the beam pipe about 3 m upstream the outlet window and provides absolute nondestructive measurements of beam pulse current with the amplitude > 25 μA, that corresponds to ~10^{10} p/pulse with typical durations 50÷150 μs (full range is 0.3÷180 μs). For less intensive beams more sensitive diagnostic instruments are foreseen.

† s.gavrilov@gmail.com

MULTIANODE GAS COUNTER

A multianode gas counter (MGC) was proposed initially as the main detector for low intensity diagnostics at the PIF. MGC is a combination of ionization and proportional air chambers, formed by an array of five plates (Fig. 2), which are fabricated as a standard 5 accuracy class printed-circuit boards made of FR4 with 0.5 mm width. Electrodes consist of 18 μm nickel, plated with 0.5 μm immersive gold.

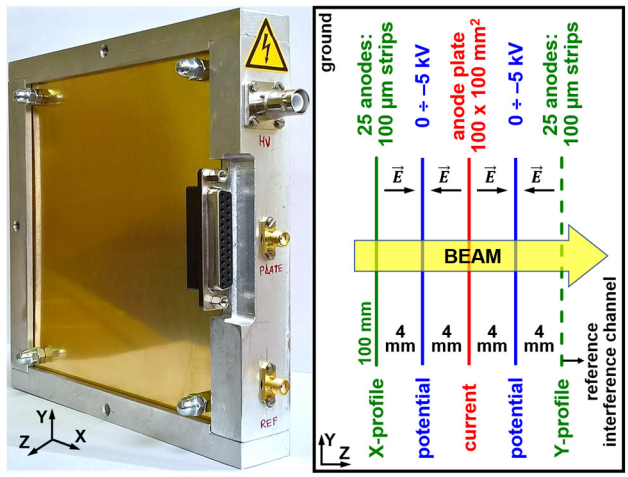

Figure 2: MGC photo and layout.

Central region operates as an ionization chamber to count particles in a beam pulse. A quasi-uniform electrostatic field is formed by two electrodes under negative potential and anode electrode under virtual ground of read-out electronics. All three electrodes have a duplex geometry, straddling the FR4 plate. Ionization electrons move to the current electrode from both sides, forming a relative beam intensity signal.

Lateral regions are proportional chambers for beam position and profile measurements. Each chamber is formed by the potential electrode and a multichannel structure, which consists of 25 anode stripes with 100 μm width, 100 mm length and 4 mm spacing. Strong non-uniform field around stripes (Fig. 3) leads to electron avalanches, increasing the desired signal.

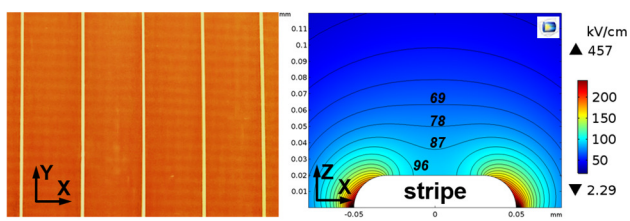

Figure 3: Photo of 100 μm stripes at the FR4 plate and distribution of electric field near a stripe at -4 kV potential.

Content from this work may be used under the terms of the CC BY 3.0 licence (© 2018). Any distribution of this work must maintain attribution to the author(s), title of the work, publisher, and DOI.

ISBN: 978-3-95450-201-1 doi:10.18429/JACoW-IBIC2018-MOPA09

OVERVIEW OF BEAM INSTRUMENTATION AND COMMISSIONING RESULTS FROM THE COHERENT ELECTRON COOLING EXPERIMENT AT BNL*

T. A. Miller†, J. C. Brutus, W. Dawson, D. M. Gassner, R. Hulsart, P. Inacker, J. Jamilkowski, D. Kayran, V. N. Litvinenko[1], C. Liu, R. Michnoff, M. Minty, P. Oddo, M. Paniccia, I. Pinayev, Z. Sorrel, J. Tuozzolo, C-AD, BNL, 11973 Upton, NY, USA
[1] also at Department of Physics and Astronomy, SBU, 11794, Stony Brook, NY, USA

Abstract

The Coherent Electron Cooling (CeC) Proof-of-Principle experiment [1], installed in the RHIC tunnel at BNL, has completed its third run. In this experiment, an FEL is used to amplify patterns imprinted on the cooling electron beam by the RHIC ion bunches and then the imprinted pattern is fed back to the ions to achieve cooling of the ion beam. Diagnostics for the CeC experiment have been fully commissioned during this year's run. An overview of the beam instrumentation is presented. This includes devices for measurements of beam current, position, profile, bunch charge, emittance, as well as gun photocathode imaging and FEL infra-red-light emission diagnostics. Design details are discussed and beam measurement results are presented.

INTRODUCTION

During CeC's operation this year [2], its complete array of instrumentation proved useful in measuring the parameters of the 1.5 MeV electron beam, with bunch charges of 50 pC – 5 nC, 10 – 500 ps long, produced by the CeSb 112 MHz SRF Photoinjector and transported through the 704 MHz SRF 5-cell Linac [3]. The 15 MeV accelerated beam passes into the RHIC common section through the modulation drift section, undulator (or wiggler) amplification section, and kicker drift section before being diverted down the extraction line into the high-power aluminium beam dump, as shown in the layout in Fig. 1. Pulsed beam operation ran at a 1 Hz rate with trains of pulses spaced at 78 kHz (the RHIC revolution frequency).

The transport is equipped with differential current transformers and beam position monitors with positions alarms that provide the two primary machine protection measures. Plunging YAG:Ce profile monitors measure beam profile with a multi-slit mask in the injection section to measure emittance. The high power and low power beam dumps are isolated to measure beam charge. The gun is equipped with cathode imaging optics in conjunction with the laser delivery system. Infrared (IR) emission from the undulators is characterized by an IR optics instrument array [4] beneath a diamond viewport in the RHIC beamline downstream of the CeC experiment.

BEAM CURRENT AND CHARGE

In order to display and log the charge in the electron bunch, beam current can be collected in one of two beam dumps and is measured in two integrating current transformers (ICT).

Faraday Cups

The two beam dumps in the beamline are electrically isolated to function as Faraday Cups (FC) to collect and measure the beam charge. These are the high-power beam dump at the end of the CeC transport and the low power dump at the end of the injection straight section. They are connected by ¼"-Heliax cable to integrating charge amplifiers located outside the tunnel to measure the collected charge and display in pC with an update rate of 1Hz. The FC's are terminated in the tunnel each with a 10 MΩ resistor and a 1nF capacitor. The signals are brought to a multiplexer for monitoring the signal on an oscilloscope or to be digitized. The majority of operations were made with the signals going to the oscilloscope.

Temperature The thermal mass of the high-power beam dump is fitted with two rad-hard thermocouples. The low power beam dump is fitted with an RTD-type probe. These probes are monitored by analog type 4-20 mA thermocouple transmitters mounted near the beam dumps. The thermocouple, made by Okazaki [5], is an AEROPAK

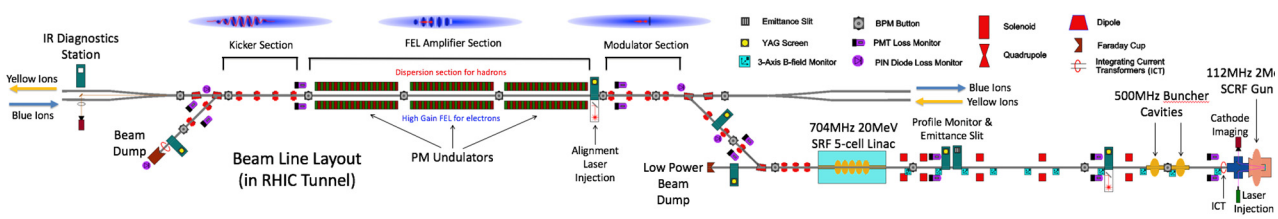

Figure 1: CeC beam line layout as installed at the 2 O'clock interaction point it the RHIC tunnel.

*Work supported by U.S. DOE under contract No DE-AC02-98CH10886 with the U.S. DOE
†tmiller@bnl.gov

Content from this work may be used under the terms of the CC BY 3.0 licence (© 2018). Any distribution of this work must maintain attribution to the author(s), title of the work, publisher, and DOI.

ISBN: 978-3-95450-201-1 doi:10.18429/JACoW-IBIC2018-MOPA12

THE DESIGN AND USE OF FARADAY CAGE IN LINAC TEMPORARY LINE OF CSNS

Ming Meng†, Taoguang Xu, Jilei Sun, Anxin Wang, Fang Li, Peng Li, Institute of High Energy Physics, Chinese Academy of Sciences (CAS), Beijing 100049, China and Dongguan Neutron Science Center, Dongguan 523803, China

Abstract

In the end of linac temporary line in CSNS, we need a faraday cage to absorb the beam. in the experiment it will be mounted and used twice. according to the beam energy and current of CSNS, we choose water-cooled pipe structure with tilted panel after simulation with Ansys. the main principle of the faraday cage is to simplify the structure and reduce the radiation activation of it, to do this, we also do the simulation of radiation. to make sure the faraday cage is safe in beam experiment, we also plug in a pt100 Platinum resistance to monitor the temperature. after faraday cage is built and mounted on the line, it works well and sustain the beam bombardment.

INTRODUCTION

China spallation neutron source (CSNS) is the first spallation neutron source in developing countries. In linac, there are a 50 keV H- iron source, a 3 MeV Radio Frequency Quadrupole(RFQ), and a 80 MeV Drift Tube Linac(DTL). In the first stage of beam experiment, when the H- come to the end of Medium Energy Beam Transport(MEBT) with 3 MeV energy and the end of DTL1 with energy 26.7 MeV, we need a temporary line with some beam measuring equipment like BPM, wire scanner to check the parameter of beam is right. And at the end of temporary line, we need to design a faraday cage to absorb the beam safely.

MACHINE DESIGN OF FARADAY CAGE

Plan Selection

In the 973 foundation project, we use "V" type beam stop as in Fig. 1, it is built with Oxygen free copper covered with aluminium using water cooling, and contain vacuum structure, the angle between the center line and surface is 8°. This beam stop is designed for 3.5 MeV proton, 20 mA beam current and 15% duty cycle, inside it , we use quadrate tunnel structure to improve cooling efficiency.

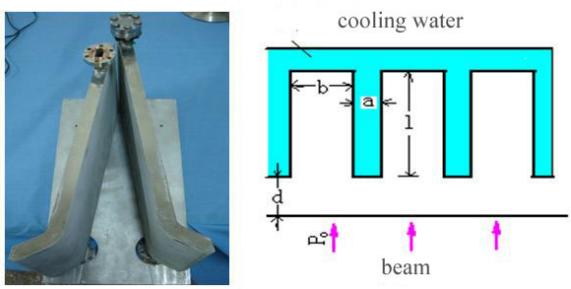

Figure 1: External shape and quadrate tunnel.

In the CSNS temporary line, because the "V" type cooling system is too complex that the welds leaks sometime, to simplify the design and machining, we decide to use just one tilted board and set the welds of water cooling pipe out of the vacuum structure. The faraday cage should be able to absorb beam as in Table 1.

Table 1: Parameter of Beam in Temporary Line

Energy	26.7 MeV	3 MeV
Peak current	15 mA	15 mA
Beam frequency	5 Hz	5 Hz
width	500 μs	500 μs

Physical Design

To start the simulation, first we should get the peak heat flux from Eq. (1), in it we set up the beam sigma size to 2.5 mm temporarily,

$$A \cdot \int_0^{0.025}\int_0^{0.025} e^{-\frac{x^2+y^2}{2\times 0.0025^2}} dx \cdot dy = 400\text{kW} \cdot \quad (1)$$

then we should get the heat exchange coefficient h as in Eq. (2), which is the thermal conductivity of cooling water, d is the equivalent diameter of cooling pipe, 4 times of cross-sectional area divide by perimeter, Nu is the Nusselt number as in Eq. (3),

$$h = \frac{\lambda \bullet Nu}{d} . \quad (2)$$

for forced convection heat transfer of turbulent flow in the tube, the Dietus-Belt formula is widely used to get Nusselt number, for cooling water n=0.3, Pr is Prandtl number, and Re Critical Reynolds number.

$$Nu = 0.023\,\text{Re}^{0.8}\,\text{Pr}^{n} . \quad (3)$$

After all this is done, we build model and set the cooling water pipe to different size, while the interval between pipe is fixed to 4mm as in Fig. 2, and in the calculation before we find that if the faraday cage is vertical to beam we can't get temperature under melting point, so we set up a slope between faraday cage and central axis to 10° ,and the beam size σ to 2.5 mm, with the slope of faraday board, the actual area of beam will become bigger to make the heat flux less.

† mengming@ihep.ac.cn

Content from this work may be used under the terms of the CC BY 3.0 licence (© 2018). Any distribution of this work must maintain attribution to the author(s), title of the work, publisher, and DOI.

ISBN: 978-3-95450-201-1 doi:10.18429/JACoW-IBIC2018-MOPA13

FAST LUMINOSITY MONITORING FOR THE SuperKEKB COLLIDER (LumiBelle2 PROJECT)

C. G. Pang*, P. Bambade, S. Di Carlo, D. Jehanno, V. Kubytskyi, Y. Peinaud, C. Rimbault
LAL, Univ. Paris-Sud, CNRS/IN2P3, Université Paris-Saclay, 91400 Orsay, France
Y. Funakoshi, S. Uehara, KEK, 305-0801 Tsukuba, Japan

Abstract

LumiBelle2 is a fast luminosity monitoring system prepared for SuperKEKB. It uses sCVD diamond detectors placed in both the electron and positron rings to measure the Bhabha scattering process at vanishing photon scattering angle. Two types of online luminosity signals are provided, Train-Integrated-Luminosity signals at 1 kHz as input to the dithering feedback system used to maintain optimum overlap between the colliding beams in horizontal plane, and Bunch-Integrated-Luminosity signals at about 1 Hz to check for variations along the bunch trains. Vertical beam sizes and offsets can also be determined from collision scanning. This paper will describe the design of *LumiBelle2* and report on its performance during the Phase-2 commissioning of SuperKEKB.

INTRODUCTION

SuperKEKB uses the so-called *nano-beam scheme* to reach a very high instantaneous luminosity of $8 \times 10^{35}\,\mathrm{cm}^{-2}\,\mathrm{s}^{-1}$ [1]. It consists of using a large crossing angle at the interaction point (IP) to enable colliding 2500 ultra-low emittance bunches with very small beam sizes (design value σ_y ~50 nm). The luminosity is very sensitive to beam-beam offsets, e.g., caused by vibration of mechanical supports induced by ground motion. In order to maintain the optimum beam collision condition, orbit feedback systems are essential at the IP [2]. At SuperKEKB, the beam-beam deflection method is used for orbit feedback for the vertical plane, while for the horizontal plane, a dithering orbit feedback system using the luminosity as input, similar to that operated in the past at PEP-II, has been adopted [3, 4].

For this purpose, a fast luminosity monitor based on sCVD diamond detectors, named *LumiBelle2*, was developed and tested during the Phase-2 commissioning of SuperKEKB. By measuring the rate of Bhabha events on each side of the IP at vanishing photon scattering angle, *LumiBelle2* can provide both Train-Integrated-Luminosity (TIL) signals and Bunch-Integrated-luminosity (BIL) signals simultaneously, over a large range of luminosities. TIL signals are needed by the dithering orbit feedback system at 1 kHz, with relative precisions better than 1 % [5]. BIL signals are important to probe potential luminosity differences between the numerous bunches along the trains. Another luminosity monitoring system named Zero Degree Luminosity Monitor (ZDLM) is also installed in the immediate vicinity. It uses Cherenkov and scintillator detectors [6], providing important complementary measurements. In addition, the Electromagnetic Calorimeter Luminosity On-line Measurement (ECL-LOM) is operated in the backward and forward end-caps of the Belle II detector, measuring the coincidence rates of back-to-back Bhabha events in the opposite sectors, with the ability to provide absolute values of the luminosity after proper internal calibration [7].

In this paper, we describe the design of *LumiBelle2*, including results of detector tests with a Sr-90 electron isotope source, the experimental set-up and the DAQ based on an FPGA, and the report on obtained luminosity monitoring performances, based on simulation and measurements pursued during the Phase-2 commissioning period, both with colliding beams, and with single beams, for background evaluations.

DESIGN AND LAYOUT

The placement of the *LumiBelle2* detectors was carefully studied with respect to signal rates and background contamination, resulting in choosing locations 10 and 29 m downstream of the IP in the Low Energy Ring (LER) and High Energy Ring (HER), to measure, respectively, Bhabha scattered positrons and photons [8]. To increase the rate of extracted positrons, a custom made beam pipe section with a depression of 15 mm and 45° inclined windows is used in the LER, see Figure 1. A Tungsten radiator with an effective thickness of 4 Radiation Lengths (1RL=3.5 mm) was added to enhance the electromagnetic showers and boost the detection efficiency [9].

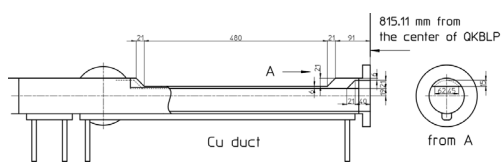

Figure 1: Designed window shape beam pipe.

The RF of SuperKEKB is about 500 MHz, with bunches stored nominally almost every other bucket (so called quasi 2-bucket fill pattern), which implies collisions every 4 ns. For BIL monitoring at high counting rate, signals from neighbouring bunches must be separated. A new diamond detector with a thickness of 140 µm, coupled with a broadband 2 GHz 40 dB current amplifier from CIVIDEC [10] at the front-end, are used for this purpose. Low attenuation half-inch HELIAX coaxial cables are used to avoid signal broadening

* pang@lal.in2p3.fr

Content from this work may be used under the terms of the CC BY 3.0 licence (© 2018). Any distribution of this work must maintain attribution to the author(s), title of the work, publisher, and DOI.

ISBN: 978-3-95450-201-1 doi:10.18429/JACoW-IBIC2018-MOPA14

ELECTRON SPECTROMETER FOR A LOW CHARGE INTERMEDIATE ENERGY LWFA ELECTRON BEAM MEASUREMENT

K.V. Gubin, ILP SB RAS, Novosibirsk, Russia,
A.V. Ottmar, Yu.I. Maltseva, T.V. Rybitskaya, BINP SB RAS, Novosibirsk, Russia

ABSTRACT

The Laser-driven Compton light source is under development in ILP SB RAS in collaboration with BINP SB RAS. Electron spectrometer with energy range 10-150 MeV for using in this project is presented. Spectrometer based on permanent magnet and phosphor screen with CCD registrar and this geometry was optimized for best measurements resolution in compromise with size limitations. Preliminary collimation of electron beam allows achieving energy resolution up to 5-10 % of top limit. System has been tested at the VEPP-5 linear electron accelerator and obtained results corresponds to design objectives. Sensitivity of beam transverse charge density was experimentally fixed at 0.03 pC/mm^2, that is practically sufficient for our LWFA experiments.

INTRODUCTION

At the present time, the impressive progress in laser wakefield acceleration (LWFA) of charged particles gives grounds to consider LWFA as a perspective method of electron beam production in the GeV energy range.

The project of laser-driven Compton light source started in ILP SB RAS in collaboration with BINP SB RAS [1]. The first stage of the project is creation and studying laser based accelerated electron beam from the supersonic gas jet. At the next stage, it is planned to obtain a high-energy gamma-ray beam by means of Compton backscattering of a probe light beam on LWFA-accelerated electrons.

General parameters of the first stage LWFA stand are:

- laser system: repetition rate is 10 Hz, pulse energy is 100÷300 mJ, pulse duration is ~20 fs, central wavelength is 810 nm;
- acceleration area: diameter is ~ 10÷15 μm, length is ~ 0.5 mm;
- supersonic He jet: diameter is ~1.2 mm, gas density is 10^{18}÷10^{19} cm^{-3}, Mach number is 3.5÷4, gas backpressure is 5÷10 atm;
- expected parameters of the electron beam are: up to 100-150 MeV of energy, 1-10 pC of charge, 1-10 mrad of angular divergence, ≤ 0.1 ps of beam duration.

SPECTROMETER PURPOSE AND REQUIREMENTS

Beam energy measurement is a necessary constituent of any accelerator facility. We choose the wide-used in LWFA experiments layout of spectrometer with magnetic dipole, phosphor screen and CCD camera as a signal register.

The spectrometer development is constrained by the following general demands:

- Compact size (full dimensions 20-25 cm) because of device must be placed inside limited volume of experimental vacuum chamber (Fig. 1) with diameter 70 cm and height 50 cm. It determines length and value of analizing magnetic field: 0.7-1.2 T and 30-50 mm. It follows the use of permanent magnets.
- Materials must be nonactivated and vacuum usable. It determines the use permanent magnets for dipole.
- The use of special electron beam collimator to improve energy resolution (see below).
- Taking into account a very small beam charge (several pC per pulse), registration system (phosphor screen + CCD camera) must have high quantum efficiency and sensitivity. Also we should take into account that CCD camera will be placed maximally near to screen but, from other hand, outside the vacuum volume. It means the distance between camera and screen will consist 35-40 cm, and the objective should be an appropriate angle of view to project the screen (about 10cm) on the CCD (11 mm).

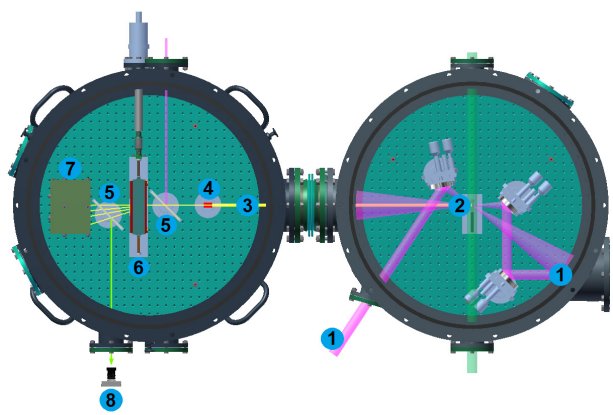

Figure 1: Experimental vacuum chamber. (1) Laser beams, (2) supersonic gas jet, (3) electronic beam, (4) collimator, (5) screens, (6) magnet dipole, (7) faraday cap, (8) CCD.

Content from this work may be used under the terms of the CC BY 3.0 licence (© 2018). Any distribution of this work must maintain attribution to the author(s), title of the work, publisher, and DOI.

ISBN: 978-3-95450-201-1 doi:10.18429/JACoW-IBIC2018-MOPA16

DESIGN OF A COMPACT PERMANENT MAGNET SPECTROMETER FOR CILEX/APOLLON

M. Khojoyan, A. Cauchois, J. Prudent, A. Specka
LLR (Laboratoire Leprince-Ringuet), CNRS and Ecole Polytechnique, Palaiseau UMR7638, France

Abstract

Laser Wakefield acceleration experiments make extensive use of small permanent magnets or magnet assemblies for analyzing and focusing electron beams produced in plasma accelerators. This choice is motivated by the ease of operation inside vacuum chambers, absence of power-supplies and feedthroughs, and potentially lower cost. Indeed, in these experiments space is at premium, and compactness is frequently required. At the same time, these magnets require a large angular acceptance for the divergent laser and electron beams which imposes constraint of the gap size. We will present the optimized design and characterization of a 100 mm long, 2.1 Tesla permanent magnet dipole. Furthermore, we will present the implementation of this magnet in a spectrometer that will measure the energy spectrum of electrons of ~ [60-2000] MeV with a few percent resolution in the CILEX/APOLLON 10PW laser facility in France.

INTRODUCTION

CILEX (Centre Interdisciplinaire de la Lumiere Extrême / Interdisciplinary Center for Extreme Light) is a research center which aims at using the Apollon-10P laser for exploring laser-matter interaction at extremely high laser intensities ($\sim 10^{22} W/cm^2$). The long focal length area of CILEX will be used to investigate plasma acceleration and radiation generation. It will be equipped with two interaction chambers able to accommodate laser focal lengths ranging from 3 m to 30 m. The spectrometer magnet presented here is designed to be compatible with the mentioned laser parameters.

A sketch of the laser-plasma interaction chamber is shown in Fig. 1. The total volume of interaction chamber is about $3m^3$ and it is practical to use permanent magnets for characterization of electron beam. Permanent magnets as compared to electromagnets, do not need power supplies (and consequently cooling system) and can be more compact due to smaller apertures. In our case, the apertures of the magnets will be limited by the laser envelope size, which according to our requirements, should pass through the magnets unobstructed. The paper is organized as follows. First, the design considerations of a permanent magnetic dipole are introduced together with analytical and computational field estimations. Next, construction of a permanent dipole magnet and magnetic field measurements are presented. Finally, beam dynamics simulation results are obtained by applying the magnet as a spectrometer inside the interaction chamber of the CILEX facility.

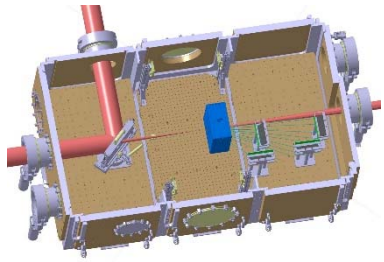

Figure 1: Schematic of interaction chamber at CILEX with laser envelope shown in red and magnetic dipole shown in blue. Measurement screens and reference electron trajectories are shown as well.

Let us consider a simple C shaped dipole (Fig. 2). The field in the gap of height h_g is driven by a permanent magnet of the same height $h_{pm} = h_g$ and of width w_{pm}.

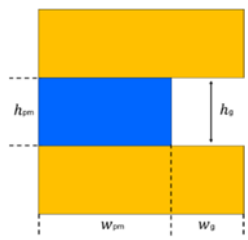

Figure 2: 2D view of a C shaped dipole with a permanent magnet shown in blue and steel/iron in yellow colors.

Assuming constant field in the gap (no horizontal field component) it is straightforward to calculate the magnetic flux density using Ampere's and flux conservation laws:

$$B_g = -\frac{B_r w_{pm}}{w_g + \frac{\mu_r h_g w_{pm}}{h_{pm}}} \quad (1)$$

with B_r and μ_r being the remnant field and relative permeability of the permanent magnet. From Eq. 1 it follows that the maximum achievable field in the gap cannot exceed the remnant induction field of the magnet independent of how small the gap width (w_g) and how large the magnet width (w_{pm}) are. It becomes clear that for a permanent magnet (PM) dipole, to reach fields higher than remnant field of an individual magnet, a special arrangement of magnetic sub-materials is necessary. Common structures are Halbach [1] and Stelter [2] configurations. In [3] a cylindrical structure was originally proposed by Halbach and

Content from this work may be used under the terms of the CC BY 3.0 licence (© 2018). Any distribution of this work must maintain attribution to the author(s), title of the work, publisher, and DOI.

ISBN: 978-3-95450-201-1 doi:10.18429/JACoW-IBIC2018-MOPA17

MOMENTUM COMPACTION MEASUREMENT USING SYNCHROTRON RADIATION

L. Torino*, N. Carmignani, A. Franchi, ESRF, 38000 Grenoble, France

Abstract

The momentum compaction factor of a storage ring can be obtained by measuring how the beam energy changes with the RF frequency. Direct measurement of the beam energy can be difficult, long or even not possible with acceptable accuracy and precision in some machines such as ESRF. Since the energy spectrum of the Synchrotron Radiation (SR) depends on the beam energy, it is indeed possible to relate the variation of the beam energy with a variation of the produced SR flux. In this proceeding, we will present how we obtain a measurement of the momentum compaction using this dependence.

INTRODUCTION

The variation of path length (L) with momentum (p) is determined by the momentum compaction factor (α_c) defined by:

$$\frac{\Delta L}{L} = \alpha_c \frac{\Delta p}{p}, \tag{1}$$

with $\frac{\Delta p}{p} \ll 1$ [1].

Assuming that particles are ultra-relativistic ($v \simeq c$, where c is the speed of light), ΔL is directly related with RF frequency variation, Δf_{RF}:

$$\frac{\Delta L}{L} = -\frac{\Delta f_{\mathrm{RF}}}{f_{\mathrm{RF}}}, \tag{2}$$

while the measurement of the momentum variation leads to some difficulties.

Using the same assumption, the momentum p can be approximated to the beam energy E and:

$$\frac{\Delta p}{p} \simeq \frac{\Delta E}{E}. \tag{3}$$

Substituting Eq. (2) and Eq. (3) in Eq. (1) one obtains:

$$\frac{\Delta E}{E} = -\alpha_c \frac{\Delta f_{RF}}{f_{RF}}. \tag{4}$$

In high-energy accelerators, and in particular in synchrotron light sources, the most accurate way to measure the energy is via the "spin depolarization" [2–4]. Unfortunately this technique cannot be used in all the machines depending on the complexity of the lattice [5]. Moreover the whole measuring process is time consuming.

On the other hand the momentum compaction factor measurement can be obtained by measuring the relative energy variation $\frac{\Delta E}{E}$. A method to obtain this quantity has been proposed based on the observation of the shift of the spectral peaks produced by an undulator [6, 7]. The observation is also quite complex and time consuming since it involves the access to a full beamline to measure the full SR spectrum.

The new technique to obtain α_c, proposed in this proceeding, is based on the measure of $\frac{\Delta E}{E}$ by using the relation between the produced SR flux and the beam energy.

MOMENTUM COMPACTION AND SYNCHROTRON RADIATION

The total SR power emitted by a charged particle with unit charge in a bending magnet is given by:

$$P_0 = \frac{8}{3}\pi\varepsilon_0 r_0^2 c^3 \frac{E^2 B^2}{(mc^2)^2}, \tag{5}$$

where ε_0 is the vacuum permittivity, r_0 is the classical electron radius, m is the rest mass of the particle, and B is the magnetic field [8]. From Eq. (5), it is clear that P_0 depends on the beam energy E, however a direct measurement of the total SR power is not possible.

A good observable is instead the intensity of the hard portion of the SR, which depends on P_0. The flux produced by an electron beam with an energy of 6.04 GeV, and one produced by increasing the beam energy of 5% are presented in Fig. 1: the fluxes start to be consistently different for photon energies larger than 100 keV.

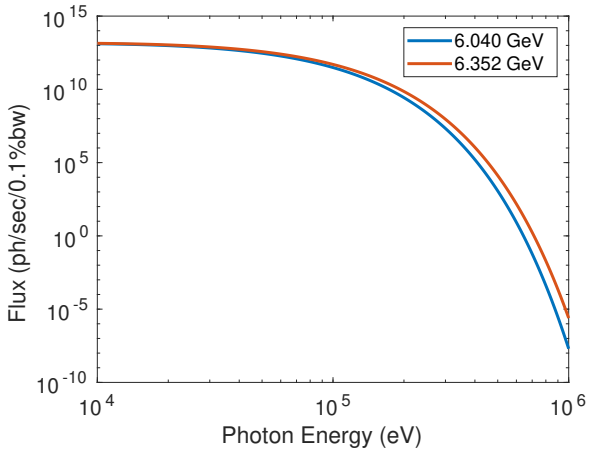

Figure 1: Photon flux produced by a beam of 6.04 GeV (blue) and the one produced by increasing the beam energy of 5% (orange).

High-energy photons can be selected by filtering the SR using an absorber, and detected by using, for example, a scintillator and a CCD camera.

The total intensity of the signal hence depends on the beam energy and although it is not possible to relate it with

* laura.torino@esrf.fr

Content from this work may be used under the terms of the CC BY 3.0 licence (© 2018). Any distribution of this work must maintain attribution to the author(s), title of the work, publisher, and DOI.

ISBN: 978-3-95450-201-1 doi:10.18429/JACoW-IBIC2018-MOPB02

ARIES-ADA: AN R&D NETWORK FOR ADVANCED DIAGNOSTICS AT ACCELERATORS*

P. Forck†, M. Sapinski, GSI Helmholtzzentrum für Schwerionenforschung, Darmstadt, Germany
U. Iriso, F. Perez, ALBA Synchrotron, Cerdanyola del Vallès, Barcelona, Spain
R. Jones, CERN, Geneva, Switzerland
Ch. Gerth, K. Wittenburg, Deutsches Elektronen-Synchrotron, Hamburg, Germany
R. Ischebeck, Paul Scherrer Institut, Villigen, Switzerland

Abstract

Accelerator Research and Innovation for European Science and Society, ARIES, is an initiative funded by the European Union. The activity comprises three major categories: Joint Research Activities; Transnational Access; Network Activities. One of 17 activities is a network related to Advanced Diagnostics at Accelerators, ADA with the task of strengthening collaborations between international laboratories and for coordinated R&D in beam diagnostics. This is performed by organizing Topical Workshops on actual developments and supporting interchange of experts between different labs. Since the start of the project in May 2017 four Topical Workshops were organized, each with 30-45 participants. Future workshops will address actual topics.

THE INITIATIVE ARIES

Accelerator Research and Innovation for European Science and Society, ARIES [1], is an Integrating Activity which aims to develop European particle accelerator infrastructures, co-funded under the European Commission's Horizon 2020 Research and Innovation programme.

Within a four year funding period, the key aim of the initiative ARIES is related to the development of novel concepts and further improve existing accelerator technology. This is realized by improving the performance, availability, and sustainability of particle accelerators, transferring the benefits and applications of accelerator technology to both science and society, and enlarging and integrating the European accelerator community. Moreover, it aims to support innovative technologies with market potential by advancing concepts and designs for medical, industrial and environmental applications of accelerators for the benefits of European society as a whole. The consortium consists of 41 institutions form academia, accelerator laboratories and industry of 18 European countries. The initiative is organized in 17 scientific work-packages of three different categories:

- Within the 5 so called '*Joint Research Activities'* several intuitions are working together on key technologies for accelerators like for super-conducting rf-cavities or very high gradient accelerators.
- As a second branch 5 so called '*Transnational Access'* provides infrastructure for equipment testing like fully equipped test benches for rf-cavities, access to electron and hadron accelerators with a wide range of beam parameters.
- The third branch comprises of 7 *'Network Activities'* which aims for strengthening the collaborations concerning the worldwide accelerator research and development. These activities are related to e.g. the design of novel accelerators, efficient energy management, design of ultra-low emittance light sources, industrial applications, beam diagnostics and novel methods for student education.

THE NETWORK ARIES-ADA

One of the Network Activities is related to '*Advanced Diagnostics at Accelerators'*, ADA [2]. To meet the demands of new accelerator facilities, novel beam instrumentation and diagnostics methods are required. Knowledge exchange between experts from worldwide research institutes is an efficient way of developing such systems efficiently. Topical Workshops with about 20 to 40 international participants ranging from novices to world-leading experts is an excellent way of summarizing state of the art developments in the field and transferring this knowledge to the young generation. A workshop duration of typically two days seems to be adequate to summarize the current status of a dedicated subject, provide the possibility to discuss novel ideas and trigger the collaboration between the participants. The collection of contributions acts as a comprehensive summery of the current R&D status. The subject of the workshops is oriented on actual topics; four of such dedicated workshops were organized in the first 14 month of the funding period (i.e. between May 2017 and June 2018).

The funding form the European Union for ARIES-ADA is administrated by the four beneficiary institutions ALBA, CERN, DESY and GSI. The budget covers mainly the general workshop costs as well as possible additional costs to enable the participations of the worldwide experts. The workshops are announced to the general audience from the ARIES website [1, 2]; key-speakers are invited directly by the workshop organizers.

In addition to the workshops, the exchange of experts for a typical duration of 2 weeks for common discussions and to carry out experiments were organised in the frame of ARIES-ADA to further strengthen the collaboration between the accelerator institutions. Within the first year of ARIES-ADA four of such visits were financed.

* This project has received funding from the European Union's Horizon 2020 programme under Grant Agreement No 730871
† email address: p.forck@gsi.de.

Content from this work may be used under the terms of the CC BY 3.0 licence (© 2018). Any distribution of this work must maintain attribution to the author(s), title of the work, publisher, and DOI.

ISBN: 978-3-95450-201-1 doi:10.18429/JACoW-IBIC2018-MOPB03

HIGH-ENERGY SCRAPER SYSTEM FOR THE S-DALINAC EXTRACTION BEAM LINE – COMMISSIONING RUN*

L. Jürgensen#, M. Arnold, T. Bahlo, R. Grewe, J. Pforr, N. Pietralla, A. Rost, S. Weih, J. Wissmann,
Technische Universität Darmstadt, Germany
F. Hug, Johannes Gutenberg-Universität Mainz, Germany
C. Burandt, T. Kürzeder, Helmholtz-Institut Mainz, Germany

Abstract

The S-DALINAC is a thrice recirculating, superconducting linear electron accelerator at TU Darmstadt. It delivers electron beams in cw-mode with energies up to 130 MeV. The high-energy scraper system has been installed in its extraction beam line to reduce the energy spread and improve the energy stability of the beam for the experiments operated downstream. It comprises three scraper slits within a dispersion-conserving chicane consisting of four dipole magnets and eight quadrupole magnets. The primary scraper, located in a dispersive section, allows to improve and stabilize the energy spread. In addition energy fluctuations can be detected. Scraping of x- and y-halo is implemented in two positions enclosing the position of the primary scraper. We will present technical details and results of the first commissioning run of the recently installed system at the S-DALINAC. Besides improving on the energy spread, it proved to be a valuable device to observe energy spread and energy fluctuations as well as to reduce background count rates next to the experimental areas.

INTRODUCTION

Since 1987 the S-DALINAC serves nuclear- and astrophysical experiments at the Technical University of Darmstadt [1]. It is fed by either a thermionic or a photoemission gun which delivers a spin-polarized beam [2]. After pre-acceleration by the injector module the electron beam can either be used for experiments at the NRF-setup [3] or it is guided through a 180°-arc to enter the main linac. By passing the linac up to four times the maximum energy of about 130 MeV can be reached. The beam current can be adjusted from several pA up to 20 µA. The layout of the S-DALINAC is given in Fig. 1.

The high-energy beam of the S-DALINAC is used for nuclear physics experiments with a need for high energy resolution and low noise next to the experimental area. The recently installed scraper system [4] is placed between the accelerator hall and the experimental hall and provides beam-cleaning and –monitoring features. The energy spread can be reduced by sending the dispersive beam through a narrow slit which determines the energy and the energy range that continues towards the experimental areas. Blocked parts of that beam deposit their charge onto the high- and the low-energy side of that slit which allows for an online monitoring of energy fluctuations during long beam times.

If not optimized, γ-ray background from brems-strahlung processes can prevent sensitive detection of photons from searched-for nuclear reactions. The background is produced by beam losses resulting from collisions of beam halo with beam line components. In order to remove beam halo the installed scraper system also contains halo scrapers that work in horizontal as well as in vertical direction.

CONSTRUCTION

The presented high energy scraper system resembles a chicane which consists of four dipole magnets, eight quadrupole magnets, four vertical steerers and the three scraper chambers themselves. The system is depicted in Fig. 2. Beam scraping will be done in three different positions. This is necessary because beam dynamics have to be adjusted individually for halo scraping and for the energy defining scraper (see section *Beam Dynamics*). The system consists of three spherical vacuum chambers, each measuring 9” in diameter. The two chambers for halo scraping contain guided, water cooled copper blocks which are positioned using a stepping motor outside the vacuum. In this set-up a positioning accuracy better than 0.01 mm is possible. Downstream of the halo scrapers, BeO-screens can be inserted to check for beam position and shape. The amount of beam current, which is stopped during halo-scraping, is in the order of 1% of the total beam intensity. The energy defining scraper is however outlaid to deal with the full beam power. Additionally to the extensive cooling water system, both scraper brackets are mounted electrically isolated from the beam pipe. By measuring the current, one gains information about the amount of beam current which is stopped on each bracket. This helps to find the optimal position of the slit and in addition identify energy fluctuations of the beam. Monitoring this quantity will also help to detect and cure irregularities of the rf-system to further decrease the potential of failure.

*Funded by Deutsche Forschungsgemeinschaft under grant No. GRK 2128
#ljuergensen@ikp.tu-darmstadt.de

Content from this work may be used under the terms of the CC BY 3.0 licence (© 2018). Any distribution of this work must maintain attribution to the author(s), title of the work, publisher, and DOI.

ISBN: 978-3-95450-201-1 doi:10.18429/JACoW-IBIC2018-MOPB04

PROGRESS IN THE STRIPLINE KICKER FOR ELBE

C. Schneider†, A. Arnold, J. Hauser, P. Michel, HZDR, Dresden, Germany

Abstract

The linac based cw electron accelerator ELBE operates different secondary beamlines one at a time. For the future different end stations should be served simultaneously, hence specific bunch patterns have to be kicked into different beam-lines. The variability of the bunch pattern and the frequency resp. switching time are one of the main arguments for a stripline-kicker. A design with two tapered active electrodes and two ground fenders was optimized in time and frequency domain with the software package CST. From that a design has been transferred into a construction and was manufactured. The presentation summarises the recent results and the status of the project.

INTRODUCTION

The electron beam with max. 40 MeV is mainly used for conversion into secondary radiation at different end stations; infrared, terahertz, gamma, positron, neutron und electron laser interaction (Figure 1). For every beam line dedicated energies and optimized settings have to be adjusted, but not every experiment demands the full 13 MHz cw capability of ELBE.

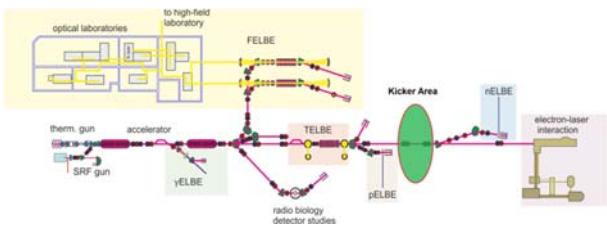

Figure 1: Overview of the ELBE layout with the position of the kicker station.

As an example the end stations from neutron an electron laser interaction are using high bunch charge but 200 kHz and 10 Hz respectively and are separated by just one beam line branch. Therefore a kicking device in front of the neutron and laser interaction beam line can serve both beam lines at a time.

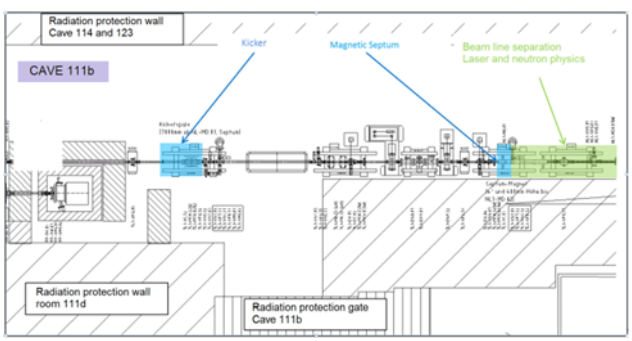

Figure 2: Detailed sketch of the ELBE kicker area.

A magnetic septum is installed to align the beam either to the neutron or laser interaction beamline (see Figure 2). The separation for the magnetic septum is about 10 mm beam displacement. The distance between kicker and septum will be around 7 m. Hence a kick angle of around 1.5 mrad must be realized. In the simulation with the CST software package a voltage of 427 V per strip-line and an electrode distance of 30 mm was used. This results in a mean kicking angle of the phase space distribution of 1.5 mrad.

DESIGN AND OPTIMISATION

The ELBE strip-line kicker design uses the common approach [1, 2, 3] with two tapered active electrodes and two ground fenders. The slightly difference is the placing of the two ground fenders in the outer area of the electrodes.

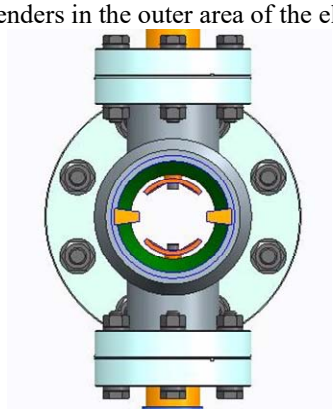

Figure 3: Sectional drawing of the ELBE kicker in the area of the connection ports.

The distance between the electrodes was chosen to 30 mm having a balance of lower HV supply and still feeding the electron beam in a homogenous field area through the kicker (Figure 3). The design was optimized with the CST package to fit best to 50 Ω impedances, for optimal S-parameters in the frequency domain as well as having best field flatness (Figure 4) in the significant area between the electrodes.

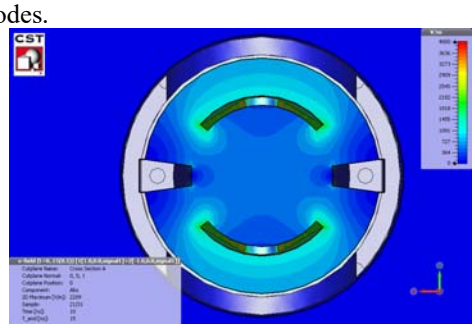

Figure 4: Sectional plot of the electric field in the medium section of the kicker structure.

KICKER SETUP AT ELBE

The kicker will be installed in the radiation shielded cave 111b (see Figure 5). The HV-device to power the kicker

* Work supported by BMBF
† Christof.Schneider@hzdr.de

Content from this work may be used under the terms of the CC BY 3.0 licence (© 2018). Any distribution of this work must maintain attribution to the author(s), title of the work, publisher, and DOI.

ISBN: 978-3-95450-201-1 doi:10.18429/JACoW-IBIC2018-MOPB06

DAΦNE LUMINOSITY MONITOR

A. De Santis*, C. Bisegni, O. R. Blanco-García, O. Coiro, A. Michelotti, C. Milardi, A. Stecchi
INFN - Laboratori Nazionali di Frascati, Frascati 00044 (Roma), Italy.

Abstract

The DAΦNE collider instantaneous luminosity has been measured identifying Bhabha scattering events at low polar angle (~10°) around the beam axis by using two small crystal calorimeters shared with the KLOE-2 experiment. Independent DAQ setup based on !CHAOS, a novel Control System architecture, has been designed and realized in order to implement a fast luminosity monitor, also in view of the DAΦNE future physics runs. The realized setup allows for measurement of Bunch-by-Bunch (BBB) luminosity that allows to investigate the beam-beam interaction for the Crab-Waist collisions at DAΦNE and luminosity dependence on the bunch train structure.

INTRODUCTION

The luminosity of DAΦNE during KLOE-2 Physics run [1] has been measured by the experiment selecting on-line a special class of Bhabha scattering events directly at the trigger level while taking data [2, 3]. KLOE-2 dedicated DAQ process was used to provide a instantaneous luminosity measurement every 15 seconds with 3-5% relative uncertainty typically.

Furthermore two independent gamma monitors were installed to measure single bremsstrahlung [4] from both electron and positron beams. This diagnostic is well suited for collisions fast fine tuning because of the high rates of the observed process. The usage of gamma monitors for absolute luminosity measurement however is not possible because the acceptance of the detectors has a strong dependence on the machine setup and a large background hitting the diagnostic is observed.

The realization of a further luminometer based on the observation of the Bhabha scattering events emitted at low angle aims at combining accuracy and high repetition rate in the same diagnostic

EXPERIMENTAL SETUP

The experimental apparatus is based on the small angle Crystal CALorimeters with Time measurement (CCALT) [5] of the KLOE-2 detector that measures the Bhabha scattering events, the dominant process in that angular region.

Detector Layout

The CCALT is constituted by two identical crystal calorimeters installed in front of the permanent defocusing quadrupole QD0 of the DAΦNE low-β doublet providing the proper focusing of the beams at the Interaction Point (IP).

The detector covers the polar angle between 8° and 18°. Each calorimeter is segmented in 48 small LYSO[1] crystal. Each segment is readout with Silicon Photo-Multiplier (SiPM). Signals from group of four crystal are analogically summed in CCALT sectors, acquired independently with respect the KLOE-2 data, to measure the luminosity. Each sectors covers an azimuthal angle of 30°. The detector assembly and final installation are shown in Fig. 1.

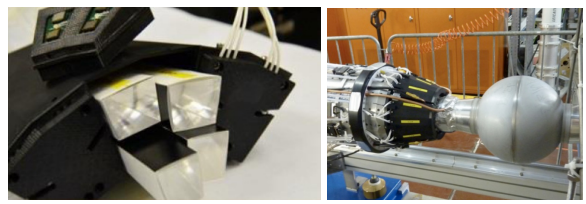

Figure 1: Left: CCALT detector macro-sector before the SiPM installation. The four crystal per sector are clearly visible. Each side of the detector is made of four macro-sectors. This segmentation is needed in order to leave space for the Beam position Monitor feed-trough.
Right: Detector fully assembled and installed in front of the QD0 magnets. The spherical beam pipe around the IP is also shown. Only one side of the detector is visible.

DAQ and Control System

The DAQ scheme is sketched in Fig. 2. CCALT sectors signals are split and compared with a constant fraction discriminator[2] in order to measure arrival time and integrated charge.

Discriminated signals are used to feed the trigger logic: same side pulses are logically merged to reduce multiplicity, then time coincidence between the two side of the detector are used to form trigger pulses when single side signals overlap for at least 4 ns. When trigger pulse is received by the TDC[3] signals arrival time are determined.

The luminometer dedicated DAQ is completed with a programmable FPGA[4] that allows monitoring of DAQ rates and the acquisition dead-time. The most relevant source of dead-time is the injection trigger veto that must be used in order to reduce the trigger rate observed during the first 50 ms after the injection pulse. The veto length caused at least a detector efficiency loss of 10% (50 ms veto every 500 ms corresponding to the single shot of the injection cycle) that has to be taken into account for online measurement of the luminosity.

* antonio.desantis@lnf.infn.it

[1] Cerium-doped Lutetium Yttrium Orthosilicate.
[2] CAEN N843
[3] CAEN V775N.
[4] CAEN V1495

Content from this work may be used under the terms of the CC BY 3.0 licence (© 2018). Any distribution of this work must maintain attribution to the author(s), title of the work, publisher, and DOI.

ISBN: 978-3-95450-201-1 doi:10.18429/JACoW-IBIC2018-MOPB07

BEAM PARAMETER MEASUREMENTS FOR THE J-PARC HIGH-INTENSITY NEUTRINO EXTRACTION BEAMLINE

M. Friend*, High Energy Accelerator Research Organization (KEK), Tsukuba, Japan
for the J-PARC Neutrino Beam Group

Abstract

Proton beam monitoring is absolutely essential for the J-PARC neutrino extraction beamline, where neutrinos are produced by the collision of 30 GeV protons from the J-PARC MR accelerator with a long carbon target. Continuous beam monitoring is crucial for the stable and safe operation of the extraction line high intensity proton beam, since even a single misfired beam spill can cause serious damage to beamline equipment at 2.5×10^{14} and higher protons-per-pulse. A precise understanding of the proton beam intensity and profile on the neutrino production target is also necessary for predicting the neutrino beam flux with high precision. Details of the suite of monitors used to continuously and precisely monitor the J-PARC neutrino extraction line proton beam are shown, including recent running experiences, challenges, and future upgrade plans.

OVERVIEW OF J-PARC AND THE NEUTRINO PRIMARY BEAMLINE

The J-PARC proton beam is accelerated to 30 GeV by a 400 MeV Linac, a 3 GeV Rapid Cycling Synchrotron, and a 30 GeV Main Ring (MR) synchrotron. Protons are then extracted using a fast-extraction scheme into the neutrino primary beamline, which consists of three sections containing a series of normal- and super-conducting magnets used to bend the proton beam towards a neutrino production target. Generated neutrinos travel 295 km towards the Super-Kamiokande detector for the Tokai-to-Kamioka Long-Baseline Neutrino Oscillation Experiment (T2K) [1], which started operation in 2009.

Table 1: J-PARC Proton Beam Specifications

	Protons/Bunch	Spill Rate
Current (2018)	3.13×10^{13}	2.48 s
Upgraded (2021~)	$2.75 \rightarrow 4.00 \times 10^{13}$	1.32→1.16 s

The J-PARC 30 GeV proton beam has an 8-bunch beam structure with 80 ns (3σ) bunch width and 581 ns bucket length. J-PARC currently runs at 485 kW with the plan to upgrade to 750+ kW in 2020 and 1.3+ MW by 2026. This will be achieved by increasing the beam spill repetition rate from the current one spill per 2.48 s, to 1.32 s and finally 1.16 s, along with increasing the number of protons per bunch from $\sim 3 \times 10^{13}$ to 4×10^{13}, as shown in Table 1.

The 30 GeV proton beam is extracted into the neutrino beamline preparation section. In the preparation section, the position and width of the extracted beam are tuned by normal-conducting magnets in order to match the beam optics in the following arc section, where the beam is bent by 80.7° using super-conducting combined function magnets. Finally, in the final focusing section, normal-conducting magnets are used to direct the beam downward by 3.647° and tune the beam position and size to focus the beam onto the center of the neutrino production target.

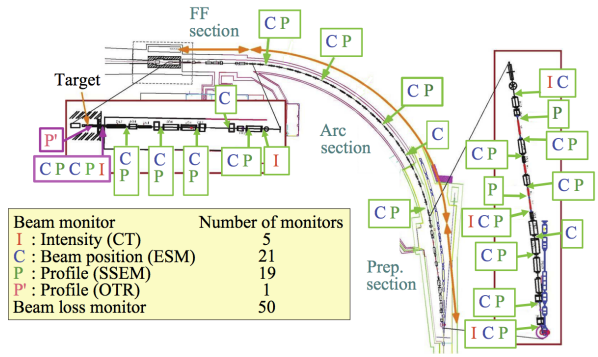

Figure 1: Beam monitor positions along the neutrino primary beamline.

Beam monitoring is essential for protecting beamline equipment from possible mis-steered beam as part of a machine interlock system, where even a single mis-steered beam shot can do serious damage at high intensities. Information from proton beam monitors is also used and as an input into the T2K physics analysis, and imprecisions on proton beam measurements can have a direct effect on the precision of the final T2K physics results.

MONITORS IN THE J-PARC NEUTRINO PRIMARY BEAMLINE

The proton beam conditions are continuously monitored by a suite of proton beam monitors along the neutrino primary beamline, as shown in Fig. 1.

Five Current Transformers (CTs) are used to continuously monitor the proton beam intensity. Fifty Beam Loss Monitors (BLMs) continuously measure the spill-by-spill beam loss and are used to fire an abort interlock signal in the case of a high-loss beam spill. Twenty-one Electro-Static Monitors (ESMs) are used as Beam Position Monitors to continuously monitor the beam position and angle.

The proton beam profile (beam position and width) is monitored bunch-by-bunch during beam tuning by a suite of 19 Segmented Secondary Emission Monitors (SSEMs) distributed along the primary beamline, where only the most downstream SSEM (SSEM19) is used continuously. An

* mfriend@post.kek.jp

Content from this work may be used under the terms of the CC BY 3.0 licence (© 2018). Any distribution of this work must maintain attribution to the author(s), title of the work, publisher, and DOI.

ISBN: 978-3-95450-201-1 doi:10.18429/JACoW-IBIC2018-MOPB08

EVALUATION OF THE TRANSVERSE IMPEDANCE OF PF IN-VACUUM UNDULATOR USING LOCAL ORBIT BUMP METHOD

O. A. Tanaka†, N. Nakamura, T. Obina, K. Harada, Y. Tanimoto, N. Yamamoto, K. Tsuchiya, R. Takai, R. Kato, M. Adachi,
High Energy Accelerator Research organization (KEK), 305-0801 Tsukuba, Japan

Abstract

When a beam passes through insertion devices (IDs) with narrow gap or beam ducts with small aperture, it receives a transverse kick from the impedances of those devices. This transverse kick depends on the beam transverse position and beam parameters such as the bunch length and the total bunch charge. In the orbit bump method, the transverse kick factor of an ID is estimated through the closed orbit distortion (COD) measurement at many BPMs for various beam currents [1]. In the present study, we created an orbit bump of 1 mm using four steering magnets, and then measured the COD for two cases: when the gap is opened (the gap size is 42 mm) and when the gap is closed (the gap size is 3.83 mm). The ID's kick factors obtain by these measurements are compared with those obtain by simulations and analytical evaluations.

INTRODUCTION

At KEK Photon Factory (PF) light source, we have four newly installed in-vacuum undulators (IVUs). They are located in short straight sections as shown in Fig. 1. The vacuum chambers of those IVUs have complex geometry: narrow gaps inside the undulators (the minimum gap is 3.83 mm) and tapers at the ends of undulators. Those gaps are much smaller than the typical aperture of the PF normal vacuum ducts.

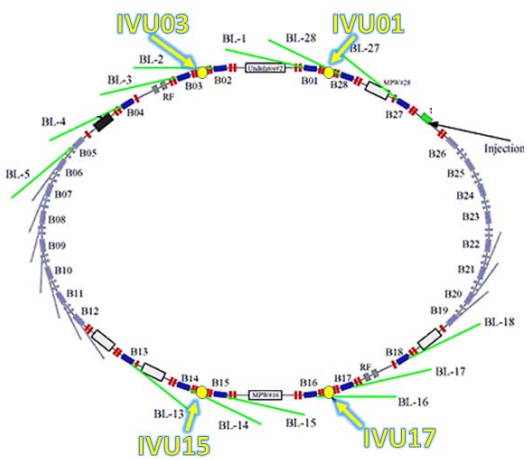

Figure 1: Locations of the IVUs in the PF ring.

First, the kick factors of the four IVUs were estimated analytically and by CST Studio simulations [2]. The total vertical kick factor due to 1 IVU including dipolar and quadrupolar kicks of the taper and resistive-wall kick of the undulator copper plates is summarized in Fig. 2.

To confirm the accuracy of the calculated transverse kick factors, we have measured the transverse tune shift with a single bunch based on the RF-KO (RF Knock Out) method [3]. The additional tune shift corresponds to a difference of the vertical tune shifts for ID open (the gap size is 42 mm) and ID closed (the gap size is 3.83 mm) cases. The result of the tune shift measurement is shown at Fig. 3. All the three evaluations demonstrated very good agreements. Thus, theory gives the tune shift value per unit of bunch current of $\Delta\nu / I_b = -10.60\times10^{-6}$ mA^{-1}. The CST Studio simulation gives those of $\Delta\nu / I_b = -10.06\times10^{-6}$ mA^{-1}. And the tune shift measurement yields the value of $\Delta\nu / I_b = -10.96\times10^{-6} \pm 1.86\times10^{-6}$ mA^{-1} including the fitting error.

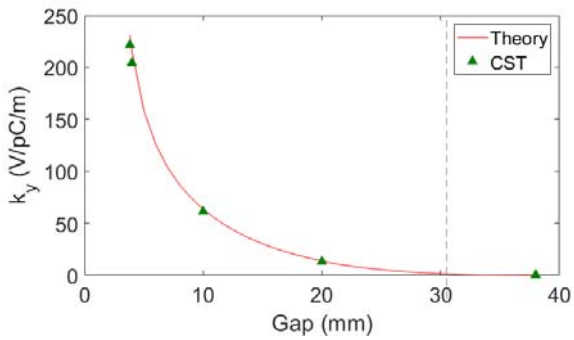

Figure 2: Total vertical kick factor due to 1 IVU (gap dependence, width fixed to 100 mm) by theory (red line), and by simulations (green triangle).

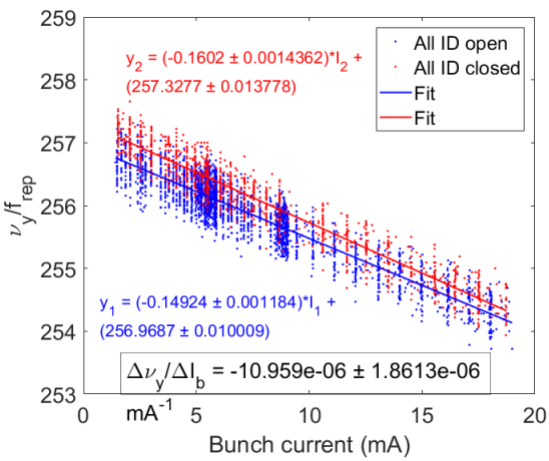

Figure 3: One of the measurement results of the additional tune shift due to the four IVU at PF.

† olga@post.kek.jp

Content from this work may be used under the terms of the CC BY 3.0 licence (© 2018). Any distribution of this work must maintain attribution to the author(s), title of the work, publisher, and DOI.

ISBN: 978-3-95450-201-1 doi:10.18429/JACoW-IBIC2018-MOPB09

COMPARISON AMONG DIFFERENT TUNE MEASUREMENT SCHEMES AT HLS-II STORAGE RING*

L. T. Huang*, T. Y. Zhou*, Y. L. Yang, J. G. Wang, P. Lu, X. Y. Liu, J. H. Wei, M. X. Qian, F. F. Wu†, B. G. Sun‡
National Synchrotron Radiation Laboratory,
University of Science and Technology of China, 230029 HeFei, China

Abstract

Tune measurement is one of the most significant beam diagnostics at HLS-II storage ring. When measuring tune, higher tune spectral component and lower other components are expected, so that the tune measurement will be more accurate. To this end, a set of BBQ (Base Band Tune) front-end based on 3D (Direct Diode Detection) technique has previously developed to improve the effective signal content and suppress other components. Employing the BBQ front-end, four different tune measurement schemes are designed and related experiments performed on the HLS-II storage ring. Experimental results and analysis will be presented later.

INTRODUCTION

The electron storage ring is the major part of HLS-II, and some of its main parameters are shown in Table 1 [1].

Table 1: Main HLS-II Storage Ring Main Parameters

Parameter	Value
Energy	800MeV
Beam current	300mA
RF frequency	204MHz
Revolution frequency	4.534MHz
Emittance	40nm*rad
Tune(fractional part)	0.45/0.35

The fractional part of the tune for a storage ring can be measured by observing the betatron sidebands on either side of the revolution harmonics [2]. The past tune measuring method is usually to put the signals from the beam position pick-up directly into the spectrum analyzer after some addition, subtraction, filtering and amplification processing, and then analyze the spectral data to obtain the fractional part of the tune. In general, beam pulse signals from the position pick-up is very narrow in the time domain, resulting in energy dispersion in a wide spectrum. This way only uses one betatron sideband, which causes most of the betatron energy to be wasted. This means that substantial beam excitation is necessary in this method, which can lead to significant emittance degradation, so the system cannot be used during normal operation [3]. To solve this problem, 3D technique was initially developed at CERN for LHC to meet the requirements for measuring the tune of beam betatron oscillations with amplitudes below a micrometre [4]. The core of 3D technique is simple peak diode detector that can time-stretch the narrow beam pulses from the pick-up into slowly changing signals, meaning it's capable of moving most of the betatron energy to the baseband and improving the used betatron sideband intensity [5]. Using the BBQ front-end based on 3D technique, four different tune measurement schemes are designed for comparative experiments.

*Supported by the National Science Foundation of China (Grant No. 11705203, 11575181), Anhui Provincial Natural Science Foundation(Grant No. 1808085QA24), Chinese Universities Scientific Fund (Grant No. WK2310000057)
† Corresponding author (email: wufangfa@ustc.edu.cn)
‡ Corresponding author (email: bgsun@ustc.edu.cn)

3D AND BBQ FRONT-END

3D technique uses two simple envelope detectors (also known as peak diode detector) connected to opposing electrodes of a pick-up. Followed by two DC blocking capacitors and a high impedance differential amplifier, a simplified BBQ front-end is completed, as shown in Fig. 1.

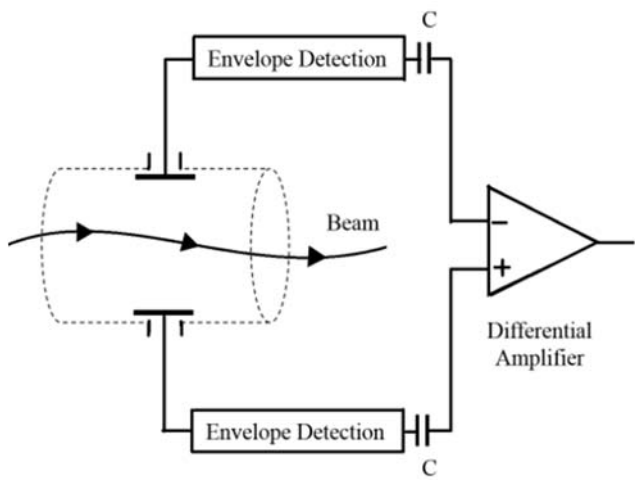

Figure 1: A simplified BBQ front-end schematic block diagram.

Based on the schematic block diagram above, a BBQ front-end was developed previously for HLS-II storage ring (see Fig. 2). The left two green parts are two peak diode detectors. The right box contains the rest: two capacitors and one differential amplifier.

Content from this work may be used under the terms of the CC BY 3.0 licence (© 2018). Any distribution of this work must maintain attribution to the author(s), title of the work, publisher, and DOI.

ISBN: 978-3-95450-201-1 doi:10.18429/JACoW-IBIC2018-MOPB10

A STUDY ON THE INFLUENCE OF BUNCH LONGITUDINAL DISTRIBUTION ON THE CAVITY BUNCH LENGTH MEASUREMENT*

Q. Wang, Q. Luo†, B. G. Sun‡, F. F. Wu
NSRL, University of Science and Technology of China, 230029 Hefei, China

Abstract

Cavity bunch length measurement is used to obtain the bunch length depending on the eigenmodes exciting inside the cavity. For today's FELs, the longitudinal distribution of particles in electron bunch (bunch shape) may be non-Gaussian, sometimes very novel. In this paper, the influence of bunch shape on the cavity bunch length measurement is analyzed, and some examples are given to verify the theoretical results. The analysis shows that the longitudinal distribution of particles in electron bunch has little influence on the cavity bunch length measurement when the bunch length is less than 1 ps and the eigenmodes used in measurement are below 10GHz.

INTRODUCTION

Bunch length is one of the important characteristics of charged particle beam in accelerators. Compared with the traditional methods, bunch length monitor based on resonant cavities has great potential especially for high quality beam sources, for it has superiority, such as simple structure, wide application rage, and high signal to noise ratio [1]. What's more, the eigenmodes of cavities are used in combined measurement of bunch length, beam intensity, position and quadrupole moment. For example, the monopole modes can be used to measure the bunch length and the beam intensity [2]. At the same time, the dipole modes are always utilized to obtain the beam position offset [3]. What's more, we could decide the quadrupole moment by analyzing the TM220 modes of the square resonators [4]. Therefore, the measurement device shows the characteristic of terseness and compaction.

The present FELs show characteristic of very short bunch. For example, the bunch length of Shanghai soft X-ray free Electron laser (SXFEL) is several hundred femtoseconds. At the same time, the longitudinal distribution of particles in electron bunch (bunch shape) may be non-Gaussian, sometimes very novel. While analyzing the beam-cavity interaction, we assume the longitudinal distribution of particles in electron bunch is Gaussian in a general way. Then what is the impact of the non-Gaussian bunch on the cavity bunch length monitor? In this paper, the influences of the different bunch shapes on the cavity bunch length measurement are analyzed under different circumstances, and the results provide theoretical support for the future FEL bunch length measurements using resonant cavities.

MESUREMENT OF GAUSSIAN BUNCH

While passing through a cavity, an electron whose charge is q can excite a series of eigenmodes. The voltage amplitude of an eigenmode can be expressed as

$$V_q = 2k_n q \tag{1}$$

Where k_n is the loss factor which is related to R/Q of the eigenmode [5]. It can be seen that the voltage is related to the charge q. As for a bunch whose total charge is Q_b, the voltage amplitude of an eigenmode excited inside the cavity is the superposition of the electrons in the bunch which arrive at the cavity at different times. The moments when the electrons arrive at the cavity depend on the longitudinal distribution of particles in electron bunch. Assume an electron bunch whose longitudinal normalized distribution function of electrons is f(t). The moment when the center of the bunch arrives at the center of the cavity is defined as zero time. So the voltage amplitude of an eigenmode when the charge arriving at the cavity at time t can be expressed as

$$dV = 2k_n dq \tag{2}$$

Considering the voltage phases excited by electrons in different places is disparate, the voltage amplitude of an eigenmode can be written as

$$\begin{aligned} V_b &= \int_{-t_m}^{t_m} \mathrm{e}^{i\omega_n t}\, dV \\ &= 2k_n \int_{-t_m}^{t_m} \mathrm{e}^{i\omega_n t} dq \\ &= 2k_n \int_{-t_m}^{t_m} I(t) \times \mathrm{e}^{i\omega_n t} dt \\ &= 2k_n Q_b \int_{-t_m}^{t_m} f(t) \times \mathrm{e}^{i\omega_n t} dt \end{aligned} \tag{3}$$

Where ω_n is the frequency of the eigenmode, t_m is the range of the bunch longitudinal distribution, and I(t) represents beam current. In a general way, the longitudinal distribution of the bunch is regarded as Gaussian distribution, so

$$f(t) = \frac{1}{\sqrt{2\pi}\sigma} \exp\left(-\frac{t^2}{2\sigma^2}\right) \tag{4}$$

* Supported by National Key R&D Program of China (Grant No. 2016YFA0401900, 2016YFA0401903), the National Science Foundation of China (Grant No. 11375178, 11575181) and the Fundamental Research Funds for the Central Universities (WK2310000046).
† Corresponding author (email: luoqing@ustc.edu.cn)
‡ Corresponding author (email: bgsun@ustc.edu.cn)

Content from this work may be used under the terms of the CC BY 3.0 licence (© 2018). Any distribution of this work must maintain attribution to the author(s), title of the work, publisher, and DOI.

ISBN: 978-3-95450-201-1 doi:10.18429/JACoW-IBIC2018-MOPB13

ACTIVE MAGNETIC FIELD COMPENSATION SYSTEM FOR SRF CAVITIES

L. Ding, Laboratory GREYC, Caen, France
Jian Liang, Hanxiang Liu, Zaipeng Xie†, Hohai Ubiversity, Nanjing, China

Abstract

Superconducting Radio Frequency (SRF) cavities are becoming popular in modern particle accelerators. When the SRF cavity is transitioning from the non-conducting to the Superconducting state at the critical temperature (Tc), the ambient magnetic field can be trapped. This trapped flux may lead to an increase in the surface resistance of the cavity wall, which can reduce the Q-factor and efficiency of the cavity. In order to increase the Q-factor, it is important to lower the surface resistance by reducing the amount of magnetic flux trapped in the cavity wall to sub 10- G range during the Tc transition.

In this paper, we present a 3-axis automatic active magnetic field compensation system that is capable of reducing the earth magnetic field and any local disturbance field. Design techniques are described to enhance the system stability while utilizing the flexibility of embedded electronics. This paper describes the system implementation and concludes with initial results of tests. Experimental results demonstrate that the proposed magnetic field compensation system can reduce the earth magnetic field to sub 1 mG even without shielding.

Introduction

An important limiting factor in the performance of superconducting radio frequency (SRF) cavities in medium and high field gradients is the intrinsic quality factor and, thus, the surface resistance of the cavity [1]. The exact dependence of the surface resistance on the magnitude of the RF field is not well understood [2]. Lower Q factors may come from several sources, one of which is the presence of a trapped magnetic field inside the cavity walls at cool down [3], known as remanent magnetization,

Remanent magnetisation is often a function of the grain boundaries of the niobium material [4] used to construct the cavities. It is affected by the ambient field during the cooling cycle that necessary to superconductivity, and below 3 Gauss, 100% of the field is trapped [5]. A number of studies have been carried out on cool-down speed, and one report concludes that fast cool-down will be more uniform and can be expected to result in less trapped magnetic flux because perturbations to the phase boundary will be larger on average during slow cool-down [6] while others advocate a fast cool-down [7].

Therefore, if the magnetic field can be reduced during the cooling cycle this will reduce the remanent magnetisation in the SRF cavity.

Current state of the art is to place the SRF cavity in a tubular magnetic shield [8]. This tube and the SRF cavity must then be located in an east-west orientation [8] [9]. In addition coils are then placed around the tube to provide further compensation. There is effectively no safety margin with this arrangement [8]. During the cool down phase fluxgate magnetometers monitor the magnetic field.

The typical remanent magnetic field requirement is less than 3-4 mG [10]. The earth's magnetic field is circa 500 mG so approximately 45dB attenuation of the earth field is required.

This paper proposes that the SRF cavity is placed inside a three axis Helmholtz coil system (Figure 1). Fluxgate magnetometers positioned as close to the cavity as possible, are used as feedback sensors for the cancellation system. With this active compensation in place, it is possible to achieve < 1 mG of trapped field in the cavity, thereby improving its RF performance.

Prior to the cooling cycle the compensation system is energized so the field in the SRF cavity is minimized. The monitoring and field adjustment continues during the cooling cycle.

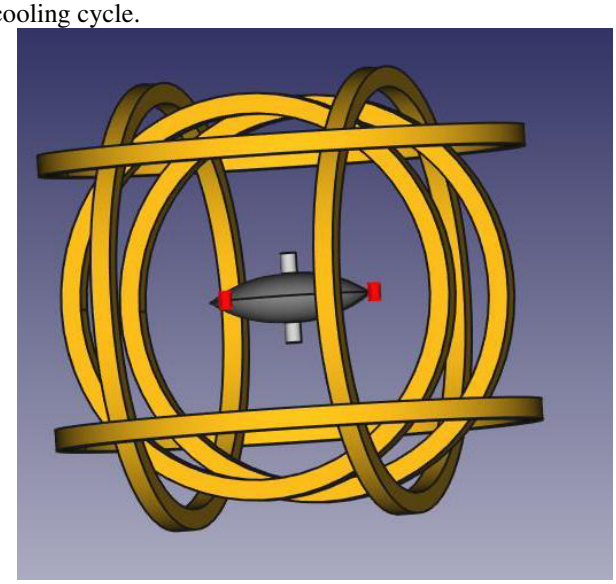

Figure 1: Coil setup with magnetometers in red.

SYSTEM DESIGN

The system consists of a three axis Helmholtz coil around the SRF cavity, 3 axis fluxgate sensor mounted to the cavity, optional additional single axis sensors around the circumference of the cavity, and the control electronics. The sensors monitor the field seen by the SRF cavity to the control electronics. This signal is in analog form, so is digitized to provide a real-time update. The control electronics compares the signals from the sensors and immediately adjusts the current in the Helmholtz coils, thereby maintaining a very low level of magnetic field

† email address: zaipengxie@impcas.ac.cn

Content from this work may be used under the terms of the CC BY 3.0 licence (© 2018). Any distribution of this work must maintain attribution to the author(s), title of the work, publisher, and DOI.

ISBN: 978-3-95450-201-1 doi:10.18429/JACoW-IBIC2018-MOPB14

SSRF BEAM OPERATION STABILITY EVALUATION USING BUNCH BY BUNCH BEAM POSITION METHOD *

Ning Zhang †, Yimei Zhou, Yongbin Leng*, Shanghai Institute of Applied Physics, CAS, Shanghai 201808, China

Abstract

In order to improve the efficiency and quality of light in Top-up mode at SSRF, disturbance caused by leakage fields mismatch during injection should be minimized and stable. This could be evaluated by analysis of bunch by bunch residual betatron oscillation data, using this method, instability of tune distribution and damping repeatability could also be calculated. So we could evaluate the beam operation stability by the data analysis and discuss in the paper.

INTRODUCTION

In Shanghai Synchrotron Radiation Facility (SSRF), the accelerator injection mode has been upgraded from Decay mode to Top-up mode since late 2012[1], aiming to achieve uniform filling. This method results in more frequent beam injections (about 2 minutes per one injection period). Since the injection process involves a variety of equipment, Parameter imperfections can lead to a closed orbit distortion, which will leave a residual betatron oscillation during injection. For beam light users, this disturbance should be as little as possible.

Usually, parameter mismatches during injection mainly refers to:

(1) Kicker excitation current mismatch (current waveform amplitude and timing).

(2) Energy or phase mismatch, between the injected bunch from the booster and the stored bunches in the storage ring.

(3. Mechanical error in the kickers.

Injection performance evaluation and analysis have been done by SSRF BI group [2][3]. In the experiment, bunch by bunch position measurement system was employed. A complete residual oscillation distribution was obtained by combining several groups of injection, which could be used for evaluate issue(1), and by harmonic analysis, The spectrum of the injected bunch position signal can be obtained for issue(2). Turn by turn SA data from Libera was used to observe the effect of issue (3).

For SSRF beam operation, the closed orbit distortion caused by kicker leakage field mismatch as well as tune and damping time should be as stable as possible, which would be good for further optimization. So operation stability should be evaluated by long-term measurement and evaluating the variation of parameters from different period.

Work supported by National Natural Foundation of China (11375255 and11375254)

† Email: zhangning@sinap.ac.cn *Email: lengyongbin@sinap.ac.cn

MESUREMENT SYSTEM

Raw position signals of beam in storage ring are excited by BUTTON BPMs installed in vacuum pipe. For building a bunch-by-bunch position measuring system to obtain the disturbance details of each bunch, the bandwidth of the system should be larger than 250 MHz, the data rates should be equal to or greater than 499.654 MHz (storage ring RF frequency), and the data buffer should be greater than 10 Mb.(determined by the loop damping time 5-6 ms).

The latest bunch by bunch position measurement method in SSRF is synchronous peak sampling at RF frequency [4]. The sampled pulse peak data with same phase from 4 input channels were calculated to obtain position and sum value for each bunch. For this purpose, ADQ14 data acquisition board developed by SP-devices Company was employed as Data Processing Board, used for raw BPM signals sampling and bunch position calculation in real-time. The board and chassis component were shown in Figure 1.

Figure 1: Data acquisition board and PXIe chassis forBTB position on-line measurement.

PC-based controller (Data I/O Unit) as well as Data Processing Board, was inserted into NI chassis, which controlled Data Processing Board using PXIe interface. We have designed an EPICS IOC running in Linux OS of the controller to implement DAQ control and data output.

Data Processing Board and Data I/O Unit consists the basic framework of bunch by bunch data acquisition system. By applying different front-end and IOC algorithm, the system could achieve transverse and longitudinal parameters [5] measurement. For bunch by bunch position, the front-end was designed for Phrase adjustment, Delay adjustment, Signal attenuation and Generating RF frequency doubling phrase-lock signal for external clock. The system structure is shown in Figure 2.

Content from this work may be used under the terms of the CC BY 3.0 licence (© 2018). Any distribution of this work must maintain attribution to the author(s), title of the work, publisher, and DOI.

ISBN: 978-3-95450-201-1 doi:10.18429/JACoW-IBIC2018-MOPB16

CONTINUOUS BEAM ENERGY MEASUREMENTS IN DIAMOND LIGHT SOURCE

N. Vitoratou*, P. Karataev
John Adams Institute at Royal Holloway, University of London, Egham, UK
G. Rehm, Diamond Light Source, Oxfordshire, UK

Abstract

Resonant Spin Depolarization (RSD) is a high precision technique that has been employed by Diamond Light Source (DLS) for beam energy measurements. In this project, we study a new approach to make RSD compatible with user beam operation and provide a continuously updated online measurement. An array of four custom-made scintillation detectors has been installed around the beam pipe, downstream of collimators to capture the highest fraction of lost particles and maximize the count rate. The excitation is gated to half of the stored bunches and the acquisition system counts losses in both halves independently. Using the count in the un-excited part for normalisation suppresses external factors that modify the loss rate. Different parameters of the measurement, like excitation kick strength and duration have been explored to optimise depolarisation and to increase the reliability of the measurement.

INTRODUCTION AND MOTIVATION

The technique of RSD takes advantage of the natural spin polarisation due to synchrotron radiation emission and provides a high precision energy measurement with a relative uncertainty of typically 10^{-6} [1]. A continuous beam energy measurement employing this technique could reveal any correlations with the photon energy fluctuations and give information about the stability of the bending magnets power supply. Thus, in Diamond Light Source, a method is being developed to make these measurements compatible with the user operation, where the main challenges are not to disturb the stored beam and counteract external factors that could influence the measurement.

BEAM POLARISATION

The spin of the electron beam will develop a polarisation, due to the emission of the spin-flip radiation, according to Sokolov-Ternov effect, which is antiparallel with the magnetic field of the main bending magnets. In an ideal ring, in the absence of depolarizing effects, the maximum expected beam polarization is 92 % [2]. The amount of polarisation will be a combination of the polarising and depolarising effects that is given by [3] :

$$P(t) = P_{ST}\frac{\tau_d}{\tau_d + \tau_{ST}}\left[1 - \exp\left(-\frac{t}{\tau_{ST}}\left(\frac{\tau_d + \tau_{ST}}{\tau_d}\right)\right)\right] \quad (1)$$

where P_{ST} and τ_{ST} are the Sokolov-Ternov values for the equilibrium polarisation level and time constant respectively, and τ_d the depolarisation time constanst. Depolarising effects can occur by horizontal magnetic fields due to closed orbit distortions or quadrupoles misalignments. However, excellent alignment, orbit correction schemes and small vertical emittance in DLS weakens these effects and allow the beam to have an equilibrium polarisation level of 82 % .

Another limit in the polarisation level is introduced by wigglers. The wigglers increase the energy spread which is related with the asymptotic polarisation level given by Sokolov-Ternov effect [4]. This effect will reduce the polarisation level to 60 % for the case of DLS, as it is shown in Fig. 1.

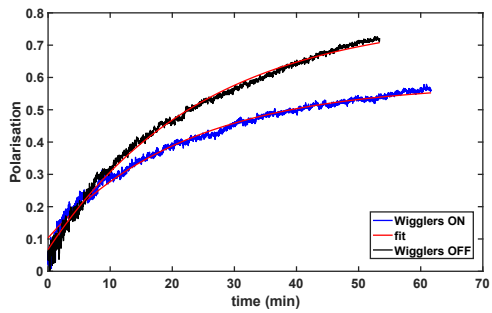

Figure 1: Polarisation build-up of stored beam with wigglers on and off, one hour after injection. The polarisation level is expressed as the relative increase of the lifetime. The lifetime is calculated by the inverse of the recorded beam losses normalised by the beam current [5]. The applied fit is based on Eq. (1).

BEAM DEPOLARISATION

The spin precession frequency of an ultra-relativistic electron in a magnetic field follows the Thomas–BMT equation which for a light source storage ring where there are no significant solenoid magnetic fields, nor transverse electric fields, can be simplified to the below form [6]:

$$\Omega_z = \omega_0(1 + \alpha\gamma) \quad (2)$$

where ω_0 is the revolution frequency, α the gyromagnetic anomaly and γ the relativistic factor. The product $\alpha\gamma$ is the number of revolutions the spin vector makes about the vertical axis in one revolution of the storage ring defined as the spin tune. The equation above shows the relation between the energy of the beam and the spin precession frequency and by determining the unknown frequency, the energy can be calculated.

* Niki.Vitoratou.2016@live.rhul.ac.uk

Content from this work may be used under the terms of the CC BY 3.0 licence (© 2018). Any distribution of this work must maintain attribution to the author(s), title of the work, publisher, and DOI.

ISBN: 978-3-95450-201-1 doi:10.18429/JACoW-IBIC2018-MOPB17

USING A TE011 CAVITY AS A MAGNETIC MOMENTUM MONITOR*

J. Guo#, J. Henry, M. Poelker, R. A. Rimmer, R. Suleiman, H. Wang,
JLAB, Newport News, VA 23606, USA

Abstract

The Jefferson Lab Electron-Ion Collider (JLEIC) design relies on cooling of the ion beam with bunched electron beam. The bunched beam cooler complex consists of a high current magnetized electron source, an energy recovery linac, a circulating ring, and a pair of long solenoids where the cooling takes place. A non-invasive real time monitoring system is highly desired to quantify electron beam magnetization. The authors propose to use a passive copper RF cavity in TE011 mode as such a monitor. If such a cavity is powered actively, it is also possible to be used as a beam magnetizer.

INTRODUCTION

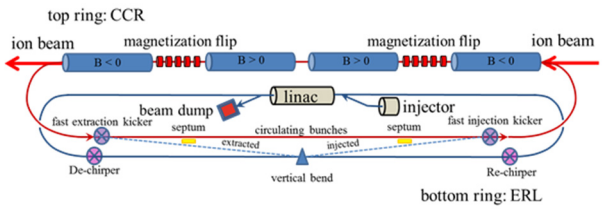

Figure 1: JLEIC Circulating Cooler Ring (CCR).

The proposed JLEIC is a high luminosity electron ion collider. The key to achieve JLEIC's luminosity goal is to maintain low ion emittance through bunched beam electron cooling in solenoid channels during the collision, as shown in Fig. 1. To avoid rotation of the electron beam in the cooling channel, the JLEIC cooling electron beam needs to be magnetized before entering the cooling channel [1]. Magnetized DC electron cooling is also necessary during the JLEIC ion beam formation.

Non-invasive measurement of the magnetic moment of a charged particle beam has long been on the wish-list of beam physicists. The previous efforts were mainly focused on measuring the beam polarization [2, 3, 4], which is in the order of $\hbar/2$ per electron or proton. Even after enhanced by the Stern-Gerlach polarimetry, the RF signal in the cavity generated by the beam is still extremely hard to measure.

The magnetic moment per particle of the magnetized beam is typically a few orders of magnitude higher. As a demonstration of the source for the JLEIC e-cooler, the magnetized beam generated at JLab GTS [5] can have a magnetic moment M=200 neV-s or 3.0×10^8 $\hbar$. The JLab GTS beam also has a typical energy of 300 keV and a low γ. These parameters make the magnetic moment more likely to be detected with an RF cavity.

One potential concern of the resonance type magnetic moment monitor is the signal excited by the non-magnetized current, usually due to the longitudinal component of electric field along the beam path. TE011 mode in a cylindrical symmetric cavity will only have azimuthal E-field, making it an ideal candidate for magnetic moment measurement.

INTERACTION BETWEEN PILLBOX TE011 MODE AND MAGNETIZED BEAM

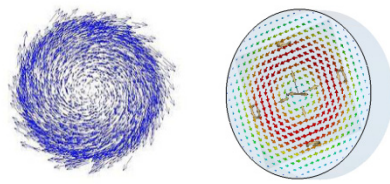

Figure 2: Left: Transverse motion of a longitudinally magnetized beam; Right: Transverse electric field in TE011 mode of a pillbox cavity.

The angular momentum and magnetic momentum of a charged particle is determined by its motion in azimuthal direction, as shown in Fig. 2, left.

$$L = \gamma m \rho^2 \dot{\varphi}$$
$$M = L\frac{e}{2mc} \quad (1)$$

For a cylindrical symmetric RF cavity, the electric field of TE011 mode has only azimuthal component, and will be zero in other directions (radial or longitudinal), as shown in Fig. 2, right. In the vicinity of the cavity axle, the TE011 mode azimuthal E-field's amplitude can be approximated as

$$E_\varphi(z,t,\rho) = E_\varphi(z,t)\rho \quad (2)$$

Assuming that the beam-cavity interaction has negligible perturbation on beam trajectory, $\rho^2\dot{\varphi}$ is almost constant during the beam's path through the cavity. By integrating E-field tangential to the particle trajectory, the acceleration voltage when a particle travels through the cavity can be calculated as

$$V_\perp = \int E_\varphi(z,t,\rho)\rho d\varphi$$
$$= \frac{\rho^2\dot{\varphi}}{\beta c}\int E_\varphi\left(z, t = \frac{z-z_0}{\beta c}\right)dz \quad (3)$$

* Authored by Jefferson Science Associates, LLC under U.S. DOE Contract No. DE-AC05-06OR23177 and supported by Laboratory Directed Research and Development funding. The U.S. Government retains a non-exclusive, paid-up, irrevocable, world-wide license to publish or reproduce this manuscript for U.S. Government purposes
#jguo@jlab.org

Content from this work may be used under the terms of the CC BY 3.0 licence (© 2018). Any distribution of this work must maintain attribution to the author(s), title of the work, publisher, and DOI.

ISBN: 978-3-95450-201-1 doi:10.18429/JACoW-IBIC2018-MOPC02

IDENTIFICATION OF FAULTY BEAM POSITION MONITOR BASED CLUSTERING BY FAST SEARCH AND FIND OF DENSITY PEAKS *

R. T. Jiang†, Y. B.Leng‡, F.Z.Chen, Z.C.Chen
Shanghai Institute of Applied Physics, Chinese Academy of Sciences, 201800 Shanghai, China

Abstract

The accuracy and stability of beam position monitors (BPMs) are important for all kinds of measurement systems and feedback systems in particle accelerator field. A proper method detecting faulty beam position monitor or monitoring their stability could optimize accelerator operating conditions. With development in machine learning methods, a series of powerful analysis approaches make it possible for detecting beam position monitor's stability. Here, this paper proposed a clustering analysis approach to detect the defective BPMs. The method is based on the idea that cluster centres are characterized by a higher density than their neighbours and by a relatively large distance from points with higher densities. The results showed that clustering by fast search and find of density peaks could classify beam data into different clusters on the basis of their similarity. And that, aberrant data points could be detected by decision graph. So the algorithm is appropriate for BPM detecting and it could be a significant supplement for data analysis in accelerator physics.

INTRODUCTION

The storage ring in SSRF is equipped with 140 BPMs located at 20 cells of the storage ring to monitor the beam dynamics [1]. The BPMs at the beam lines after the insertion devices (ID) or the bending magnets are of great importance, because they also serve as the orbit feedback system to ensure stability of the electron Beams [2]. Meanwhile, the BPM confidence levels included in the feedback system can be used to estimate stability of the beam dynamics. Some BPMs can be also used to do measurements other than the beam position, such as the (relative) beam current or life time. Therefore, an abnormal BPM should be found and treated and a beam position monitor (BPM) system is an essential diagnostic tool in storage ring of a light source.

A typical BPM system consists of the probe (button-type or stripline-type), electronics (Libra Electronics/ Brilliance in SSRF) and transferring component (cables and such). Ever since the SSRF commissioning in 2009, the BPM have occurred all kinds of malfunction. They were permanently damage of individual probe or corresponding cable, misaligned (position/angle) probes, high-frequency vibrations, electronics noise, and others. These faults mean totally useless of the signals from the BPM, which should be ignored until its replacement or repair. Hence, it is essential to find an effective method to detect the faulty BPM for operation of the storage ring.

With development in machine learning methods, a series of powerful analysis approaches make it possible for detecting beam position monitor's stability. Cluster analysis is one of machine learning methods. It is aimed at classifying elements into categories on the basis of their similarity [3]. Its applications range from astronomy to bioinformatics, bibliometric, and pattern recognition. Clustering by fast search and find of density peaks is an approach based on the idea that cluster centres are characterized by a higher density than their neighbours and by a relatively large distance from points with higher densities [4]. This idea forms the basis of a clustering procedure in which the number of clusters arises intuitively, outliers are automatically spotted and excluded from the analysis, and clusters are recognized regardless of their shape and of the dimensionality of the space in which they are embedded. In addition to, it is able to detect nonspherical clusters and to automatically find the correct number of clusters.

Based on the advantage of clustering by fast search and find of density peaks, this study researches the stability of beam position monitors to locate the BPM malfunctions at SSRF.

EXPERIMENTAL DATA AND ANALYSIS METHOD

In this study, the experimental data were collected from the transverse oscillation of X direction. In general, the fluctuation of transverse oscillation of X direction means the stability of beam position monitors and the malfunctions could be judged by the abnormal fluctuations. It also has an important problem that is to detect the performance differences of different BPMs. Therefore, this study research the accuracy and stability of beam position monitors based on the data of transverse oscillation of X direction. Theoretically, the BPM could be considered as malfunction when its fluctuation ranges beyond the range of horizontal β-function which is reference value. On the other hand, the performance differences of different BPMs were be expect to distinguish by different cluster centres based on cluster analysis.

The clustering by fast search and find of density peaks has its basis in the assumptions that cluster centres are surrounded by neighbours with lower local density and that they are at a relatively large distance from any points with a higher local density. For each data point i, we compute two quantities: its local density ρi and its distance δi from points of higher density. Both these quantities depend only

* Work supported by National Nature Science Foundation of China (No.11375255)
† jiangruitao@sinap.ac.cn
‡ lengyongbin@sinap.ac.cn

Content from this work may be used under the terms of the CC BY 3.0 licence (© 2018). Any distribution of this work must maintain attribution to the author(s), title of the work, publisher, and DOI.

ISBN: 978-3-95450-201-1 doi:10.18429/JACoW-IBIC2018-MOPC03

PRECISE MEASUREMENT OF SMALL CURRENTS AT THE MLS

Y. Petenev†, J. Feikes, J. Li, A. N. Matveenko, Y. Tamashevich, HZB, 12489 Berlin, Germany
R. Klein, J. Lubeck, R. Thornagel, PTB, 10587 Berlin, Germany

Abstract

The Physikalisch-Technische Bundesanstalt (PTB), the National Metrology Institute of Germany, utilizes an electron storage ring – the Metrology Light Source (MLS), located in Berlin, as a radiation source standard in the VIS, UV and VUV spectral range. In order to be able to calculate the absolute intensity of the radiation, the electron beam current has to be measured with low uncertainty. In this paper we focus on the measurement of the beam current in a range of several nA to 1 pA (one electron) by means of Si photodiodes, detecting synchrotron radiation from the beam. Electrons are gradually scraped out of the ring and the diode signal is analyzed afterwards. The exact number of stored electrons then can be derived from the signal. The measurement is carried out automatically with an in-house developed software.

INTRODUCTION

The Metrology Light Source (the MLS) is the electron storage ring owned by the Physikalisch-Technische Bundesanstalt located in Berlin and dedicated to metrology and technological developments in the spectral ranges from far IR to extreme UV [1]. The main parameters of the MLS are presented in Tab. 1.

Table 1: Main Parameters of the MLS

Parameter	Value
Circumference	48 m
Injection energy	105 MeV
Operation Energy	50 to 629 MeV
Revolution frequency	6.25 MHz
Beam Current	1 pA (1 electron) to 200 mA

The MLS is utilized as a primary source standard and, therefore, PTB has installed and is operating all the equipment required for the measurement of the storage ring parameters required for calculation of the spectral photon flux with high accuracy [2]. The spectral intensity of the synchrotron radiation can be calculated by means of the Schwinger equation [3]. One of the contributors into the spectral power accuracy is the value of the electron beam current, therefore it has to be measured and controlled with a lowest possible uncertainty.

At the MLS the beam current can be varied in the range from 200 mA to 1 pA (a current of a single electron). The current is controlled over the whole range with a good accuracy (typical relative uncertainty < 10^{-2} to 10^{-4}). In this paper the main point of interest is the lower range of the electron beam current (a few nA and less). In this range the accuracy of the current measurement can be significantly improved by counting the exact number of the electrons circulating in the storage ring. Since the revolution frequency of the ring can be measured with high precision (better than 10^{-8}), the electron beam current is also known to this accuracy.

MEASUREMENT OF THE ELECTRON BEAM CURRENT

In the upper range (from 1 mA and more), the current is measured by two commercially available DC parametric current transformers (PCTs, made by Bergoz Instrumentation, France) [4]. The PCTs have a relative uncertainty of about 10^{-4} in this current range.

In the lower ranges the beam current is measured by 4 sets of Si photodiodes (AXUV100 and SXUV100 diodes with 10 mm x 10 mm area, made by Opto Diode Corp.). In each set there are 3 diodes (see Fig. 1) with a different attenuation of synchrotron radiation. The attenuation is made using two different Aluminum filters (3 diodes (D1) with a thick filter (8 μm) cover the range of 20 mA and less, and 3 diodes (D2) with a thin filter (0.8 μm) are used for the range below 0.01 mA. The third type is the unfiltered diode (D3 and D4) which covers the range of low currents (10 nA and less).

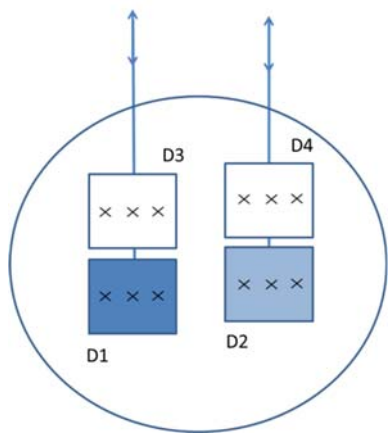

Figure 1: Photodiodes set-up at the MLS.

When the synchrotron light is hitting the diode, it produces a photocurrent which can be amplified, transferred into a voltage and then measured via a volt meter. All filtered diodes and two unfiltered diodes (1 on each set D3 and D4) are connected to Keithley 617 electrometers [5]. The rest of the diodes – 4 unfiltered diodes – are connected to the FEMTO current-voltage converters (I/U) [6] (FEMTO diode) followed by Agilent 34401A [7] a digital voltmeter (DVM), which have better signal to noise ratio than the Keithleys. The diodes connection scheme is presented in Fig. 2.

† yuriy.petenev@helmholtz-berlin.de

Content from this work may be used under the terms of the CC BY 3.0 licence (© 2018). Any distribution of this work must maintain attribution to the author(s), title of the work, publisher, and DOI.

ISBN: 978-3-95450-201-1 doi:10.18429/JACoW-IBIC2018-MOPC04

BEAM CHARGE MEASUREMENT AND SYSTEM CALIBRATION IN CSNS *

W. L. Huang†, F. Li, L.Ma, S. Wang, T. G. Xu
Institute of High Energy Physics, Chinese Academy of Sciences, Beijing 100049, China Dongguan Neutron Source Center, Dongguan 523803, China

Abstract

In China Spallation Neutron Source (CSNS), the beam charge monitors along the ring to the target beam transport line(RTBT) and the ring to the dump beam transport line(RDBT), are consisted of an ICT and three FCTs manufactured by Bergoz. The electronics includes a set of NI PXIe-5160 oscilloscope digitizer, and a Beam Charge Monitor (BCM) from Bergoz as supplementary. The beam charge monitors provide the following information: a) the quantity of protons bombarding the tungsten target; b) the efficiency of particle transportation; c) a T0 signal to the detectors and spectrometers of the white neutron source. With the calibration with an octopus 50Ω terminator in lab and an onboard 16-turn calibrating coils at the local control room, corrections for the introducing the 16-turn calibrating coils and the long cable were made. An accuracy of ±2% for the beam charge measurement during the machine operation has been achieved with the ICT/FCTs and a PXIe-5160 oscilloscope digitizer.

INTRODUCTION

The accelerator and target layout of CSNS and beam instrumentations distributed on the linac , the RCS ring and beam transport lines are presented in Figure 1. After the 50keV H- source, the 4-tank 324MHz drift tube linac (DTL) is designed to accelerate the H- beam from 3MeV to 81MeV, and the H- ions are injected into the RCS ring. During the injection, H- stripping by a carbon primary stripper foil (100μg/cm^2) and a secondary stripper foil (200μg/cm^2) is adopted for this high intensity proton synchrotron [1], then protons are accelerated to 1.6GeV in 20ms by 8 ferrite-loaded RF cavities before extraction [2]. There is an ICT sensor installed at the beginning of RTBT and RDBT beam line, one FCT sensor just in front of the R-dump, one FCT sensor in the mid of bending magnets RTB1 and RTB2 and the third FCT sensor in front of the tungsten target.

Before the installation, two sets of charge measurement methods were utilized for the sensor calibration. During the machine commissioning, the beam charge measurement was calibrated with the extracted particle numbers derived by the beam current measured by DCCT on the RCS ring and the RF frequency (round about 2.44MHz). Then we made a statistics analysis of the beam charge measurement during machine operation. It is showed that a sensitivity of 1.0×10^{10} protrons/pulse and an accuracy of less than ±2% could be achieved in the beam charge measurement.

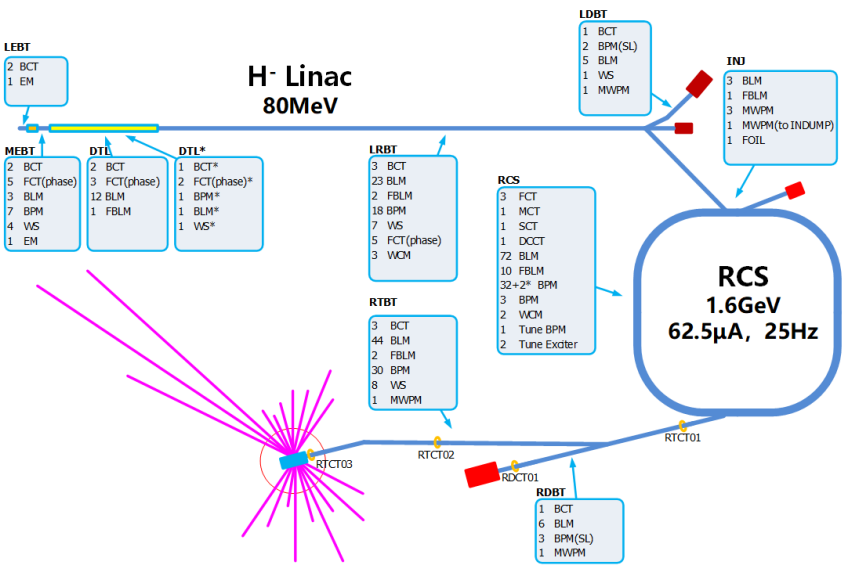

Figure 1: Accelerator and target layout and beam instrumentations of CSNS.

∗Work supported by Special fund for public welfare research and capacity building in Guangdong province, 2016A010102001
† huangwei@ihep.ac.cn

Content from this work may be used under the terms of the CC BY 3.0 licence (© 2018). Any distribution of this work must maintain attribution to the author(s), title of the work, publisher, and DOI.

ISBN: 978-3-95450-201-1 doi:10.18429/JACoW-IBIC2018-MOPC06

Content from this work may be used under the terms of the CC BY 3.0 licence (© 2018). Any distribution of this work must maintain attribution to the author(s), title of the work, publisher, and DOI.

COMPARATIVE MEASUREMENT AND CHARACTERISATION OF THREE CRYOGENIC CURRENT COMPARATORS BASED ON LOW-TEMPERATURE SUPERCONDUCTORS*

V. Tympel†, Th. Stoehlker[1, 2], Helmholtz Institute Jena, 07743 Jena, Germany
M. Fernandes[3, 4], J. Tan, CERN, 1211, Geneva 23, Switzerland
C.P. Welsch[3, 4]
[3]also at Cockcroft Institute, Sci-Tech Daresbury, WA4 4AD, Daresbury, Warrington, UK
[4]Department of Physics, The University of Liverpool, Liverpool, L69 7ZE, UK
H. De Gersem, N. Marsic, W. Müller, Department of Electrical Engineering and Information Technology, TU Darmstadt, 64283 Darmstadt, Germany
D. Haider, F. Kurian, M. Schwickert, T. Sieber,
[1]at GSI Helmholtzzentrum für Schwerionenforschung, 64291 Darmstadt, Germany
J. Golm, R. Neubert[5], F. Schmidl, P. Seidel, Institute of Solid State Physics, 07743 Jena, Germany
M. Schmelz, R. Stolz, Leibniz Institute of Photonic Technology, 07745 Jena, Germany
V. Zakosarenko, Supracon AG, 07751 Jena, Germany
[2]also at Institute for Optics and Quantum Electronics, 07743 Jena, Germany
[5]also at Thuringia Observatory Tautenburg, 07778 Tautenburg, Germany

Abstract

A Cryogenic Current Comparator (CCC) is a non-destructive, metrological-traceable charged particle beam intensity measurement system for the nano-ampere range. Using superconducting shielding and coils, low temperature Superconducting Quantum Interference Devices (SQUIDs) and highly permeable flux-concentrators, the CCC can operate in the frequency range from DC to several kHz or hundreds of kHz depending on the requirement of the application. Also, the white noise level can be optimized down to 2 pA/sqrt(Hz) at 2.16 K.

This work compares three different Pb- and Nb-based CCC-sensors developed at the Institute of Solid State Physics and Leibniz Institute of Photonic Technology at Jena, Germany: CERN-Nb-CCC, optimized for application at CERN Antiproton Decelerator (AD) in 2015 with a free inner diameter of 185 mm; GSI-Pb-CCC, designed for GSI-Darmstadt with a free inner diameter of 145 mm, 1996 completed, 2014 upgraded; GSI-Nb-CCC-XD, designed for the GSI/FAIR-project with a free inner diameter of 250 mm, 2017 completed. The results of noise, small-signal, slew-rate, and drift measurements done 2015 and 2018 in the Cryo-Detector Lab at the University of Jena are presented here.

THE SYSTEM

After 25 years of development the Cryogenic Current Comparator (CCC) has been established as a useful tool for non-destructive and metrological-traceable beam intensity measurement in the nano-ampere range [1]. The principle behind the CCC is to pick up the azimuthal magnetic field of the moving charged particles. Figure 1 shows a superconducting meander structure which shields the non-azimuthal magnetic field components. The following pickup coil, enclosing a highly permeable flux-concentrating core, and the particle beam build up a current-transformer. The very low pickup coil current can be measured, via matching electronics, by a Low-Temperature Superconducting Quantum Interference Device (SQUID). The measured raw voltage of the SQUID electronics can be linked to a corresponding CCC input current using a calibration factor defined with a metrological-traceable calibration current.

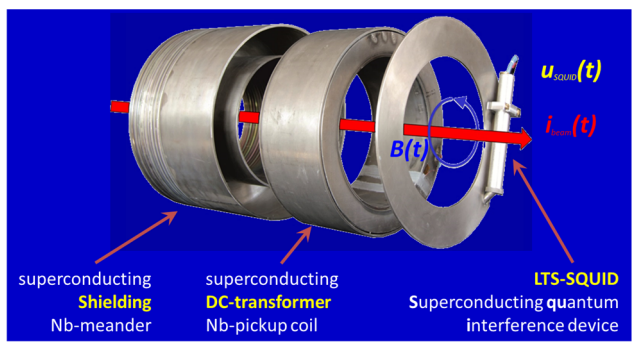

Figure 1: Components and operating principle of the CCC-sensor shown on a niobium-based system before it is assembled.

Measurement Setups

Three CCC sensors (see Table 1) with different dimensions, varying meanders, and core materials were characterized by a setup consisting of a Dynamic Signal Analyzer HP35670A, a Vector Signal Analyzer HP89410A, an Agilent Function / Arbitrary Waveform Generator 33210A and a DAkkS (Deutsche Akkreditierungsstelle)-certified Keithley 2002 Multimeter. The lab measurements are done in a shielded chamber (see Fig. 2, left).

* Work supported by BMBF, project numbers 05P15SJRBA and 05P18SJRB1.
† volker.tympel@uni-jena.de

ISBN: 978-3-95450-201-1 doi:10.18429/JACoW-IBIC2018-MOPC08

Content from this work may be used under the terms of the CC BY 3.0 licence (© 2018). Any distribution of this work must maintain attribution to the author(s), title of the work, publisher, and DOI.

BEAM INTENSITY MONITORING WITH NANOAMPERE RESOLUTION – THE CRYOGENIC CURRENT COMPARATOR (CCC)*

D. M. Haider†, P. Forck, F. Kurian, M. Schwickert, T. Sieber
GSI Helmholtzzentrum für Schwerionenforschung, 64291 Darmstadt, Germany
M. Fernandes, J. Tan, CERN, 1211 Gevena 23, Switzerland
J. Golm[1], F. Schmidl, P. Seidel, FSU Jena, 07743 Jena, Germany
T. Stoehlker[2,3], V. Tympel, Helmholtz Institute Jena, 07743 Jena, Germany
M. Schmelz, R. Stolz, V. Zakosarenko[4], IPHT, 07751 Jena, Germany
H. De Gersem, N. Marsic, TEMF, TU Darmstadt, 64289 Darmstadt, Germany
[1]also at Helmholtz Institute Jena, 07743 Jena, Germany
[2]also at GSI Helmholtz Centre for Heavy Ion Research, 64291 Darmstadt, Germany
[3]also at Institute for Optics and Quantum Electronics, 07743 Jena, Germany
[4]also at Supracon AG, 07751 Jena, Germany

Abstract

The storage of low current beams as well as the long extraction times from the synchrotrons at FAIR require non-destructive beam intensity monitoring with a current resolution of nanoampere. To fulfill this requirement, the concept of the Cryogenic Current Comparator (CCC) based on the low temperature SQUID is used to obtain an extremely sensitive beam current transformer. During the last years CCCs have been installed to do measurements of the spill structure in the extraction line of GSI SIS18 and for current monitoring in the CERN Antiproton Decelerator ring. From these experiences lessons can be learned to facilitate further development. The goal of the ongoing research is to improve the robustness of the CCC towards external influences, such as vibrations, stray fields and He-pressure variations, as well as to develop a cost-efficient concept for the superconducting shield and the cryostat.

INTRODUCTION

In modern accelerator facilities there are many applications, from rare isotopes and antiprotons in storage rings to slow extracted beams for nuclear physics experiments, which require absolute and non-destructive monitoring of ion beams with intensities down to nanoamperes. This need cannot be addressed by standard current diagnostics. Typical AC and DC current transformers are limited to intensities above microamperes. More sensitive devices like Faraday cups or secondary electron monitors (SEM) are at least partially destructive, which limits their application in storage rings, and – in case of the SEM – require elaborate calibration to compensate for aging effects. Although Schottky monitors can provide some current information, they are often not able to reach the desired accuracy at low currents and special care must be taken to calibrate them correctly, especially for their use across large frequency ranges [1].

With the high magnetic sensitivity of a SQUID sensor (Superconducting Quantum Interference Device) the cryogenic current comparator (CCC) expands the detection threshold of the traditional current transformers and can provide absolute, non-destructive current measurements independent of particle species. In the most recent installation at the Antiproton Decelerator (AD) at CERN the CCC has shown a current resolution of 5.8 nA [1] and is actively used as part of the accelerator control system during the commissioning and routine operation. In a clean lab environment, currents down to 1.3 nA with a current noise lower than 3 – 30 pA/√Hz (7 Hz – 100 kHz) can be measured [2]. Furthermore, bandwidths of up to 200 kHz with a slew rate of 0.16 µA/µs are possible [2].

With our work, we aim to further increase the current resolution by improving the stability against electromagnetic and mechanical perturbations. A custom beamline cryostat is designed to minimize interferences as well as to expand the usability by adding a self-sufficient liquid helium cooling cycle. Ultimately, we plan to install a CCC in the storage rings (CRYRING and Collector Ring) and transfer lines of FAIR in order to supply low intensity current data to both the machine experts and users, and thus have a tool to better understand the processes during slow extraction from synchrotrons as well as the physics of low intensity experiments.

In this contribution, we look at the history of the CCC to show possible applications and the problems that we encountered, followed by the latest research to address these challenges. This includes studies toward alternative (coreless) shielding geometries and superconducting materials, as well as the analysis of mechanical resonances of the housing cryostat.

HISTORIC DEVELOPMENTS

The CCC was developed in national standards laboratories to compare extremely small electric currents. One of the first who used the emerging SQUID sensors for current measurements was I.K. Harvey in 1972 [3]: see

* Work supported by the European Union's Horizon 2020 research and innovation programme under the Marie Skłodowska-Curie grant agreement No 721559 as well as by the BMBF with the project numbers 05P15SJRBA and 05P18SJRB1.
† d.haider@gsi.de

ISBN: 978-3-95450-201-1 doi:10.18429/JACoW-IBIC2018-MOPC10

UPGRADE AND IMPROVEMENT OF CT BASED ON TMR

Ying Zhao, Yaoyao Du, Ling Wang, Institute of High Engy Physics. CAS, Beijing, China

Abstract

The CT based on TMR sensor has been developed in the lab. For Improving the accuracy and linearity, reducing the influence of sensor position, a series simulation and calculation have been done which conduct an upgrade both in the mechanical structure and electronics design. Lab test shows good results and test on beam will be carried on soon.

INTRODUCTION

The CT based on TMR sensor's principle is like hall ammeter. Beam pass through a magnetic ring with a gap, a TMR sensor is put in a gap of the ring. The output of the sensor changes with the beam current [1]. The a principle diagram and the whole profile are shown in Figure 1. First test indicate that the resolution and linearity error could not meet the demand, improvement of the magnetic core and electronics design has been done, most details are present in this paper.

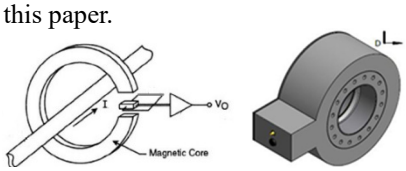

Figure 1: Principle and profile of TMR CT.

STUDY AND IMPROVEMENT OF CORE DESIGN

One of the key parameter that involves the resolution are the core with a cutoff section. The soft alloy which has been processed is used as the magnetic core.The initial permeability is changed, so does other characteristic.

The cutoff section is an air gap,for an toroid core with air gap and ignore the edge flux,a equivalent permeability μ_e can be calculate as below.

$$I_{beam} = \frac{B_{core}}{\mu_0\mu_r} l_{core} + \frac{B_{gap}}{\mu_0} l_{gap} = \frac{B_{core} l_{core}}{\mu_0\mu_r}(1 + \frac{\mu_r l_{gap}}{l_{core}})$$

$$\mu_e = \frac{1}{\frac{1}{\mu_r} + \frac{l_{gap}}{l_{core}}}$$

l_{core} is average core circumference $2\pi r_{core}$ (r_{core}=(r_{out}+ r_{in})/2, r_{out} and r_{in} are outer and inner radius of the core), l_{gap} is length of the air gap. When μ_r is large enough, the μ_e is related to the l_{gap} and l_{core}. It means the core magnetic permeability is decreased and linearized.

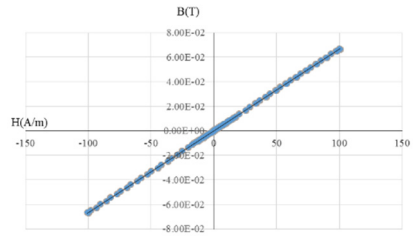

Figure 2: Magnetization curve test result of the core with air gap.

The magnetization curve of the core with air gap is test in the lab as shown in Figure 2. The magnetization curve with air gap can be seen as the synthesis of magnetization characteristic of the core and air gap. The air gap reduces the remanence and the core saturation.It also means most of the loss is garthered in the gap instead of the core.

High frequency signal brings hysteresis loss. If the magnetic core cross section area is A_{core},, the exciting signal are u(t) and i(t). As indicate in Figure 3, the area A_1 of $-B_r$ ->S -> B_m -> - B_r, means the exciting signal varies from zero to the maximum, in the half period T/2 ,the total energy can be calculate below:

$$\int_{\alpha}^{\alpha+\frac{T}{2}} u(t)i(t)dt = \int_{-B_r}^{B_r} A_{core}\frac{dB}{dt} Hl_{core}dt$$

The area A_2 from S to B_m is the part of recoverable energy. The energy of the core loss is proportional to the area around the hysteresis loop, is related to the area of A_1-A_2. With air gap the A_1-A_2 is small enough to be ignored.[2]

$$A_{core}l_c(\int_{-B_r}^{B_s} HdB - \int_{B_s}^{B_r} HdB) = A_{core}l_c(A_1 - A_2)$$

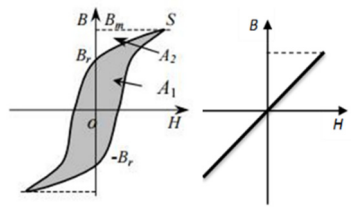

Figure 3: Magnetization curve without (left) and with (right) air gap.

Primary design and test result shows that output resolution is influenced by sensor's position and angle in the gap. Focusing on how to uniform the magnetic field distribution doesn't show effective improvement. As the sensing area is 2mm much smaller than the gap section area 20mm x 20mm, gathering the magnetic field is a feasible option. A perpendicular cutoff is made to reduce the cross section as shown in the Figure 4. The gap section area is 10mm x 20mm after this improvement.

Content from this work may be used under the terms of the CC BY 3.0 licence (© 2018). Any distribution of this work must maintain attribution to the author(s), title of the work, publisher, and DOI.

ISBN: 978-3-95450-201-1 doi:10.18429/JACoW-IBIC2018-MOPC11

DATA ACQUISITION SYSTEM FOR BEAM INSTRUMENTATION OF SXFEL AND DCLS*

Y.B. Yan†, Y.B. Leng, L.W. Lai, L.Y. Yu, W.M. Zhou, J. Chen, H. Zhao, C.L. Yu
Shanghai Synchrotron Radiation Facility (SSRF)
Shanghai soft X-ray Free-Electron Laser facility (SXFEL)
Shanghai Institute of Applied Physics, Chinese Academy of Sciences
Shanghai 201204, P.R. China

Abstract

The high-gain free electron lasers have given scientists hopes for new scientific discoveries in many frontier research areas. The Shanghai X-Ray Free-Electron Laser (SXFEL) test facility is commissioning at the SSRF campus. The Dalian Coherent Light Source (DCLS) has successfully commissioned in the northeast of China, which is the brightest vacuum ultraviolet free electron laser facility. The data acquisition system for beam instrumentation is based on the EPICS platform. The field programmable gate array (FPGA) and embedded controller are adopted for the signal processing and device control. The high-level applications are developed using Python. The details of the data acquisition system will be reported in this paper.

OVERVIEW

The Shanghai soft X-ray Free-Electron Laser facility (SXFEL) is being developed in two steps, the SXFEL test facility (SXFEL-TF) and the SXFEL user facility (SXFEL-UF). The SXFEL-TF is a critical development step towards the construction a soft X-ray FEL user facility in China, and is under commissioning at the Shanghai Synchrotron Radiation Facility (SSRF) campus. The test facility is going to generate 8.8 nm FEL radiation using an 840 MeV electron Linac passing through the two-stage cascaded HGHG-HGHG or EEHG-HGHG (echo-enabled harmonic generation, high-gain harmonic generation) scheme, as shown in Figure 1. The construction of the SXFEL-TF started at the end of 2014. Its accelerator tunnel and klystron gallery were ready for equipment installation in April 2016. The installation of the SXFEL-TF Linac and radiator undulators were completed by the end of 2016. In the meantime, the SXFEL-UF, with a designated wavelength in the water window region, began construction in November 2016. It was based on upgrading the Linac energy to 1.5 GeV, and the building of a second undulator line and five experimental end-stations. It is scheduled to be open to users in 2019[1].

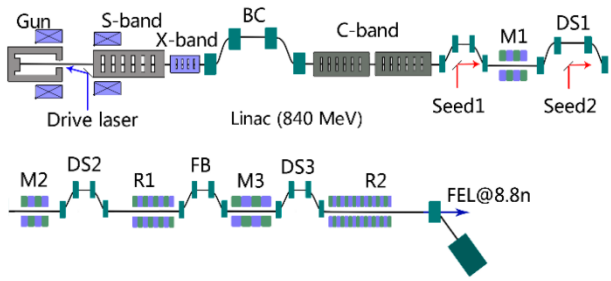

Figure 1: Schematic layout of the SXFEL-TF.

The Dalian coherent Light Source (DCLS) is a FEL user facility, which can deliver world's brightest FEL light in the energy range from 8 to 24 eV, making it unique of the same kind that only operates in the Vacuum Ultra Violet (VUV) region. It use a 300MeV Linac to produce fully coherent photon pulses in the wavelength range between 50-150nm by HGHG scheme. This project was launched at the beginning of 2012, and has successfully commissioned by the end of 2016. It was a close collaboration between the scientists and engineers from Dalian Institute of Chemical Physics and Shanghai Institute of Applied Physics, two institutes of Chinese Academy of Sciences.

The data acquisition system for beam instrumentation is a part of the SXFEL and DCLS control system, which is based on the EPICS (Experimental Physics and Industrial Control System) platform. The system architecture is shown in Figure 2. The FPGA (Field Programmable Gate Array) and embedded controller (such as Raspberry Pi, BeagleBone Black) are adopted for the signal processing and device control. The high-level applications are developed using Python.

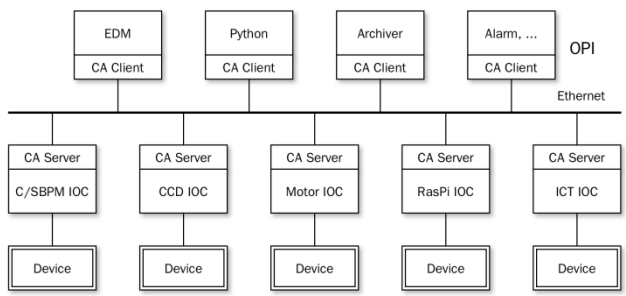

Figure 2: Data acquisition system architecture for beam instrumentation.

* Work supported by the National Development and Reform Commission (NDRC) and the National Natural Science Foundation of China (NSFC)
† yanyingbing@sinap.ac.cn

Content from this work may be used under the terms of the CC BY 3.0 licence (© 2018). Any distribution of this work must maintain attribution to the author(s), title of the work, publisher, and DOI.

ISBN: 978-3-95450-201-1 doi:10.18429/JACoW-IBIC2018-MOPC12

THE RADIAL DETECTOR IN THE CYCLOTRON OF HIMM

Min Li[1], Shenpeng Li[2], Xincai Kang[1,3],Weilong Li[1,4], Ruishi Mao[1], Haihong Song[1], Tiecheng Zhao[1], Yucong Chen[1], Yonggan Nie[1],Yongchun Feng[1,3], Yan Yin[1], Yanmou Wang[1], Weinian Ma[1].
[1]Institute of Modern Physics, Chinese Academy of Science, Lanzhou 730000, China;
[2]Lanzhou Kejintaiji Corporation, LTD, Lanzhou 730000, China
[3]Lanzhou University of Technology, Lanzhou 730050, China
[4]University of Chinese Academy of Sciences, Beijing 100049, China

Abstract

The cyclotron is designed as the injector of the Heavy Ion Medical Machine (HIMM) in Wuwei city, China. It provides 10 uA carbon beams to fulfill the requirement of the accumulation in the following synchrotron. The Radial detector is used to measure the beam current and beam turn motion in this Cyclotron. The beam current signal gathered by radial detector is acquired by four picoammeters, meanwhile the beam time structure is measured with FPGA and real time operating system. This paper introduces the design of radial detector, the motion control and data acquisition system for it of the cyclotron.Finally, the beam current and turn pattern measurement results at HIMM are presented in this paper.

INTRODUCTION

The first Heavy Ion Medical Machine (HIMM) has passed the registration tests and now enters the clinical trials phase which was constructed at the Institute of Modern Physics, China [1]. A compact cyclotron is designed as the injector of a synchrotron which forms the HIMM, and it accelerates the $^{12}C^{5+}$ from ion source to 7.0MeV/u, meanwhile the extracted beam current is more than 10uA [2].

As its compact structure of the cyclotron, there are 2 radial probes installed on the hill and in the valley respectively of Cyclotron. The one installed in the valley is used to monitor the beam current during the injection period, and the other one installed between the extraction deflector and extraction dipole is used to monitor the extraction beam current. Furthermore, the beam centre measurement can be done with the two targets during the acceleration period. The radial probe installed on the hill is shown in Fig.1. And for each radial probe, it is driven with a servo motor. The moving distance of the radial probe is 795 mm.

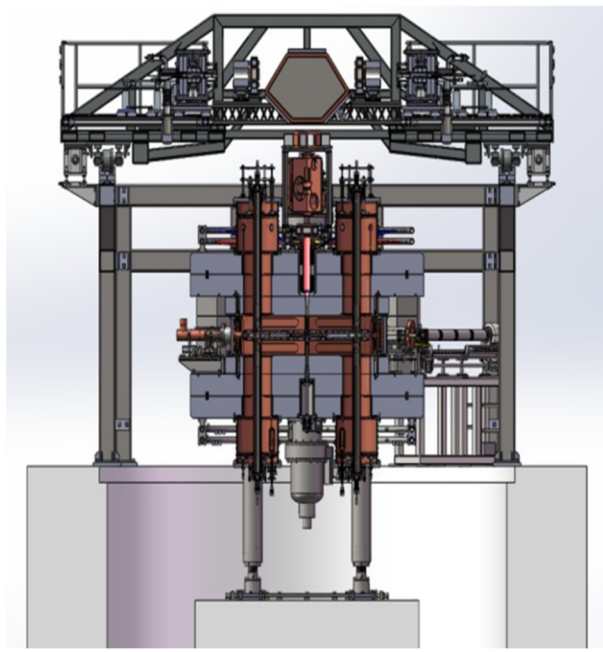

Figure 1: Radial probe installed on the Cyclotron.

DESIGN OF RADIAL PROBE

Mechanical Design

The radial probe target tip, making up by one integral block and 3 differential fingers which are distributed concurrently in the horizontal direction, measure the beam distribution on axial and radial directions by blocking the beam [3]. The 3 differential fingers are distributed uniformly in the vertical direction with the gap of 5mm. The sizes of the integral and differential target tips are listed in table 1.The radial probe target tips are made by copper. The top view of the radial probe is displayed in Fig.2 and the target probe structure is shown in Fig.3.

Table 1: The Size of Four Fingers

Finger Name	Size(mm)
Integral Finger	40
Differential Top	10
Differential Middle	10
Differential Bottom	10

Content from this work may be used under the terms of the CC BY 3.0 licence (© 2018). Any distribution of this work must maintain attribution to the author(s), title of the work, publisher, and DOI.

ISBN: 978-3-95450-201-1 doi:10.18429/JACoW-IBIC2018-MOPC14

THE DESIGN OF DOSE PARAMETER ACQUISITION AND CONTROL SYSTEM FOR A PENCIL BEAM SCANNING SYSTEM IN HUST-PTF*

Y.Y. Hu, P. Tan†, Y.J. Lin, X.Y. Li, Y.C. Yu, H. Lei, H.D. Guo
State Key Laboratory of Advanced Electromagnetic Engineering and Technology,
School of Electrical and Electronic Engineering,Huazhong University of Science and Technology,
Wuhan 430074, China

Abstract

Pencil beam scanning (PBS) technology is a flexible and accurate dose delivery technology in proton therapy, which can deliver beams adapting to irregularly shaped tumors, while it requires precise diagnostic and real-time control of the beam dose and position. In this paper，a dose parameter acquisition and control system for the pencil beam scanning system based on the EPICS and LabVIEW is designed for HUST-PTF. The EPICS environment is built to realize the data exchange function between the front-end devices and control system. A channel access server（CAS）is designed to convert treatment parameters into the process variables (PVs) and expose them to the network for data sharing. Under current experimental conditions, the simulated beam current is generated according to the dose parameters in the treatment plan file. The current are processed by a digital electrometer and transmitted to the EPICS database in real time. Then the control system user interface based on LabVIEW is realized for displaying and parameter analysis.

INTRODUCTION

The pencil beam scanning nozzle is located at the end of the proton therapy machine in Huazhong University of Science and Technology Proton Therapy Facility (HUST-PTF). It is composed of scanning magnets, ionization chambers and other beam diagnostic equipment as well as related electronic devices and controllers. It is the last guarantee to accurately deliver the proton beam to the designated location of the tumor with accurate dose. This paper mainly focuses on the technology of controlling dose safety, and the dose parameter acquisition and control system has been designed by using software and hardware redundancy analysis.

Firstly, the dose monitoring system of the nozzle needs to obtain the treatment plan accurately from the Treatment Control System (TCS), extract the scan dose parameter, convert it into the actual machine parameters correctly, and confirm and display these data. Then, the control software needs to transmit data with the front-end devices efficiently. It sends the corresponding instrument parameters to the hardware devices in the nozzle accurately and gets feedback data, so as to control and monitor the beam dose accurately in real time. At the same time, fast interlocking protection can be carried out under exceptional conditions.

* Work supported National Key R&D Program of China (No.2016YFC0105308).
† Corresponding author, tanping@mail.hust.edu.cn

As the main equipment for dose monitoring, two separate working ionization chambers are designed as redundant measures to ensure that the ionization chamber operates normally all the time. And the alarm threshold of the second ionization chamber is set to be 5% larger than that of the first device to ensure that when the first ionization chamber fails, the other device can still work normally, and the fault signal can be transmitted to the superior system.

In order to make the operation of the control system more intuitive and convenient, the graphical user interface (GUI) of the system is built with the LabVIEW development platform. The interface displays treatment plan parameters, actual treatment data, treatment progress, the working status of front-end devices and so on.

Finally, the treatment results are uploaded to the TCS when the treatment is finished. Also, if treatment is interrupted, the dose already applied must be uploaded in order to allow correct continuation after interruption. The corresponding framework of the control system is shown in Fig.1.

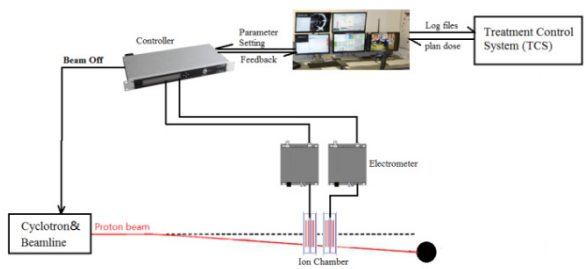

Figure 1: Control system framework.

LOGICAL DESIGN OF THE SYSTEM

Before the start of treatment, the first step is to accurately analyse the treatment plan file and obtain the ideal dose parameters. In order to ensure the safety of the transmission and correct interpretation of the treatment plan file, the DICOM standard data format is uniformly used for data interaction throughout the whole treatment process. The essence of the DICOM file is the binary file. Each data element contains four parts: Tag (Data element Identification)、VR (Value Representation)、 VL (Value Length)、VF (Value Field) [1].By identifying the Tag of the dose parameter, the data element of planned dose parameter can be extracted out. Dose parameters are stored in VF part in hexadecimal from. Then we convert them to

Content from this work may be used under the terms of the CC BY 3.0 licence (© 2018). Any distribution of this work must maintain attribution to the author(s), title of the work, publisher, and DOI.

ISBN: 978-3-95450-201-1 doi:10.18429/JACoW-IBIC2018-MOPC16

THE DEVELOPMENT AND APPLICATIONS OF DIGITAL BPM SIGNAL PROCESSOR ON SSRF *

L.W. Lai, Y.B. Leng†, Y.B. Yan, W.M. Zhou, F.Z. Chen, N. Zhang
SSRF, SINAP, Shanghai, China

Abstract

The development of Digital BPM Signal Processors (DBPM) for SSRF started from 2008. The first prototype for SSRF storage ring was completed in 2012, with turn-by-turn resolution better than 1μm. From 2016 to 2017, SSRF successively constructed two FEL facilities in China, DCLS and SXFEL test facilities. The second version DBPM was developed and used in large scale during this period to meet the requirements of signal processing for stripline BPMs and cavity BPMs. After that, we turned to the development of DBPM for SSRF storage ring based on the second version hardware, including FPGA firmware, EPICS IOC, EDM control panel. The development was completed and tests were carried out in early 2018. Test results showed that the position data is accurate and can monitor beam movement correctly, and online turn-by-turn position data resolution reaches 0.46μm. This paper will introduce the design of DBPM for the SSRF storage ring and the tests carried out to verify the data accuracy and evaluate the system performance.

INTRODUCTION

SSRF is the first 3rd-generation synchrotron light source built in China, which came into service in 2009. The circumference of the storage ring is 432 meters, and the ring contains 20 cells that can serve up to 40 beamlines. The 499.654 MHz RF system produces 720 buckets of which typically 500 contain charge distributed in 4 bunch trains to minimize ion accumulation. There are 7 BPM electronics in each cell totaling more than 140 sets Libera BPM electronics around the ring measuring the beam orbit for beam control and feedback.

SSRF started the development of Digital BPM Processor (DBPM) in 2008. A first version prototype was developed in 2012 for the SSRF storage ring[1]. Later a second version DBPM hardware was developed in 2016[2,3], which was more compact and more versatile. The new DBPM was first used on two FEL facilities, DCLS and SXFEL, in large scale. The development of new SSRF DBPM based on the new version hardware was taken from that design.

Table 1 lists the DBPM requirements based on considering accelerator performance and current technical level. After years of on and off development and improvement, a second version DBPM was developed and tested on SSRF this year.

*Supported by The National Science Foundation of China (Grant No.11375255, 11575282); The National Key Research and Development Program of China (Grant No. 2016YFA0401990, 2016YFA0401903).
† lengyongbin@sinap.ac.cn

Table 1: DBPM Requirements

Requirements	Value
ADC	4 channels, 16bits
Central Frequency	499.654MHz
Sampling clock	External/internal
Sampling rate	117.2799MHz
Turn-by-turn rate	693.964kHz
Trigger	External/internal/period
Signal processing	FPGA
Data	ADC/TBT/FA/SA
Resolution	~1μm@TBT
OS	ArmLinux
Control	EPICS

FIRMWARE AND SOFTWARE DESIGN

The DBPM was designed to provide position data at five different rates, including raw ADC data, turn-by-turn data, 50kHz fast acquisition (FA) data, 10kHz FA data, 10Hz slow acquisition (SA) data. Figure 1 shows the DBPM signal processing diagram, with the processing including four steps, and data rate reduced after each step. Position data is read out in small scale streaming mode or large scale capture mode.

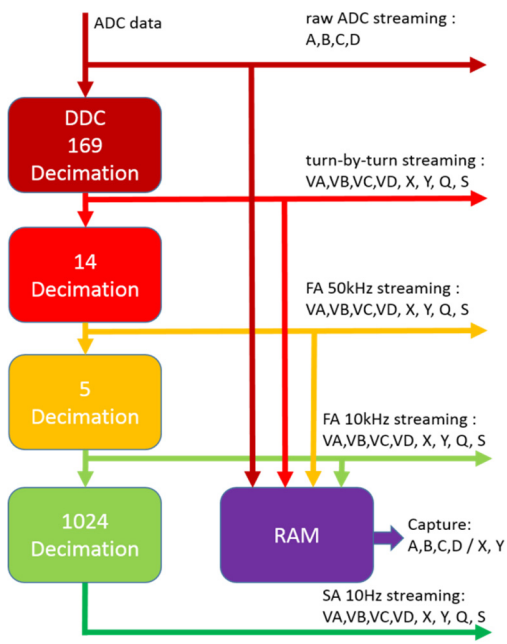

Figure 1: DBPM signal processing diagram.

Content from this work may be used under the terms of the CC BY 3.0 licence (© 2018). Any distribution of this work must maintain attribution to the author(s), title of the work, publisher, and DOI.

ISBN: 978-3-95450-201-1 doi:10.18429/JACoW-IBIC2018-MOPC17

ON-LINE CROSSTALK MEASUREMENT AND COMPENSATION ALGORITHM STUDY OF SXFEL DIGITAL BPM SYSTEM*

F. Z. Chen†[1], Y. B. Leng‡, J. Chen[1], L. Y. Yu, L. W. Lai, R. X. Yuan, T. Wu[1]
Shanghai Institute of Applied Physics, Chinese Academy of Sciences, 201800 Shanghai, China
[1]also at University of Chinese Academy of Sciences, 100049 Beijing, China

Abstract

Shanghai soft X-ray Free Electron Laser (SXFEL) has acquired the custom designed Digital BPM processor used for signal processing of cavity BPMs and stripline BPMs. In order to realize monitor the beam position accurately, it has high demand for DBPM system performance. Considering the crosstalk may introduce distortion and influence beam position resolution, it is important to analyze and compensate the crosstalk to improve the resolution. We choose the CBPM signal to study the crosstalk for its narrowband and sensitive for phase position. The main experiment concept is successive accessing four channels to form a signal transfer matrix, which including amplitude frequency response and phase response information. And the compensation algorithm is acquire four channel readouts, then using the signal transfer matrix to reverse the true signal to ensure the accurate beam position measurement. This concept has already been tested at SXFEL and hopeful to compensate the crosstalk sufficiently.

BACKGROUND

SXFEL

SXFEL is one of the high-gain FELs constructed in China. Key technologies have been tested through prototype developments. Based on the research and development prototype of hard X-ray FEL. The construction of the user facility in soft XFEL has already finished. The SXFEL facility consists of an electron injector with a thermionic cathode, main accelerate section including C-band high-gradient accelerators along with S-band accelerators, and in-vacuum undulators. Figure 1 is SXFEL undulator layout [1, 2].

SXFEL is designed to generate a coherent x-ray beam using a self-amplified spontaneous emission (SASE) process. In order to meet the harsh demands, the beam diagnostic system achieving high precision resolution is one of the most important technical issues. Cavity BPM meets the hash demands for the precise measurement of the resolution of the SXFEL undulators system. Figure 2 is the picture of one Cavity BPM installed in the tunnel.

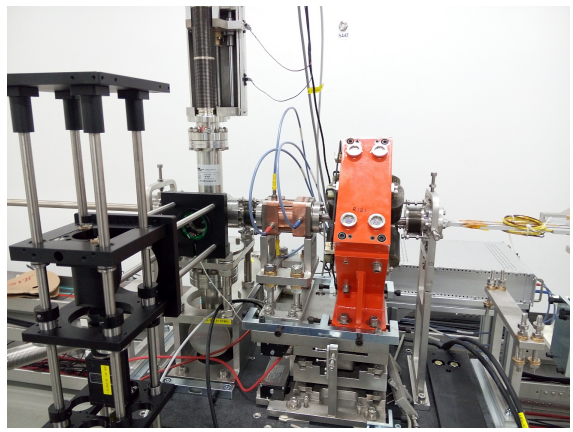

Figure 2: Cavity BPM installation spot picture.

Cavity BPM CBPM is a key beam instrumentation component for SXFEL beam diagnostics. As the requirement of undulator should reach sub-micron level position resolution. The high Q cavity BPM. As the key beam diagnostics tool, BPM systems are widely equipped in all kinds of accelerators. Cavity Beam Position Monitors are main beam diagnostic instruments in SXFEL. There are more than 20 CBPM conducted in SXFEL used for the measurement and adjustment of beam orbit. Moreover, the sum of four SBPM electrodes signal can also apply in relative beam charge measurement. RF cable extract beam signal from CBPM pickup, RF front-end module modulated signal to proper amplitude, then led the signal to digital BPM processor.

* Work supported by National Science Foundation of China (No.11375255)
† chenfangzhou@sinap.ac.cn
‡ lengyongbin@sinap.ac.cn

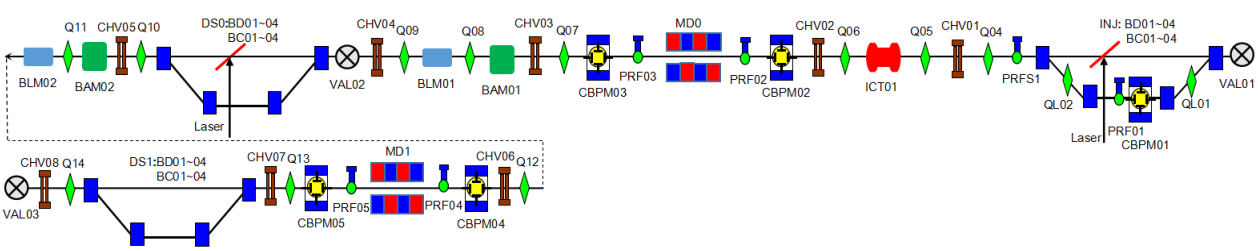

Figure 1: Partial layout of SXFEL undulator.

Content from this work may be used under the terms of the CC BY 3.0 licence (© 2018). Any distribution of this work must maintain attribution to the author(s), title of the work, publisher, and DOI.

ISBN: 978-3-95450-201-1 doi:10.18429/JACoW-IBIC2018-MOPC18

DEVELOPMENT OF AN EXPERT SYSTEM FOR THE HIGH INTENSITY NEUTRINO BEAM FACILITY AT J-PARC

K. Nakayoshi*, K. Sakashita, Y. Fujii, T. Nakadaira,
High Energy Accelerator Research Organization (KEK), Tsukuba, Japan

Abstract

A high intensity neutrino beam is utilized by a long-baseline neutrino oscillation experiment, T2K at J-PARC. To generate a high intensity neutrino beam, a high intensity proton beam is extracted from a 30GeV Main Ring Synchrotron (MR) to the neutrino primary beamline. In the beamline, one mistaken shot can potentially do serious damage on the beamline equipment. To avoid such a consequence, many beamline equipment interlocks to stop the beam operation are implemented. Once an interlock is activated, prompt and proper error handling is necessary. We are developing a beamline expert system for prompt and efficient understanding of the status to quickly resume the beam operation. The beamline expert system consists of three components such as a data collection component, inference engines and a result presenting component. The data collection component continuously collects the beamline information and the inference engines infer beamline status from the beamline monitor data. Finally the result presenting component presents the inferred results. The inference engines are a key component in the expert system. We are developing a Machine-Learning(ML) based inference engine for our expert system. ML is one of the most active research fields in computing, we adopt the technology from it. We report the progress of development of the expert system, especially the prototype of ML based inference engine.

INTRODUCTION

The T2K (Tokai-to-Kamioka) experiment [1] is a long-baseline neutrino oscillation experiment at J-PARC (Japan Proton Accelerator Research Complex). A high intensity neutrino/anti-neutrino beam is produced and propagates 295 km from J-PARC to Super-Kamiokande. In August 2017, T2K excluded CP-conservation at 95% confidence level using the data until April 2017. In order to keep generating interesting physics, steady operation of the facility is very important.

Figure 1 shows a layout of the neutrino experimental facility (neutrino facility). The neutrino facility is composed of the primary/secondary beamline and a near detector (ND280). In the primary beamline, the high intensity proton beam is extracted from the Main Ring synchrotron (MR) and guided through super/normal conducting magnets to the target station. In the secondary beamline, the proton beam hits a graphite target and produces pions. These pions decay into muons and muon neutrinos in a decay volume. The high intensity proton beam reached 485 kW in 2018. The MR plans to upgrade the beam power up to 1.3MW.

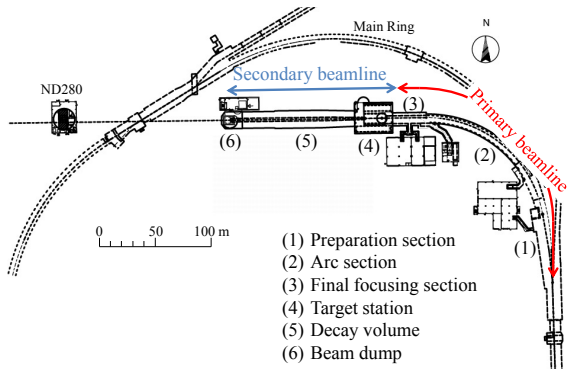

Figure 1: Layout of the T2K experimental facility.

MOTIVATION

We handle a high intensity proton beam at the neutrino facility. In the beamline, one mistaken shot can potentially do serious damage to the beamline equipment. To avoid such a consequence, a lot of beamline equipment interlocks, called MPS (Machine Protection System) to stop the beam operation are implemented. We have more than 800 interlock sources. Multiple sources can cause an interlock at the same time. For example, many BLM (Beam Loss Monitors) sometimes issue an interlock simultaneously. In that case, it is difficult for the beamline operators to understand quickly what happened in the beamline and these can lead to a time loss of the beamline operation.

When an essential beamline equipment fails, it may take a long time to restore the beam operation. For example, a helium compressor in the helium circulation system at the target station was broken in January 2017. We lost about two weeks of the beam time due to this trouble.

To improve these situations, we plan to introduce a beamline expert system to the neutrino facility.

BEAMLINE EXPERT SYSTEM

Figure 2 shows a schematic diagram of the beamline expert system. The beamline expert system consists of three components such as a data collection component, inference engines and a result presenting component. The data collection component continuously collects beamline information and the inference engines infer the beamline status from

* kazuo.nakayoshi@kek.jp

Content from this work may be used under the terms of the CC BY 3.0 licence (© 2018). Any distribution of this work must maintain attribution to the author(s), title of the work, publisher, and DOI.

ISBN: 978-3-95450-201-1 doi:10.18429/JACoW-IBIC2018-MOPC19

VIRTUAL SIGNAL SPECTRUM ANALYZER DEVELOPMENT BASED ON REDPITAYA AND EPICS FOR TUNE MEASUREMENT IN BEPC-II

Y.H Lu†, J. He, BEPCII, IHEP, 100049 Beijing, P. R. China

Abstract

An independent tune measurement system was developed in BEPCII using Direct Diode Detect (3D) technique. The system includes two diagonal electrode signals of a set of BPMs, a self-designed board based on Direct Diode Detect (3D) technique, and a commercial spectrum analyzer. For replacement of the commercial spectrum analyzer and integrated to the central EPICS system, an EPICS device driver is developed based on the EPICS base and ASYN module support, using an open source digital electronics Red Pitaya and its software "Spectrum". According to the application requirements of tune measurement in BEPCII, the device driver finds the frequency point and power value corresponding to the X&Y tune between 631 to 874 kHz. The spectral resolution is 119 Hz. An EPICS IOC is built and run on Red Pitaya for accessing the device driver. A CSS-based user interface shows the signal's power spectra and the tune frequency directly.

INTRODUCTION

The betatron tune is one of the most important parameters of the storage ring, especially for colliders. It plays a crucial role in brightness optimization. At present, the tune measurement system in BEPCII [1] can only be monitored when the beam betatron oscillation amplitude is large enough due to its sensitivity problem. In order to solve the defect, a high-sensitivity tune measurement system based on a diode peak hold circuit is under development and being teseted, which is refered to as Direct Diode Detection (3D) tune measurement system. An original 3D tune measurment system was developed by Marek Gasior originally in CERN according to the work of predecessors [2, 3].

The 3D tune measurement system requires a spectrum analyzer to perform spectrum observation. And its results are expected to be integrated to the central control system EPICS and database system of BEPCII. The commercial spectrum analyzers are usually expensive, and the integration with the central control system cannot be achieved easily for non-open-source.

This paper presents development of a virtual spectrum analyzer for the 3D tune measurement system in BEPCII. It is based on a digital electronics platform named Red Pitaya [4] with an embedded linux operating system on it. An API for BEPCII 3D tune measurement is developed firstly based on the open source code "Spectrum" of Red Pitaya, allowing users to survey frequencies corresponding to the X&Y tunes of the collider. Then, an EPICS driver support for spectrum analyzer is written, based on ASYN [5], redpitaya-epics [6] and the API source code. An EPICS IOC for 3D tune measurement system is built and tested with a CSS-BOY interface.

† luyh@ihep.ac.cn, BI Group, Accelerator Centre, IHEP

HARDWARE ARCHITECTURE

The hardware architecture of 3D tune measurement system is demonstrated in Fig. 1. Signals from the two BPM diagonal pickups, with main frequency range 499.8±1.262MHz, are processed by the 3D tune measurement electronics, and then transferred to an EPICS virtual spectrum analyzer running on the Red Pitaya board. The graphical user interface was developed using CSS (Control System Studio) which executes on a remote PC, which located in the same LAN (Local Area Network) with the Red Pitaya board.

Red Pitaya is built around a Xilinx Zynq-7010 SoC processor combined with an FPGA. The board has two 14 bits ADCs with sampling rates up to 125MHz and a SD-Card slot for holding a Linux operating system. Spectrum Analyzer turns Red Pitaya into a 2-channel DFT Analyzer, with frequency span from DC up to 62.5MHz.

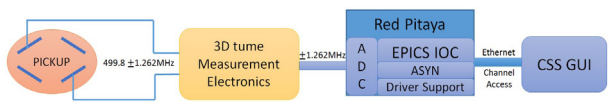

Figure 1: The hardware architecture of the 3D tune measurement system for BEPCII.

SPECTRUM ANALYZE API FOR BEPCII 3D TUNE MEASUREMENT

All Red Pitaya applications are web-based and do not require any software configurations on the remote PC. Users can access APIs via a web browser (such as Firefox). Red Pitaya is known for its open source, but the spectrum analyzer API that is currently in use is spectrumPro. The original open source code of spectrum analyzer API we use is outdated and written in the C language and is independent of the present header files like rp.h which are responsible for data interaction with the DDR3 memory.

To solve "Application Not Loaded" problem when access the spectrum Analyzer API, lots of debug statements are added to the C source code. Then according to error or warning messages in the debug.log file, the API can be accessed remotely via a web browser after many "nignx [7]: worker process: symbol lookup error" errors are excluded.

Data sampled and initially processed by Red Pitaya is located in the internal storage area of Zynq, and its storage depth is limited to 16×1024×14 bits. However, considering the problems of network traffic and data refresh rates on the web browser, the spectrum analyzer extracts

Content from this work may be used under the terms of the CC BY 3.0 licence (© 2018). Any distribution of this work must maintain attribution to the author(s), title of the work, publisher, and DOI.

ISBN: 978-3-95450-201-1 doi:10.18429/JACoW-IBIC2018-TUOA01

THE DIAGNOSTIC SYSTEM AT THE EUROPEAN XFEL: COMMISSIONING AND FIRST USER OPERATION*

D. Nölle†, DESY, 22603 Hamburg, Germany
on behalf the European XFEL Diagnostic Team

Abstract

The European XFEL is now commissioned and user operation has started. Long bunch trains up to 500 bunches are established. The role of and experience with the electron beam diagnostic will be reported. Highlights, problems and their solutions will be discussed

INTRODUCTION

The European XFEL (Fig. 1) is an X-ray free-electron-laser based light source with soft and hard X-ray beamlines that will finally provide intense radiation from about 0.25 to 25 keV at TW level with pulse durations of a few 10 fs [1].

The length of the facility is about 3.5 km and the accelerator tunnel is crossing below inhabited areas in the city of Hamburg. It offers 5 photon tunnels ending in a big experimental hall. In the current configuration two hard X-ray FELs and one soft X-Ray FEL are in operation. The FELs are driven by a superconducting accelerator based on TESLA technology [2] with up to 17.5 GeV electron beam energy. The long RF pulse of 650 µs allows to accelerate up to 2700 bunches per RF pulse. With a repetition rate of 10 Hz this corresponds to up to 27000 X-ray pulses per second that can be distributed between the different undulator lines to allow for simultaneous operation of experiments.

Only 9 months after the cool down of the superconducting accelerator and initial beam commissioning first user experiments started. The total operation time in 2017 was about 7000 h. Currently the facility is mainly operated at 14 GeV with 1 – 60 bunches per RF pulse and photon energies around 9.3 keV, based on the users demands.

Up to now two photon beamlines served by the hard X-ray FEL device SASE1 are in operation and have started their user program. The soft X-ray FEL SASE3 driven by the spend electron beam of SASE1 is lasing routinely at photon energies around 900 eV and the commissioning of the photon beamline is in an advanced state. The user program of this beamline will start in fall 2018. The second hard X-ray FEL SASE2 is also lasing. Even lasing with all 3 devices in parallel was already demonstrated.

During special tests a photon energy range of 7.2 to 19.3 keV was easily achieved by tuning the gaps of the variable gap undulators. In test runs an average power of the X-ray beam of up to 6 W, running a bunch train of 500 bunches per RF pulse, as well as the design energy of 17.5 GeV have already been demonstrated.

LAYOUT OF THE FACILITY

The accelerator has an injector located in a separate vault. It consists of the normal conducting gun, one accelerating module of the TESLA type and a 3.9 GHz module [3] for phase space linearization, a laser heater system [4], followed by a diagnostic section. This installation was completed and commissioned one year before the main LINAC, so that most essential parts of almost all systems could be commissioned during this time [5, 6].

From the injector the beam is fed to the main accelerator tunnel. The accelerator is laid out with a 3 stage bunch compression and bunch compressors B0 at 130 MeV, B1 at 700 MeV and the final stage B2 at 2.4 GeV. The stages are separated by the LINAC systems L1 and L2, consisting of 4 and 12 accelerator modules, respectively. At 700 MeV and 2.4 GeV the compressors include diagnostic sections; the high energy one is equipped with a transverse deflecting system (TDS) for longitudinal phase space diagnostics [7]. After bunch compression to a few 10 fs, the beam is accelerated in the main LINAC build out of 80 accelerator modules. The RF system is designed such, that one RF station serves four modules.

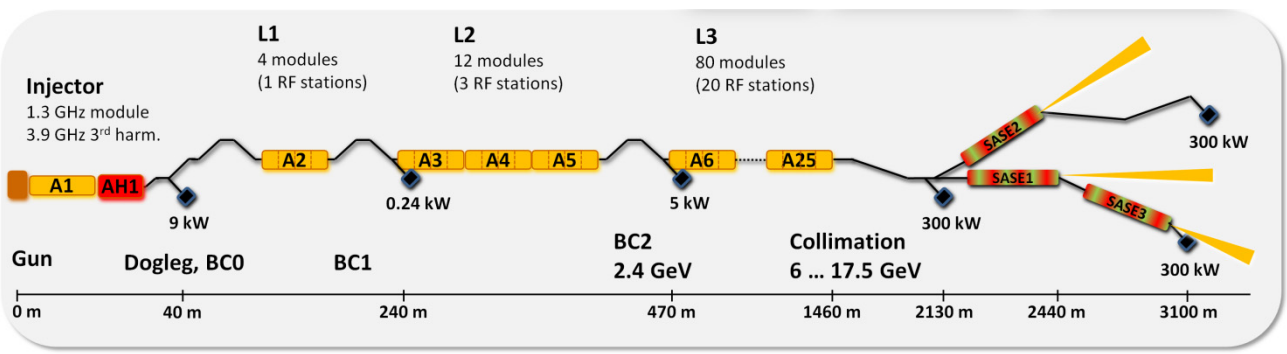

Figure 1: Block Diagram of the EXFEL.

* Work supported by the respective funding agencies of the contributing institutes; for details please see http:\\www.xfel.eu
† dirk.noelle@desy.de

Content from this work may be used under the terms of the CC BY 3.0 licence (© 2018). Any distribution of this work must maintain attribution to the author(s), title of the work, publisher, and DOI.

ISBN: 978-3-95450-201-1 doi:10.18429/JACoW-IBIC2018-TUOA02

APPLICATION OF MACHINE LEARNING TO BEAM DIAGNOSTICS

E.Fol†, J. Coello de Portugal, R. Tomas, CERN, CH-1211, Geneva, Switzerland
†also at Johann Wolfgang Goethe-University Frankfurt, 60323 Frankfurt am Main, Germany

Abstract

Machine learning (ML) techniques are widely used in science and industry as a powerful tool for data analysis and automation. Currently, in accelerator physics ML is represented as a young research field, demonstrating mixed results in the latest attempts. The presented work is devoted to exploration of appropriate ML methods for beam diagnostics. The target is to provide an overview of ML techniques which can be applied to improve beam diagnostics and general accelerator performance. Besides the results of ML tools currently used in modern accelerators and evaluation of these tools, we also demonstrate possible concepts with the potential for further investigation and give recommendations on efficient use of ML techniques in accelerators.

HISTORICAL MOTIVATION

Traditional Optimization Techniques

Various optimization problems arise in modeling and operation of accelerators. Multi-parameter optimization can be performed using well established methods such as simplex, as it was shown at KEKB [1] applied on minimization of vertical emittance in injector linac. Another examples for the application of simplex as optimization technique for accelerators can be found in [2], where the method was applied on tuning of beam delivery system in CLIC simulations.

Linear optics corrections using optimization algorithms to find a minimum beam size with multi-parameter knobs as input were performed already in 1993 [3]. Luminosity maximization and beam lifetime are typical multivariate optimization tasks also in circular colliders [4, 5].

For light sources, such methods as random-walk optimization are being used to reduce the vertical beam size [6]. Also online optimization using various measures of accelerator performance as objective functions is being successfully applied in operation [7]. An illustrating example towards applying ML is the development of machine based optimization using genetic algorithms, which have been used as well in accelerator design [8–10].

Limitations of Traditional Methods

The described examples demonstrate successful performance of traditional optimization tools in applications on linear optics corrections and problems with limited amount of optimization targets. Bigger challenges emerge when diagnostics of complex non-linear behavior is required and several variables have to be taken into account as final objective. The amount of time and computational power required by traditional methods might become unacceptable for future accelerators such HE-LHC and FCC. The main limitation of traditional optimization methods is that the objective function or specific rules and thresholds have to be known. In opposite, Machine learning (ML) methods can learn from given examples without requiring explicit rules.

RELEVANT MACHINE LEARING CONCEPTS

ML techniques aim to build computer programs and algorithms that automatically improve with experience by learning from examples with respect to some class of task and performance measure, without being explicitly programmed [11].

Depending on problem and existence of learning examples, different approaches are preferred. If pairs of input and desired output are available, an algorithm can generalize the problem from the given examples and produce prediction for unknown input. ML algorithms that learn from input/output pairs are called *supervised learning* algorithms. Opposite to supervised learning, *unsupervised learning* algorithms solve the tasks where only input data is known. Unsupervised learning is suitable for the problems such anomaly detection, signal denoising, pattern recognition, dimensionality reduction and feature extraction. In the following a brief overview on significant machine learning concepts that can be used as supervised as well as unsupervised approaches is presented.

Artificial Neural Network

Artificial Neural Networks (ANNs) are well suited for learning tasks, where data is represented by noisy, complex sensor signals and the target output function may consist of several parameters. A basic ANN consists of a single processing unit (*neuron*), that takes the *weighted* inputs and an additional activation function to introduce the nonlinearity in the output. For more complex practical problems, ANNs are composed of several interconnected *hidden layers* with multiple neurons stacked.

ANNs can be used for both regression and classification problems. In case of classification the output can be either a class label or a probability of an item belonging to a class. The learning of ANN is performed using *backpropagation* algorithm [12] on a set of examples. For each example the training algorithm computes the derivatives of the output function of the network. The obtained gradients with respect to all weights are then used to adjust the weights in order to achieve a better fit to the target output. In backpropagation *stochastic gradient descent* or one of its improved extensions Adam [13] and AdaGrad [14] is applied as optimization method in order to minimize the loss between the network output values and the target values for these outputs by updating the connection weights.

Content from this work may be used under the terms of the CC BY 3.0 licence (© 2018). Any distribution of this work must maintain attribution to the author(s), title of the work, publisher, and DOI.

ISBN: 978-3-95450-201-1 doi:10.18429/JACoW-IBIC2018-TUOB02

OPTICS MEASUREMENTS IN STORAGE RINGS: SIMULTANEOUS 3-DIMENSIONAL BEAM EXCITATION AND NOVEL HARMONIC ANALYSIS

L. Malina[1], J. Coello de Portugal, J. Dilly, P. K. Skowroński and R. Tomás,
CERN, Geneva 23, Switzerland
[1] also at University of Oslo, 0316 Oslo, Norway

Abstract

Optics measurements in storage rings employ turn-by-turn data of transversely excited beams. Chromatic parameters need measurements to be repeated at different beam energies, which is time-consuming. We present an optics measurement method based on adiabatic simultaneous 3-dimensional beam excitation, where no repetition at different energies is needed. In the LHC, the method has been successfully demonstrated utilising AC-dipoles combined with RF frequency modulation. It allows measuring the linear optics parameters and chromatic properties at the same time without resolution deterioration. We also present a new accurate harmonic analysis algorithm that exploits the noise cleaning based on singular value decomposition to compress the input data. In the LHC, this sped up harmonic analysis by a factor up to 300. These methods are becoming a "push the button" operational tool to measure the optics.

INTRODUCTION

One of the ways to perform optics measurements in a storage ring is to excite the beam and acquire turn-by-turn (TbT) beam position monitor (BPM) data showing the coherent betatron motion [1]. The beam is excited using either kickers or AC-dipoles [2]. AC-dipoles can ramp up and down the oscillation adiabatically [3], i.e. without any measurable emittance growth. Typical optics measurements consist of several excitations at different beam energies, in order to measure the linear optics as well as the chromatic properties.

Based on the experience with optics measurements in the LHC, there are two main time-consuming tasks during the measurements. First, the human intervention to change beam energy by adjusting the RF-frequency and check other beam parameters, which usually takes up to 15 minutes. Second, the AC-dipole needs about 70 seconds to cool down after every single excitation. Addition of longitudinal excitation [4] can be used to speed up the measurement when performed adiabatically.

In the analysis process, TbT BPM data is first cleaned of noise using methods [5–7] based on Singular Value Decomposition (SVD). The SVD of a matrix $\mathbf{A}$ is given by: $\mathbf{A} = \mathbf{USV}^{\mathbf{T}}$. Cleaning keeps only the modes corresponding to the largest singular values, in this way it improves precision and accuracy. It also reduces the amount of information without changing the size of the data, typically about a factor 40 larger than the reduced $\mathbf{U}$, $\mathbf{S}$ and $\mathbf{V}^{\mathbf{T}}$ matrices.

Later the harmonic analysis is performed on cleaned TbT data BPM by BPM (further reffered to as "bpm" method). The Discrete Fourier Transform (DFT) is obtained performing Fast Fourier Transform (FFT). The refined frequency of the strongest signal obtained from FFT is found using Jacobsen frequency interpolation with bias correction [8] based on 3 DFT peaks. The refined complex amplitude of the signal is obtained as an inner product of a unit signal corresponding to the refined frequency with the TbT data. This signal is subtracted from the TbT data and the whole procedure starting with FFT is repeated [9], typically 300 times in the LHC. As a result the TbT data is approximated by the sum of the 300 strongest harmonics.

The framework presented here implements new methods to also increase the speed of harmonic analysis by its combination with precedent data cleaning.

ADIABATIC BEAM EXCITATION

In the LHC, the beam is excited using AC-dipoles in both transverse directions simultaneously. This gives the BPM reading as shown in Figure 1, for one of the planes. Once the beam energy is changed the measurement is repeated. This time-consuming process can be avoided by fast modulation of RF-frequency. RF-frequency change is normally used to adjust the beam energy, or it is modulated in order to measure the chromaticity. However, the frequency of the modulation for the chromaticity measurement is typically about 0.1 Hz, such that the Base-Band Tune (BBQ) system [10] can measure the tune.

We employ the RF-modulation at its maximal frequency of 5 Hz, which is still far from the natural synchrotron frequency of about 20 Hz. The RF-frequency modulation is ramped up before the actual AC-dipole excitation starts. Three periods of adiabatic energy variation (forced synchrotron oscillation) fit within acquired 6600 turns (with LHC's revolution frequency of 11.3 kHz). A sample of TbT reading at a dispersive BPM is shown in Figure 2.

The adiabaticity of this mode of excitation has been experimentally demonstrated in the LHC, as it can be seen from the beam size measurement from Beam Synchrotron Radiation Telescope (BSRT) during the 3-dimensional (3D) excitations shown in Figure 3.

Content from this work may be used under the terms of the CC BY 3.0 licence (© 2018). Any distribution of this work must maintain attribution to the author(s), title of the work, publisher, and DOI.

ISBN: 978-3-95450-201-1 doi:10.18429/JACoW-IBIC2018-TUOB03

Content from this work may be used under the terms of the CC BY 3.0 licence (© 2018). Any distribution of this work must maintain attribution to the author(s), title of the work, publisher, and DOI.

DEMONSTRATION OF A NEWLY DEVELOPED PULSE-BY-PULSE X-RAY BEAM POSITION MONITOR IN SPring-8*

Hideki Aoyagi†, Yukito Furukawa, Sunao Takahashi, Atsuo Watanabe
Japan Synchrotron Radiation Research Institute (JASRI), Hyogo, Japan

Abstract

A newly designed pulse-by-pulse X-ray beam position monitor (XBPM), which is photoemission type, has been demonstrated successfully in the SPring-8 synchrotron radiation beamline. Conventional XBPMs work in the direct current (DC) mode, because it is difficult to measure a beam position in the pulse mode under the severe heat load condition. The key point of the design is aiming at improving heat-resistance property without degradation of high frequency property. This monitor is equipped with microstripline structure for signal transmission line to achieve pulse-by-pulse beam position signal. A photocathode is titanium electrode that is sputtered on a diamond heat sink to achieve high heat resistance. We have manufactured the prototype, and demonstrated feasibility at the SPring-8 bending magnet beamline. As a result, we observed a unipolar single pulse with the pulse length of less than 1 ns FWHM and confirmed that it has pulse-by-pules position sensitivity. Furthermore, this monitor can be also used in the DC mode with good stability and good resolution. The operational experience will be also presented.

INTRODUCTION

Development of a pulse-by-pulse X-ray beam position monitor (XBPM) aiming at measuring every isolated pulses for insertion devise (ID) beamline of the synchrotron radiation facility SPring-8 is being advanced. Conventional XBPMs used widely are photoemission type, and blade-shaped tungsten is usually employed as a detector head to raise heat-resistance [1]. However, it is impossible to measure the beam position of every isolated pulses with the conventional XBPMs, because of long time constant of the current signal and ringing due to stray capacitance and impedance mismatch. Therefore, we tried to settle this problem by adopting polycrystalline diamond as a heat sink to improve the heat resistance, and downsized detector heads to reduce the stray capacitance [2]. In addition, the microstripline structure [3-6] is adopted in the vacuum chamber of the monitor to prevent attenuation and reflection of the unipolar single pulse.

DESIGN AND MANUFCTURE

The pulse-by-pulse XBPM that we have been developing is photoemission type in the same way as the conventional XBPMs, and having four blade-shaped diamond heat sinks with titanium plated electrodes (detector heads) in top/bottom and right/left near the beam axes to measure the beam position in horizontal and vertical directions. The detector heads are inclined by 1/20 against the beam axis to be irradiated mainly on the unilateral side of the blade. As a result, photoemission can be controlled efficiently with the applied voltage of the charge collecting electrodes (collectors).

Figure 1 (a) shows a photograph of diamond heatsinks mounted on the water-cooling base. According to the thermal finite element analysis [7, 8], the thermal contact conductance between the heat sink and the cooling holder needs to be $>10^4$ W/(m^2·K). Therefore, indium foils of the 50μm thickness are inserted between them to improve the thermal contact conductance. Figure 1 (b) shows a photograph of a signal transmission line with microstripline structure, which is mounted on an ICF70 flange. According to the high frequency properties test, the time domain reflectometry using the pilot model of the detector head has been performed in advance. It was confirmed that the unipolar single pulse of sub-nanosecond can be obtained [7, 8].

Figure 2 shows a 3D image of the combination of the detector head (Fig. 1 (a)) and the microstripline structure (Fig. 1 (b)). The structure of the pulse-by-pulse XBPM is shown in Fig. 3. The shading mask is mounted directly on the upstream side of the 6-way cross-chamber to prevent the cooling base from irradiation. By arranging a pair of collectors on both sides of left and right of the detector heads, photoelectron emitted from the detector heads can be attracted or retarded according to the polarity of the collector. In the direct current (DC) mode operation, in the same way as the conventional XBPM, current signal can be stabilized by applying the voltage, which is usually +100 V. In the pulse-mode operation, the negative voltage is applied to retard the emission of low energy photoelectron that distort the pulse waveform.

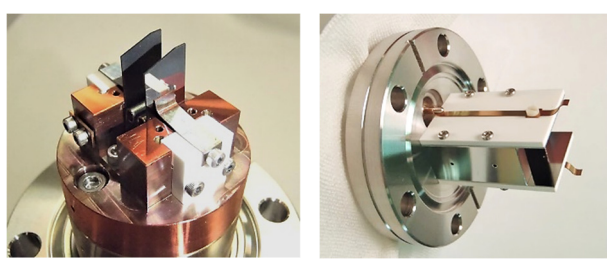

(a) (b)

Figure 1: (a) Photograph of diamond heatsinks (20 mm × 8 mm × 0.3 mm). (b) Photograph of signal transmission lines with microstripline structure.

* This work was partly supported by Japan Society for the Promotion of Science through a Grant-in-Aid for Scientific Research (c), No. 20416374 and No. 18K11943.
† aoyagi@spring8.or.jp

ISBN: 978-3-95450-201-1 doi:10.18429/JACoW-IBIC2018-TUOB04

Content from this work may be used under the terms of the CC BY 3.0 licence (© 2018). Any distribution of this work must maintain attribution to the author(s), title of the work, publisher, and DOI.

A VERTICAL PHASE SPACE BEAM POSITION AND EMITTANCE MONITOR FOR SYNCHROTRON RADIATION

N. Samadi* , University of Saskatchewan, S7N 5E5 Saskatoon, Canada
L. Dallin, Canadian Light Source, S7N 2V3 Saskatoon, Canada
D. Chapman[1], Canadian Light Source, S7N 2V3 Saskatoon, Canada
[1]also at University of Saskatchewan, S7N 5E5 Saskatoon, Canada

Abstract

We report on a system (ps-BPM) that can measure the electron source position and angular motion at a single location in a synchrotron bend magnet beamline using a combination of a monochromator and an absorber with a K-edge to which the monochromator was tuned in energy. The vertical distribution of the beam was visualized with an imaging detector where horizontally one part of the beam was with the absorber and the other part with no absorber. The small range of angles from the source onto the monochromator crystals creates an energy range that allows part of the beam to be below the K-edge and the other part above. Measurement of the beam vertical location without the absorber and edge vertical location with the absorber gives the source position and angle.

Measurements were made to investigate the possibility of using the ps-BPM to correct experimental imaging data. We have introduced periodic electron beam motion using a correction coil in the storage ring lattice. The measured and predicted motions compared well for two different frequencies.

We then show that measurement of the beam width and edge width gives information about the vertical electron source size and angular distribution.

INTRODUCTION

The stability of the photon beam which is dependent on the stability of the electron source in a synchrotron is critical and essential to the performance of the machine and the beamlines. It is becoming a more important issue as fourth generation storage rings are planned and coming alive and as many other facilities are upgrading their existing rings. The fourth-generation light sources are pushing to very low emittance, so the stability of the electron beam becomes increasingly important as it has a direct effect on the emittance of the machine.

The vertical position of the photon beam at some distance from the source is determined by the vertical position and angle of the electron beam.

We have developed a method to measure the vertical position and angle of the synchrotron electron beam at a single location in a bend magnet beamline at the Canadian Light Source (CLS). The discovery of this system came during an imaging experiment at the Biomedical Imaging and Therapy (BMIT) beamline [3-5] at CLS [1]. Normally to measure the beam angle, two measurements of the beam position at two separated distances from the source are required. This is a difficult task in a beamline due to both lack of space and presence of many beamline optics and components that will interfere with the location and operation of beam position monitors.

The system we have developed relies on measurements of the photon beam profile with and without an absorption edge filter and at the same location in the beamline. In the initial experiments a Bragg type (reflection geometry) Double Crystal Monochromator (DCM)[2] was used to prepare the photon beam at an energy of the filter's absorption edge.

In this paper we present the implementation and results of a system using (1) a single Laue monochromator setup which is compact and is less susceptible to beam power loading and thus energy drift. We have used this system to assess the ability to (2) measure periodic beam motion with the future intent of (3) using these measurements both to show some of the temporal features of the system and to use the beam position and angle measurements to correct experimental imaging data.

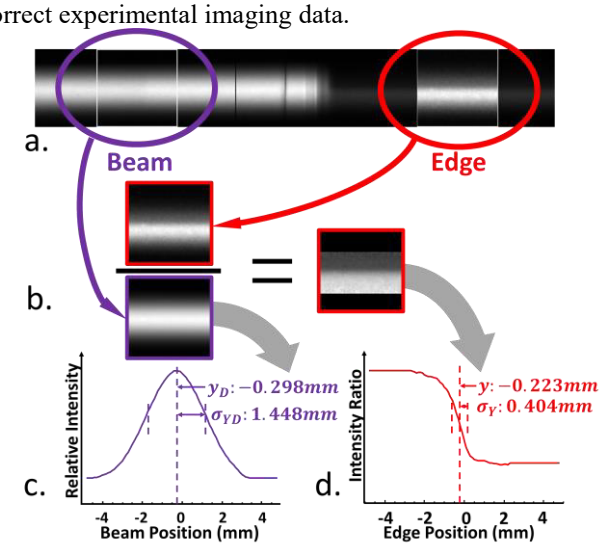

Figure 1:: Beam and edge data (a) plus schematic representation of the data analysis steps (b,c,d).

Synchrotron

The vertical photon distribution of a bend magnet or wiggler synchrotron beam can be well fitted with a Gaussian function for photon energies what are well above the critical energy of the device (see Fig. 1c where the Gaussian center and width are shown). In our case, the critical energy of the CLS bend is 7.57keV and the absorption edge of the iodine filter is 33.17keV. Figure

* email address Nazanin.Samadi@usask.ca

ISBN: 978-3-95450-201-1 doi:10.18429/JACoW-IBIC2018-TUOC01

INTEGRATION OF A PILOT-TONE BASED BPM SYSTEM WITHIN THE GLOBAL ORBIT FEEDBACK ENVIRONMENT OF ELETTRA

G. Brajnik*, S. Bassanese, G. Cautero,
S. Cleva, R. De Monte, Elettra-Sincrotrone Trieste, Trieste, Italy

Abstract

In this contribution, we describe the advantages of the pilot tone compensation technique that we implemented in a new BPM prototype for Elettra 2.0. Injecting a fixed reference tone upstream of cables allows for a continuous calibration of the system, compensating the different behaviour of every channel due to thermal drifts, variations of cable properties, mismatches and tolerances of components. The system ran successfully as a drop-in substitute for a Libera Electron not only during various machine shifts, but also during a user dedicated beamtime shift for more than 10 hours, behaving in a transparent way for all the control systems and users. The equivalent RMS noise (at 10 kHz data rate) for the pilot tone position was less than 200 nm on a 19 mm vacuum chamber radius, with a long-term stability better than 1 µm in a 12-hour window. Two main steps led to this important result: firstly, the development of a novel RF front end that adds the pilot tone to the signals originated by the beam, secondly, the realisation of an FPGA-based double digital receiver that demodulates both beam and pilot amplitudes, calculating the compensated X and Y positions.

INTRODUCTION

Like many other lightsources, also Elettra (the Italian synchrotron) is planning its upgrade to Elettra 2.0, a low emittance machine. To obtain the promised figures of merit (high stability, reduced emittance, etc. [1,2]), these new generation machines need several beam diagnostics improvements. In particular, for what concerns electron beam position monitors (eBPMs), the following features are mandatory: nanometer-scale accuracy, long-term stability, reduced current dependence, compensation of different channel behaviours.

Previous experiences in developing analog front end have shown that eBPMs based on pilot tone compensation can fulfil most of these requirements [3,4]. So, we decided to go one step further to demonstrate its usefulness in a real environment, firstly with the realisation of an FPGA-based double digital receiver that demodulates both beam and pilot amplitudes and calculates the compensated beam positions, secondly with the integration of this system in the Elettra Global Orbit Feedback (GOF), replacing a Libera Electron during the normal machine operation.

ELECTRON BPM PROTOTYPE

In order to have maximum flexibility and to compensate the different channel behaviours, including the cables, a modular approach that allows to place the front end in service area is essential. The modules are essentially two, the RF analog front end and the FPGA-based Digital Receiver.

Improved Analog Front End

The front end is similar to the one presented at IBIC 2016 [4], but enhanced and re-engineered in a more compact solution. In the present version the low-noise PLL has been integrated in the box (Fig. 1), together with diagnostic functionalities (voltage and temperature sensors) and complete Ethernet control. Figure 2 illustrates the block diagram of the front end, with the following elements:

1. low-pass filter;
2. high reverse-isolation combiner for the pilot tone;
3. band-pass filter;
4. variable attenuator;
5. low-noise amplifier;
6. splitter;
7. low-noise PLL for the pilot tone generation.

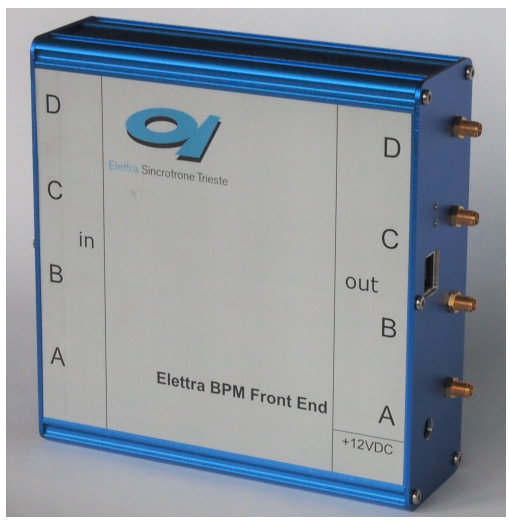

Figure 1: Elettra eBPM analog front end.

FPGA-based Digital Receiver

In the previous publications [4, 5] we described an in-house assembled digitiser (based on Linear Technology LTC2209 ADCs and Altera Stratix III FPGA) developed for first tests of the system, catching only the raw ADC data and transmitted via an Ethernet link thanks to an FPGA. The major limitation of that approach was the off-line processing with the FFT technique. To overcome this issue, the FPGA code has been completely rewritten, implementing a parallel double digital receiver.

* gabriele.brajnik@elettra.eu

Content from this work may be used under the terms of the CC BY 3.0 licence (© 2018). Any distribution of this work must maintain attribution to the author(s), title of the work, publisher, and DOI.

ISBN: 978-3-95450-201-1 doi:10.18429/JACoW-IBIC2018-TUOC03

COMMISSIONING OF THE OPEN SOURCE SIRIUS BPM ELECTRONICS

D. O. Tavares*, G. B. M. Bruno, S. R. Marques, L. M. Russo, H. A. Silva, LNLS, Campinas, Brazil

Abstract

Sirius is a 3 GeV 4th generation circular light source designed to achieve an emittance of 0.25 nm·rad [1]. During the early stages of the machine design, the BPM electronics was selected as one of the projects to be developed by the LNLS team. This paper will report on the manufacturing and deployment processes of the referred electronics as well as the achieved reliability and performance.

INTRODUCTION

All units of the Sirius BPM Electronics have been manufactured and are currently being prepared for deployment in the machine. In total, 21 BPM racks will be deployed along the accelerator, of which 20 racks are dedicated to booster's and storage ring's electron BPMs, white photon beam BPMs and fast orbit feedback, and 1 rack is dedicated to transfer lines BPMs. A 22nd BPM rack will be kept in the Beam Diagnostics laboratory as a homologation rack for repairs and new developments . Not included in this list are the Linac BPM electronics, which were supplied by SINAP as part of a turnkey Linac contract. They will not be covered in this paper.

SIRIUS BPM ELECTRONICS

As shown in Fig. 1 the assembly of a BPM rack is composed of the following parts: (i) one 12-slot MicroTCA.4 crate; (ii) several RF Front-End (RFFE) modules, one per BPM; (iii) one 24-port Ethernet switch; (iv) one isolated AC/DC linear power supply serving the RFFE modules; (v) RF coaxial cables between RFFE modules and digitizer boards; (vi) Ethernet cables for RFFEs and crate.

The MicroTCA.4 crate is populated with modular FPGA carrier boards following PICMG AMC [2] and VITA FMC [3] standards, each of them playing the role of either a timing receiver, a 4-channel RF signals digitizer or a 4-channel digital picoammeter, depending on the I/O mezzanine modules attached to it. In the future, an additional crate slot will be used as fast orbit feedback (FOFB) processor and fast orbit correctors' power supply, for which multi-gigabit optical I/O mezzanines and an open hardware 10 kHz bandwidth linear power supply rear-transition module (RTM) will be employed.

The RFFE is an Ethernet-controlled analog front-end module providing the following core functions to the BPM system: (i) low-pass filtering of high accelerator RF frequency harmonics; (ii) 2x2 switching of diagonally opposed BPM antenna signals, with optional RF switches temperature stabilization; (iii) narrow band-pass filtering to avoid aliasing of revolution harmonics to the baseband; (iv) RF signals amplification with digitally controlled gain.

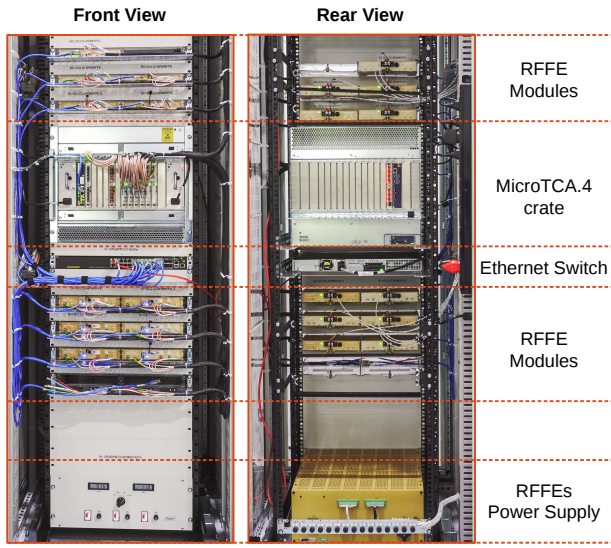

Figure 1: BPM rack layout.

Following ESRF's and Soleil's approach [4], the signals from the BPM pick-ups will be brought to the electronics by delay-matched cable assembly with (160 ps peak-to-peak error), composed of four LMR195 coaxial cables extruded within a common encapsulation, aiming at minimizing the position drifts caused by unequal thermal variations of cables' characteristics. This is a critical part of the system, since such drifts could not be calibrated by the RFFEs switching scheme. Cables lengths vary from 25 m to 70 m.

Another bundle of cables connect the 4 RFFE RF outputs and switching clock signal input to the digitizer's 4 ADC RF inputs and trigger output of one BPM, respectively. The 4 RF cables are also delay-matched with peak-to-peak error below 20 ps. They are double-shielded 2 m long RG316 coaxial cables providing more than 100 dB isolation.

The digitizer sampling clock is generated in each FMC ADC module and is synchronized with the accelerator's master oscillator by means of a timing receiver in the crate [5]. A reference clock is delivered by the timing receiver and sent to all BPM digitizers through one of the MicroTCA.4 backplane's low jitter clock line.

Each RFFE is controlled via Ethernet (TCP/IP) by the crate CPU. They are physically connected to the rack's Ethernet switch but logically isolated from the accelerator's control network by means of Virtual LANs. Only the crate CPU has access to the RFFE IP addresses of the corresponding rack. The AMC FPGA boards are in turn accessed via PCI Express. The BPM EPICS IOC of each BPM run in the crate CPU and publish the BPM PVs to the control network.

The BPM project followed an open source design philosophy aiming at facilitating collaboration with other institutes [6]. The RFFEs, RF digitizers, FPGA carrier and

* daniel.tavares@lnls.br

Content from this work may be used under the terms of the CC BY 3.0 licence (© 2018). Any distribution of this work must maintain attribution to the author(s), title of the work, publisher, and DOI.

ISBN: 978-3-95450-201-1 doi:10.18429/JACoW-IBIC2018-TUOC04

DEVELOPMENT OF BEAM POSITION MONITOR FOR THE SPring-8 UPGRADE

H. Maesaka†, RIKEN SPring-8 Center, 679-5148 Sayo, Hyogo, Japan
H. Dewa, T. Fujita, M. Masaki, S. Takano[1], Japan Synchrotron Radiation Research Institute, 679-5198 Sayo, Hyogo, Japan
[1]also at RIKEN SPring-8 Center, 679-5148 Sayo, Hyogo, Japan

Abstract

A precise and stable beam position monitor (BPM) system has been developed for the low-emittance upgrade of SPring-8. The requirements for the BPM system are: (1) a single-pass resolution of 100 μm rms for a 100 pC single-bunch and an electric center accuracy of 100 μm rms for the initial beam commissioning to achieve the first turn, (2) a closed-orbit distortion (COD) resolution better than 0.1 μm rms for a 100 mA stored beam and a position stability of less than 5 μm to maintain a photon beam axis. We designed a button electrode and a BPM block and produced some prototypes for performance evaluation. The development of readout electronics based on the MicroTCA.4 standard and the evaluation of a commercial electronics have also been conducted. The prototype BPM system was installed to the present SPring-8 storage ring to confirm the performance with an actual electron beam. We obtained sufficient signal intensity, electric center accuracy, position resolution, position stability, etc. by the beam test. Thus, the new BPM system is almost ready for the SPring-8 upgrade.

INTRODUCTION

SPring-8 has a low-emittance upgrade plan of the storage ring, SPring-8-II, to provide much more brilliant X-rays to users [1]. The beam energy is lowered to 6 GeV from the current 8 GeV and the lattice is changed to 5-bend achromat (5BA). As a result, the emittance is ~140 pm rad without radiation damping of insertion devices (IDs) and further reduced to ~100 pm rad by radiation damping of IDs, while the emittance of the present storage ring is 2.4 nm rad. The X-ray brilliance below 60 keV is expected to be more than 20 times higher than the present SPring-8 ring. In order to utilize brilliant X-rays, it is quite important to maintain the optical axis well within its intrinsic divergence by stabilizing the electron beam orbit. In addition, the beam orbit must be aligned to the magnetic center of each quadrupole or sextupole magnet at the commissioning stage to achieve the first beam storage, since the dynamic aperture of the new ring is narrower than the amplitude of closed orbit distortion caused by alignment error of magnets. Therefore, the resolution and the accuracy of the single-pass BPM measurement is crucial.

For the stability of the optical axis, the tolerances of the source point and the direction of X-rays are approximately 1 μm and 1 μrad, respectively, since the electron beam size is 28 (H) x 6 (V) μm^2 std. and since the divergence of X-rays is 5 (H) x 17 (V) μrad^2 std. for 10 keV photon energy. Thus, we set the closed-orbit distortion (COD) mode BPM stability to 5 μm peak-to-peak for 1 month. In this case, the angular stability of 1 μrad can be expected, because the distance between the two BPMs at the both ends of a straight section for an insertion device is 5 m.

For beam commissioning, the beam must be steered within a narrow dynamic aperture of approximately 10 (H) x 2 (V) mm^2. The required single-pass (SP) position resolution is 100 μm std. for a 100 pC single-bunch. Furthermore, the electric center of each BPM must be aligned within 100 μm std. (±200 μm max.) with respect to the magnetic center of an adjacent quadrupole magnet.

In order to satisfy these requirements, we designed a button BPM electrode, BPM block and readout electronics. Some prototypes of BPM components were produced and some of them have been tested with an actual electron beam at the present SPring-8 storage ring. In this article, we describe design of the BPM system, evaluation of prototypes, result of beam test, etc.

DESIGN AND BASIC PERFORMANCE OF THE BPM SYSTEM

BPM Electrode and Block

We took the following things into account for the design of a BPM electrode and block.

- Sufficient signal intensity for the SP-mode.
- Small heat generation by trapped modes etc.
- Nonmagnetic materials not to distort the field of adjacent magnets.
- Same cross-section as the vacuum chamber to be connected.

As a result, we designed a BPM electrode and block, as illustrated in Fig. 1.

Button electrodes are arranged on 20 mm-wide flat surfaces on the top and bottom of the vacuum chamber with a vertical aperture of 16 mm. The button diameter was set to 7 mm and the horizontal span of the electrodes was to 12 mm in order to obtain a signal as large as possible and to fit the electrodes to the flat top. Each electrode is inserted into the hole with 8 mm diameter, and hence the gap between the hole and the electrode is 0.5 mm. A cooling water channel is equipped with the block so as to suppress the temperature rise due to an electron beam.

We selected molybdenum for the material of the electrode. Since molybdenum has a good electric and thermal conductivity, the heat generation due to trapped modes can be reduced and the temperature rise can be sup-

† maesaka@spring8.or.jp

Content from this work may be used under the terms of the CC BY 3.0 licence (© 2018). Any distribution of this work must maintain attribution to the author(s), title of the work, publisher, and DOI.

ISBN: 978-3-95450-201-1 doi:10.18429/JACoW-IBIC2018-TUPA01

PIN DIODE IN A MEDICAL ACCELERATOR – A PROOF OF PRINCIPLE AND PRELIMINARY MEASUREMENTS

A. Pozenel[1], M. Eichinger, S. Enke, M. Furtinger, C. Kurfurst, M. Repovz
EBG MedAustron, 2700 Wr. Neustadt, Austria

Abstract

The MedAustron Ion Therapy Center located south of Vienna, Austria, is a cancer treatment facility utilizing a particle therapy accelerator optimized for protons and carbon ions. The beam is injected into the synchrotron, accelerated to the desired speed and extracted to be guided into one of four irradiation rooms. During extraction a certain amount of particles is lost which is measured with a PIN diode. In this paper the measurement method of this system is presented, as well as some measurement attempts documented.

INTRODUCTION

MedAustron is a therapy center capable of both offering cancer treatment with proton and carbon beams up to 250 MeV and 400 MeV/n, respectively. In addition to that higher energy beams up to 800 MeV will be available soon for non-clinical research purposes.

The particle beam is circulated in a synchrotron until it has reached a given energy and is then extracted to reach one of three irradiation rooms. Naturally one wants to extract in an efficient way and avoid particle losses on physical components of the accelerator. As such, thorough commissioning of the extraction process and components is needed, which heavily relies on beam diagnostic devices. One of these devices at MedAustron is the PIN system described in this paper [1].

A description of the measurement principle will be given, followed by the theoretical implementation at MedAustron and concluded by the development process, challenges and lessons learned. Finally, an outlook on further plans at MedAustron regarding the PIN system and extraction efficiency investigation will be given.

PRINCIPLE OF OPERATION

A PIN diode is a diode with a wide intrinsic region, compared to a standard diode which has a much narrower P and N junction. The idea is to operate the diode in reverse bias mode so it does not conduct in normal conditions, except for a small dark current. When a charged particle impacts on the intrinsic region it creates electron-hole pairs. The carriers are immediately swept out of the region by the reverse bias field which creates a measureable current. The depletion region extends almost over the complete intrinsic region of the diode, and naturally the bigger the intrinsic region is, the more area there is where impacting particles can be detected.

By adjusting the reverse bias voltage across the diode anode and cathode the size of the depletion region can be influenced. Naturally, a higher voltage results in a wider region. However, a higher voltage also results in a higher dark current, which can be a problem for small signals.

IMPLEMENTATION AT MEDAUSTRON

In MedAustron's case (see Figure 1) the diode is made from hydrogenated[2] amorphous silicon (a-Si:H) with chromium-gold metallization on both surfaces. The active detector area is 15 mm by 40 mm and has a thickness of 0.3-0.5 mm.

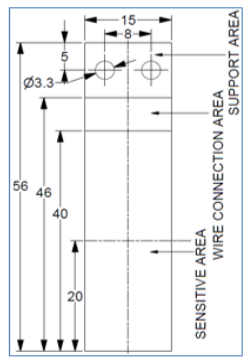

Figure 1: Mechanical structure of PIN.

The PIN diode used at MedAustron is suited for voltages from -10 V to +1 V. However, these reverse bias levels only apply for vacuum and should be applied gradually (e.g. over 30 s). Depending on the voltage level it can take up to one hour until a stable dark current is reached [2].

Connections to the electrodes are established using two clamps made from copper beryllium that can be adjusted with screws, with cables leading to two SMA connectors.

The PIN is mounted on a flange that is fixed to the beamline and located in the extraction magnetic septum in a way that the active detector area covers most of the wall area (see Figure 2). This way, close to all particles that are lost on this surface during extraction should be detected.

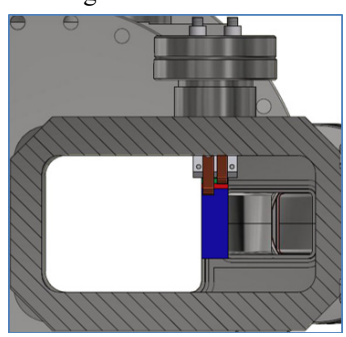

Figure 2: PIN as seen by beam.

1 alexander.pozenel@medaustron.at

[2] Hydrogenation is necessary to improve photoconductivity in amorphous silicon

Content from this work may be used under the terms of the CC BY 3.0 licence (© 2018). Any distribution of this work must maintain attribution to the author(s), title of the work, publisher, and DOI.

ISBN: 978-3-95450-201-1 doi:10.18429/JACoW-IBIC2018-TUPA02

A MICROMEGAS BASED NEUTRON DETECTOR FOR THE ESS BEAM LOSS MONITORING

L. Segui*, H. Alves, S. Aune, T. Bey, J. Beltramelli, Q. Bertrand, M. Combet, D. Desforge, F. Gougnaud, T. Joannem, M. Keibiri, C. Lahonde-Hamdoun, P. Le Bourlout, P. Legou, O. Maillard, Y. Mariette, J. Marroncle, V. Nadot, T. Papaevangelou, G. Tsiledakis, IRFU-CEA, Université Paris-Saclay, F-91191 Gif-sur-Yvette, France
I. Dolenc Kittelmann, T. J. Shea, European Spallation Source ERIC, Lund, Sweden

Abstract

Beam loss monitors are of high importance in high-intensity hadron facilities where any energy loss can produce damage or/and activation of materials. A new type of neutron BLM has been developed aiming to cover the low energy part. In this region typical BLMs based on charged particle detection are not appropriate because the expected particle fields will be dominated by neutrons and photons. Moreover, the photon background due to the RF cavities can produce false beam loss signals. The BLM proposed is based on gaseous Micromegas detectors, designed to be sensitive to fast neutrons and insensitive to photons (X-rays and gamma). In addition, the detectors will be insensitive to thermal neutrons, since part of them will not be directly correlated to beam loss location. The appropriate configuration of the Micromegas operating conditions will allow excellent timing, intrinsic photon background suppression and individual neutron counting, extending thus the dynamic range to very low particle fluxes. The concept of the detectors and the first results from tests in several facilities will be presented. Moreover, their use in the ESS nBLM system will be also discussed.

INTRODUCTION

In the new high-intensity hadron linear accelerators, a small loss of the beam is capable of damaging or activating materials in the machine. Thus Beam Loss Monitors (BLM) detectors with a sensitivity to very small fraction of beam losses are required. This limit approaches the 0.01 W/m loss value, which, in the case of the ESS, means a 0.001 ‰of the total 5 MW power lost over 600 m.

Moreover, an important background of photon fluxes is induced by the RF cavities due to the acceleration of electrons emitted from the cavity surfaces. The electrons will generate bremsstrahlung photons when interacting with some material of the accelerator. The spectrum of the produced photons ranges from X-rays to gammas of few MeV. If the BLM is photon-sensitive this implies an irreducible background that can mislead to a false beam loss or hide a real one [1]. This is of particular relevance in the low energy part of the accelerators where only photons and neutrons are produced in a beam loss situation. For this reason, a detector insensitive to photons is proposed.

Another requirement of a BLM is to obtain information about the loss location. In the low energy part, only neutrons and photons are emitted, as indicated above. With thermal neutrons their location information is lost, while fast neutrons can still provide such information.

In this paper the concept and first experimental results of a new neutron Beam Loss Monitor sensitive to fast neutrons and insensitive to X-rays and gammas are presented. It is based on the Micromegas detector technology. This new neutron BLM (nBLM) was already discussed in IBIC2016 [2] presenting results from MonteCarlo simulations that had proof the concept. In this paper experimental results will be discussed. The use of these detectors is planned for the ESS nBLM system.

NEUTRON BEAM LOSS MONITOR CONCEPT

Micromegas detectors (MICRO-MEsh GAseous Structures) [3] are a type of Multi-Pattern Gaseous Detectors (MPGD). As other MPGD detectors, Micromegas have a high gain, fast signals, and a very good spatial and energy resolution. They are largely in use in nuclear and particle physics experiments since their invention in 1996. In addition, among the Micromegas family, the bulk Micromegas technology [4] appears as a very robust detector, with a simplified manufacturing process that reduces its cost and allows its industrialization.

Micromegas detector is a two-stage avalanche chamber with three electrodes: the cathode or drift, a micromesh and an anode. The micromesh separates the two regions. First region between the cathode and the micromesh is the conversion region. The second region is defined by the micromesh and the anode and is a very narrow amplification region of the order of $\sim 128\ \mu$m. When a charged particle enters in the conversion region it ionizes the gas producing primary electrons that are drifted towards the amplification gap by a constant electric field. In the amplification region an avalanche of electrons takes place due to the higher electric field applied in this region ($\sim 10^5$ V/cm). The Micromegas detector itself consists of the anode and the micromesh, usually constructed as a unity. The planarity between both is obtained by insulator pillars established by lithographic process. To detect neutrons (neutral particles) a neutron-to-charge converter is placed at the entrance of the drift.

The neutron BLM is conceived to be tunable to specific experimental conditions. It can be adapted to a wide range of neutron measurements with appropriate neutron-to-charge converters and neutron absorber and moderators [5]. More-

* laura.segui@cea.fr

Content from this work may be used under the terms of the CC BY 3.0 licence (© 2018). Any distribution of this work must maintain attribution to the author(s), title of the work, publisher, and DOI.

ISBN: 978-3-95450-201-1 doi:10.18429/JACoW-IBIC2018-TUPA03

TEST OF NEW BEAM LOSS MONITORS FOR SOLEIL

N. Hubert†, M. El Ajjouri, D. Pédeau, Synchrotron SOLEIL, 91192 Saint-Aubin, France

Abstract

SOLEIL is currently testing new beam loss monitors to replace its pin-diode based system. The new detectors are made of plastic scintillators associated with photomultiplier and connected to Libera BLM dedicated electronics. This new detector should provide both fast (turn by turn) and slow loss measurement, post mortem capabilities and should be less sensitive to the beam directivity compared to the pin-diodes. Different methods for a relative calibration of the modules are under investigation, either using a photodiode or a cesium radioactive source. Calibration results and first measurements in SOLEIL storage ring are presented.

INTRODUCTION

In the storage ring, the electron beam is subjected to Touschek effects and to interactions with the residual gas, causing particle losses and impacting the lifetime. These losses may be regular or irregular, fast or slow, localized or distributed.

In order to monitor these losses, 36 loss monitors have been installed along the storage ring since the commissioning of SOLEIL in 2006. These monitors consist of two PIN diodes in coincidence [1] used in counting mode (Fig 1). This system has been in operation during 12 years but with some limitations. Only slow losses are detected and the high directivity of the sensor makes the comparison between two detectors quite difficult. The count rate is indeed very sensitive to the orientation of the detector with respect to the loss source.

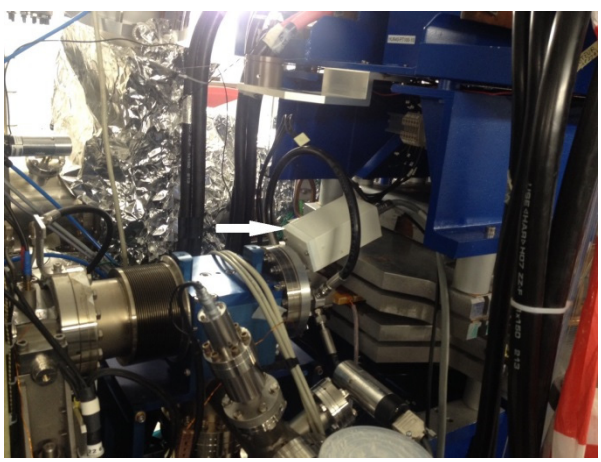

Figure 1: PIN diode loss monitor in its lead housing installed upstream of the HU640 undulator in the SOLEIL storage ring.

In order to prepare the upgrade of the system, we have decided to test new Beam Loss Monitors (BLMs) based on a scintillator and a photomultiplier.

SYSTEM DESCRIPTION

The new BLM system has to fit the following requirements:

- Allow a relative calibration in between the detectors to enable a comparison of the losses amplitudes around the machine.
- Provide slow and fast losses measurement.

Based on the work conducted by ESRF [2], we have tested BLM modules made of a scintillator (or a quartz Cerenkov radiator) and a photomultiplier. The plastic scintillator is a rod EJ-200 [3] wrapped into high reflectivity aluminum foil to improve photon flux on photosensor input. The photomultiplier is a photosensor module from Hamamatsu (series H10721, models 110, 113 and 210 [4]).
Those two elements are embedded in a compact aluminium housing (Fig.2).

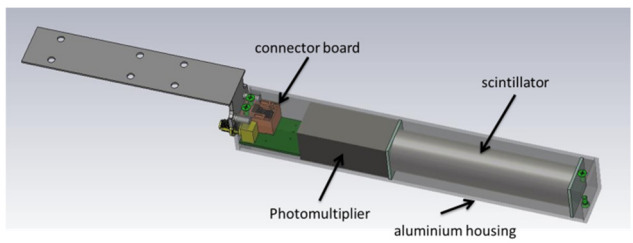

Figure 2: New BLM components and their Al housing.

The acquisition is performed by the Libera BLM electronic module which provides four 14 bits-125 MS/s ADCs together with a power supply and again control for the photosensor modules [5].

SYSTEM CALIBRATION

Having a relative calibration between the modules in order to be able to compare the losses amplitude measured by different detectors was one of the motivations for the upgrade of the system. We ideally targeted a relative calibration between all detectors better than 10%. Two different calibration methods have been investigated: using a LED or using a cesium source.

Diode

A dedicated housing has been realized to install a diode emitting at 455 nm, i.e. close to the maximum of the photosensor spectral response (250nm to 650 nm). The flux of the diode can be adjusted with a dedicated power-supply, whereas the photosensor is connected to the Libera BLM for acquisition and gain control (Fig. 3).

Content from this work may be used under the terms of the CC BY 3.0 licence (© 2018). Any distribution of this work must maintain attribution to the author(s), title of the work, publisher, and DOI.

ISBN: 978-3-95450-201-1 doi:10.18429/JACoW-IBIC2018-TUPA04

ANALYSIS OF INTERLOCKED EVENTS BASED ON BEAM INSTRUMENTATION DATA AT J-PARC LINAC AND RCS

N. Hayashi*, S. Hatakeyama, A. Miura, M. Yoshimoto, JAEA/J-PARC, Tokai, Ibaraki, Japan
K. Futatsukawa, T. Miyao, KEK/J-PARC, Tokai, Ibaraki, Japan

Abstract

J-PARC is a multi-purpose facility. Accelerator stability is the one of important issues for users of this facility. To realize stable operation, we must collect data on interlocked events and analyze these data to determine the reasons for the occurrence of such events. In J-PARC Linac, data of interlocked events have been recorded using several some beam loss monitors and current monitors, and these data have been are analyzed and classified. In J-PARC RCS, new instrumentation is being introduced to obtain beam position. We discuss the present status and future plans related to this subject.

INTRODUCTION

The Japan Proton Accelerator Research Complex (J-PARC) is a complex research facility consisting of three accelerators [1] and three experimental facilities. The first accelerator, Linac, was upgraded in 2014 by adding the Annular-ring Coupled Structure (ACS) after the separated drift-tube-linac (SDTL) and by replacing front-end system, a RF-driven ion source and a 50-mA Radio-frequency Quadrupole (RFQ). The injection system of the second accelerator, a 3-GeV Rapid-Cycling Synchrotron (RCS), was upgraded as well to accept 400 MeV H^- beams. Nominal RCS beam power of the Materials and Life Science Experimental Facility (MLF) was recovered to 500 kW in 2018. Because of the two neutron target failures in 2015, the beam power recovery program was executed with a very conservative schedule.

The design beam power for 1-MW operation was demonstrated for 1 h recently. Some fraction of the RCS beam is delivered to either the Neutrino Experimental Facility (NU) or the Hadron Experimental Facility (HD) through the Main Ring (MR) at intervals of 2.48 or 5.2 s, respectively. The beam power supplied to these two facilities was increased gradually to about 490 kW and 50 kW, respectively [2].

Availability of the facilities is as important as high beam power. To this end, the numbers of un-scheduled beam stoppage events, also called interlocked events, should be reduced. At least, it is necessary to understand the causes underlying accelerator interruption. Hence, we record and analyze interlocked events in detail. One of the J-PARC interlock subsystems is called Machine Protection System (MPS). There are several sources of MPS, for instance, mal-function of an apparatus, vacuum problem, or beam loss signal from the proportional-type Beam Loss Monitor (BLMP). Individual BLM MPS events lead to short down-times, but the number of Linac BLMP MPS events is large and comparable to the number of RFQ MPS events. The total down-time of such events is non-negligible [2]. BLMP MPS events are classified into three categories: events associated with other machine MPS, multiple BLMP MPS events without other MPS and finally single BLMP MPS events [3].

Especially, for the Linac, most of events are single BLMP triggered MPS. Neighboring BLMPs show no specific sign of being affected. In such an event,it may not be necessary to stop operation because the beam loss signal of single BLMP event continues only for one intermediate pulse length, which is less than 1 μs. However, in the case of RF-interlock-associated BLMP signal, the beam loss signal extends over multiple intermediate pulses. We believe that the single BLMP MPS does not represent significant beam loss. Hence, we are of the opinion that such events can be eliminated.

INSTRUMENTATION

Beam Loss Monitor

Most BLMs are proportional chambers [4]. The BLM detectors used in the Linac and the RCS are the same, but their operational conditions are different. In the Linac, the high voltage of the BLM detector is -2 kV, and its pre-amp input impedance is 50 Ω for better time response. Raw output signals from the signal amplifier are used for MPS in the Linac. By contrast, integral signals from BLMP are used to trigger MPS in the RCS. Different HV is applied to each BLMP because of individual optimization. High pre-amp input impedance is selected.

The present setting is excessively sensitive for the Linac, as discussed later. Therefore, we investigate a new parameter setting to reduce the number of single BLMP events. To this end, we decrease HV from -2 kV to -1.5 kV and select high impedance (10 kΩ). Pre-amp gain is maintained at ×100. The new settings are applied gradually because the pre-amp or the other filter module sets off an alarm if HV is lower than a certain value. Some pre-amps have a pre-set value is higher than -1.5 kV. Recent MPS statistics are presented in later.

BLMP detectors are located all over the accelerator bodies (93 in Linac and 90 in RCS). Particularly, one of the most important detectors is at the beam transport line from Linac to the 3-GeV RCS (L3BT). It is called L3BT:BLMP21, and it is located just before the first bending magnet BM01 of the 90-degree arc section. SCT12, a Slow Current Transformer for detecting beam current, is located between the last accelerating cavity ACS21 and BM01.

* naoki.hayashi@j-parc.jp

Content from this work may be used under the terms of the CC BY 3.0 licence (© 2018). Any distribution of this work must maintain attribution to the author(s), title of the work, publisher, and DOI.

ISBN: 978-3-95450-201-1 doi:10.18429/JACoW-IBIC2018-TUPA07

COLLIMATOR FOR BEAM POSITION MEASUREMENT AND BEAM COLLIMATION FOR CYCLOTRON

Lexing Hu[1], Yuntao Song†, Kaizhong Ding, Juniun Li, Qingxi Yang,
Institute of Plasma Physics, Chinese Academy of Sciences, Hefei, Anhui, China
Kai Yao, Yucheng Wu, Yonghua Chen,
Hefei CAS Ion Medical and Technical Devices Co., Ltd, Hefei, Anhui, China
[1]also at University of Science and Technology of China, Hefei, Anhui, China

Abstract

In order to restrict the beam dispersion and diffusion at the extraction area of the cyclotron and to detect abnormal beam loss, a beam collimator system has been designed to collimate the beam and to measure its transverse positions. The collimator system is composed of a vacuum cavity, two pairs of beam targets, a set of driving and supporting mechanism, and a measurement and control unit. The beam target with the size determined by the diameter of the beam pipe, the particle energy and beam intensity, will generate current signal during particle deposition. Each pair of beam targets has bilateral blocks which forms a slit in either horizontal or vertical direction. Servo motor and screw rod are used so that the target can reciprocate with the repeatability of less than 0.1mm. The measurement and control system based on LabVIEW can realize the motion control and current measurement of the targets and then calculate the beam transverse positions.

INTRODUCTION

The project of superconducting cyclotron for proton therapy SC200 is under development at ASIPP (Hefei, China) and JINR, which will be able to accelerate protons to the energy 200 MeV with the maximum beam current of 400 nA [1-3].

The collimator has been developed to reduce beam diffusion at the extraction area of the cyclotron and to detect abnormal beam loss, and then to measure the beam positions in horizontal and vertical directions.

The beam collimation system works in high-radiation areas and requires high heat dissipation, radiation resistance, positioning accuracy, stability and high vacuum performance, while considering the remote operation and maintenance functions of the collimator [4].

STRUCTURAL DESIGN

Mechanical Design

The collimator system is composed of a support gantry, servo drive unit, a vacuum chamber, bellows, and tungsten targets.

The vacuum chamber of the collimator is connected to the beam line through the flange before and after, and the overall leak rate is less than 1.0×10^{-11} Pa·m^2/s. Four tungsten targets are installed respectively in the upper, lower, left and right directions of the vacuum chamber to collimate the beam and to measure its transverse positions.

The tungsten target is connected to the slide table of the lead screw through a transmission rod. A bellows is used to ensure the vacuum of the vacuum chamber. The lead screw is driven by a servo motor.

The entire collimator is mounted on the support structure, and four bolts are used to achieve height adjustment and level adjustment of the collimator.

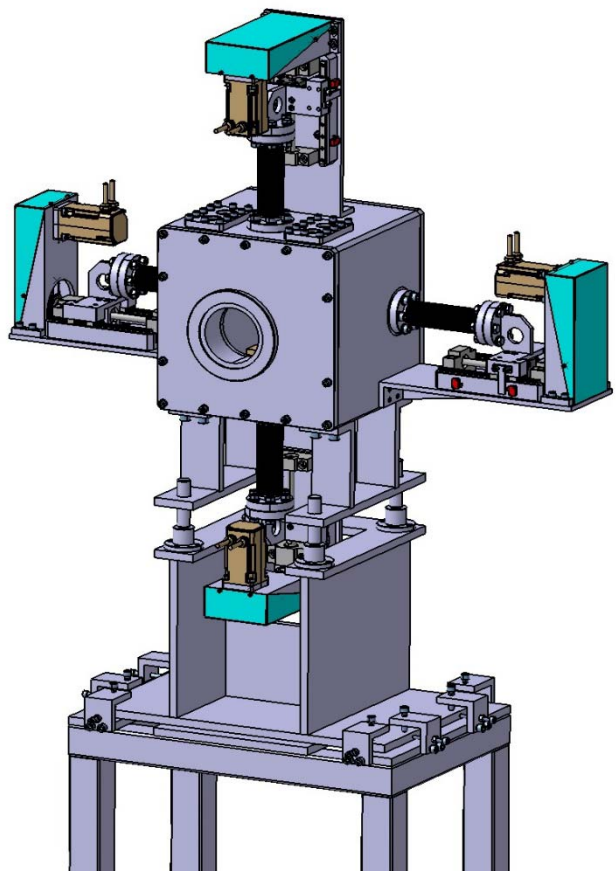

Figure 1: Layout of the collimator.

* Work supported in part by grants 1604b0602005 and 1503062029.
† email address: hulx@ipp.ac.cn

Content from this work may be used under the terms of the CC BY 3.0 licence (© 2018). Any distribution of this work must maintain attribution to the author(s), title of the work, publisher, and DOI.

ISBN: 978-3-95450-201-1 doi:10.18429/JACoW-IBIC2018-TUPA08

ARC DISCHARGE DETECTORS FOR THE CiADS SUPERCONDUCTING RF CAVITIES*

Zaipeng Xie†, Jian Liang, Yukai Ding, Hanxiang Liu
Hohai University, Nanjing, China
Yuan He, Yongming Li, Institute of Modern Physics,
Chinese Academy of Sciences, Lanzhou, China

Abstract

Arc discharge due to the electron emission is one of the key issues in the CW superconducting RF(SRF) for the CiADS particle accelerator. Arc discharges can deteriorate the SRF cavities and damage the facility. Monitoring arc discharges is important for the purpose of machine protection. In this paper, an arc discharge detector has been designed to provide fast response upon events of arc discharge using open-source hardware and LabVIEW software. Electronic design techniques are described to enhance the system stability while utilizing the flexibility of embedded electronics. The proposed detector system gives about 700 ns of response time and it employs a LabVIEW based graphic user interface. The system has the capability of detecting the instantaneous arc discharge events in real time. Timestamps of the event will be recorded to assist beam diagnostics. This paper describes the hardware/software implementation and concludes with initial results of tests at CiADS.

INTRODUCTION

The superconducting proton LINAC has been built for the China initiative accelerator driven subcritical(CiADS) facility. In the LINAC [1], a 1.5 GeV, 10 mA proton beam is produced using the CW superconducting RF(SRF) cavities that requires a high availability for the beam diagnostics. In the CiADS SRF cavity, field emission can start at the emitters located on the cavity surface and result in electron emission. Secondary electrons can be produced from multipacting by ions, radicals, or photons. Electron emissions from cavity surfaces by thermionic and field emissions can occur in a small area of the surface and lead to a voltage breakdown that yields a gas discharge such as an arc or a glow discharge [2]. The onset of the discharge is usually accompanied by local temperature rises that can melt a small region of the emitter and produce starburst craters on the cavity surface. This process can deteriorate the cavity performance by eroding the electrode and lead to catastrophic failure in the insulator, which can eventually damage the SRF facility. Methods [3], such as the high-pressure water rinsing (HPR) and the high pulse power processing (HPP) technique, have been explored to mitigate the electron emission and arc discharge at CiADS. However, since the sources of electron emitters are caused by random material defects and contaminants introduced during assembling, arc discharge can still occur occasionally. Arcs can be suppressed by shutting the RF power down and it requires a minimal response time on detecting an SRF arc event. Hence, fast response detectors are desired that can detect the arc discharge and abort the machine to prevent further damages.

There are only a few commercial products available for the application and they require an increased expense. Recent advances in the Internet of Things (IoT) technology has made low cost and open access scientific tools accessible to researchers in vast industrial applications. For example, Hughes et al. [4] developed a hyperion particle-γ detector array that employs an Arduino based open source hardware to control its cryogenic fill system. Tavares et al. [5] implemented an open-source hardware platform for the BPM and orbit feedback system at the Brazilian Synchrotron Light Laboratory. Open source hardware for instrumentation and measurement [6] has been adopted in several scientific applications [7] at CERN.

This paper explores an open-source hardware solution for the arc discharge detector that can provide modularity and economic viability. One of the main consideration of this paper is to provide a fast development and deployment open-source solution with a reasonable system reliability. This paper present the basic building elements for delivering an open-hardware based infrastructure of the arc discharge detector that brings flexibility and manageability.

SYSTEM OVERVIEW

The arc discharge detector for the CiADS superconducting RF cavities is designed as a machine protection instrument that requires a maximum 10 µs response time on detecting an arc event. The system is triggered by the incident light near its installation site. A optical sensor is employed in the system that is connected with a fast circuit for the signal processing. Since the arc has to be in the line-of-sight, the detector is installed to the monitoring of specific elements such as the T-junction and the vacuum feed-through. The detector system requires a high level of reliability and dust deposition or irradiation of the optical fibers are also major issues that require attention. The system efficiency is determined by the maximum false alarm rate of the detector. Maintenance and testing operations are also factors that need to be taken into consideration.

Figure 1 shows a diagram of the system. The arc discharge detector is composed of a hardware and a software platform. The hardware employs an optical sensor, a cus-

* Work supported by the National Natural Science Foundation of China (Grant No.11505255, No.91026001) and the Fundamental Research Funds for the Chinese Central Universities(2015B29714)
† zaipengxie@impcas.ac.cn

Content from this work may be used under the terms of the CC BY 3.0 licence (© 2018). Any distribution of this work must maintain attribution to the author(s), title of the work, publisher, and DOI.

ISBN: 978-3-95450-201-1 doi:10.18429/JACoW-IBIC2018-TUPA09

THE MONTE CARLO SIMULATION FOR THE RADIATION PROTECTION IN A NOZZLE of HUST-PTF*

Y.C. Yu, P. Tan†, H.D. Guo, L.G. Zhang, Y.J. Lin, X.Y. Li, Y.Y.Hu
State Key Laboratory of Advanced Electromagnetic Engineering and Technology,
School of Electrical and Electronic Engineering, Huazhong University of Science and Technology,
Wuhan 430074, China

Abstract

Nozzle is the core component in proton therapy machine, which is closest to the patient and is necessary to consider the radiation impacts on patients and machine. The ionization chamber and the range shifter in active scanning nozzle are the main devices in the beam path that affect the proton beam and produce secondary particles during the collision, causing damage to the patients and machine. In this paper, the spatial distribution of energy deposited in all regions, the distribution of the secondary particles of 70-250MeV proton beam in the nozzle in Huazhong University of Science and Technology Proton Therapy Facility(HUST-PTF) are studied with Monte Carlo software FLUKA in order to provide reference for radiation shielding design. Six types of materials commonly used today as range shifters are analyzed in terms of the influence on radiation,so that the most suitable material will be selected.

INTRODUCTION

In order to ensure the safety of the patients, as well as the machine, the effect of radiation should be considered when designing the nozzle. Due to the application of the active scanning nozzle in HUST-PTF, the collimator and scatter are not required on the beam path, so the scattering and secondary particle radiation will be significantly reduced[1].However, it is still necessary to analyze the radiation distribution in the nozzle and develop a corresponding radiation shielding scheme. At the end of nozzle, a range shifter is placed very close to the patient in order to decrease the proton beam energy so that the shallow tumors can be treated. Selecting a suitable material for the range shifter will significantly reduce its radiation impacts on patients.

The scanning nozzle is mainly composed of a vacuum window, a pixel ionization chamber, a helium pipe, an ion chamber, and a series of mechanical support structures in Huazhong University of Science and Technology Proton Therapy Facility(HUST-PTF). The vacuum window, made of 30μm kapton, is installed at the end of the beamline as a boundary between the beamline transmission system and the nozzle system. The pixel ionization chamber is used to monitor the initial beam states which is located 100mm away from the vacuum window. The helium pipe, passing through two scanning magnets, is placed behind the pixel ionization chamber to reduce energy loss and transverse scattering. The plate ion chamber is placed 800 mm from the isocenter plane and is used to monitor the position and the dose of the proton beam，so that the accuracy of the dose and position can be ensured. The structure of pixel ionization chamber and plate ion chamber in HUST-PTF is shown in Fig.1. In order to simulate the human body composition, a water phantom is placed after the isocenter plane. The structure of nozzle in HUST-PTF is shown in Fig. 2.

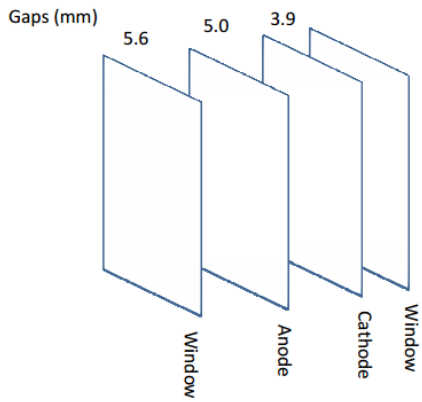

a. The structure of pixel ionization chamber

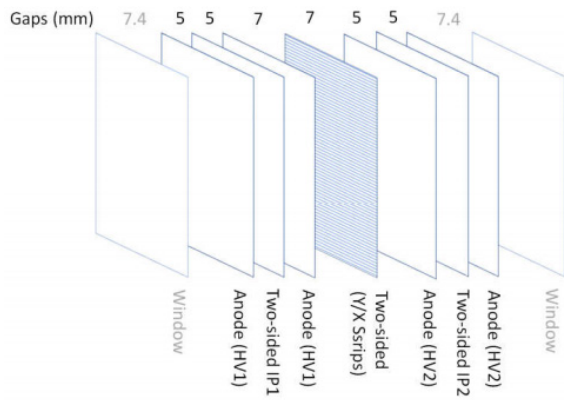

b. The structure of plate ion chamber

Figure 1: The structure of pixel ionization chamber and plate ion chamber.

In this paper, the model of the nozzle in HUST-PTF is constructed in three dimensions by using the Monte Carlo software FLUKA[2]. The energy loss when the proton beam passes through the nozzle，the secondary particle yield, the spatial distribution of neutrons and photons are calculated by using FLUKA. At the same time, the

* Work supported by National Key R&D Program of China（No.2016YFC0105308）
† Corresponding author, tanping@mail.hust.edu.cn

Content from this work may be used under the terms of the CC BY 3.0 licence (© 2018). Any distribution of this work must maintain attribution to the author(s), title of the work, publisher, and DOI.

ISBN: 978-3-95450-201-1 doi:10.18429/JACoW-IBIC2018-TUPA14

BEAM LOSS MONITORING IN THE ISIS SYNCHROTRON MAIN DIPOLE MAGNETS

D. M. Harryman*, S. A. Fisher†, W. A. Frank, B. Jones, A. Pertica, D. W. Posthuma de Boer, C. C. Wilcox, STFC, Rutherford Appleton Laboratory, Oxfordshire, UK

Abstract

Beam loss monitoring at the ISIS Neutron and Muon Source is primarily carried out with gas ionisation chambers filled with argon. Thirty-nine ionisation chambers are distributed evenly around the inner radius of the synchrotron, with additional devices for the linac and beam transport lines. To improve loss control, a programme has been implemented to install six scintillator Beam Loss Monitors (BLMs), each 300 mm long, inside each of the ten main dipole magnets of the synchrotron. Using these scintillator BLMs the accelerator can be fine-tuned to reduce areas of beam loss that were previously unseen or hard to characterise. Installation of the system is now complete and this paper reviews: the installation of the scintillator BLMs, the electronic hardware and software used to control them, and the initial measurements that have been taken using them.

INTRODUCTION

ISIS Beam Loss Monitoring

ISIS has two systems for beam loss detection: a main "global" system using thirty-nine argon filled ionisation chambers [1]; and a finer system, using BC-408 plastic scintillators, that provides additional monitoring in selected areas [2]. The gas ionisation chambers in the synchrotron are 3 m long and distributed evenly around the inner radius, about 2 m from the beam axis. As beam losses inside the synchrotron's main dipole magnets are shielded by the magnet yokes, they can be undetectable using the existing ionisation chambers. Therefore, to supplement these monitors, scintillator BLMs were initially installed inside the main dipole magnet downstream of the collimation straight, Dipole 2, as this had occasionally suffered beam related damage. This initial set of scintillators detected beam losses which were not measured on the ionisation chambers, and as such the decision was taken to install scintillators inside all ten of the main dipole magnets around the synchrotron. Each of the main dipole magnets is 4.4 m long, and for the initial set-up of Dipole 2, twelve BC-408 detectors were installed between the vacuum vessel and magnet yoke. Based on experience from Dipole 2, a configuration of six detectors has been installed in each of the main ring dipoles, which provided an optimal balance of cost, complexity and resolution. A key benefit of the scintillator detector design, with their entirely non-metallic construction, is that they avoid potentially serious problems with Eddy currents in the fast cycling ISIS magnets.

* daniel.harryman@stfc.ac.uk
† sarah.fisher@stfc.ac.uk

System Overview

Figure 1 shows an outline of a scintillator system for one dipole, including main hardware, subsystems, locations, and connections.

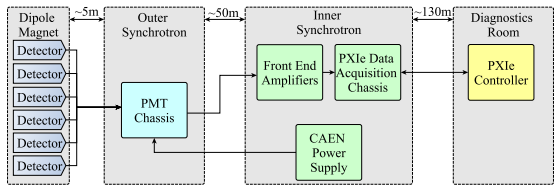

Figure 1: Overview of system hardware used for a single dipole.

As with the initial installation in Dipole 2, all detectors are installed within the main dipole magnets, between the magnet yoke and the vacuum vessel. All of the detector assemblies are installed on the inside radius of each dipole. Approximately 5 m from each dipole is a Photo Multiplier Tube (PMT) chassis holding six PMTs, one for each detector. The PMTs convert the light generated by the detectors into electrical "beam loss" signals. Each PMT is connected to a high voltage power supply and front end amplifiers, which are both located in the inner synchrotron area. This area is shielded by several metres of concrete, meaning radiation levels there are relatively low during accelerator operations. The CAEN power supply provides high bias voltages for each PMT. The front end amplifiers buffer the PMT outputs into a voltage which can be read by the PXIe data acquisition system.

Although the inner synchrotron area is shielded, some sensitive equipment, like the PXIe controller, can suffer from radiation-induced failure. Therefore, while the data acquisition cards for the system are located in the inner synchrotron area, the controller is located 100 m away, where radiation levels are negligible and access is unrestricted. The long distance connections between the two PXIe sub-systems is achieved with a custom optical fibre link, as detailed below.

DETECTORS

Detector Design

The detectors are based on the same design as those described in [2], based on BC-408 plastic scintillators. When high-energy particles interact with BC-408, light is generated [3]. The detector is covered in a light proof cover to eliminate background light, and connected to a PMT via optical fibres (see Fig. 2). As each detector has slightly different characteristics and responses, each detector and PMT pair is calibrated with a known radiation source in the

Content from this work may be used under the terms of the CC BY 3.0 licence (© 2018). Any distribution of this work must maintain attribution to the author(s), title of the work, publisher, and DOI.

ISBN: 978-3-95450-201-1 doi:10.18429/JACoW-IBIC2018-TUPA15

ADAPTIVE COLLIMATOR DESIGN FOR FUTURE PARTICLE ACCELERATORS*

T. Furness[1†], S. Fletcher[1], J. Williamson[1], A. Bertarelli[2], F. Carra[2], L. Gentini[2], M. Pasquali[2], S. Redaelli[2]
[1]The University of Huddersfield, Queensgate, Huddersfield, UK
[2]The European Organisation for Nuclear Research (CERN), Genève, CH

Abstract

The function of collimators in the Large Hadron Collider (LHC) is to control and safely dispose of the halo particles that are produced by unavoidable beam losses from the circulating beam. Even tiny proportions of the 7TeV beam have the stored energy to quench the superconducting magnets or damage parts of the accelerator if left unchecked. Particle absorbing Low-Z material makes up the active area of the collimator (jaws). Various beam impact scenarios can induce significant temperature gradients that cause deformation of the jaws. This can lead to a reduction in beam cleaning efficiency, which can have a detrimental effect on beam dynamics. This has led to research into a new Adaptive Collimation System (ACS). The ACS is a re-design of a current collimator already in use at CERN, for use in the HL-LHC. The ACS will incorporate a novel fibre-optic-based measurement system and piezoceramic actuators mounted within the body of the collimator to maintain jaw straightness below the 100µm specification. These two systems working in tandem can monitor, and correct for, the jaw structural deformation for all impact events. This paper details the concept and technical solutions of the ACS as well as preliminary validation calculations.

INTRODUCTION AND COLLIMATOR DESIGN

The current energy stored in nominal LHC beams is two times 362MJ [1]. For the High-Luminosity LHC upgrade (HL-LHC), this is expected to be higher than 700MJ [2]. As little as 1mJ/cm^3 at 7TeV of deposited energy can quench the super-conductive magnets or cause more major damage to other sensitive areas of the accelerator complex [3]. In efforts to counter this, the LHC collimation system is designed to intercept and safely dispose of the halo particles that are produced from the unavoidable beam losses generated from the circulating beam core.

Broadly speaking, the collimation system comprises of primary, secondary and tertiary collimators presented in a variety of geometrical configurations, working in union to clean the circulating beam. Each collimator consists of three main areas: the jaw assemblies, the actuation system, and the vacuum tank, shown in figure 1.

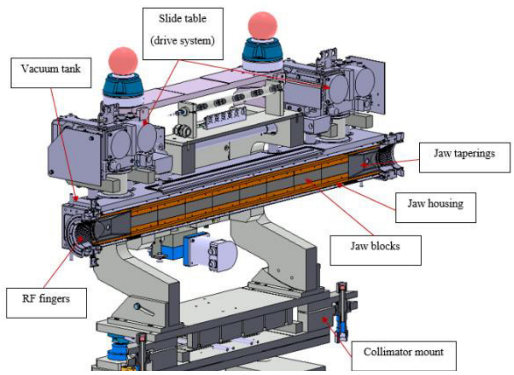

Figure 1: Section view of a typical horizontal secondary collimator.

The main component of the jaw assembly is the active absorption area. In primary and secondary collimators, this is made up of several blocks of low-Z material, such as a graphite composite or carbon reinforced carbon, to ensure low electrical induced impedance whilst maintaining mechanical robustness. These blocks are then clamped to a dispersion strengthened copper (Glidcop®) housing. The blocks are clamped to the housing rather than being rigidly fixed as this is not easily achieved. This is also to ensure a certain amount of slippage as the thermal expansion of Glidcop® is far greater than the thermal expansion of the low-Z blocks. Within the Glidcop® housing is also the jaw cooling system. The cooling system is designed to be able to evacuate the high heat loads generated by loss absorption (up to 47kW for HL-LHC cases) in an effort to minimise thermal deformations, which may be induced [4]. The cooling pipes are sandwiched between the block-housing stiffener on the front and an intermediate stiffener on the back then vacuum brazed together to ensure a good thermal conductivity, as shown in figure 2.

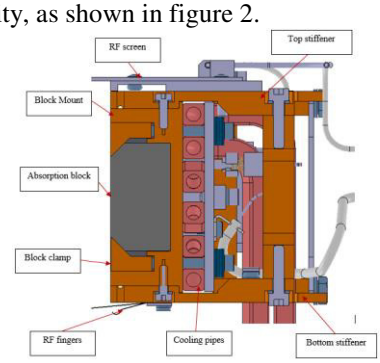

Figure 2: Cross section of current HL-LHC jaw assembly.

†t.furness@hud.ac.uk
*This work has been funded by Science and Technology facilities Council (STFC) and by the European Organisation for Nuclear Research (CERN)

Content from this work may be used under the terms of the CC BY 3.0 licence (© 2018). Any distribution of this work must maintain attribution to the author(s), title of the work, publisher, and DOI.

ISBN: 978-3-95450-201-1 doi:10.18429/JACoW-IBIC2018-TUPA16

SIGNAL PROCESSING FOR BEAM LOSS MONITOR SYSTEM AT JEFFERSON LAB

J. Yan, T. Allison, S. Bruhwel, W. Lu, Jefferson Lab, Newport News, VA 23606, U.S.A.

Abstract

Ion Chambers and Photomultiplier Tubes (PMT) are both used for beam loss monitoring in the Machine Protection System (MPS) at Jefferson Lab. These detectors require different signal processing, so two VME-based signal processing boards, Beam Loss Monitor (BLM) board and Ion-Chamber board, were developed. The BLM board has fast response (< 1 μs) and 5 decades of dynamic range from 10 nA to 1 mA, while the Ion-Chamber board has a slower response but 8 decades of dynamic range from 100 pA to 10 mA. Both boards feature machine protection and beam diagnostics, in addition to a fast shutdown (FSD) interface, beam sync interface, built-in-self-test, remotely controlled bias signals, and on-board memory buffer.

INTRODUCTION

The Beam Loss Monitor (BLM) system is an important part of the Jefferson Lab Machine Protection Systems (MPS) [1]. It detects bremsstrahlung radiation from low level beam loss during tune-up and beam operations and provides a machine protection trip well before the beam can damage accelerator components. Two types of radiation detectors, 931B PMT [2] and CERN Ion Chamber [3], are installed for the beam loss monitor system of the CEBAF at Jefferson Lab. An 8-channel VME based BLM board, which has replaced the original 4-channel CAMAC based board, are developed as the current acquisition electronics for PMT detectors, with negative current between -5 nA to -1 mA and a fast response time. Meanwhile, a newly designed 5-channel Ion Chamber (IC) VME board provides the current acquisition for CERN Ion Chamber, which has a slow time response and a large dynamic range.

NEW BLM BOARD DESIGN

The new 8-channel BLM signal processing board has a functional block diagram that consists of analog signal processing and digital processing. The analog processing includes linear signal tuning, operational amplifier (op-amp) integrating signal processing, Howland voltage-to-current converter circuits, and logarithmic current signal processing. The digital processing includes FSD signal logic, analog-to-digital (ADC) data acquisition, and FPGA digital control. The linear tuning is an op-amp circuit with a gain of 5490. It converts negative current from PMT to voltage, referred to as the pre-amplified voltage. The pre-amplifier voltage signal then serves as the input for both integrating and log circuits. Figure 1 shows the diagram of the analog signal processing for each channel. The integrating processing circuit is op-amp based and performs the mathematical operation of integration to cause the output voltage to respond to changes of the input voltage over time. The integrated output voltage is connected both to the ADC for data sampling and to a fast voltage comparator for FSD detection. The equation of the ideal voltage of the op-amp integrator is

$$V_{\text{int}} = -\int_0^t \frac{V_{in}}{R_{in} \cdot C} dt \,.$$

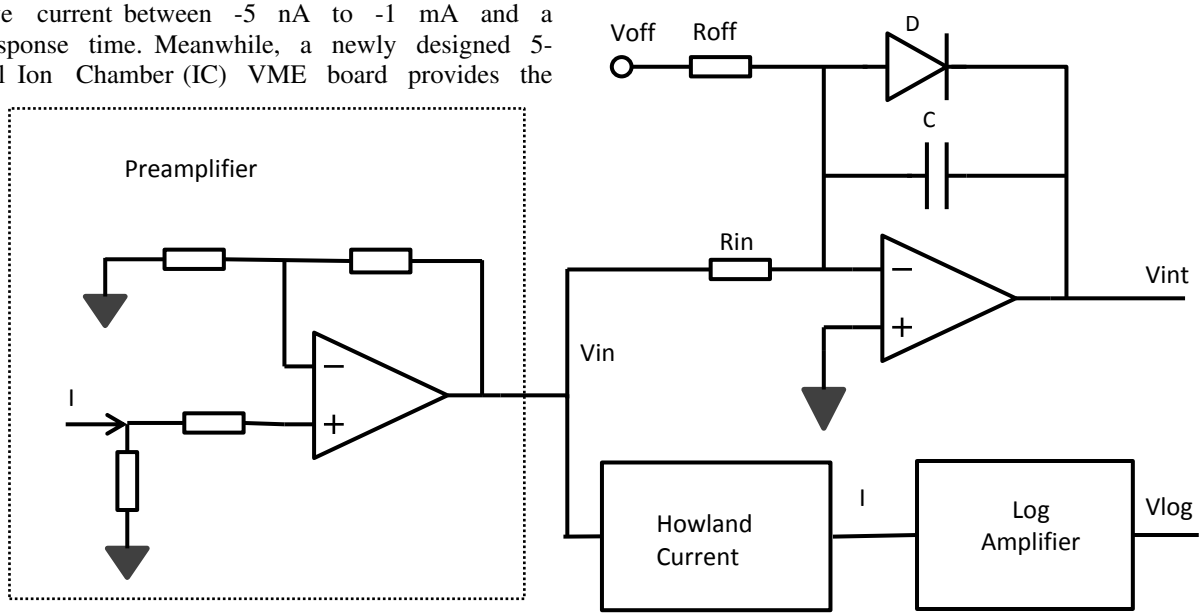

Figure 1: Diagram of the analog signal processing.

Content from this work may be used under the terms of the CC BY 3.0 licence (© 2018). Any distribution of this work must maintain attribution to the author(s), title of the work, publisher, and DOI.

ISBN: 978-3-95450-201-1 doi:10.18429/JACoW-IBIC2018-TUPA17

STATUS OF THE BNL LEReC MACHINE PROTECTION SYSTEM*

S. Seletskiy†, Z. Altinbas, D. Bruno, M. Costanzo, A. Drees, A. Fedotov, D. M. Gassner, X. Gu, L. Hammons, J. Hock, R. Hulsart, P. Inacker, J. Jamilkowski, D. Kayran, J. Kewisch, C. Liu, K. Mernick, T. Miller, M. Minty, M. Paniccia, W. Pekrul, I. Pinayev, V. Ptitsyn, V. Schoefer, L. Smart, K. Smith, R. Than, P. Thieberger, J. Tuozzolo, W. Xu, Z. Zhao
BNL, Upton, USA

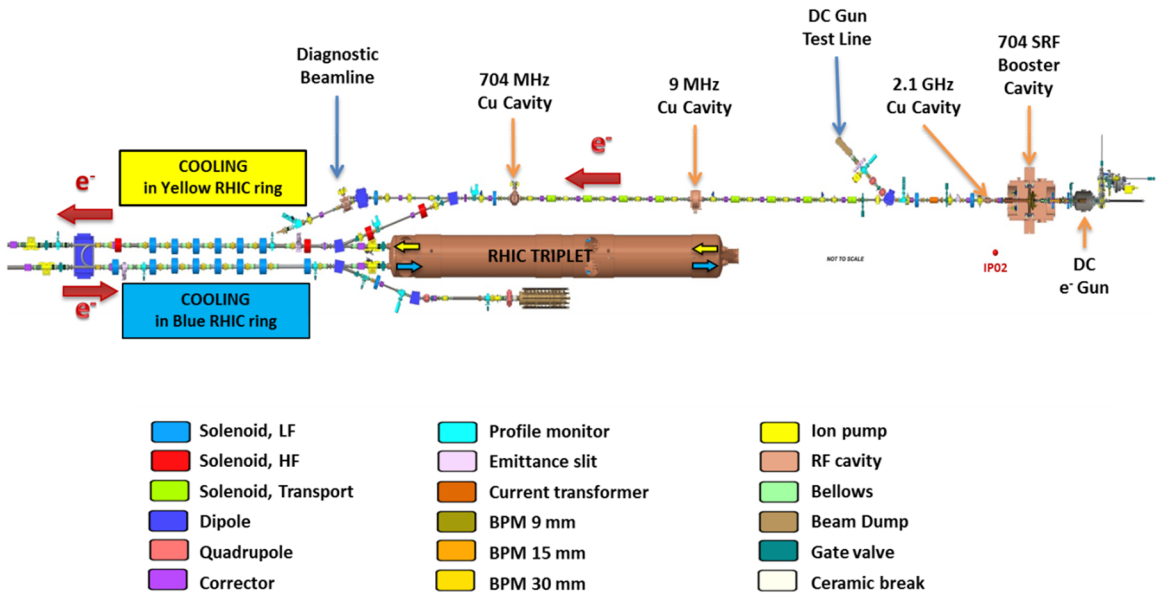

Figure 1: LEReC layout.

Abstract

The low energy RHIC Electron Cooler (LEReC) will be operating with 1.6-2.6 MeV electron beams having up to 140 kW power. It was determined that under the worst case scenario the missteered electron beam can damage the vacuum chamber and in-vacuum components within 40 us. Hence, the LEReC requires a dedicated fast machine protection system (MPS). The LEReC MPS has been designed and built and currently is under commissioning. In this paper we describe the most recent developments with the LEReC MPS.

LEREC LAYOUT AND PARAMETERS

The LEReC accelerator [1] consists of the 400 kV DC photo-gun followed by the 1.2-2.2 MV SRF Booster, the transport line and the merger that brings the beam to the two cooling sections (CS1 and CS2) followed by the 140 kW dump. The LEReC also includes two dedicated diagnostic beamlines: the low-power beamline capable of accepting 15 kW beam (DC Gun Test Line) and the RF diagnostic beamline.

The LEReC layout is schematically shown in Fig. 1.

The LEReC beam train consists of 9 MHz macro-bunches. Each macro-bunch (MB) consists of N_b=30 bunches repeated with 704 MHz frequency. The length of each bunch at the cathode is 40 ps. The charge per bunch (Q_b) can be as high as 200 pC.

The LEReC can work with macro-bunch trains of various length (Δt), various number of macro-bunches per train (N_{mb}), and various time delay (T) between the trains.

The nominal LEReC beam parameters pertinent to the MPS design are summarized in Table 1.

Table 1: LEReC Beam Parameters.

Kinetic Energy, MeV	1.6	2	2.6
Electron bunch (704 MHz) charge, pC	130	170	200
Bunches per macro-bunch (9 MHz)	30	30	24-30
Charge per macro-bunch, nC	4	5	5-6
Average current, mA	35	46	44-55
Average power, kW	56	93	114-142

In addition to the baseline operational modes listed in Table 1 the LEReC might also be operated with CW 704 MHz beam of 85 mA (at 1.6 MeV) and 68 mA (at 2 MeV).

There are also several additional beam modes required for accelerator commissioning, study and transition to operational conditions. All these modes of operation comprise the MPS beam modes.

The relation between the MPS beam mode and allowed destinations of the beam will be discussed in the following sections.

The LEReC MPS beam modes and their use are summarized in Table 2.

* Work supported by Brookhaven Science Associates, LLC under Contract No. DE-AC02-98CH10886 with the U.S. Dept. of Energy.
† seletskiy@bnl.gov

Content from this work may be used under the terms of the CC BY 3.0 licence (© 2018). Any distribution of this work must maintain attribution to the author(s), title of the work, publisher, and DOI.

ISBN: 978-3-95450-201-1 doi:10.18429/JACoW-IBIC2018-TUPB01

THE INSTALLATION AND COMMISSIONING OF THE AWAKE STRIPLINE BPM*

Shengli Liu†, Victor Alexandrovich Verzilov, Paul Eric Dirksen, TRIUMF, Vancouver, BC, Canada
Franck Guillot-Vignot, Lars Soby, David Medina Godoy, Spencer Jake Gessner,
CERN, Geneva, Switzerland

ABSTRACT

AWAKE (The Advanced Proton Driven Plasma Wakefield Acceleration Experiment at CERN) stripline BPMs are required to measure the position of the single electron bunch to a position resolution of less than 10 μm rms for electron charge of 100 pC to 1 nC. This paper describes the design, installation and commissioning of a such BPM system developed by TRIUMF (Canada). Total 12 BPMs and electronics had been installed on AWAKE beam lines and started commissioning since Fall of 2017. The calibration and measurement performance are also reviewed.

SYSTEM OVERVIEW

AWAKE facility is a proof-of-principle R&D experiment at CERN and the world's first proton driven plasma Wakefield acceleration experiment [1]. Its construction has been completed and the commissioning has been started since Fall of 2017, which includes the stripline BPMs for tuning the electron beam. Refer to Fig. 1 for the layout of the AWAKE electron beamline and the common beamline, the electron BPMs locations and other diagnostic devices.

A total 12 BPMs have been installed on the AWAKE, with 6 on the electron beamline, and 6 on the common beamline. Those on the electron beamline are 40 mm aperture, while those on the common beamline are 60 mm aperture. They both have coverage angle of 38 degree, and with longitudinal length of 120 mm and 124 mm. Because of these parameters, their sensitivities are supposed to be slightly different. The processing electronics, i.e. BPM DSP (Digital Signal Processor), is in the hall way which has about 30 ~ 60 meters to the BPMs. The radiation dose rate level there is low enough that the electronics is not designed to be radiation hard. Refer to Fig. 2 for the system diagram, which describes the electronics, network and data acquisition computer. All the BPM DSPs are powered through the power bars that support Ethernet interface, which allows the DSP boxes to be power cycled in the situation that the communication becomes dead. Such situation happened several times during the commissioning, this remote reset scheme prevented human access to the site which is difficult or impossible during SPS operation. Besides the FEC (Front End Computer) which runs the DAQ software FESA server (FESA: What also is shown in the diagram is the triggers which signal the presence of the electron or proton beam bunches.

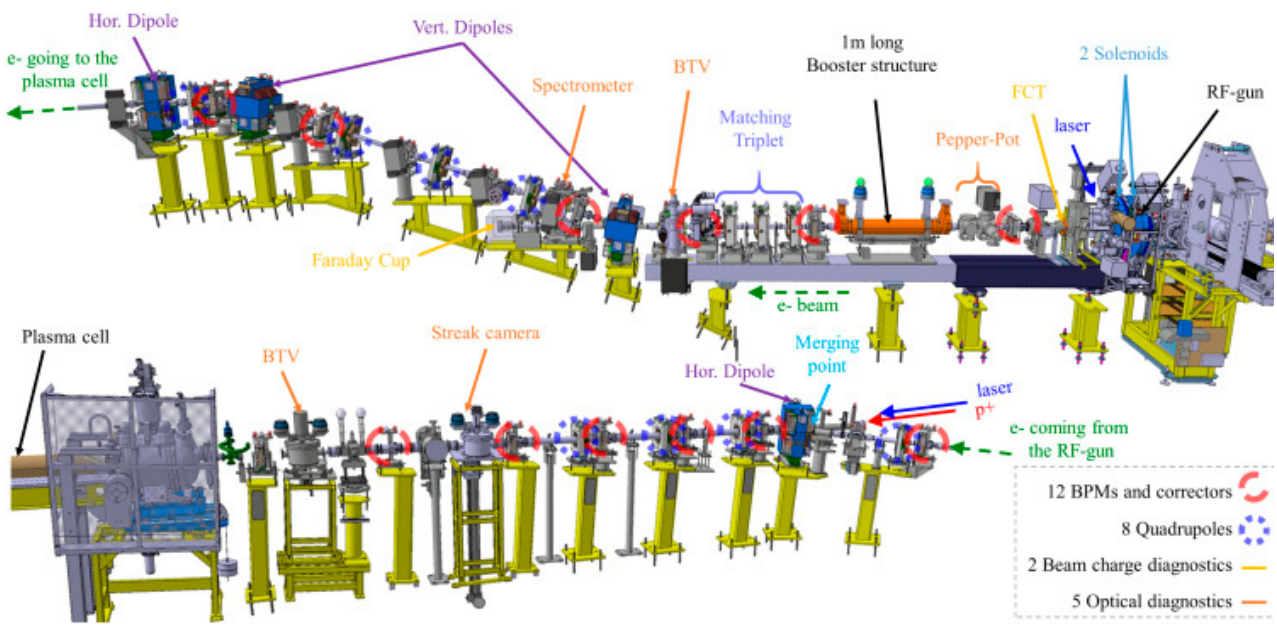

Figure 1: AWAKE beam lines and BPM locations.

* TRIUMF contribution was supported by NSERC and CNRC
† sliu@triumf.ca

Content from this work may be used under the terms of the CC BY 3.0 licence (© 2018). Any distribution of this work must maintain attribution to the author(s), title of the work, publisher, and DOI.

ISBN: 978-3-95450-201-1 doi:10.18429/JACoW-IBIC2018-TUPB02

COMPLETE TEST RESULTS OF NEW BPM ELECTRONICS FOR THE ESRF NEW LE-RING

B.K. Scheidt, ESRF, Grenoble, France

Abstract

Among the 320 BPMs in the ESRF new low-emittance ring, a set of 128 units will be equipped with new electronics, while the other set (192) will be served by the existing Libera-Brilliance electronics. These new electronics are an upgraded version of the low-cost Spark electronics originally developed 3 years ago for the ESRF's injector complex. All these 128 units have been installed in the first half of 2018 on existing BPM signals (through duplication with RF-splitters) and subsequently been tested thoroughly for performance characteristics like stability, resolution and reliability. It shows that while these Sparks have a very straightforward and simple concept, i.e. completely omitting calibration schemes like RF-cross-bar switching, pilot-tone introduction or active temperature control, they are fully compatible with all the beam position measurement requirements of this new ring.

OVERVIEW OF THE BPM SYSTEM

The BPM system in this new storage ring will be a hybrid type with both two types of BPM-block geometries, and two types of BPM electronics. The lattice parameters of the new ring are given in Fig. 1 that represents one complete cell out of the total of 32, with the 10 BPMs indicated in triangles.

The Fig. 2 shows some numeric details of that lattice, the distribution in a cell of the large and the small geometry, and the distribution of the 2 types of electronics.

For the latter we will use a) 192 Liberas that were bought nearly 10 years ago and b) 128 newly developed and procured Sparks. [1]

The old storage ring with 224 BPMs is served with an equal number of Libera-Brilliance units with satisfactory performance and reliability over these 10 years and therefore the logical choice would have been to procure more of them to make-up for the new total number of 320 BPMs. [2]

However, these units had become obsolete. In looking for a satisfactory alternative, we have turned towards a different device that was developed, 3 years earlier, for new Booster BPMs. These relatively simple, straight-forward and of moderate cost Spark electronics offered enough scope for upgrading in order to make them comply with our overall BPM needs and requirements of this new storage ring. [3, 4]

By re-using 192 Libera units out of the 224 presently active units we have increased our cover for spares.

These two different electronics provide data-streams, and buffers with identically synchronised sampling-rates. However, the Fast-Orbit-Correction will only use the 10 kHz stream provided by the 192 Liberas. [5]

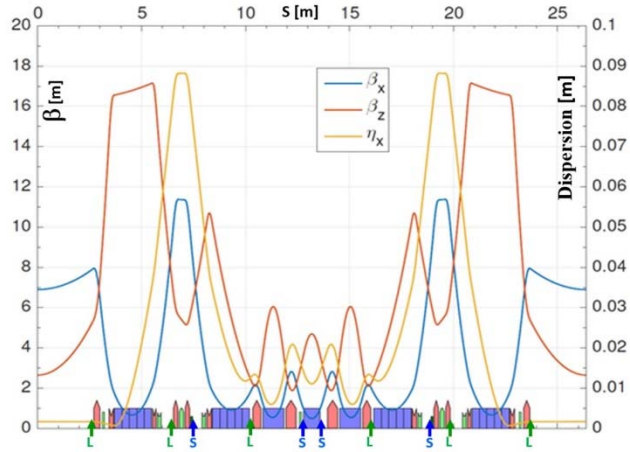

Figure 1: The lattice of one complete cell with the 10 BPM positions indicated by blue/green triangles

BPM	Geom.	Libera/Spark	S [m]	β Hor [m]	β Vert [m]	Disp.[cm]
1	Large	Libera	2.65	7.92	5.30	0.2
2	Large	Libera	6.48	9.50	7.17	8.0
3	Large	Spark	7.52	7.82	6.54	7.3
4	Small	Libera	10.29	1.93	2.33	1.3
5	Small	Spark	12.73	1.13	3.39	1.5
6	Small	Spark	13.64	1.13	3.39	1.5
7	Small	Libera	16.08	1.93	2.33	1.3
8	Large	Spark	18.86	7.82	6.54	7.3
9	Large	Libera	19.90	9.50	7.17	8.0
10	Large	Libera	23.72	7.92	5.30	0.2

Figure 2: The BPM geometry and the type of electronics.

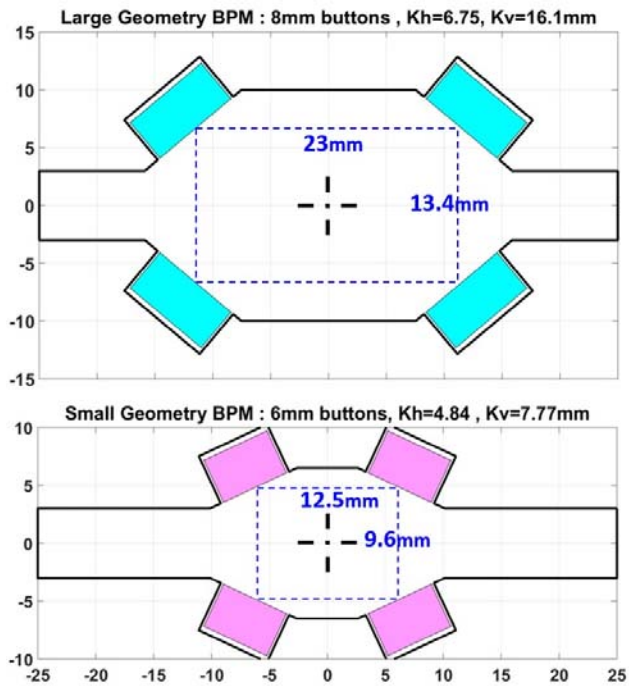

Figure 3: The distinct geometries of the two BPM blocks.

Content from this work may be used under the terms of the CC BY 3.0 licence (© 2018). Any distribution of this work must maintain attribution to the author(s), title of the work, publisher, and DOI.

ISBN: 978-3-95450-201-1 doi:10.18429/JACoW-IBIC2018-TUPB03

RESULTS OF SPIRAL2 BEAM POSITION MONITORS ON THE TEST BENCH OF THE RFQ

M.B. Abdillah †, P. Ausset, Institut de Physique Nucléaire, IPN, Orsay, France
R.Ferdinand, Grand Accélerateur National d'Ions Lourds, GANIL, Caen, France

Abstract

SPIRAL2 project is based on a multi-beam superconducting LINAC designed to accelerate 5 mA deuteron beams up to 40 MeV, proton beams up to 33 MeV and 1 mA light and heavy ions (Q/A = 1/3) up to 14.5 MeV/A. The accurate tuning of the LINAC is essential for the operation of SPIRAL2 and requires measurement of the beam transverse position, the phase of the beam with respect to the radiofrequency voltage, the ellipticity of the beam and the beam energy with the help of Beam Position Monitor (BPM) system. The commissioning of the RFQ gave us the opportunity to install two BPM sensors, associated with their electronics, mounted on a test bench. The test bench is a D-plate fully equipped with a complete set of beam diagnostic equipment in order to characterize as completely as possible the beam delivered by the RFQ and to gain experience with the behaviour of these diagnostics under beam operation. This paper addresses the measurements carried with the two BPMs on the Dplate: energy, transverse position and ellipticity under 750 keV proton beam operation.

GENERAL DESCRIPTION OF SPIRAL2

SPIRAL2 facility is being installed in Caen, France. It includes a multi-beam driver accelerator (5mA/40Mev deuterons, 5mA/14.5MeV/A heavy ions). The injector is constituted by an ECR ion source (Q/A= 1/3), an ECR deuteron/proton source, a low energy beam line (LEBT) followed by a room temperature RFQ which accelerates beam up to an energy of 0,75MeV/u. A medium energy line (MEBT) transfers the beam to the superconducting Linac.

The Linac is composed of 19 cryomodules: 12 contain one $\beta = 0.07$ cavity and 7 contain two $\beta = 0.12$ cavities. The cavities operate at $F_{acc} = 88.0525$MHz.

Main beams accelerated by the superconducting Linac are mentioned in table 1.

Table 1: SPIRAL2 Main Beams Parameters

Particle	Current(mA)	Energy(MeV/u)
Proton	0.15-5	2 -33
Deuteron	0.15-5	2 -20
Q/A = 1/3	0.15-1	2 -14.5
Q/A = 1/6	0.15-1	2 -8

SPIRAL2 nominal mode of operation is planned to be C.W. mode. The considerations on commissioning and tuning periods of the LINAC lead to a pulsed mode operation in order to minimize the mean power of the beam. The shortest duration of a macro-pulse will be 100 µs. The repetition period varies from 1ms to 1s. The intermediate configurations have to be taken in account in order to reach the C.W. operation. The step to increase or decrease either the macro pulse duration or the repetition rate will be 1µs.

SPIRAL2 BEAM POSITION MONITORS

A doublet of magnetic quadrupoles is placed between the cryomodules for the horizontal and vertical transverse focusing of the beam. Beam Position Monitors (BPMs), of the electrostatic type, is inserted in the vacuum pipe located inside the quadrupoles of the LINAC.

20 BPMs are installed along the SPIRAL2 linac. They enable the measurement of Beam transverse position, phase and transverse beam ellipticity as defined in [1]. The combination of the measured phases of two adjacent BPMs enables the measurement of Beam energy.

SPIRAL2 BPM [1] is composed of 4 capacitive sensors. Each BPM was characterized on a dedicated test bench based on a coaxial transmission line. The characterization delivers BPM electrical centre coordinates, position and ellipticity sensitivities and offsets at $\beta \approx 1$ [2].

Each BPM sensor feeds an electronic module through 23 meters long coaxial cables. The 20 BPM electronics modules are located in four VME 64x crates. Each module contains an analog and a digital board. The design of the analog module of the card is based on the scheme of auto-gain equalization using offset tone having frequency slightly offset from the RF reference [3]. The electronic module works either at F=88.0525 MHz or at 2*F=176.1050 MHz to deliver the required information.

Two prototypes of the BPM readout electronics module were qualified in IPN leading to several upgrades in order to meet specifications. Series of 22 electronic modules is presently under qualification at IPN.

THE SPIRAL2 INTERMEDIATE TEST BENCH (SP2-ITB)

An "Intermediate Tests Bench" (ITB) has been assembled as part of the injector commissioning plan [4]. The ITB is positioned after the focusing quadrupole following the first re-buncher of the M.E.B.T. Two other focusing quadrupoles are placed between the re-buncher, and the RFQ. A beam stopper able to withstand nearly the full power of the beam terminates the ITB which includes 18 beam diagnostics identical to the SPIRAL2 driver ones. The aim of the ITB is to fully characterize the properties of the beam accelerated by the RFQ and also to study the behaviour of these diagnostics. Figure 1 shows the ITB.

† abdillah@ipno.in2p3.fr

Content from this work may be used under the terms of the CC BY 3.0 licence (© 2018). Any distribution of this work must maintain attribution to the author(s), title of the work, publisher, and DOI.

ISBN: 978-3-95450-201-1 doi:10.18429/JACoW-IBIC2018-TUPB04

DEVELOPMENT OF A NEW BUTTON BEAM-POSITION MONITOR FOR BESSY VSR*

J.-G. Hwang †, G. Schiwietz, A. Schälicke, M. Ries, V. Dürr, D. Wolk
Helmholtz-Zentrum Berlin für Materialien und Energie GmbH (HZB), Berlin, Germany

Abstract

An extreme operation mode such as the BESSY-VSR conditions stimulates the development of a high accuracy bunch-by-bunch beam-position monitor (BPM) system which is compatible with the bunch-selective operation for the orbit feedback system. Such a system will also greatly benefit to accelerator R&D such as transverse resonance island buckets (TRIBs). Compensation of the long-range ringing signal produced by the combined effect of impedance mismatching inside the button and trapped TE-modes in the aluminum-oxide insulator (Al_2O_3) material is required essentially to improve the resolution. This is important since the ringing causes a misreading of the beam position and current of following bunches. We show the design study of a new button-type BPM to mitigate the influence of the ringing signal as well as to reduce wake losses by improving the impedance matching in the button and by replacing the insulator material.

INTRODUCTION

Since 2017, the Helmholtz-Zentrum Berlin launches the BESSY variable-pulse-length storage ring (BESSY VSR) project which is an upgrade project of the existing storage ring of BESSY II to fulfill the future increasing demands to study sub-picosecond, picosecond and longer dynamics in complex systems. This is feasible by installing additional superconducting cavities with harmonic frequencies of 1.5 GHz and 1.75 GHz [1]. The cavities will be installed in a straight section of BESSY II to create long and short photon pulses simultaneously for all beam lines. This also provides a high degree of flexibility in a bunch filling pattern. Potentially, it will lead to more complex filling patterns, such as shown in Fig. 1 [2].

The filling pattern, however, has the disparity in the beam current of long and short bunches since the long bunch buckets have relatively high bunch charge to preserve the present average brilliance of BESSY II. The short bunches are added to relax beam lifetime and to supply THz power as well as high repetition rate short X-ray pulses.

PRESENT BESSY II BUTTON BPM

From the measurement of the present button-type beam position monitor (BPM) signal with 1 mA single bunch with 1.25 MHz revolution frequency in the BESSY storage ring, we observed long-range and strong trapped modes inside the BPM. The trapped modes are also not fully damped

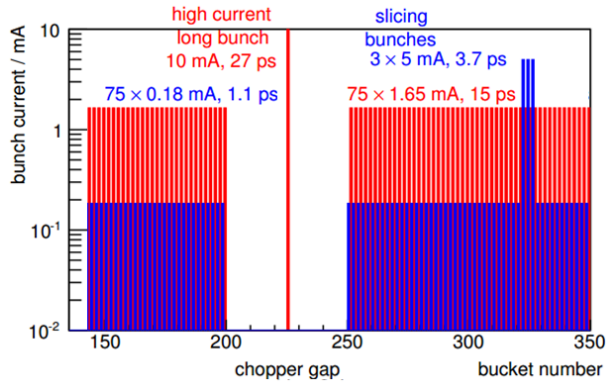

Figure 1: Section of a possible filling pattern with short bunches (blue) and long bunches (red). Trains of short bunches are added to supply THz power as well as high repetition rate short x-ray pulses.

within 2 ns, which corresponds to the bunch spacing in the ring, and it causes a signal superposition for neighboring bunches. Especially, the future filling pattern which has a large disparity in the beam charge between the short and long bunches such as BESSY VSR can cause a misreading of the beam position of the short (low-intensity) bunches. The measured BPM signal during single-bunch operation is shown in Fig. 2.

In the spectrum of the measured BPM signal, two strong trapped modes are present at the frequencies of 5.2 GHz and 5.5 GHz. Since the desirable transverse electromagnetic (TEM) mode is allowed to propagate at all frequencies, but at frequencies above the cutoff frequency (f_{cut}), the first higher-order mode (TE_{11}) is also allowed to propagate. The low-frequency cutoff for the undesired TE_{m1}-mode in a coaxial waveguide can be defined as [3]

$$f_{\mathrm{cut}}^{\mathrm{TE}_{m1}} = \frac{1}{\sqrt{\epsilon_r}} \frac{c}{\pi} \frac{m}{r_i + r_o}, \qquad (1)$$

where r_i and r_o are the radii of the inner and outer conductors, respectively, $m = 1, 2, 3, \ldots$, which indicates the field variation in azimuthal direction, and ϵ_r is dielectric constant. Since the f_{cut} in a coaxial waveguide is inversely proportional to the square root of a dielectric constant of the insulator, the button has minimum f_{cut} value at the insulator.

In the BESSY II, the present button BPM has a diameter of 10.8 mm and gap of 0.3 mm. The thickness of button electrode is 2.6 mm and an aluminium oxide (Al_2O_3) insulator with the diameter of 11.4 mm and thickness of 3 mm was used for a vacuum seal. Therefore, the cutoff frequency at the insulator is 5 GHz. The source of the trapped mode is

* Work supported by German Bundesministerium für Bildung und Forschung, Land Berlin, and grants of Helmholtz Association.
† ji-gwang.hwang@helmholtz-berlin.de

Content from this work may be used under the terms of the CC BY 3.0 licence (© 2018). Any distribution of this work must maintain attribution to the author(s), title of the work, publisher, and DOI.

ISBN: 978-3-95450-201-1 doi:10.18429/JACoW-IBIC2018-TUPB05

DESIGN OF A CAVITY BEAM POSITION MONITOR FOR THE ARES ACCELERATOR AT DESY

D. Lipka*, M. Dohlus, M. Marx, S. Vilcins, M. Werner, DESY, Hamburg, Germany

Abstract

The SINBAD facility (Short and INnovative Bunches and Accelerators at DESY) is foreseen to host various experiments in the field of production of ultra-short electron bunches and novel high gradient acceleration techniques. The SINBAD linac, also called ARES (Accelerator Research Experiment at SINBAD), will be a conventional S-band linear RF accelerator allowing the production of low charge (within a range between 0.5 pC and 1000 pC) electron bunches. To detect the position of low charge bunches, a cavity beam position monitor is being designed based on the experience from the European XFEL. It will consist of a stainless steel body with a quality factor of 70, a resonance frequency of 3.3 GHz and a relative wide gap of 15 mm to reach a high position sensitivity of 4.25 V/(nC mm) of the dipole resonator. The design considerations and simulation results of the dipole and reference resonator will be presented.

INTRODUCTION

SINBAD is a dedicated accelerator R&D facility currently under construction at DESY, Hamburg, and will host the ARES linac (Accelerator Research Experiment at SINBAD). It will consist of a normal conducting photo-injector and a 100 MeV S-band linear accelerator with beam repetition rates between 10 and 50 Hz for the production of low charge beams (0.5–30 pC) with (sub-) fs duration and excellent arrival time stability [1–3]. For dedicated user experiments bunch charges up to 1000 pC are foreseen. To observe the beam transverse position with highest precision the requirements include a resolution of 5 µm for a beam charge between 5 and 100 pC. To achieve this requirement a cavity beam position monitor (CBPM) is developed.

DESIGN

For the general design the resonance frequency and quality factor have to be chosen for the dipole and reference resonator of the CBPM. Both parameters should be similar for the dipole and reference resonator to simplify the signal processing. Since the inner tube diameter is 34 mm with a cut-off frequency of 6.75 GHz the resonance frequency should be smaller. To receive a reliable resonance field with this tube diameter a resonance frequency of $f = 3.3$ GHz is defined. The relative low beam repetition rate would allow to use a long *ringing* signal to analyze the waveform. Therefore a relative high quality factor with a long decay time could be applied. But the voltage amplitude and following the sensitivity would be small therefore a low loaded quality factor of $Q_L = 70$ is chosen which results in a bandwidth of 47 MHz. This allows a monitor production in stainless steel. The basic design is depicted from the SACLA facility [4] which was modified for the European XFEL [5]. The quality factor and resonance frequency of the new design are similar to the European XFEL CBPMs for synergy but with other tube diameter and resonator thickness of the dipole resonator.

Dipole Resonator

The TM_{11} mode of the dipole resonator provides a signal proportional to beam offset and charge. The amplitude sensitivity $S = \pi f \sqrt{\frac{Z}{Q_{\text{ext}}}\left(\frac{R}{Q}\right)}$ [1] [6], with the line impedance $Z = 50\,\Omega$ and the normalized shunt impedance $\left(\frac{R}{Q}\right)$, is increased by a relative small external quality factor Q_{ext}. The antenna position defines the value of the external quality factor; a low value dominates the loaded quality factor because $\frac{1}{Q_L} = \frac{1}{Q_{\text{ext}}} + \frac{1}{Q_0}$ with Q_0 the internal quality factor (which is still relative large compared to Q_{ext} for stainless steel). To obtain a larger sensitivity the normalized shunt impedance can be increased by using a large resonator thickness l because $\left(\frac{R}{Q}\right) \propto l$ [7], in this design $l = 15$ mm is applied. The Eigenmode solver of the simulation tool CST [8] is used to design and investigate the resonator properties. The resulting geometry is shown in Figs. 1 and 2.

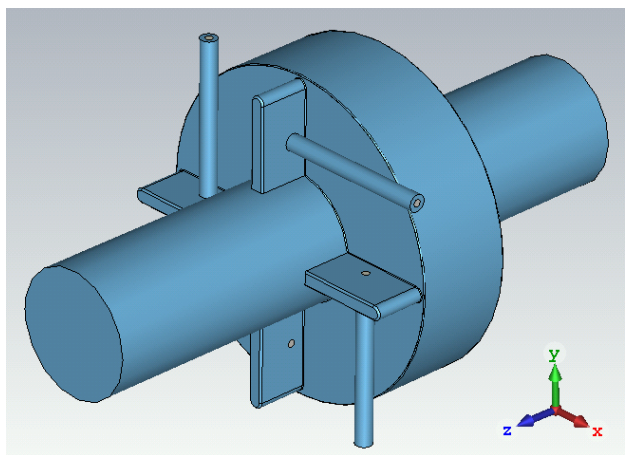

Figure 1: 3-dimensional simulation view of the vacuum part of the dipole resonator.

The resonator has a kink to decrease the resonator diameter which bends the dipole field. This is an advantage for a smaller overall monitor transverse size. The dipole field is propagating into the four slots where the dominating

* dirk.lipka@desy.de

[1] The development of this equation is described in the appendix.

Content from this work may be used under the terms of the CC BY 3.0 licence (© 2018). Any distribution of this work must maintain attribution to the author(s), title of the work, publisher, and DOI.

ISBN: 978-3-95450-201-1 doi:10.18429/JACoW-IBIC2018-TUPB07

STABILITY STUDY OF BEAM POSITION MEASUREMENT BASED ON HIGHER ORDER MODE SIGNALS AT FLASH

J. H. Wei†, NSRL, University of Science and Technology of China, 230026 Hefei, P. R. China
and Deutsches Elektronen-Synchrotron, 22607 Hamburg, Germany
L. Shi, Paul Scherrer Institut, 5232 Villigen PSI, Switzerland
N. Baboi, Deutsches Elektronen-Synchrotron, 22607 Hamburg, Germany

Abstract

FLASH is a free-electron laser driven by a superconducting linac at DESY in Hamburg. It generates high-brilliance XUV and soft X-ray pulses by SASE (Self Amplified Spontaneous Emission). Many accelerating cavities are equipped with HOMBPMs (Higher Order Mode based Beam Position Monitors) to align the beam and monitor the transverse beam position. However, these lose their position prediction ability over time. In this paper, we applied an efficient measurement and signal analysis with various data process methods including PLS (Partial Least Square) and SVD (Singular Value Decomposition) to determine the transverse beam position. By fitting the HOM signals with a genetic algorithm, we implemented a new HOMBPM calibration procedure and obtained reliable beam prediction positions over a long time. A stable RMS error of about 0.2 mm by using the spectra of signals and 0.15 mm by using the new method over two months has been observed.

INTRODUCTION

FLASH [1] was originally a test facility for various physics studies of the superconducting technologies. It serves nowadays as a Free Electron Laser (FEL) user facility as well as a test facility for advanced Linac facilities such as the European XFEL and ILC. Figure 1 shows the schematic layout of FLASH with three beam lines. FLASH1, FLASH2 are used for generation of high brilliance ultra-short ultraviolet (XUV) and soft X-ray pulses. They are able to provide a beam for two experiments simultaneously. The third beamline accommodates FLASH-Forward, a beam-driven plasma-wakefield experiment. There are seven accelerating cryo-modules along the linac. Each module contains eight TESLA superconducting cavities with 1.3 GHz working frequency. There is also one module with four 3.9 GHz cavities to linearize the energy chirp induced by the first accelerating module in the longitudinal phase space.

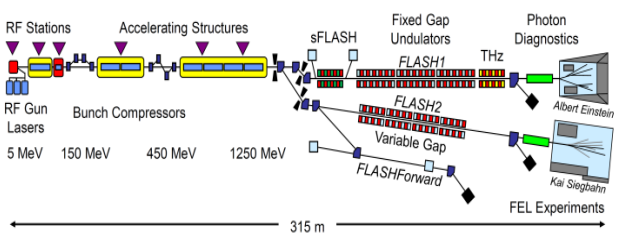

Figure 1: Schematic layout of FLASH [1].

† junhao.wei@desy.de.

When an electron beam passes through the cavities, it excites wakefields, which can deteriorate the beam quality and may result in a beam-break-up instability in the worst case [2]. Therefore two couplers installed at both sides of the TESLA cavity are specially designed to extract them (see Fig. 2). The wakefields can be expanded as a multipole series of so-called modes. The modes with higher frequency than the accelerating mode are named Higher Order Modes (HOMs). Among these, dipole modes can be utilised to determine the beam position since their amplitude has linear dependence on the beam offset. Based on this, a HOMBPM system was built. A 4 μm resolution rms was observed in one cavity [3]. However, the beam position readout calibration is unstable over time [4]. In order to solve this problem, we use a method based on genetic algorithm (GA) to fit the beam excited signals. After that, several methods are applied to predict the beam position.

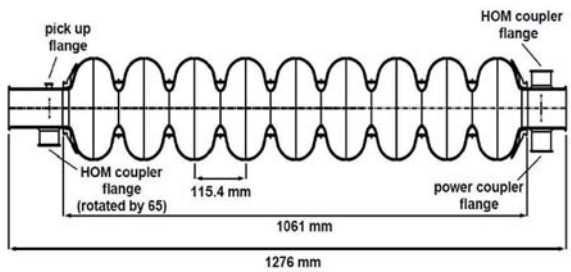

Figure 2: Drawing of the TESLA cavity with nine cells, one power input coupler, one probe antenna and two HOM couplers.

Next section introduces the measurement principle of the dipole mode signal and the GA fitting procedure. The following section presents the results of the HOMBPMs in several cavities with different calibration methods. The paper ends with conclusions.

DIPOLE MODE SIGNAL

The dipole mode signal from the HOM ports excited by a traversing bunch can be affected by four beam parameters: the bunch charge, the trajectory offset, the trajectory tilt and the bunch tilt [5]. For short bunches, as is the case at FLASH, the bunch tilt signals are vanishingly small compared with beam offset signals. A 5 mrad trajectory tilt will excite the signal with the same amplitude as 1 mm bunch offset for 1.3 GHz cavities [6]. In our measurement, the

Content from this work may be used under the terms of the CC BY 3.0 licence (© 2018). Any distribution of this work must maintain attribution to the author(s), title of the work, publisher, and DOI.

ISBN: 978-3-95450-201-1 doi:10.18429/JACoW-IBIC2018-TUPB09

THE EVALUATION OF BEAM INCLINATION ANGLE ON THE CAVITY BPM POSITION MEASUREMENT*

J. Chen[1], Y. B. Leng†, L. Y. Yu, L. W. Lai, R. X. Yuan
Shanghai Institute of Applied Physics, Chinese Academy of Science, 201204 Shanghai, China
[1]also at University of the Chinese Academy of Science, 100049 Beijing, China

Abstract

Cavity beam position monitor (CBPM) is widely used to measure the transverse position in free-electron laser (FEL) and international linear collider (ILC) facilities due to the characteristic of high sensitive. In order to study the limiting factors of the position resolution of cavity BPM, the influence of beam inclination angle on the measurement of CBPM position and the direction of beam deflection was analyzed. The simulation results show that the beam inclination angle is an important factor limiting the superiority of CBPM with extremely high position resolution. The relative beam experiments to change the relative inclination angle between the cavity and the electron beam based on the kicker were performed in Shanghai Soft X-ray FEL (SXFEL) facility, the experiment results will also be mentioned as well.

INTRODUCTION

The free electron laser (FEL) is a fourth-generation light source based on the interaction between electromagnetic fields and ultra-relativistic electron bunches which travel along the axis of a vacuum beam-pipe. In order to achieve high efficiency operation of FEL, the electron beam and the generated photo beam need to be overlapped strictly and that both can pass through the entire undulator section. Therefore, requirements on the BPM system for the FEL are very stringent, especially on position stability.

Cavity BPM systems [1] adopt a resonant cavity structure and through the use of anti-symmetric characteristic mode, coupled from the cavity, to measure the beam position which can meet that requirements, so it is widely used in FEL facilities. In order to maximize the advantages of cavity BPM with extremely high-resolution, a detailed analysis of the limiting factors affecting CBPM performances is needed, especially the effect of beam inclination angle on CBPM performance. Based on this purpose, the influence of beam trajectory angle on the amplitude of position signal and the direction judgement of beam position was simulated in this paper.

Shanghai soft X-ray FEL facility is a user experiment facility with an expected capacity to generate 9-nm X-ray laser by adopting an FEL frequency doubling of ultraviolet band seeded laser of 265 nm. A total of 20 CBPM systems are installed in the undulator section for the beam position measurement. Therefore, SXFEL is also an excellent test platform for experiment verification of beam trajectory angle simulation which mentioned above. Detailed calculation principles, simulation results and online beam verification results will be given in the following sections.

CALCULATION PRINCIPLE

In order to calculate the signal intensity generated when the beam trajectory has an angle through the cavity, a method of dividing a large cavity into a plurality of small cavities is adopted. As shown in Fig. 1. The position of the bunch in each small cavity can be considered to be parallel to the Z axis. Then, all the small cavities can be integrated to obtain the signal intensity when the beam has an angle and pass through the entire cavity.

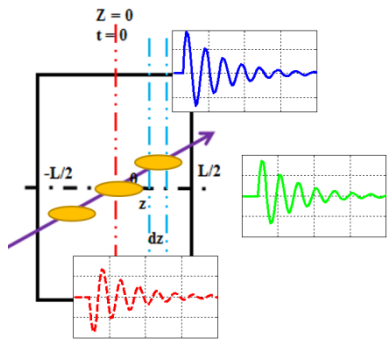

Figure 1: Model of cavity segmentation.

When the beam is parallel to the Z axis and the distance from the electrical center is x, the cavity excitation signal can be expressed by Eq.(1):

$$V_p = \frac{\omega q}{2}\sqrt{\frac{Z}{Q_{ext}}[\frac{R}{Q}]_0} * e^{-\frac{\omega^2\sigma_z^2}{c^2}} * \frac{x}{x_0} * e^{-\frac{t}{2\tau}} * \sin(\omega t) \qquad (1)$$

Assume that the length of the bunch is constant during this process, the cavity parameters are also fixed, and the constant term can be separated, it can expressed by Eq. (2) briefly:

$$V_p = Ax * e^{-\frac{t}{2\tau}} * \sin(\omega t) \qquad (2)$$

When the beam passes through the center of the cavity but with an inclination angle θ, the excitation voltage of the small cavity whose cavity length is dz can be written by Eq. (3):

$$dv = A * z * \tan(\theta) * e^{-\frac{t}{2\tau}} * \sin(\omega t) * \frac{dz}{L} \qquad (3)$$

So the signal intensity when the beam has an angle θ and pass through the entire cavity can be calculated by

*Work supported by The National Key Research and Development Program of China (Grant No. 2016YFA0401903, 2016YFA0401900)
†lengyongbin@sinap.ac.cn

Content from this work may be used under the terms of the CC BY 3.0 licence (© 2018). Any distribution of this work must maintain attribution to the author(s), title of the work, publisher, and DOI.

ISBN: 978-3-95450-201-1 doi:10.18429/JACoW-IBIC2018-TUPB10

DESIGN AND SIMULATION OF STRIPLINE BPM FOR HUST PROTON THERAPY FACILITY

J.Q. Li, K.J. Fan†, Q.S Chen, K. Tang, P. Tian
State Key Laboratory of Advanced Electromagnetic Engineering and Technology
Huazhong University of Science and Technology,
Wuhan 430074, China

Abstract

Proton beams used in Huazhong University of Science and Technology Proton Therapy Facility（HUST-PTF）have extreme low currents of the order of nanoampere，which is a great challenge to beam diagnostics due to low signal level. Conventional destructive beam diagnostic devices will affect the quality of the beam and cannot work online during the patient treatment, so a non-destructive stripline beam position monitor (BPM) is designed. This study will introduce some analysis and simulation results of the stripline BPM, such as the coupling between the electrodes, impedance matching, signal response, etc. We also discussed how to increase the output signal by geometry optimization.

INTRODUCTION

Huazhong University of Science and Technology Proton Therapy Facility（HUST-PTF）is a dedicated proton therapy facility [1]. As shown in Fig. 1, it is made up of a 250_MeV superconducting cyclotron, an energy selection system, two rotating gantries, the beam line and a fixed treatment room. The beam current becomes ultra low after the proton beam passes through a degrader, which is a great challenge to measure the beam position. The beam main parameters after the degrader are described in Tab.1. Conventional measurements, such as using an ionization chamber, will introduce some degradation of the beam energy dispersion. From experience of iThemba LABS [2], we plan to design a stripline BPM for HUST-PTF.

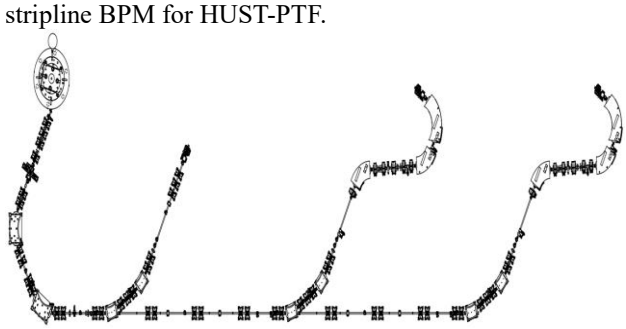

Figure 1: Layout of HUST-PTF.

* Work supported by national key R&D program,2016YFC0105303.
† email address:kjfan@hust.edu.cn

Table 1: Beam Parameters After a Degrader

Parameters	value
Bunch length	~200mm
Bunch frequency	73MHz
Bunch radius	2-10mm
Beam energy	70-230Mev
Average current	0.4-4nA

The stripline BPMs can be regarded as transmission-line circuits in microwave engineering. The schematic of stripline BPM is shown in Fig. 2. It is suited for short bunch measurement because the signal propagation is considered. When a Gaussian bunch passes through the BPM, the voltage signal of the upstream port is:

$$V_U(t)=\frac{\phi Z}{4\pi}\left(\exp\left(\frac{-(t+l/c)^2}{2\sigma^2}\right)-\exp\left(\frac{-(t-l/c)^2}{2\sigma^2}\right)\right)I_b(t) \quad (1)$$

Where σ represents bunch length. l represents electrode length. ϕ represents electrode radius. The frequency domain expression of the output signal can be written as:

$$V_U(\omega)=\frac{\phi Z}{\sqrt{2\pi}}I_b(\omega)\sin\left(\frac{\omega l}{c}\right) \quad (2)$$

$V_U(\omega)$ is made up of a series of maximum for $f=(2n-1)c/4l$. For a given electronic device the first voltage maxima is located at $l=c/4f$. Because of Libera Single Pass [3] we plan to work at 500_MHz ± 5_MHz in frequency domain, the electrode length is 150_mm to get the voltage maxima at 500_MHz.

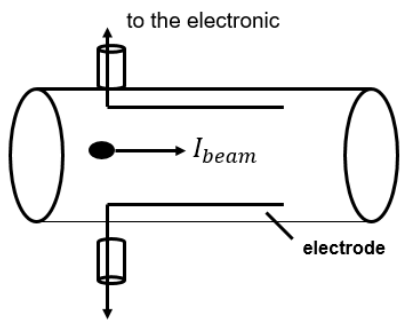

Figure 2: Schematic of stripline electrodes.

IMPEDANCE MATCHING

From Fig. 3 it is clear that the stripline BPM has four electrodes, which support four independent TEM modes, namely a sum mode, two dipole modes (horizontal dipole and vertical dipole), and a quadrupole mode. As shown in Figs. 4 and 5, the electrodes and vacuum pipe can be

Content from this work may be used under the terms of the CC BY 3.0 licence (© 2018). Any distribution of this work must maintain attribution to the author(s), title of the work, publisher, and DOI.

ISBN: 978-3-95450-201-1 doi:10.18429/JACoW-IBIC2018-TUPB12

MACHINE STUDIES WITH LIBERA INSTRUMENTS AT THE SLAC SPEAR3 ACCELERATORS*

S. Condamoor, D. Martin, S. Wallters, J. Corbett†, SLAC, Menlo Park, CA 94025, USA
Q. Lin, Donghua University, Shanghai, China
L. Lai, Shanghai Synchrotron Radiation Facility, Shanghai, China
P. Leban, M.Cargnelutti, Instrumentation Technologies, Solkan, Slovenia

Abstract

Turn-by-turn BPM readout electronics were tested on the SPEAR3 booster synchrotron and storage ring to identify possible improvements in data acquisition. For this purpose, Libera Spark [1] and Libera Brilliance+ [2] instruments were customized for the booster (358.4 MHz) and SPEAR3 storage ring (476.3 MHz) radio-frequencies, and tested during machine studies. Even at low single-bunch booster beam current, the dynamic range of the Libera Spark provided excellent transverse position resolution during the linac-to-booster beam capture process, the energy ramp phase and during beam extraction. Booster injection efficiency was analyzed as a function of linac S-band bunch train arrival time. In SPEAR3, turn-by-turn Libera Brilliance+ measurement capability was evaluated for single and multi-bunch fill patterns as a function of beam current. The single-turn measurement resolution was found to be better than 15 microns for a single 1.5 mA bunch. The horizontal single-bunch damping time was then observed with the 238 MHz bunch-by-bunch feedback system ON and OFF, and the multibunch fill pattern stability evaluated as a function of total beam current.

INTRODUCTION

SPEAR3 is a 3rd generation, 3 GeV synchrotron light source with 234 m circumference. The storage ring nominally operates with 500 mA circulating beam current and approximately 1.8 mA/bunch (1.4nC). Topup occurs every 5 minutes using about 50 pulses of single-bunch charge at a 10 Hz rate. The booster synchrotron features a 10 Hz resonant-driven White circuit with a 100 MeV to 3 GeV energy ramp in ~37 ms. Of significance, injection into the booster consists of about 7 S-band bunches selected from a 1 μs S-band bunch train produced in a thermionic RF electron gun. The S-band bunches are not phase-locked to the booster and the arrival time can vary due to thermal and electronic drift over time.

Libera BPM processor electronics were installed in the booster ring and in the SPEAR3 storage ring to study measurement performance under different beam conditions. The Libera Spark was configured for highest sensitivity and was able to accurately measure single bunch position during the 37 ms booster ramp phase. Analog signals from four booster BPM striplines were connected to the Libera Spark front end processor equipped with 352 MHz bandpass filters. The filters stretch the response which is then sampled by PLL-controlled ADCs clocked at 109.8 MHz. The baseband signals were sampled 49 times each revolution (1 turn=466 ns).

For SPEAR3 a Libera Brilliance+ module was installed to monitor beam position from a set of four botton-style BPM electrodes. In this case the sampling clock was 112.7 MHz and the baseband signal was sampled 88 times during the 781 ns revolution period. At this sampling rate the Brilliance+ module can resolve two diametrically opposite bunches separated by 390 ns in SPEAR3.

BOOSTER BPM MEASUREMENTS

The SPEAR3 charge transfer sequence starts in a 100 MeV linac followed by a 3 GeV booster and finally injected into SPEAR3 at a 10 Hz repetition rate every 5-minute topup cycle. At each 10 Hz injection event, the single-bunch booster beam is accelerated and extracted in about 37 ms.

The original 1990's-era booster BPM system consists of a commercial multiplexor that switches individual BPM button signals through an electronic peak detector followed by a sample-hold-digitization circuit chain. As a result, the measurement resolution for the electron beam position is sub-optimal and can only read the beam orbit every 1.5 ms during the energy ramp.

By introducing the Libera Spark module, it is now possible to measure the single bunch beam position turn-by-turn and with much higher resolution throughout the ramp. Figure 1 for example shows raw turn-by-turn data over three turns from one booster ring BPM pickup.

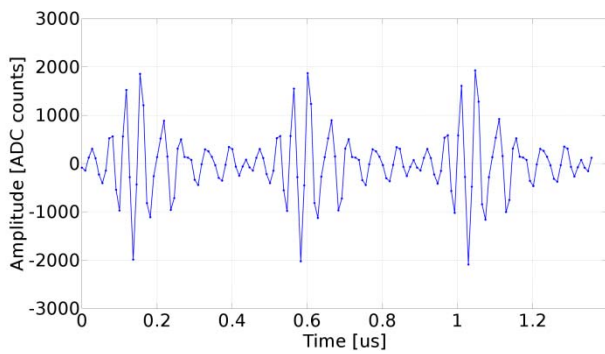

Figure 1: Three-turn single bunch measurement in the SPEAR3 booster ring.

Figure 2 shows the beam position and charge (SUM) throughout the full booster acceleration cycle. The turn-by-turn data was clocked using the injection timing trigger and processed in the time domain.

* Work sponsored by US Department of Energy Contract DE-AC03-76SF00515 and Office of Basic Energy Sciences, the China Scholarship Council and Instrumentation Technologies.
†corbett@slac.stanford.edu

Content from this work may be used under the terms of the CC BY 3.0 licence (© 2018). Any distribution of this work must maintain attribution to the author(s), title of the work, publisher, and DOI.

ISBN: 978-3-95450-201-1 doi:10.18429/JACoW-IBIC2018-TUPB13

STABILITY TESTS WITH PILOT-TONE BASED ELETTRA BPM RF FRONT END AND LIBERA ELECTRONICS

M. Cargnelutti*, P. Leban, M. Žnidarčič, Instrumentation Technologies, Solkan, Slovenia
S. Bassanese, G. Brajnik, S. Cleva, R. De Monte, Elettra-Sincrotrone Trieste, Trieste, Italy

Abstract

Long-term stability is one of the most important properties of the BPM readout system. Recent developments on pilot tone capable front end have been tested with an established BPM readout electronics. The goal was to demonstrate the effectiveness of the pilot tone compensation to varying external conditions. Simulated cable attenuation change and temperature variation of the readout electronics were confirmed to have no major effect to position data readout. The output signals from Elettra front end (carrier frequency and pilot tone frequency) were processed by a Libera Spark with the integrated standard front end which contains several filtering, attenuation and amplification stages. Tests were repeated with a modified instrument (optimized for pilot tone) to compare the long-term stability results. Findings show the pilot tone front end enables great features like self-diagnostics and cable-fault compensation as well as small improvement in the long-term stability. Measurement resolution is in range of 10 nanometers RMS in 5 Hz bandwidth.

INTRODUCTION

The recent developments about eBPMs analog front ends capable of pilot tone compensation [1,2] have shown a growing interest towards this topic. In order to verify the usefulness of this approach and its benefits with an existing BPM readout electronics, the eBPM analog front end developed at Elettra has been coupled with an Instrumentation Technologies' Libera Spark.

ELETTRA EBPM RF FRONT END

The front end is similar to the one presented at IBIC 2016 [2], but enhanced and re-engineered in a more compact solution. In the present version the low-noise PLL has been integrated in the box, together with diagnostic functionalities (voltage and temperature sensors) and complete Ethernet control. Figure 1 shows the block diagram of the system: a low-phase-noise PLL (7) generates the pilot tone (whose frequency and amplitude are programmable), which is split into four paths by a high-reverse-isolation splitter (6) that guarantees more than 52 dB of separation between the outputs. A coupler (2) sums the tone with the signal from the pick-ups, adding further 25 dB of isolation to prevent inter-channel crosstalk from the path of the pilot tone. At this point, all the signals pass through a bandpass filter (3), centered at 500 MHz with a bandwidth of 15 MHz, and two variable-gain stages, composed of low-noise, high-linearity amplifiers (5) (G=22 dB, F=0.5 dB, OIP3=+37 dBm, P1dB=+22 dBm) and

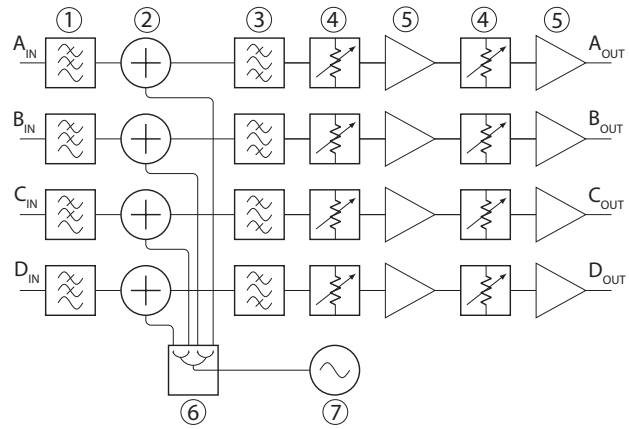

Figure 1: Analog front end block diagram.

Figure 2: Frequency response of the front end at full gain.

digitally controlled attenuators (4) (7 bits, up to 31.75 dB of attenuation, steps of 0.25 dB).

In order to achieve the expected results, the splitter must be temperature-insensitive, as well as the four couplers. Indeed, this architecture allows us to compensate the part of the system after the couplers, i. e. filters, attenuators, amplifiers. It has to be noted that being the front end a separate unit, it can be placed as near as possible to the pick-ups (tunnel area), with two main advantages: better signal-to-noise ratio and the possibility to compensate the cables (which are usually long). The frequency response of the front end is shown in Fig. 2.

LIBERA ELECTRONICS

Libera Spark was used to process the A, B, C and D signals from the Elettra eBPM analog front end. Libera Spark is

* manuel.cargnelutti@i-tech.si

Content from this work may be used under the terms of the CC BY 3.0 licence (© 2018). Any distribution of this work must maintain attribution to the author(s), title of the work, publisher, and DOI.

ISBN: 978-3-95450-201-1 doi:10.18429/JACoW-IBIC2018-TUPB14

NEW BEAM POSITION MONITORS FOR THE CERN LINAC3 TO LEIR ION BEAM TRANSFER LINE

G. Baud, M. Bozzolan, R. Scrivens, L. Søby
CERN, 1211, Geneva, Switzerland

Abstract

The ion injection line into the CERN Low Energy Ion Ring (LEIR) has recently been equipped with nine, new, electrostatic Beam Position Monitors (BPMs) in order to measure and optimize the trajectory of the low intensity ion beams coming from Linac3. In this paper, we describe the design of the BPM, the low noise charge amplifier mounted directly on the BPM, and the digital acquisition system. There is special emphasis on the first commissioning results where the measured beam positions were perturbed by EMI and charging of the BPM electrodes by secondary particles. The effect of mitigation measures, including repelling voltages on the electrodes and external magnetic fields, are also discussed.

INTRODUCTION

The CERN Linac3 provides heavy ions, mainly Pb^{54+} at an energy of 4.2MeV/u, to the Low Energy Ion Ring (LEIR). Here the ions (pulses of up to 30µA, 200µs) are accelerated to 72MeV/u, extracted to the PS and further to the SPS where the fully stripped ions are either extracted for fixed target physics, or transferred to the LHC for ion collisions. In order to optimize the injection efficiency into LEIR, the transfer line between Linac3 and LEIR has recently been equipped with nine highly sensitive electrostatic BPMs (Figure 1).

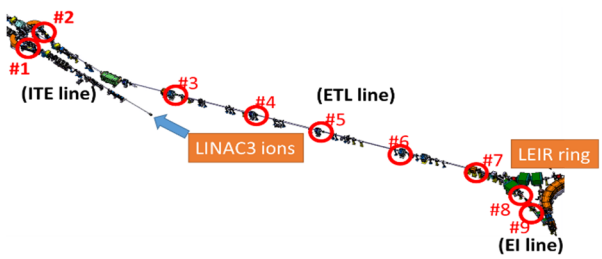

Figure 1: Linac3 to LEIR transfer line BPM layout.

BPM DESIGN

Table 1 summarises the BPM system specifications.

Table 1: BPM Specifications

Parameter	Value	Comment
Accuracy	0.5mm	-
Resolution	0.2mm	For 4uA current
Time resolution	1us	Along 200us pulse
Max. Beam displ.	±15 mm	-
Max beam current	50uA	-
Nb. of injections	1-13	Every 100-200ms

The BPMs are of a dual plane electrostatic type with an aperture of 196mm and a length of 200mm. The azimuthal width of the electrodes is 75° and the distance to ground is 21.5mm. The ~20pF electrodes are connected to high impedance charge amplifiers mounted directly onto the BPM body, via 75Ω cables, see Figure 2. The transfer impedance is about 30Ω yielding an electrode signal of ~0.1mV for a centred beam. All parts are of 316 LN stainless steel. The two BPMs nearest the LEIR ring have a non-evaporable getter (NEG) coating on the chamber walls to lower the overall vacuum level in this region.

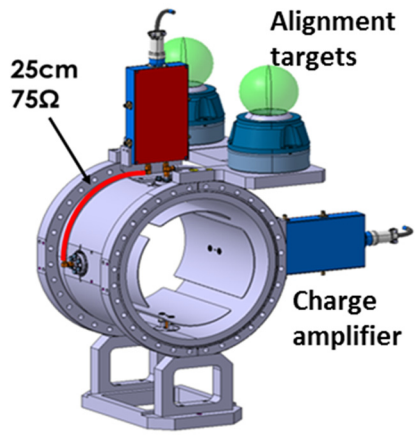

Figure 2: 3D model of the BPM.

ACQUISITION SYSTEM

Electronics

The input stage of the front-end electronics mounted directly on the BPMs is a charge amplifier. Gain calibration is performed by injecting a known charge into each input through a low capacitance calibration capacitor (1pF). After charge amplification, further amplifier stages generate the sum (3×10^{12} V/C gain) and difference (6×10^{12} V/C gain) signals. The -3dB bandwidth is 60Hz to 2MHz. A more detailed description of the head amplifier can be found in [1]. Coaxial cables transmit the signals to the control room where commercial, 8 channel, 12 bit Analogue to Digital Converters (ADCs) sample the signals.

Front-End Software: FESA

The Front-End Software Architecture (FESA) is a C++ framework used at CERN to design, develop, test and deploy real-time control software. It is used to provide software control and monitoring of the acquisition triggers, data read-out, processing and calibration. It also allows the data to be easily integrated with standard tools such as the beam steering Graphical User Interface (GUI) or long-term logging database.

Content from this work may be used under the terms of the CC BY 3.0 licence (© 2018). Any distribution of this work must maintain attribution to the author(s), title of the work, publisher, and DOI.

ISBN: 978-3-95450-201-1 doi:10.18429/JACoW-IBIC2018-TUPC01

AUSTRALIAN SYNCHROTRON BPM ELECTRONICS UPGRADE

Y.-R. E. Tan*, R. Hogan, Australian Synchrotron - ANSTO, Clayton, Australia

Abstract

The storage ring at the Australian Synchrotron (AS) had been originally equipped with 98 Libera Electrons. In late 2017 the all 98 of the BPM electronics has been upgraded to Libera Brilliance+. This report will outline plans that were put in place for the transition and the results from commissioning the new system.

INTRODUCTION

The Australian Synchrotron (AS) is a 3rd generation light source that was commissioned in 2006. The storage ring is a Chassman-Green lattice with 14 sectors each equipped with 7 Beam Position Monitors (BPMs) connected to Instrumentation Technology's Libera Electrons (98 Electrons) [1–3]. The booster ring is a FODO lattice with 4 sectors each equipped with 8 BPMs connected to Bergoz MX processors that is then digitized by NI DAQ cards [4]. Since an upgrade to the booster BPM system in 2010 increasing hardware problems has resulted in a continuous decline in the number of usable BPMs. Simultaneously, between 2013 and 2016 the Libera Electrons in the storage ring began to display an increasing number of hardware problems. In 2016 the decision was made to replace the storage ring Libera Electrons with Brilliance+ electronics [5] and to re-purpose the Libera Electrons in the booster ring.

Additional improvements to the system has also been the integration of the Brilliance+ directly into the Micro-Research Timing Event system with the EVR module and the option to increase the fast acquisition (FA) data rate from 10 kHz to 30 kHz. The increase in the FA data rate was added to push the performance of our Fast Orbit Feedback System (FOFB) [6] by reducing the group delay of the FA data.

PERFORMANCE MEASUREMENTS

To get the Libera Brilliance+ units ready for installation and to confirm that the performance met the requirements a initial configuration script and acceptance testing script were used. The configuration script configured the Linux subsystem to use some of the standards at the AS. The acceptance test script confirmed that the basic functionality was working such as locking to the machine clock and the unit was correctly reading the event data stream. The script would sweep the input power to each of the BPM cards in the Brilliance+ unit from −2 dB to −63 dB (Instrumentation Technology RF clock generator and power splitter) and log the position data at Turn-by-Turn (TbT; 1.389 MHz) and FA data rates (10 kHz) at different power levels. The average and spread of $\sigma_{x,y}$ across 110 cards is shown in Fig. 1.

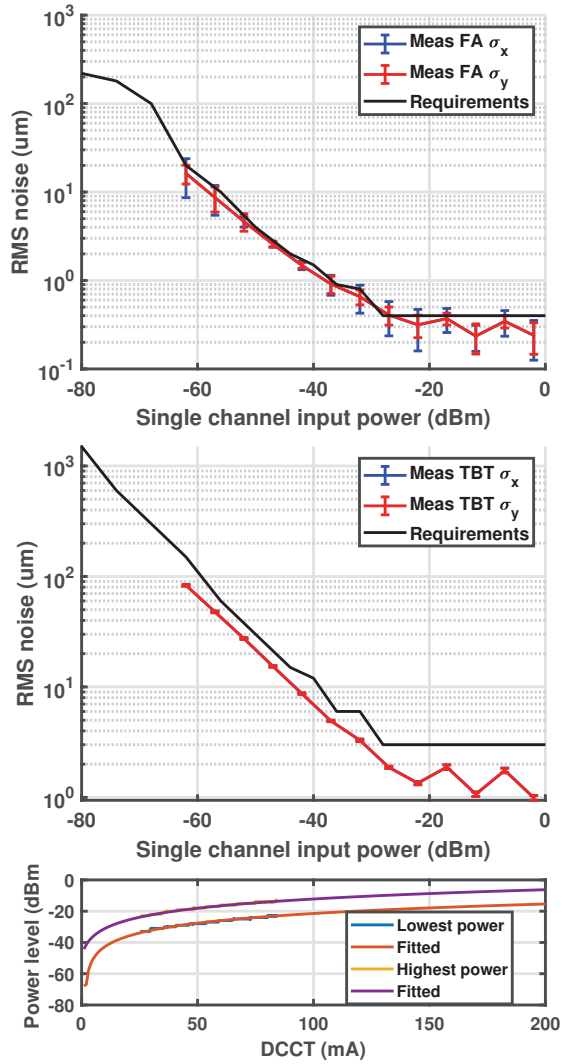

Figure 1: The average and spread of $\sigma_{x,y}$ across 110 BPM modules measured at TbT (1.389 MHz) and FA (10 kHz) data rates. The spread of the FA data rate is higher than expected where there was not enough time allowed for the digital signal conditioning learning cycle to complete before taking measurements. The corresponding input power graphs shows that below 30 mA the position resolution starts to increase.

The beam current/input power dependence was measured at the FA data rate and shown to be less than 1 µm from −60 dBm to −5 dBm which covers the range from 5 mA up to 200 mA in the storage ring.

The temperature dependence was measured by restricting the air flow to the crate, causing a 10 degree change in temperature. Using the internal airflow temperature sensors the temperature dependence was found to be an average of 0.8 µm/°C (switching enabled) and 0.4 µm/°C (switching

* eugene.tan@ansto.gov.au

Content from this work may be used under the terms of the CC BY 3.0 licence (© 2018). Any distribution of this work must maintain attribution to the author(s), title of the work, publisher, and DOI.

ISBN: 978-3-95450-201-1 doi:10.18429/JACoW-IBIC2018-TUPC03

BEAM QUALITY MONITORING SYSTEM IN THE HADES EXPERIMENT AT GSI USING CVD DIAMOND MATERIAL*

A. Rost[1†], J. Adamczewski-Musch[2], T. Galatyuk[1,2], S. Linev[2], J. Pietraszko[2], M. Traxler[2]
[1]Institut für Kernphysik, TU Darmstadt, Darmstadt, Germany
[2]GSI Helmholtzzentrum für Schwerionenforschung GmbH, Darmstadt, Germany

Abstract

In this contribution a beam monitoring system which consists of a chemical vapor deposition (CVD) diamond sensor, a fast readout electronics and a monitoring and visualization software used at GSI will be introduced. The sensor has been designed to measure the reaction time (T0) in the HADES Spectrometer, but also possesses beam quality monitoring capabilities which is of great importance to ensure high efficiency data recording. In the following, the diamond based sensor, its read-out chain and the online analysis and visualization software are described. Special emphasis will be put on an online visualization of important beam parameters namely the beam intensity, its position during extraction and the beam particle time structure.

INTRODUCTION

For experiments with the HADES [1] detector at GSI in Darmstadt and for the future CBM [2] experiment at the FAIR facility, radiation hard and fast beam detectors are required. The detectors should feature high rate capability, low interaction probability and perform precise T0 measurements ($\sigma_{T0} < 50$ ps). In addition, the sensors should offer beam monitoring capabilities. These tasks can be fulfilled by utilizing single-crystal Chemical Vapor Deposition (scCVD) diamond based detectors. This material is well known for its radiation hardness and high drift velocity of both electrons and holes, making it ideal not only as Time-of-Flight (ToF) detectors placed in the beam but also as luminosity monitors. With the help of striped read-out electrodes position information can be obtained for beam monitoring purposes. The main detector system used for this purpose in the HADES experiment consists of two diamond based sensors made of pcCVD and scCVD materials. Both sensors are equipped with a double-sided strip segmented metallization (300 µm width) which allows a precise position determination of the beam position. Those sensors are able to deliver a time precision <100 ps RMS and can handle rate capabilities up to 10^7 particles/channel. Having the precise time measurement and precise position information of the incoming beam ions one can monitor important beam parameters namely the beam intensity, its position during extraction and the beam particle time structure. The read-out of the sensors is based on the NINO [3] chip in combination with the already well established TRB3 (Trigger Readout Board - Version 3) platform [4], developed by the TRB Collaboration [5]. On this platform high precision multi-hit TDCs (up to 264 channels, time precision <10 ps RMS) are implemented inside FPGAs. The TRB3 system serves as a fast and flexible Data Acquisition System (DAQ) with integrated scaler capability. The analysis and online visualization is performed using the Data Acquisition Backbone Core (DABC) [6] framework.

CVD DIAMOND BASED BEAM DETECTOR

The detector, which is used in HADES in order to construct the reaction time determination (T0) and beam quality monitoring, is made of single crystal chemical vapor deposition (scCVD) diamond material with an active area of 4.7 mm × 4.7 mm. The sample thickness of 70 µm is chosen in order to reduce the nuclear interaction probability of the beam ions in the detector material. For example for an Au beam at 1.25 AGeV the interaction probability is about 0.36 %. The sensor is metalized with a 50 nm Cr layer, annealed at 500 °C for 10 min, deposited on the scCVD diamond and covered by a 150 nm Au layer. A similar detector [7] was used as T0 sensor in HADES for a $^{197}Au^{69+}$ beam, with a kinetic energy of 1.25 AGeV and currents between 10^6–10^7 ions/s delivered from the SIS 18 accelerator. The metallization is arranged in 16 strips (each 300 µm wide) on each side which allows a beam profile measurements in x and y directions. A close-up picture of the multi-strip segmentation of the diamond based sensor is shown on in Fig. 1.

The diamond sensor is glued to a Printed Circuit Board (PCB), which serves as a holder and provides electrical con-

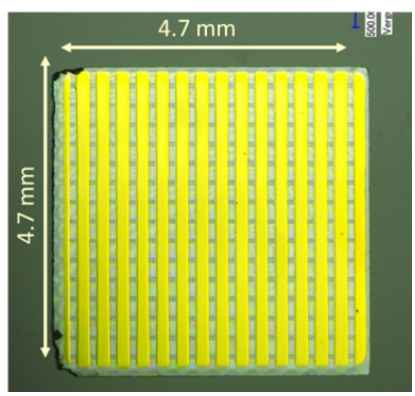

Figure 1: Close-up photography of the scCVD diamond based sensor. The metallization is arranged in 16 strips (each 300 µm wide) on each side which allows beam profile measurements.

* Work supported by the DFG through GRK 2128 and VH-NG-823.
† a.rost@gsi.de

Content from this work may be used under the terms of the CC BY 3.0 licence (© 2018). Any distribution of this work must maintain attribution to the author(s), title of the work, publisher, and DOI.

ISBN: 978-3-95450-201-1 doi:10.18429/JACoW-IBIC2018-TUPC04

BPM SYSTEM UPGRADE AT COSY

I. Bekman, C. Böhme, V. Kamerdzhiev, B. Lorentz, S. Merzliakov,
P. Niedermayer, K. Reimers, M. Simon, M. Thelen
FZJ, Jülich, Germany

Abstract

The beam position monitoring system of the Cooler Synchrotron (COSY) has been upgraded in 2017. The upgrade was driven by the requirement of the JEDI collaboration to significantly improve the orbit control and by the electronics approaching end-of-life. The entire signal processing chain has been replaced. The new low noise amplifiers, mounted directly on the BPM vacuum feedthroughs, were developed in-house and include adjustable gain in 80 dB rage and in-situ test and calibration capabilities. The signals are digitized and processed by means of commercial BPM signal processing units featuring embedded EPICS IOC. The decision path, technical details of the upgrade and performance of the new system are presented.

INTRODUCTION

The necessity of upgrading the COSY Beam Position Monitor (BPM) system arose from the requirement of the JEDI collaboration to significantly improve the beam orbit control and by the electronics approaching end-of-life. The upgrade affected all electronics sub-systems: amplifiers and their control, data collection and processing, networks, and the way measurement results are stored and presented. New sub-systems were added, for example, the calibration sub-system utilizing in-situ test signal generation and fine control of amplifier gain and as the main part - the Hadron Beam Position Processor Libera. Below the block-diagram (Fig. 1) and a brief description of the main components of BPM system are presented. 31 capacitive BPM are installed in the COSY ring. This number includes two BPM of the 2 MeV electron cooler which are also capable of measuring proton orbit. These are not affected by the upgrade presented here. Each COSY BPM utilizes 4 electrically isolated electrodes that make beam position measurements in both X and Y planes possible. The electrodes are connected via N-type vacuum feedthroughs to the amplifiers. Close to the amplifiers high precision ($4 \cdot 10^{-4}$) four-way splitters are placed to feed test signals from generators of the calibration sub-system into the amplifiers. The 116 amplified signals are transmitted from the tunnel via coaxial cables to eight Libera beam position processors [1] installed at 6 location in the accelerator hall (Fig. 2). The 19-inch racks house also the crates of the trigger system as well as additional crates accommodating the amplifier power supply and calibration sub-system. Newly developed graphical user interfaces based on Control System Studio allow for display of measured beam orbit and turn-by-turn data, amplifier gain control and calibration as well as provide additional software tools for display and control of Libera parameters, ADC data etc.

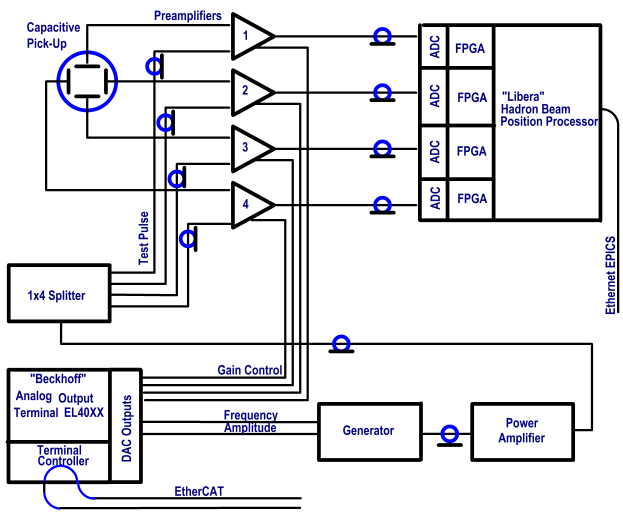

Figure 1: Block diagram of the new COSY BPM system. Only one pickup and corresponding electronics are shown.

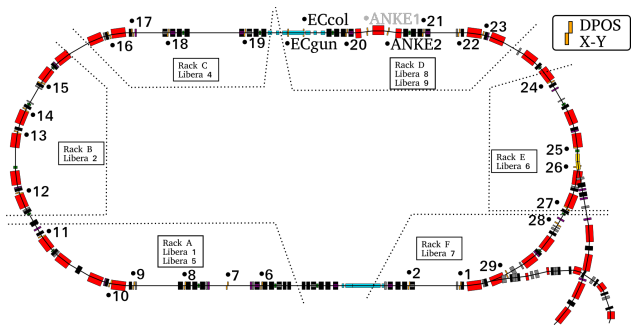

Figure 2: Operational BPM hardware around the COSY ring.

BPM AMPLIFIERS

The BPM amplifiers are housed in a 100·50·25 mm die-cast aluminum case and are installed directly on the vacuum feedthroughs. They are connected to the Libera beam position processors and the calibration sub-system. For analog signals RG214 coaxial cables are used. CAT 6 Ethernet cables are used to power the amplifiers and for gain control. Figure 3 shows the block diagram of a BPM amplifier.

Each unit consists of two stages: input stage and amplification stage. Table 1 summarizes the properties and performance of the input stage. The amplification stage is based on the variable gain amplifier chip AD8330 and features variable gain up to 80 dB. Control of the amplifier gain is done by means of commercial EtherCAT DACs.

Content from this work may be used under the terms of the CC BY 3.0 licence (© 2018). Any distribution of this work must maintain attribution to the author(s), title of the work, publisher, and DOI.

ISBN: 978-3-95450-201-1 doi:10.18429/JACoW-IBIC2018-TUPC05

INFLUENCE OF SAMPLING RATE AND PASSBAND ON THE PERFORMENCE OF STRIPLINE BPM

T. Wu[1], Y. B. Leng, L. W. Lai, S. S. Cao, J. Chen, F. Z. Chen, Y. M. Zhou,
Shanghai Institute of Applied Physics, Chinese Academy of Science, Shanghai, China
[1]also at University of the Chinese Academy of Science, 100049 Beijing, China

Abstract

It is obviously that the property of strip-line BPM is influenced by data acquisition system, but how the procedure of data acquisition and processing takes effect is still room for enquiring into it. This paper will present some data simulation and experiment results to discuss the function between resolution and passband, sampling rate or other influence factor. We hope that this paper would give some advice for building up data acquisition system of SBPM.

INTRODUCTION

Thanks to its compact design and high precision, SBPM is widely used for bunch position measurement just as what was in SXFEL [1]. As part of the modularization and generalization of the system, the digital BPM parameter settings used in SBPM measurements are the same as that in other part of beam diagnostics system. As a result, the analog signal measured by SBPM passes through a filter with a passband of 495 MHz-505 MHz, and then is undersampled by a sampling rate of 119 MHz and converted into a digital signal for subsequent processing.

The final measurement accuracy meets the need for beam position measurement of beam diagnostics system in SXFEL. However, With the improvement of machine performance requirements, the optimization of SBPM performance has gradually become more realistic and urgent. Under the premise that it is difficult to greatly optimize the performance of probes, it is a good choice to optimize the filter passband and sampling rate in electronics front-end design.

NUMERICAL SIMULATION

The corresponding signal and spectrum of strip-line BPM are showed below in Figure 1. We assume that the photon in the beam bunch Gaussian distribution, so as the signal waveform [2].

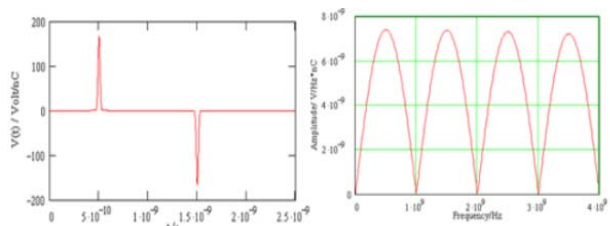

Figure 1: SBPM output signal(left) and the spectrum under the ideal conditions [3].

According to the spectrum, when center of the passband is nearing 500 MHz, the resolution would be optimal. That is the reason why passband is 490 MHz-510 MHz. But when put SBPM in a data measurement system, the conclusion may be different.

In SXFEL, the analog signal of SBPM will be transferred into digital signal before data processing [4]. Considering the influence of ADC, the spectrum of SBPM is shown in Figure 2.

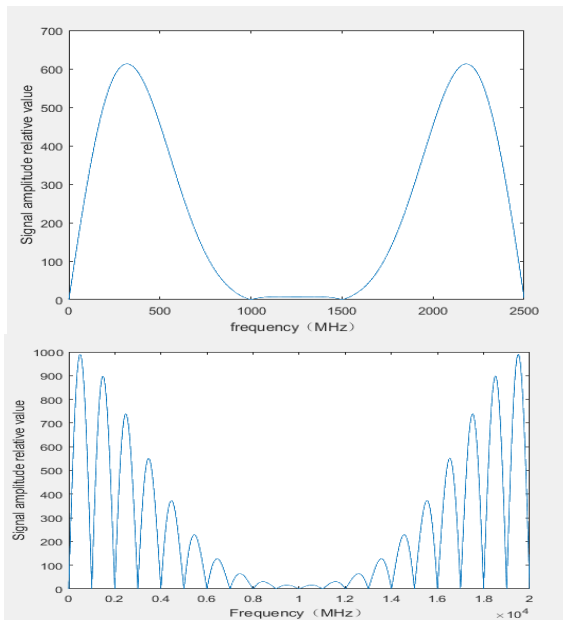

Figure 2: SBPM output spectrum influenced by ADC. Sampling rate are 2.5 GHz (top) or 10 GHz (bottom).

The result of numerical simulation reflects in one aspect how the sampling rate affects SBPM performance. 500 MHz is no longer the peak of the signal frequency after analog to digital conversion. Instead, a lower frequency takes its place. This phenomenon becomes more pronounced as the sampling rate of the ADC decreases. Considering undersampling, the spectral characteristics changes brought by ADC will be more complicated and need to be calculated according to the specific scheme [5].

The above is discussing the effect of the sampling rate on the peak of signal in frequency domain. On the other hand, the bandwidth of passband would also effect the resolution of SBPM. However, how it matters is more complicated. It depends on the noise composition. When the signal noise from SBPM probe is the main part of the

Content from this work may be used under the terms of the CC BY 3.0 licence (© 2018). Any distribution of this work must maintain attribution to the author(s), title of the work, publisher, and DOI.

ISBN: 978-3-95450-201-1 doi:10.18429/JACoW-IBIC2018-TUPC07

FIRST RESULTS OF BUTTON BPMS AT FRIB*

S. Cogan†, S. Lidia, J. Crisp, T. Ford, Facility for Rare Isotope Beams, East Lansing, MI, USA

Abstract

Commissioning and tuning the linac driver for the Facility for Rare Isotope Beams (FRIB) requires a large network of warm and cryogenic beam position monitors (BPMs), with apertures of 40 - 150 mm, sensitivity to beam currents of 100 nA to 1 mA, and accurate for beams with velocities as low as 0.03c. We present initial results of the BPM system, analog and digital signal processing, and energy measurements for low energy beams.

COMMISSIONING AND TUNING

The Facility for Rare Isotope Beams (FRIB) is a new scientific user facility for low energy nuclear science. Under construction on campus and operated by Michigan State University, FRIB will provide the highest intensity beams of rare isotopes available anywhere [1].

The accelerator is being commissioned and tuned in sections. The Front End, RFQ, and first three superconducting RF cavities have been commissioned with beam [2]. BPMs are the primary tool used to determine beam position and beam energy. Beam of $^{40}Ar^{9+}$ was accelerated up to 2.3 MeV/u and BPM position and phase proved accurate down to currents as low as 100 nA. Figure 1 shows a portion of the linac and placement of 15 BPMs.

BPM Characterization and Correction

At FRIB, we primarily utilize two types of 4-button BPMs, with aperture diameters of 41.3 and 47.6 mm. Buttons are circular with 20 mm diameter. With a 4-button BPM, the simple formula (1) for position utilizes the ratio of difference over sum for two of the buttons signals (R, L or T, B) along with a scale factor incorporating the BPM aperture (D)

$$\mathrm{H} = \frac{\mathrm{D}}{\pi}\left(\frac{R-L}{R+L}\right), \quad \mathrm{V} = \frac{\mathrm{D}}{\pi}\left(\frac{T-B}{T+B}\right) \tag{1}$$

Formula (1) approximates beam position well, but distortion increases further away from center. A polynomial correction (2) was determined for each BPM type to correct for non-linear distortions. Each BPM was characterized using a translation stage to raster scan wire positions within the BPM aperture. Fiducials on the BPM housing, shown in Fig. 2, allow accurate position survey and correlation with pre-installation wire measurements to within 100 µm. Consistent BPM manufacturing allows the use of the same correction for all BPM assemblies of the same type.

$$\mathrm{H}_{\mathrm{new}} = p_{00} + p_{10}H + p_{30}H^3 + p_{50}H^5 + p_{12}HV^2 + p_{14}HV^4 + p_{32}H^3V^2 \tag{2}$$

There is an additional position distortion present with very low-beta (v/c<<1) beams, resulting from the non-relativistic electric fields and asymmetrical pickup of the higher order beam harmonics when the beam is off-center [3]. = This effect is most significant when beta < 0.10, and can be ignored when beta > 0.15. Formula (3) corrects for low-beta distortion, where *a* and *b* are factors dependent on beta, frequency, and geometry [3].

$$\mathrm{H}_{\mathrm{new}} = a\mathrm{H} + b\mathrm{H}^5 \quad \mathrm{V}_{\mathrm{new}} = a\mathrm{V} + b\mathrm{V}^5 \tag{3}$$

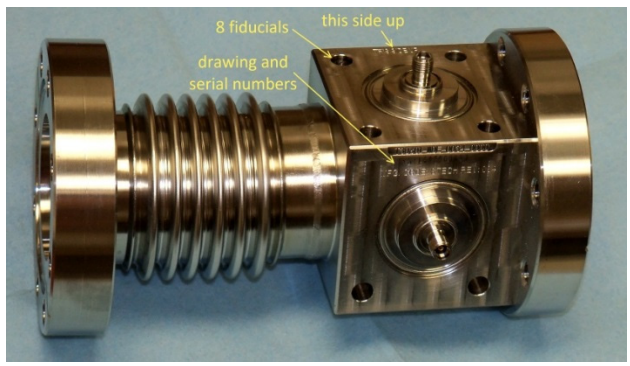

Figure 2: FRIB BPM assembly.

DAQ ELECTRONICS AND SIGNAL PROCESSING

The BPM data acquisition electronics were designed to be MicroTCA [4] based, where up to 10 BPM electronics boards communicate (using PCIe) to a single CPU which serves data to the control system network. The electronics consist of a rear-transition module (RTM) which includes +35 dB amplification, analog filter (either lowpass or bandpass), and ADC digitization. This RTM digitizes two 4-button BPMs plus a reference (REF) clock. An FPGA digital processing board performs digital down-conversion

Figure 1: A portion of the FRIB linac, including medium energy beam transport (MEBT), first 3x cryo-modules with 12x accelerating SRF cavities, and diagnostics station as temporary beam stop. 15 BPMs locations were studied, 6 of which were "cold" BPMs inside cryo-modules.

* This material is based upon work supported by the U.S. Department of Energy Office of Science under Cooperative Agreement DE-SC0000661, the State of Michigan and Michigan State University.
† cogan@frib.msu.edu

Content from this work may be used under the terms of the CC BY 3.0 licence (© 2018). Any distribution of this work must maintain attribution to the author(s), title of the work, publisher, and DOI.

ISBN: 978-3-95450-201-1 doi:10.18429/JACoW-IBIC2018-TUPC09

INITIAL RESULTS FROM THE LHC MULTI-BAND INSTABILITY MONITOR

T.E. Levens*, T. Lefevre, D. Valuch, CERN, Geneva, Switzerland

Abstract

Intra-bunch transverse instabilities are routinely measured in the LHC using a "Head-Tail Monitor" based on sampling a wide-band BPM with a high-speed digitiser. However, these measurements are limited by the dynamic range and short record length possible with typical commercial oscilloscopes. This paper will present the initial results from the LHC Multi-Band Instability Monitor, a new technique developed to provide information on the beam stability with a high dynamic range using frequency domain analysis of the transverse beam spectrum.

INTRODUCTION

Transverse beam instabilities are regularly observed during routine operation of the Large Hadron Collider (LHC). As many of the sources of instabilities scale with the bunch intensity and emittance, their mitigation remains an important consideration for delivering the maximum luminosity to the LHC's experiments. Regular studies into the causes of these instabilities are performed during dedicated "machine development" sessions [1] in order to find adequate mitigation techniques [2]. In addition to these studies, it is important to have instrumentation available that can diagnose any instabilities that may occur during regular operation.

A fundamental tool for the measurement of transverse instabilities is the LHC "Head-Tail Monitor" [3] which can resolve the intra-bunch beam position by sampling a wide-band beam position monitor (BPM) with a fast oscilloscope. Similar techniques have been used since the first direct observation of transverse instabilities in CERN's PS and Booster in the 1970s [4]. However, the short bunch length in the LHC ($4\sigma \approx 1.1$ns) requires sampling at a much higher rate than has been previously necessary, up to 10 GSPS in the case of the LHC.

While the Head-Tail Monitor provides a direct measurement of the intra-bunch motion, and is an important tool for instability studies, it poses a number of challenges for use during regular operation. The original oscilloscopes used in the LHC could provide a maximum of 11 turns of data every 15 seconds. Furthermore, due to the limited dynamic range of their 8-bit high-speed digitisers, only larger oscillation amplitudes were visible. These limitations lead to the development of an online trigger system to precisely trigger the acquisition during an instability [5]. For the 2018 LHC run, new 10-bit oscilloscopes have been installed which offer a higher dynamic range and longer acquisition lengths of up to 450 turns. While easing the demands for precise triggering, the increase in data size of up to 3 GB per acquisition makes data processing and storage challenging.

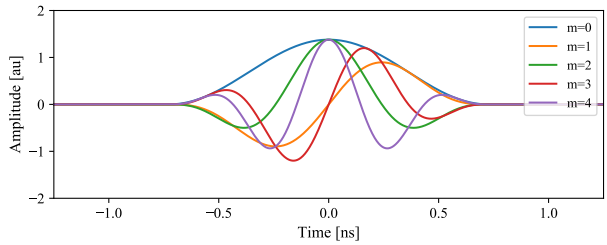

(a) time domain

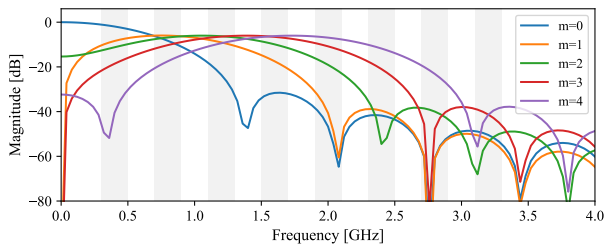

(b) frequency domain

Figure 1: Simulated comparison of time domain (a) and frequency domain (b) analysis for a typical LHC bunch with head-tail instability modes 0 to 4.

As an alternative to "brute-force" time domain sampling, the Multi-Band Instability Monitor (MIM) uses a frequency domain approach to measure intra-bunch motion. Similar techniques are often used on very short electrons bunches where the spectrum extends to frequencies that cannot be easily measured directly by temporal detection schemes [6]. As shown in Fig. 1, it is expected that for an unstable bunch there will be a shift in the spectral power to higher frequencies as the instability mode increases. In order to measure this shift, the signal from a wideband BPM is split into a number of frequency bands using a bank of radio frequency (RF) band-pass filters. Each band can then be mixed down to base-band and digitised in parallel. As the signal from each band has limited bandwidth, it can be digitised at a much higher resolution than would be possible for the wideband BPM signal. While full time domain reconstruction would require amplitude and phase information from each band, with only the amplitude it is still possible to determine the mode from the relative power in the bands. This simplification permits the use of highly sensitive diode detectors, as are used in the LHC's base-band tune (BBQ) system [7].

After the MIM concept was first demonstrated in the SPS and LHC [8], it has also been tested for short electron bunches using an "optical BPM" at the Australian Synchrotron, measuring synchrotron radiation in three frequency bands up to 12 GHz [9]. In this paper we present the first results from the fully implement MIM system in the LHC.

* tom.levens@cern.ch

Content from this work may be used under the terms of the CC BY 3.0 licence (© 2018). Any distribution of this work must maintain attribution to the author(s), title of the work, publisher, and DOI.

ISBN: 978-3-95450-201-1 doi:10.18429/JACoW-IBIC2018-TUPC10

THE DESIGN OF SCANNING CONTROL SYSTEM FOR PROTON THERAPY AT CIAE*

L. Cao†, T.Ge, F.P.Guan, S.G.Hou, L.P.Wen, X.T.Lu, Y.Wang, China Institute of Atomic Energy, Beijing, China

Abstract

A novel proton therapy facility is designed and constructed at China Institute of Atomic Energy (CIAE) in Beijing, which includes a superconducting cyclotron CYCIAE-230 to provide 230 MeV proton beams for cancer therapy. As a part of therapy control system, the scanning control is designed to scan the beam for the access of required tumour volume field. Two set of dipole magnet is driven for changing the beam path. Meanwhile, interfaces between scanning system and other systems will be built for beam control and safe considering. In order to acquire high precise feedback control, the beam position and dose monitor ionization chambers will be constructed in the nozzle. Detailed description will be presented in this paper.

INTRODUCTION

Proton therapy has proven to be an effective cancer treatment with minimal side effects. Due to the progress of superconducting devices, very compact cyclotrons, suitable for hospital installations, can be manufactured with lower cost. In order to promote the development of proton therapy in China, CIAE (China Institute of Atomic Energy) has designed a superconducting cyclotron, which would produce a 230 MeV, 300 nA proton beam [1].

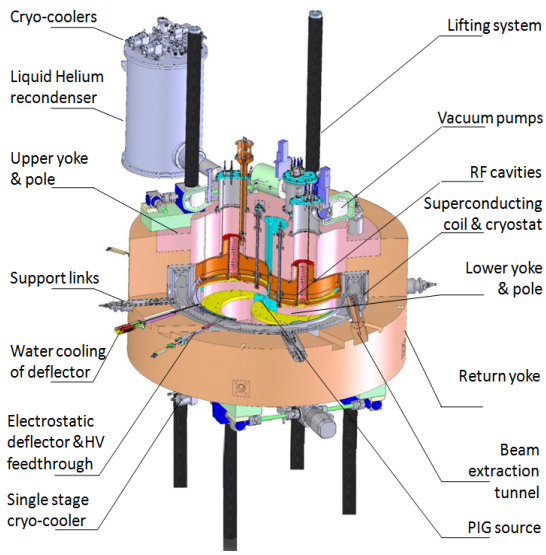

Figure 1: Layout of CYCIAE230 Cyclotron.

As the essential Part of Proton therapy, CYCIAE230 are in commissioning phase, including the cryogenic system and RF system as shown in Fig. 1. Meanwhile, the beamline and gantry are in construction. The specification of cyclotron is shown in Table1. The treatment control system is needed for whole treatment. Scanning control system belongs to the treatment control system and is the core part to do the main process. So, a dedicated scanning control system is designed for the proton therapy facility. Detailed system design will be presented below.

Table 1: Cyclotron Specifications

Parameter	Value
Extraction energy	>230MeV
Extraction current	>500nA
Injection/Extraction field	2.35 T / 2.95 T
RF frequency	~71.3 MHz
RF voltage	70 kV/110 kV

SCANNING CONTROL SYSTEM

In the whole control system of proton therapy, scanning control take a important role. Whatever any scanning mode was used. Also there are complex interfaces with other subsystems. Scanning control system require the the therapy data table to direct the scanning to target volume and the field feedback data to verify the scan process. Figure 2 shows the positon of scanning control system in the whole control system, which is essensial for proton therapy system. The device layer is mainly comprises of needed hardware for convetional process, which accept the control of relatively target front end. The lower layer is safe related function that protects the patient against over dose radiation. The central interlock system will act as a protector for treatment. The last layer is control layer. In this layer, scanning control system is the coordinator to arrange other subsystem to work together smoothly under the defined process. The interface to cyclotron is through the data exchange to cyclotron control system.

Functionalities

Fast dynamic scanning functional specification is as follows:

Interface with accelerator control system to adjust the vertical deflector to stabilize the beam current. The repetition rate is about 1kHz, and the beam off time is lower than 50usec, intensity stability is lower than 5%.

Scanning mode: step & shoot, continue scanning 'TV' or contours scanning, the two sweeper magnets should control the beam position up to 2cm/Ms.

Scanning delivery function comes out that scanning control system dynamically operate the actuators according to the feedback data which involves the position and beam intensity.

* Work supported by National Natural Science Foundation of China under Grant No.11375273 and 1146114103.
† clyoung@163.com

Content from this work may be used under the terms of the CC BY 3.0 licence (© 2018). Any distribution of this work must maintain attribution to the author(s), title of the work, publisher, and DOI.

ISBN: 978-3-95450-201-1 doi:10.18429/JACoW-IBIC2018-TUPC11

DESIGN OF AN ULTRAFAST STRIPLINE KICKER FOR BUNCH-BY-BUNCH FEEDBACK

Jianxin Wang[1,2#], Longgang Yan[1,2],Peng Li, Dai Wu, Dexin Xiao
[1]Institute of Applied Electronics, China Academy of Engineering Physics, Mianyang, 621900, P. R. China
[2]Graduate school of China Academy of Engineering Physics, Beijing, 100088, P. R. China

Abstract

The CAEP THz Free Electron Laser (CTFEL) will have a fast transverse bunch-by-bunch feedback system on its test beamline, which is used to correct the beam position differences of individual bunches with interval of about 2 ns. In this paper, we are proposing an ultrafast wideband stripline kicker, which is able to provide a kick to the bunch in a 2 ns time window. The structure design and simulation results of this kicker are also discussed

INTRODUCTION

China Academy of Engineering Physics (CAEP) has developed a terahertz free electron laser (CTFEL) facility with Peking University and Tsinghua University, which is the first high average power FEL user facility in China [1]. CTFEL is a kind of oscillator type FEL and mainly consists of a GaAs photocathode high-voltage DC gun, a 1.3 GHz 2x4-cell superconducting RF linac, a planar undulator and a quasi-concentric optical resonator. The first saturated lasing of CTFEL was obtained in 2017 [2]. Since then, CTFEL has realized stable operation and some user experiments have been done. The repetition rate of THz beams is 54.17 MHz and the THz frequency can be adjusted from 1.87 THz to 3.8 THz continuously. The average output power in macro pulse is more than 10 W and the peak power is beyond 0.5 MW [3]. Now, fast machine protection system is under developed and CW operation will be realized soon. Moreover, CTFEL is expected to upgrade to cover the THz band from 1 THz to 10 THz and greatly promote the development of THz science as well as many other cutting-edge fields in the future.

The CTFEL will have a test beam line behind the 90 degree analysis magnet, a fast transverse intra-bunch train feedback system to stabilize the beam position will be developed. The time interval of the micro-pulse will set to be about 2ns. Several beam elements and diagnostics device will be installed in the test beam line. Figure 1 shows the location of the CTFEL diagnostics device. This paper gives an overview of the design and analysis of the strip-line kicker.

A stripline kicker consists of two parallel electrodes housed in a conducting vacuum pipe: each of the electrodes is driven by an equal but opposite polarity pulse. The most technology challenges are the following: first, good power transmission by achieving good impedance matching to the electrical circuit; second, the excellent field homogeneity was need in the center region of the vacuum pipe. The stripline design has been carried out by using CST MICROWAVE STUDIO and CST EM STUDIO[4].

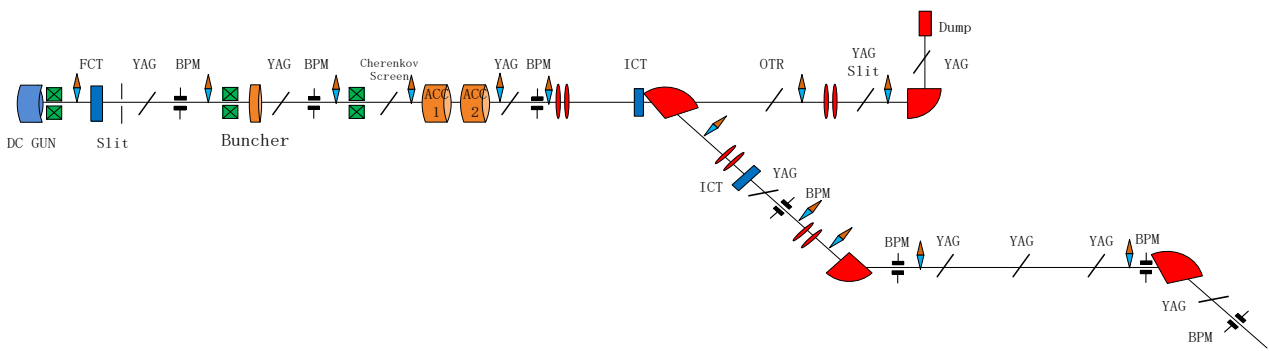

Figure 1: Location of CTFEL diagnostics device.

#jianxinwang1026@163.com

Content from this work may be used under the terms of the CC BY 3.0 licence (© 2018). Any distribution of this work must maintain attribution to the author(s), title of the work, publisher, and DOI.

ISBN: 978-3-95450-201-1 doi:10.18429/JACoW-IBIC2018-TUPC12

BEAM TRANSVERSE QUADRUPOLE OSCILLATION MEASUREMENT IN THE INJECTION STAGE FOR THE HLS-II STORAGE RING*

F.F. Wu, B.G. Sun†, T.Y. Zhou‡, F.L. Gao, J.G. Wang, P. Lu, L.T. Huang, X. Y. Liu, J. H. Wei
National Synchrotron Radiation Laboratory
University of Science and Technology of China, Hefei, 230029, China

Abstract

Beam transverse quadrupole oscillation can be excited in the injection stage if injected beam parameters(twiss parameters or dispersion) are not matched with the parameters in the injection point of the storage ring. In order to measure the beam transverse quadrupole oscillation in the injection stage for the HLS-II storage ring, some axially symmetric stripline BPMs were designed. Transverse quadrupole component for these BPMs was simulated and off-line calibrated. Beam transverse quadrupole oscillation has been measured when beam was injected into the HLS-II electron storage ring. The spectrum of the transverse quadrupole component showed that beam transverse quadrupole oscillation is very obvious in the injection stage and this oscillation isn't the second harmonic of beam betatron oscillation. The relationship between transverse quadrupole oscillation and beam current was also analyzed and the result shows that the relationship is not linear.

INTRODUCTION

When twiss parameters and dispersion of injected beam are not matched with injected point of storage ring, some oscillaitons can be excited[1, 2]. The most obvious oscillation is beam betatron(transverse dipole) oscillation, which can be used to measure betatron tune. In some machines, beam transverse quadrupole oscillation can also be excited in the injected stage. In the HLS-II electron storage ring, beam transverse quadrupole oscillation can be measured based stripline BPM in the injected stage.

TRANSVERSE QUADRUPOLE OSCILLAITON MEASUREMENT SYSTEM INTRODUCTION

Axially symmetric stripline BPM was used to measure beam transverse quadrupole oscillation in the HLS-II electron storage ring The cross-section of this stripline BPM is shown in Fig. 1.

The stripline BPM should be offline calibrated before experiment. Simulation of beam positon and transverse quadrupole component can be as shown in reference 3. Offline calibration of beam positon and transverse quadrupole component can be as shown in reference 4. Beam transverse quadrupole component can be obtained and is shown as follows:

$$\sigma_x^2-\sigma_y^2=\frac{1}{0.0011}\begin{pmatrix} Q_{\Delta/\Sigma}+0.7870-0.0011x_0^2 \\ +0.0011y_0^2-0.0006x_0-0.0004y_0 \end{pmatrix} \quad (1)$$

$Q_{\Delta/\Sigma}$ is the beam transverse quadrupole signal acquired by the difference/sum method and can be espressed as:

$$Q_{\Delta/\Sigma}=\frac{V_R+V_L-V_T-V_B}{V_R+V_L+V_T+V_B} \quad (2)$$

V_R, V_T, V_L, V_B are induced voltages on the right, top, left, bottom electrode. $Q_{\Delta/\Sigma}$ can be obtained by BPM processor(Libera Brillianceplus). Beam position(x, y) can be obtained based the eqution(4) of the reference 4. So Beam transverse quadrupole component(σ_x^2-σ_y^2) can be finally obtained.

The measurement system block diagram is shown in Fig. 2. In the injected stage, The stripline BPM electrode signals are processed by Libera Brillianceplus and the turn-by-turn data is obtained by Labview code(or Matlab code) of PC, then, the relationship between beam transverse quadrupole component(σ_x^2-σ_y^2) and injected turn number n can be obtained.

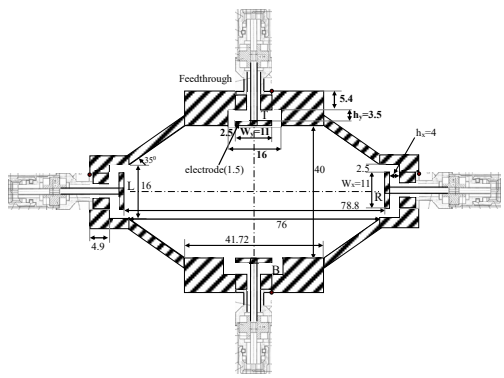

Figure 1: The cross-section of the stripline BPM.

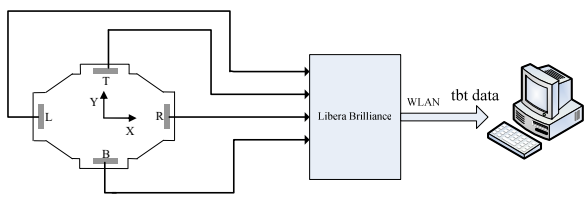

Figure 2: Measurement system block diagram for beam transverse quadrupole oscillation in the the injected stage.

EXPERIMENT AND DATA ANALYSIS

The turn-by-turn data of beam position(x, y) can be used to measure fractional part of machine tune($\Delta\nu_x$, $\Delta\nu_y$). When

* Work supported by the Anhui Provincial Natural Science Foundation(Grant No. 1808085QA24), National Science Foundation of China (Grant No. 11705203, 11575181, 11605202), Chinese Universities Scientific Fund (Grant No. WK2310000057)
†Corresponding author (email: bgsun@ustc.edu.cn)
‡Corresponding author (email: tiany86@ustc.edu.cn)

Content from this work may be used under the terms of the CC BY 3.0 licence (© 2018). Any distribution of this work must maintain attribution to the author(s), title of the work, publisher, and DOI.

ISBN: 978-3-95450-201-1 doi:10.18429/JACoW-IBIC2018-TUPC13

Content from this work may be used under the terms of the CC BY 3.0 licence (© 2018). Any distribution of this work must maintain attribution to the author(s), title of the work, publisher, and DOI.

EARLY COMMISSIONING OF THE LUMINOSITY DITHER SYSTEM FOR SuperKEKB*

M. Masuzawa†, Y. Funakoshi, T. Kawamoto, S. Nakamura, T. Oki, M. Tobiyama, S. Uehara, R. Ueki, KEK. 305-0801 Tsukuba, Japan
A. S. Fisher, M.K. Sullivan, D. Brown, SLAC, 94025 Menlo Park, CA, USA
U. Wienands, ANL 60439 Argonne, IL, USA
P. Bambade, S. Di Carlo, D. Jehanno, C. Pang, LAL, 91898, Orsay, France
D.El Khechen, CERN, 1211 Geneva, Switzerland

Abstract

SuperKEKB is an electron–positron double ring collider that aims to achieve a peak luminosity of 8×10^{35} cm^{-2}s^{-1} by using what is known as the "nano-beam" scheme. A luminosity dither system is employed for collision orbit feedback in the horizontal plane. This paper reports the dither hardware and algorithm tests during the SuperKEKB Phase II luminosity run.

INTRODUCTION

The SuperKEKB collider [1] employs a luminosity dither system that is based on the collision feedback system previously used at SLAC for PEP-II [2, 3] for finding the horizontal offset at the interaction point (IP) that maximizes luminosity. The dithering feedback is different from that used for KEKB collision orbital feedback, where beam–beam deflection was used in both the vertical and horizontal planes. With the "nano-beam" scheme, the horizontal beam–beam parameters are much smaller than those at KEKB, and the detecting luminosity maximum orbit using beam–beam deflection is not as effective as KEKB. Therefore, a dithering method was introduced for SuperKEKB. A good collision condition is sought for by dithering the positron beam (LER), and once a good collision condition is found, it is maintained by an active orbital feedback, which moves the electron beam (HER) relative to the LER by creating a local bump at the IP. The dither system was tested with colliding beams for SuperKEKB Phase II commissioning.

DITHERING SYSTEM

Principle

When an LER beam is dithered sinusoidally in the horizontal plane, where the relative offset of the LER and HER are x_0, the variation in luminosity L is described as a function of the relative offset of the two beams x, as follows:

$$L(x) = L_0 \exp\left(-\frac{x^2}{2\Sigma_x^2}\right) \tag{1}$$

where

$$x = x_0 + \tilde{x}\cos\omega_x t \tag{2}$$

and

$$\Sigma_x^2 = \sigma_{x+}^{*eff\,2} + \sigma_{x-}^{*eff\,2} \tag{3}$$

The parameters $\tilde{x}$, ω_x, σ_{x+}^{*eff}, and σ_{x-}^{*eff} represent the dithering amplitude, dithering frequency, effective horizontal LER, and HER beam size at the IP, respectively. The effective horizontal beam size is denoted as follows:

$$\sigma_{x\pm}^{*eff} = \sigma_z \sin\phi_c \tag{4}$$

where ϕ_c and σ_z are the half crossing angles of the two beams at the IP and bunch length, respectively. Figure 1 shows a conceptual drawing of the colliding beams at SuperKEKB.

Expanding Eq. (1) for small offset x_0 and dither amplitude $\tilde{x}$, L can be rewritten as follows:

$$L(x) = L_0\left(1 - \frac{x_0\tilde{x}}{\Sigma_x^2}\cos\omega_x t - \frac{\tilde{x}^2}{2\Sigma_x^2}\cos^2\omega_x t\right)\exp\left(-\frac{x_0^2}{2\Sigma_x^2}\right) \tag{5}$$

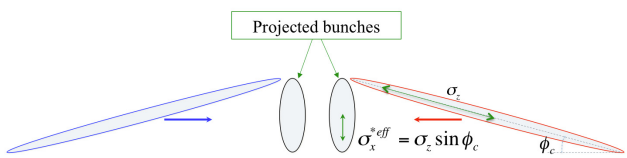

Figure 1: SuperKEKB colliding beams.

When the beam is dithered around the "center," where luminosity peaks, luminosity drops on either side of the peak, giving a modulation at 2ω. When dithered off center, there is additional modulation at the fundamental, as indicated in Fig. 2.

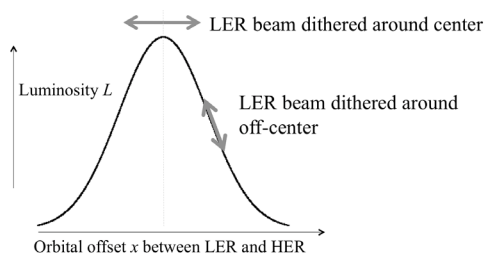

Figure 2: Luminosity dependence on the orbital offset between LER and HER at the IP.

*Work supported by U.S.-Japan Science and Technology Cooperation Program in High Energy Physics.
† mika.masuzawa@kek.jp

ISBN: 978-3-95450-201-1 doi:10.18429/JACoW-IBIC2018-WEOA02

Content from this work may be used under the terms of the CC BY 3.0 licence (© 2018). Any distribution of this work must maintain attribution to the author(s), title of the work, publisher, and DOI.

OPTICAL INVESTIGATION TO MINIMIZE THE ELECTRON BUNCH ARRIVAL-TIME JITTER BETWEEN FEMTOSECOND LASER PULSES AND ELECTRON BUNCHES FOR LASER-DRIVEN PLASMA WAKEFIELD ACCELERATORS*

S. Mattiello†, Andreas Penirschke, Technische Hochschule Mittelhessen, Friedberg, Germany
Holger Schlarb, DESY, Hamburg, Germany

Abstract

In a laser driven plasma based particle accelerators a stable synchronization of the electron bunch and of the plasma wakefield in the range of less than 2 fs is necessary in order to optimize the acceleration. For this purpose we are developing a new shot to shot feedback system with a time resolution of less than 1 fs. As a first step, stable THz pulses are generated by optical rectification of a fraction of the plasma generating high energy laser pulses in a nonlinear lithium niobate crystal. It is planed that the generated THz pulses will energy modulate the electron bunches shot to shot before the plasma to achieve the time resolution of 1fs. In this contribution we systematically investigate the influence of the optical properties as well as the theoretical description of the THz generation on the conversion efficiency of the generation of short THz pulses, in undepleted approximation. We compare different approximations for the modeling of the generation dynamics and of the dielectric function in order to investigate the importance of a detailed description of the optical properties. First results by considering intensity decreasing of the laser pump will be presented.

INTRODUCTION

Particle accelerators are important tools for fundamental research as well for the industry and human life. In fact, they allow to achieve crucial new discoveries, e.g. the Higgs boson, to test and develop the standard model and to deeply understand the strong interaction and in particular the properties of the quark gluon plasma. On the other side, accelerators have several applications in material science, biology, medicine, industry and for security purposes and point-to point communications. As examples we mention the systematic investigation of basic materials using ions beams in order to achieve new technologies, the repair of complex DNA lesions as well as cancer treatment, where the high-energy particle beams can be targeted to destroy tumors [1, 2].

The technology of standard accelerators is coming to its limit given by the physical-chemical properties of the material used for the construction as well as by the huge size of new accelerators and by the financial costs.

Because of their extremely large accelerating electric fields, plasma-based particle accelerators driven by either lasers or particle beams allow to overcome these problems. In this method, known as plasma wakefield acceleration (PWA), the accelerating gradients in plasmas can be 3–4 orders of magnitude higher than in conventional accelerators [3].

The period of these fields is in the range of 10 fs to 100 fs so that for an optimization of the acceleration a stable synchronization of the electron bunch and of the plasma wakefield in the range of few femtoseconds is necessary. Consequently, the minimizing the electron bunch arrival-time jitter becomes a central point for the realization of these accelerators. We are planning a new shot to shot feedback system, which should be able to synchronize the electron bunch with the plasma exciting laser pulse with a time resolution of less than 1 fs.

In a first step, stable Terahertz (THz) pulses should be performed by optical rectification (OR) of high energy laser pulses in a nonlinear crystal. These pulses allow an energy modulation in the modulator placed in a chicane of the electron bunch in order to achieve the required resolution. This paper focuses on the first step of the feedback system, i.e. the generation of THz pulses.

For our purpose an efficient and stable generation of THz pulses is a challenging task. Consequently, the main focus is to maximize the conversion efficiency of the THz generation defined in term of the THz frequency component of the electric field as [4],

$$\eta = \frac{\pi \epsilon_0 c \int_0^\infty \mathrm{d}\Omega \; n(\Omega) |E(\Omega, z)|^2}{F_\mathrm{p}}, \qquad (1)$$

where F_p and ε_0 indicate the pump fluence and the vacuum dielectric constant respectively.

For optical rectification the selection of the nonlinear material is fundamental aspect. Because of its high nonlinear optic coefficient, lithium niobate ($LiNbO_3$, LN) is a suitable material for THz generation.

The optical properties of the material and in particular the details of the adsorption of the THz radiation and material dispersion effects are important for the optimization of the efficiency. In this contribution we investigate the influence of the optical properties, where we focus on a periodically poled lithium niobate crystal (PPLN) [4].

The paper is organized as follows. First, we derive the general equations for the description of the THz generation and then we present the calculation of the optical properties of the material and the different approximations for the solution of the THz generation. Therefore we investigate in

* The work of S. Mattiello is supported by the German Federal Ministry of Education and Research (BMBF) under contract no. 05K16ROA.
† stefano.mattiello@iem.thm.de

ISBN: 978-3-95450-201-1 doi:10.18429/JACoW-IBIC2018-WEOA03

FIRST ELECTRO-OPTICAL BUNCH LENGTH MEASUREMENTS AT THE EUROPEAN XFEL

B. Steffen*, M.K. Czwalinna, Ch. Gerth, P. Peier†,
Deutsches Elektronen-Synchrotron DESY, Hamburg, Germany

Abstract

Three electro-optical bunch length detection systems based on spectral decoding have been installed and are being commissioned at the European XFEL. The systems are capable of recording individual longitudinal bunch profiles with sub-picosecond resolution at a bunch repetition rate 1.13 MHz. Bunch lengths and arrival times of entire bunch trains with single-bunch resolution have been measured as well as jitter and drifts for consecutive bunch trains. In this paper, we present first measurement results for the electro-optical detection system located after the second bunch compressor. A preliminary comparison with data from the bunch arrival-time monitor shows good agreement.

INTRODUCTION

The accelerator for the European X-ray Free-Electron Laser (E-XFEL) delivers femtosecond electron bunches at an energy of up to 17 GeV at a repetition rate of up to 4.5 MHz in bursts of up to 2700 bunches every 100 ms. The electron bunches can be distributed between three undulator beamlines, and the generated femtosecond X-ray laser pulses at wavelengths between 0.05 nm and 6 nm can serve up to three user experiments in parallel [1].

Short electron bunches with a high peak current are needed to drive the SASE process in the magnetic undulators. To reach these short bunches, the initially long electron bunches created at the photocathode gun are compressed in three magnetic bunch compressor chicanes BC0, BC1 and BC2 downstream of the respective accelerating sections I0, L1 and L2 (see Table 1).

Table 1: Design electron bunch lengths (rms) for different operation modes [2].

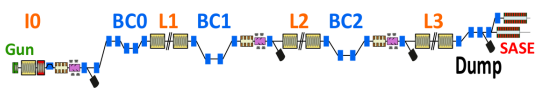

	130 MeV	700 MeV	2.4 GeV	17.5 GeV
20 pC	4.5 ps	1.5 ps	190 fs	5 fs
100 pC	4.8 ps	1.6 ps	200 fs	12 fs
250 pC	5.3 ps	1.7 ps	220 fs	25 fs
500 pC	6.0 ps	2.0 ps	260 fs	43 fs
1 nC	6.8 ps	2.2 ps	300 fs	84 fs

Various diagnostic devices have been installed along the accelerator to measure the longitudinal properties of the electron bunches. Transverse deflecting structures (TDS) have been installed in the injector [3] and downstream of BC2 at final bunch compression for the measurement of slice emittance, longitudinal phase space and longitudinal bunch profile. These properties can be measured for single electron bunches with high accuracy, since the electron bunches are streaked and imaged onto a screen. However, as a consequence, the bunch properties are degraded and these bunches are not delivered to the undulators but deflected by fast kicker magnets out of the bunch train into a dump upstream of the undulators .

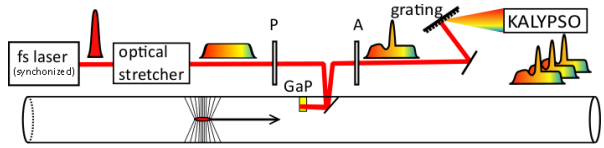

Figure 1: Schematic drawing of a spectrally encoded electro-optical detection setup. P: polarizer; A: analyzer (quarter-wave plate, half-wave plate, polarizer).

Electro-optical bunch length detection (EOD) [4] offers the possibility of measuring the longitudinal bunch profile and arrival time in a non-destructive manner with single bunch resolution for every bunch in the bunch train. Three EOD systems have been installed: One downstream of the injector linac I0 at 130 MeV, one downstream of BC0 (and L1) and one downstream of BC1 at a beam energy of 700 MeV. An EOD system was not foreseen downstream of BC2 due to the limited time resolution.

Bunch arrival time monitors (BAM) [5] have been installed downstream of the injector linac and after each of the bunch compressors BC0, BC1 and BC2. The BAMs measure the arrival time of individual electron bunches with femtosecond precision relative to an optical reference system and can be used for a feedback on the RF of the accelerating modules to stabilize the arrival time which is critical in pump-probe user experiments.

ELECTRO-OPTICAL BUNCH LENGTH DETECTION

Electro-optically active crystals like gallium phosphide (GaP) become birefringent in the presence of an electric field. The electro-optical detection techniques use this effect to transfer the temporal profile of fast changing electric fields by sampling the change in birefringence with laser pulses. Afterwards, the modulated temporal profile of the laser pulse can be analyzed with classical laser techniques.

Several different electro-optical detection techniques have been established for single-shot bunch length measurements at different electron accelerators in the past decade, among them:

* bernd.steffen@desy.de
† now at METAS, Bern, Switzerland

Content from this work may be used under the terms of the CC BY 3.0 licence (© 2018). Any distribution of this work must maintain attribution to the author(s), title of the work, publisher, and DOI.

ISBN: 978-3-95450-201-1 doi:10.18429/JACoW-IBIC2018-WEOA04

THE APPLICATION OF BEAM ARRIVAL TIME MEASUREMENT AT SXFEL *

S. S. Cao†[1,2], R. X. Yuan[1], J. Chen[1,2],Y. B. Leng*[1]
[1] Shanghai Institute of Applied Physics, CAS, Jiading campus, Shanghai 201808, China
[2] University of Chinese Academy of Sciences, Shijingshan District, Beijing 100049, China

Abstract

The Shanghai soft X-ray free electron laser (SXFEL) is able to generate high brightness and ultra-short light pulses. The generation of the light sources relies on the synchronization between seed laser and electron bunch. Beam arrival time play an important role to keep the synchronization. For the SXFEL, a beam arrival time resolution under 100 fs is required. In this paper, the application of beam arrival time measurement scheme at SXFEL has been presented. Especially, a two-cavities mixing scheme to measure the beam flight time or pseudo beam arrival time has been proposed and compared with the typical RF phase detection scheme. The experiment results of the two scheme based on the dual-cavities BAM have also been discussed.

INTRODUCTION

The Shanghai Soft X-ray Free-Electron laser facility (SXFEL) is under commissioning now [1]. Figure 1 shows the layout of the SXFEL-TF. The main parameters of SXFEL-TF is shown in Table 1.

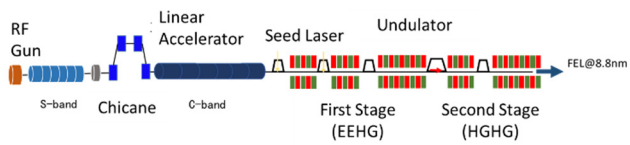

Figure 1: Electron beam characteristic.

Table 1: Main Parameters of SXFEL-TF

Parameter	Value	Unit
Beam energy	0.84	GeV
Beam charge	0.5	nC
Bunch length	~0.5	ps
Pulse repetition rate	10	Hz
Peak current	~ 0.5	A

For the FEL facility, its operation relies on the precise synchronization between the electron bunches and the seed laser pulses in three-dimensional space. Its longitudinal position can be measured by a beam arrival time monitor. The measured beam arrival time can be applied for feedback to adjust the timing of seed laser and also to reduce the timing jitter of accelerator. And the beam arrival time can be used to correct for timing drifts from the accelerator to the experiments[2]. Currently, there are typically two schemes to measure the beam arrival time, electron-optical detection scheme and RF cavity detection scheme. Although the electron-optics detection scheme can acquire better performance, it biggest limitations is its great complexity and quite expensive. In contrast, the RF cavity based detection scheme is simple and inexpensive. In addition, its best resolution can be better than 13 fs.

This paper will focus on the discussion of the RF-phase detection scheme. In detail, the scheme selection, dual-cavities design, fabrication, installation, and beam arrival time experiment as well as beam flight time experiment have been presented.

BEAM ARRIVAL TIME MEASUREMENT SCHEME

The typical RF cavity phase detection scheme is quite mature. Several FEL facility have conducted the research of beam arrival time with this scheme, such as LCLS[3], SACLA[4], PAL-XFEL[5]. Figure 2 gives the diagram of a typical RF cavity based phase detection scheme.

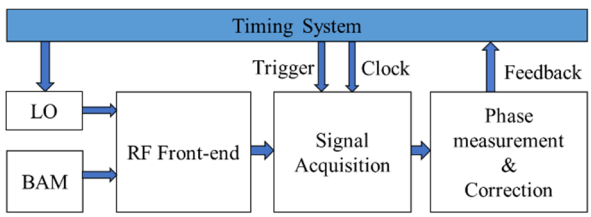

Figure 2: Diagram of a typical RF cavity based phase detection.

The typical BAM system consists of a narrow-band beam arrival time monitor, a reference signal, an RF front-end electronics, a signal acquisition system, and a phase processing/correction system. When an electron bunch passing through the BAM, a variety of electro-magnetic field modes will be excited. Typically, the strongest mode is TM010, a centro-symmetrical mode, whose signal strength is generally proportional to the bunch charge while independent of bunch offset within a paraxial approximation. However, single arrival time phase is meaningless, only when it is relative to a reference time. The two signals, a cavity signal and a reference signal, then be mixed to an intermediate frequency (IF). The beam arrival time can finally be evaluated via a signal acquisition system and phase processing system. However, its limitation is requiring a reference signal with high phase stability. Normally, the reference signal needs to be transmitted over a long dis-

* Work Supported by The National Key Research and Development Program of China (Grant No. 2016YFA0401903, 2016YFA0401900)
* lengyongbin@sinap.ac.cn

Content from this work may be used under the terms of the CC BY 3.0 licence (© 2018). Any distribution of this work must maintain attribution to the author(s), title of the work, publisher, and DOI.

ISBN: 978-3-95450-201-1 doi:10.18429/JACoW-IBIC2018-WEOB01

NEW BEAM LOSS DETECTOR SYSTEM FOR EBS-ESRF

L. Torino*, K.B. Scheidt, ESRF, 38000 Grenoble, France

Abstract

In view of the construction and the commissioning of the new Extremely Brilliant Source (EBS) ring, a new Beam Loss Detector (BLDs) system has been developed, installed and tested in the present European Synchrotron Radiation Facility (ESRF) storage ring. The new BLD system is composed of 128 compact PMT-scintillator based BLDs, distributed evenly and symmetrically at 4 BLDs per cell, controlled and read out by 32 Libera Beam Loss Monitors (BLMs). The detectors fast response and the versatility of the read-out electronics allow to measure fast losses with an almost bunch-by-bunch resolution, as well as integrated losses useful during the machine operation. In this paper the different acquisition modes will be explained and results obtained during injection and normal operation will be presented.

INTRODUCTION

Beam Loss Detectors (BLDs) are an important part of the accelerators diagnostics. They are used during normal operation to identify and locate partial beam losses that may be caused by the malfunctioning of various devices, vacuum leaks, unexpected obstacles, misalignment, and so on. BLDs may be even more relevant during machine commissioning where this kind of problems are recurrent [1].

The European Synchrotron Radiation Facility (ESRF) is a 6 GeV light source, operating in Grenoble for more than 20 years. The facility will undergo through a major update, leading to the new Extreme Brilliant Source (EBS), in which a lower emittance will guarantee a brighter and more coherent x-ray beam [2,3]. The ESRF dismantling phase will start at the very end of 2018, and the commissioning is expected to take place between the end of 2019 and mid 2020.

Since the ESRF storage ring will still be operational until December 2018, several sub-systems which will be later used in EBS, such as the BLD system, are already under test.

The opportunity of having and testing the BLD system on the current machine will not only be a great help for the EBS commissioning, but will also allow to compare levels and loss distributions of the two machine.

NEEDS FOR THE NEW BLD SYSTEM

In order to fulfill the requirement for EBS, the new BLD system has to be able to detect both "slow" and "fast" losses [1]. This capability depends on the system dynamic range and bandwidth.

Slow losses are unavoidable and are the one that determine the beam lifetime. They are usually confined in some hot-spots and are due to the presence of collimators, scraper, septa, or other aperture limits. They also depend on the beam size and the population of the buckets, which lead to a deterioration of the Touschek lifetime. The typical time scale for slow losses is in the order of the second.

Fast losses are instead related with accidental effect, or some traumatic events such as perturbation due to injection. These losses can be distributed all around the machine, and can be visible on the single bunch or the single turn time scale.

Another constrain for the new BLD system is the limited amount of space in the EBS machine. For this reason new detectors have to be compact.

These requirements lead to the choice of PMT-scintillator based detectors, read out by a commercial Libera Beam Loss Monitor (BLM) unit [4].

BEAM LOSS DETECTOR SYSTEM

Detector

A scintillator-PMT based detector has been chosen for the new BLD system [5].

The BLD has to detect losses generated by the 6 GeV electron beam. When a high-energy electron is lost, it crashes on the vacuum chamber and creates an electromagnetic shower composed by electrons, positrons, and γ-rays. In order to detect showers, a suitable plastic scintillator can be used to convert the energy deposited by particles into visible light, which can then be detected by a commercial PMT.

The scintillator chosen is a EJ-200 rod (100 mm length, 22 mm diameter), wrapped in reflective foil to minimize the light losses. The maximum emission wavelength is 425 nm [6].

The selected PMT is a Hamamatsu H10721-110, with a cathode sensitivity centered in the scintillator emission wavelength, and a 8 mm diameter active area. The PMT requires to be powered by 5 V, and has a 0-1 V control gain [7].

The PMT-scintillator system is enclosed in a metallic casing, and an electronic card has been designed to optimize PMT power supply, gain, and signal connections. The metallic casing is also sealed to provide a first ambient-light isolation. Figure 1 presents a model of the detector.

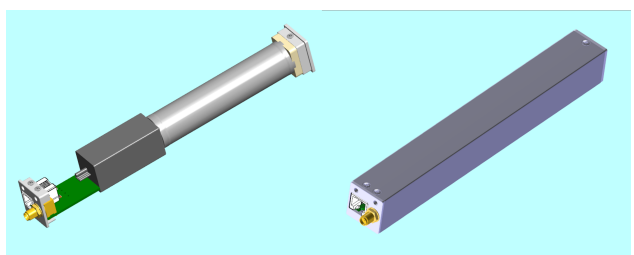

Figure 1: Model of the PMT-scintillator system without and with the metallic casing.

* laura.torino@esrf.fr

Content from this work may be used under the terms of the CC BY 3.0 licence (© 2018). Any distribution of this work must maintain attribution to the author(s), title of the work, publisher, and DOI.

ISBN: 978-3-95450-201-1 doi:10.18429/JACoW-IBIC2018-WEOB02

RadFET DOSE MONITOR SYSTEM FOR SOLEIL

N. Hubert†, F. Dohou, D. Pédeau, Synchrotron SOLEIL, 91192 Saint-Aubin, France

Abstract

SOLEIL is currently testing new dose measurement monitors based on RadFET transistors. This new monitor at SOLEIL will provide a measurement of the dose received by equipment that are damaged by the radiations in the storage ring, in order to anticipate their replacement. This monitor should be very compact to be placed in tiny areas, sensitive to all kind of radiation and low cost to install many of them around the ring. A readout electronic module is being developed in-house, and a first prototype has been built and installed on the machine. Description of the system and first results recorded on the machine are presented here.

INTRODUCTION

After more than ten years of operation, SOLEIL pieces of equipment in the storage ring are damaged by radiations. The damage level is strongly dependent on the tunnel localization [1]. In order to have a better knowledge of the deposited dose, and to anticipate the replacement of the equipment, a dose monitor system has to be deployed around the storage ring.

This system must:

- Have a compact sensor that can be installed as close as possible to the equipment, and sometimes in tiny areas.
- Be sensitive to all kind of radiation, including X-rays since we know that in some particular locations X-rays are responsible of damages.
- Be low cost to be able to deploy a large number of sensors around the ring.

RadFET sensors, which have already been used with success by the accelerator community [2, 3], fit those specifications. SOLEIL has tested one kind of RadFET during the last months. A dedicated multiplexed electronics has been designed to periodically and automatically read the dose measurements.

RADFET SENSORS

Description

RadFET are Metal Oxide Semiconductor Field Effect Transistors (MOSFET), optimized for radiation sensitivity. When ionizing radiations go through the gate oxide layer, they generate pairs of electron-hole, leading to a permanent modification of the layer with trapped positive charges (Fig. 1). As a consequence, the threshold voltage of the transistor is modified. The voltage shift depends on the amount of radiation that hits the device. By measuring the threshold voltage shift (forcing a fixed DC current in the device), the dose received by the RadFET can then be deduced.

† nicolas.hubert@synchrotron-soleil.fr

RadFETs are sensitive to all kind of radiations (X-rays, gamma, electrons…). They give a measure of the total integrated dose received.

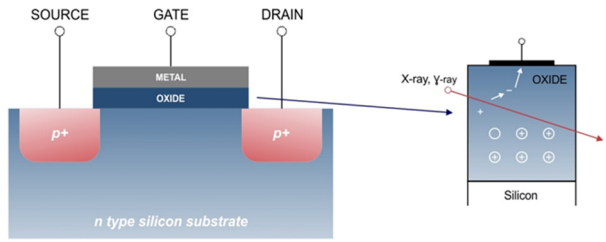

Figure 1: RadFET schematics (source Tyndall).

RadFETs used at SOLEIL are provided by Tyndall Works and manufactured by Tyndall National Institute in Ireland [4]. The TY1004 chip embeds two identical RadFETs with a gate oxide thickness of 400 nm. The active area (gate oxide surface) is very small: 300 µm by 50 µm.

Calibration

RadFETs TY1004 are given for a measurement range from 1 rd to 100 krd (1 cGy to 1 kGy). Since their response is non-linear with the deposited dose, calibration curves are provided by the manufacturer to retrieve the dose value from the measured voltage shift ΔV according to the following formula:

$$\Delta V = A * Dose^{B}$$

The A and B coefficients are obtained exposing one RADFET to discrete dose values using a Co60 source (see Fig. 2). It is then assumed that all RADFETs of a same batch follow the same calibration curve.

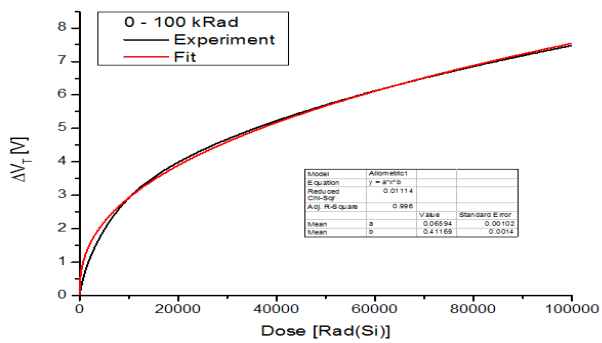

Figure 2: Calibration curve for dose range 0 – 100 krd / 1 kGy (Source: Tyndall).

A and B coefficients are not constant over the full measurement range. This is why a set of coefficients is given depending on the dose range (Table 1).

Content from this work may be used under the terms of the CC BY 3.0 licence (© 2018). Any distribution of this work must maintain attribution to the author(s), title of the work, publisher, and DOI.

ISBN: 978-3-95450-201-1 doi:10.18429/JACoW-IBIC2018-WEOB03

THE EUROPEAN XFEL BEAM LOSS MONITOR SYSTEM

T. Wamsat*, T. Lensch
Deutsches Elektronen-Synchrotron DESY, Hamburg, Germany

Abstract

The European XFEL MTCA based Beam Loss Monitor System (BLM) is composed of about 470 monitors, which are part of the Machine Protection System (MPS). The BLMs detect losses of the electron beam, in order to protect accelerator components from damage and excessive activation, in particular the undulators, since they are made of permanent magnets. Also each cold accelerating module is equipped with a BLM to measure the sudden onset of field emission (dark current) in cavities. In addition some BLMs are used as detectors for wire- scanners. Experience from the already running BLM system in FLASH2 which is developed for XFEL and tested here, led to a fast implementation of the system in the XFEL. Further firmware and server developments related to alarm generation and handling are ongoing.

The BLM systems structure, the current status and the different possibilities to trigger alarms which stop the electron beam will be presented.

INTRODUCTION

The Beam Loss Monitor (BLM) system at the European XFEL is the main system to detect losses of the electron beam, thus to protect the machine hardware from radiation damage in particular the permanent magnets of the undulators. As part of the Machine Protection System (MPS) [1] the BLM system delivers a signal which stops the electron beam as fast as possible in case the losses get too high.

In addition, there are Beam Halo Monitors (BHM) [2] in front of the beam dumps using the same digital backend as the BLM electronics.

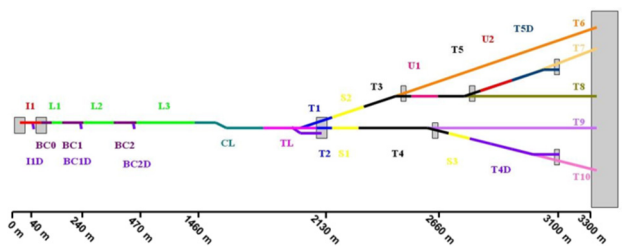

Figure 1: Section overview of the European XFEL accelerator [3].

About 470 BLMs are installed along the XFEL Linac which schematically is shown in Fig. 1. The BLMs are positioned at locations near the beamline, where losses can be expected or where sensitive components are installed, thus most of the BLMs are installed in the undulator area (see Table 1). Since even a big number of BLMs cannot provide a complete survey of losses, there is also a toroid based Beam Current Monitor system [4] installed, which provides transmission interlock system to stop the beam if too much charge gets lost along the machine. Also each superconducting accelerating module is equipped with one BLM at the end to detect the field emission produced by cavities (Correlation work still ongoing, no paper available yet).

Table 1: BLM Distribution

Section	#
I1, BC0	24
BC1	18
BC2	23
L1, L2, L3 (field emission)	98
CL, TL	71
S1, T4	80
S3	48
T4D	10
S2, T3	80
U1, T5, U2, T5D	20

Some selected BLMs are also used as additional detectors for wire scans [5].

SYSTEM OVERVIEW

The hardware consists of the BLM devices, a dedicated Rear Transition Module (RTM) in combination with the DESY Advanced Mezzanine Card DAMC2. Furthermore a MPS card is required for alarm output collection.

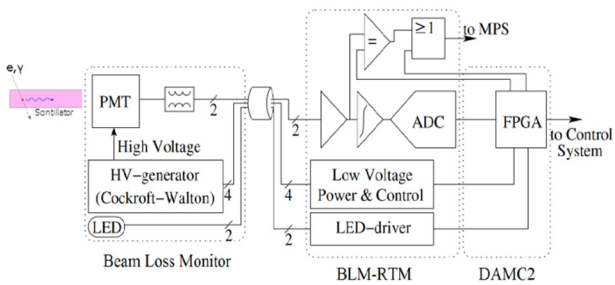

Figure 2: BLM system scheme.

The BLM includes either an EJ-200 plastic scintillator or a SQ1 quartz glass rod. The latter are used mainly in the undulator intersection. In contrast to scintillators, that are also sensitive to hard x-rays, the Quartz rods work with Cherenkov effect, that is sensitive to particle loss only.

The high voltage for the photomultiplier (PMT) is generated within the BLM, so no high voltage cables are needed (see Fig. 2), just a CAT 7 cable with RJ-45 connectors is used. A LED can be switched on within the

* thomas.wamsat@desy.de

Content from this work may be used under the terms of the CC BY 3.0 licence (© 2018). Any distribution of this work must maintain attribution to the author(s), title of the work, publisher, and DOI.

ISBN: 978-3-95450-201-1 doi:10.18429/JACoW-IBIC2018-WEOC02

REVIEW OF RECENT STATUS OF CODED APERTURE X-RAY MONITORS FOR BEAM SIZE MEASUREMENT*

J.W. Flanagan†[1], High Energy Accelerator Research Org., KEK, 305-0801 Tsukuba, Japan
[1]also at the Graduate University for Advanced Science, SOKENDAI, 305-0801 Tsukuba, Japan

Abstract

X-ray beam profile monitors based on coded aperture imaging use an array of pinholes or slits to achieve large open apertures, which provide improved photon collection efficiency over single pinholes or slits. The resulting improvement in photon statistics makes possible single-bunch, single-turn measurements at lower bunch currents than are possible with a single pinhole or slit. In addition, the coded aperture pattern provides extra information for beam profile reconstruction, which makes possible somewhat improved resolution, as compared to a single slit. The reconstruction algorithm for coded aperture imaging is more complicated and computing-intensive than that for a single slit, though with certain classes of coded apertures a faster reconstruction method is possible. This paper will provide a survey of efforts to use coded aperture imaging for beam profile diagnostics at accelerators to date, covering principles and practical experiences with the technique, as well as prospects for the future at SuperKEKB, where it forms the primary means of measuring vertical beam sizes.

INTRODUCTION

Coded aperture imaging is a form of wide-aperture imaging with roots in x-ray astronomy. This paper will start with reviews of wide-aperture imaging in x-ray astronomy, including coded aperture telescopes. This will be followed by a review of the principles of coded aperture imaging. Finally, there will be a discussion of experiences at Diamond Light Source, CesrTA, ATF2 and SuperKEKB, and a summary.

WIDE-APERTURE IMAGING IN X-RAY ASTRONOMY

The existence of x-rays coming from outside the solar system was first discovered in 1962, using non-imaging detectors [1]. This gave birth to the field of x-ray astronomy, for which Riccardo Giacconi later received the Nobel Prize. Due to the attenuation of x-rays in the atmosphere, x-ray telescopes need to be placed on rockets, high-altitude balloons, or satellites. The first fully imaging x-ray satellite dedicated to extra-solar astronomy was the HEAO-B (Einstein) satellite, which operated from 1978 to 1982 [2]. Imaging was accomplished via grazing-incidence mirrors. To increase the light collection efficiency (open aperture), a set of 4 nested mirrors was used. This worked for x-rays up to 8 keV.

* Work supported in part by Kakenhi and Japan-US Cooperation in High Energy Physics
† john.flanagan@kek.jp

This basic approach has evolved over the years, with ever-increasing numbers of nested mirrors employed. For example, the NuSTAR satellite [3] employs 133 nested mirrors. In addition, it employs multi-layers on the surface of the mirrors, made up of alternating layers of high- and low-index of refraction materials. The multi-layers enhance reflectivity through constructive interference at higher x-ray energies, giving the satellite a usable spectral range of 3-79 keV, limited by the optics.

Another approach used for x-ray and gamma-ray astronomy is coded aperture (CA) imaging, which will be discussed in the next section. An example of a CA-based x-ray telescope is the balloon-borne protoMIRAX experiment [4], which used a rectangular mask pattern of apertures to modulate the incoming x-rays. Advantages of CAs over reflective optics include wider angular and spectral acceptances (spectral acceptance being determined primarily by detector efficiency rather than optics), and a shorter required distance between optics and detector -- the NuSTAR satellite for example, requires 10 m separation between optics and detectors to focus at 79 keV (due to the required shallowness of the grazing incidence angle), while protoMIRAX reaches up to 200 keV in a much more compact package.

PRINCIPLES OF CODED APERTURE IMAGING

CA imaging is a technique developed by x-ray astronomers, gamma-ray astronomers and others using a mask made up of multiple apertures to modulate incoming light. The resulting image must be deconvolved through the mask response to reconstruct the object. The primary advantage of a CA mask over a single pinhole is increased light-collection efficiency, with typical CA masks in use having open apertures of around 50%.

X-ray astronomer R.H. Dicke proposed to use multiple pinholes to increase photon-collection efficiency [5]. He proposed a randomly-spaced arrangement of pinholes. Such an arrangement produces a complicated detector image, that can be recovered by deconvolution by cross-correlation with the original mask image.

In principle, however, any set of multiple apertures can be considered a "coded aperture." Prior to Dicke (and prior to the advent of x-ray astronomy), the use of Fresnel zone plates (FZPs) had been proposed [6]. If an FZP is detuned so as not to act like a lens, then it provides a uniformly spaced set of aperture widths and spacings, for uniform spatial resolution over a range of sizes.

A notable class of coded aperture is Uniformly Redundant Arrays (URAs) [7, 8]. URAs are made up of a pseudo-random arrangement of apertures, designed to have the

Content from this work may be used under the terms of the CC BY 3.0 licence (© 2018). Any distribution of this work must maintain attribution to the author(s), title of the work, publisher, and DOI.

ISBN: 978-3-95450-201-1 doi:10.18429/JACoW-IBIC2018-WEOC03

A SIMPLE MODEL TO DESCRIBE SMOKE RING SHAPED BEAM PROFILE MEASUREMENTS WITH SCINTILLATING SCREENS AT THE EUROPEAN XFEL

G. Kube, S. Liu, A. Novokshonov, M. Scholz, DESY, Hamburg, Germany

Abstract

Standard beam profile measurements of high-brightness electron beams based on optical transition radiation (OTR) may be hampered by coherence effects induced by the micro–bunching instability which render a direct beam imaging impossible. For the European XFEL it was therefore decided to measure transverse beam profiles based on scintillating screen monitors using LYSO:Ce as scintillator material. While it is possible to resolve beam sizes down to a few micrometers with this kind of scintillator, the experience during the commissioning of the XFEL showed that the measured emittance values were significantly larger than the expected ones. In addition, beam profiles measured at bunch charges of a few hundreds of pico-Coulomb show a 'smoke ring' shaped structure. While coherent OTR emission and beam dynamical influence can be excluded to explain this observation, it is assumed that the beam profile distortions are caused by effects from the scintillator material. A simple model is presented which takes into account quenching effects of excitonic carriers inside a scintillator in a heuristic way. Based on this model, the observed beam profiles can be understood qualitatively. Together with the model description, first comparisons with experimental results are presented.

INTRODUCTION

Transverse beam profile diagnostics in electron linacs is widely based on optical transition radiation (OTR) as standard technique which is observed in backward direction when a charged particle beam crosses the boundary between two media with different dielectric properties. Unfortunately, microbunching instabilities in high–brightness electron beams of modern linac–driven free–electron lasers (FELs) can lead to coherence effects in the emission of OTR, thus rendering it impossible to obtain a direct image of the particle beam and compromising the use of OTR monitors as reliable diagnostics for transverse beam profiles. The observation of coherent OTR (COTR) has been reported by several facilities (see e.g. Ref. [1]), and in the meantime the effect of the microbunching instability is well understood [2].

For the European XFEL it was therefore decided to use scintillation screen monitors because the light emission in a scintillator is a multistage stochastic process from many atoms which is completely insensitive to the longitudinal bunch structure. In a series of test measurements performed in the past few years, the applicability of inorganic scintillators for high resolution electron beam profile measurements was investigated [3, 4]. Most notably, the dependency of the resolution on the scintillator material and on the observation geometry was studied with respect to resolve beam profiles in the order of several tens of micrometers, and it was concluded that LYSO ($Lu_{2(1-x)}Y_{2x}SiO_5$:Ce) is a suitable material because it gives the best spatial resolution. Based on these measurements, screen monitor stations were designed for the European XFEL using 200 µm thick LYSO screens [5]. In a high resolution beam profile measurement using an XFEL–type screen it was demonstrated that it is possible to resolve a vertical beam size of $\sigma_y = 1.44$ µm [6].

However, the experience during the commissioning of the XFEL showed that the measured emittance values were significantly larger than the expected ones [7, 8]. In addition, beam profiles measured at bunch charges of a few hundreds of pico-Coulomb show a 'smoke ring' shaped structure, see e.g. Fig. 1. While the contribution of COTR emission

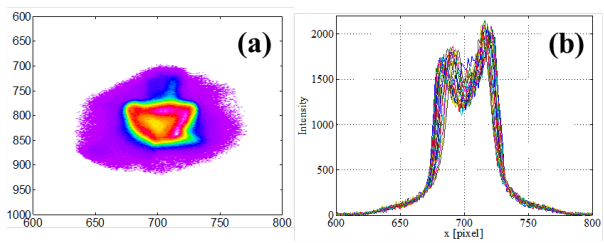

Figure 1: (a) Typical smoke ring shaped beam profile as measured with an XFEL screen monitor based on a 200 µm thick LYSO screen. (b) Various horizontal cuts through the 2D–profile demonstrate the intensity drop in the central part of the beam spot.

from the scintillator surface, beam dynamical influence, and camera effects could be excluded to explain this observation, it is assumed that the beam profile distortions are caused by effects from the scintillator material.

In the following a simple model is described which takes into account quenching effects of excitonic carriers inside a scintillator in a heuristic way. Based on this model, the observed beam profiles can be understood qualitatively.

BASIC CONSIDERATIONS

Degradation effects in scintillator based beam profile measurements are reported in a number of publications, see e.g. Refs. [9–13]. The scintillator influence is mainly interpreted as saturation of the measured profiles, caused e.g. by full excitation of the luminescent centers in some regions inside the scintillator. While inspecting Fig. 1 it is obvious that the XFEL observations cannot simply be described by a saturation effect which would result in a flattening of the measured beam profiles. It rather leads to the conclusion

Content from this work may be used under the terms of the CC BY 3.0 licence (© 2018). Any distribution of this work must maintain attribution to the author(s), title of the work, publisher, and DOI.

ISBN: 978-3-95450-201-1 doi:10.18429/JACoW-IBIC2018-WEOC04

SPACE CHARGE EFFECTS STUDIES FOR THE ESS COLD LINAC BEAM PROFILER

F. Belloni†, F. Benedetti, J. Marroncle, P. Abbon, G. Coulloux, F. Gougnaud, C. Lahonde-Hamdoun, P. Le Bourlout, Y. Mariette, J. P. Mols, V. Nadot, L. Scola,
CEA-Saclay, 91191 Gif-sur-Yvette, France
C. Thomas, ESS, 221 00 Lund, Sweden

Abstract

Five Ionisation Profile Monitors are being built by CEA in the framework of the in-kind contribution agreement signed with ESS. The IPMs will be installed in the Cold Linac where the proton energy range they need to cover extends from 90 MeV to 2 GeV. The ESS fields intensity of 1.1e+09 protons/bunch delivered at a frequency of 352 or 704 MHz, with a duty cycle of 4%, may strongly affect the trajectories of the ionised molecules and electrons created by the passage of the beam through the residual gas. In order to quantify and to develop a correction algorithm for these space charge effects, a code was initiated at ESS and completed at CEA Saclay with the possibility to include real case electric fields calculated with Comsol Multiphysics. A general overview of the code and its preliminary results are presented here.

INTRODUCTION

The first proton beam at the European Spallation Source (ESS), in construction at Lund (Sweden) is expected by 2019. A perfect beam alignment and focusing are necessary to prevent beam losses and the resulting activation of the accelerator and pipes. Transversal beam profile monitors are therefore among the diagnostics needed by the accelerator.

ESS proton fields are too intense for interceptive monitors, causing material vaporization and radiation damage. Non invasive monitors are the only option for monitoring the ESS transversal beam profile. NPMs (Non-Interceptive Profile Monitors) can rely on ionisation (IPMs) or on fluorescence emission (FPMs). The two processes have different cross sections at different energies, the latter being less likely at high proton energies than the former.

The Cold Linac, where the pressure is expected to be below 10^{-9} mbar, will be therefore equipped with 5 NPMs of IPM type: one in the Spoke section (protons in the 90 MeV - 216 MeV energy range), 3 in the Medium β section (216 MeV – 571 MeV) and one in the High β section (571 MeV – 2 GeV). Every NPM will be installed in a chamber in-between the cryomodules and is composed of two IPMs set at 90° with respect to each other, and each one measuring one transversal beam profile.

Physically, an ESS-IPM is a cube missing two opposite walls. Out of the four remaining walls, two opposite ones are metallized to be used as electrodes for imposing an electric field in the cage and the other two are in insulating material but equipped with resistors to make the field as more uniform as possible. The proton beam enters the cage through one missing wall and exits from the other missing one.

SPACE CHARGE EFFECTS

The effects of space charge are twofold: they affect the charged particle beam itself and any other charge in its proximity. Our focus is on this second aspect.

A charge generated at rest between two parallel plates kept at different voltages drifts towards the electrodes travelling parallel to the electric field lines. In an ideal case of perfectly uniform electric field, the point where the charge meets the plate will simply be the projection of its initial position on the electrode. In IPMs, charges are created via gas ionisation and the beam profile is reconstructed this way. But the presence of a charged particle beam, necessary to create ionisation charges, induces an electromagnetic field which modifies the trajectories of the electrons and of the ionised gas molecules and thus introduces a shift between the point where they should have ideally meet the electrode and the point where they really reach it. The measured beam profile therefore will differ from the real one by an amount which depends on the beam intensity, the beam size, the beam energy and the strength of the electric field applied between the electrodes.

CODE TO QUANTIFY THE SPACE CHARGE EFFECTS

ESS Core

The core of the code was written in MATLAB at ESS [1] and translated in C++ at CEA Saclay. Its mathematics is based on [2]. Briefly, let's consider the reference frames K and K, with cartesian axis respectively x,y,z and x,y and z. K is the laboratory system where a Gaussian bunch with total charge Q_b is moving with speed v_b along the z axis, while K is the reference frame co-moving with the bunch. The charge density of the bunch in the co-moving frame is given in Eq. (1)

$$\rho(\bar{x},\bar{y},\bar{z}) = \frac{Q_b}{(2\pi)^{3/2}\sigma_{\bar{x}}\sigma_{\bar{y}}\sigma_{\bar{z}}}\exp\left(-\frac{\bar{x}^2}{2\sigma_{\bar{x}}{}^2}\right) \exp\left(-\frac{\bar{y}^2}{2\sigma_{\bar{y}}{}^2}\right)\exp\left(-\frac{\bar{z}^2}{2\sigma_{\bar{z}}{}^2}\right) \quad (1)$$

†francesca.belloni@cea.fr

Content from this work may be used under the terms of the CC BY 3.0 licence (© 2018). Any distribution of this work must maintain attribution to the author(s), title of the work, publisher, and DOI.

ISBN: 978-3-95450-201-1 doi:10.18429/JACoW-IBIC2018-WEPA01

A MicroTCA.4 TIMING RECEIVER FOR THE SIRIUS TIMING SYSTEM

J. L. N. Brito*, S. R. Marques, D. O. Tavares, L. M. Russo, G. B. M. Bruno, LNLS, Campinas, Brazil

Abstract

The AMC FMC carrier (AFC) is a MicroTCA.4 AMC board which has a very flexible clock circuit that enables any clock source to be connected to any clock input, including telecom clock, FMC clocks, programmable VCXO oscillator and FPGA. This paper presents the use of the AFC board as an event receiver connected to the Sirius timing system to provide low jitter synchronized clocks and triggers for Sirius BPM electronics and other devices.

INTRODUCTION

Sirius is a 4th generation synchrotron light source based on a 5BA magnetic lattice, currently under construction in Brazil by LNLS [1]. The machine, designed to achieve a beam emittance of 0.25 nm·rad and scheduled for commissioning at the end of 2018 [2], consists of a 150 MeV Linac, a 150 MeV to 3 GeV booster and a 3 GeV storage ring with 518 meters circumference and 20 straight sections. Both booster and storage ring RF frequency is 499.658 MHz and the Linac will inject in single or multi-bunch mode at 2 Hz.

Sirius timing system [3] is a star topology optical fiber network where an event generator (EVG) broadcasts event frames to the event receivers. An event frame decoded by an event receiver can generate clock and trigger signals synchronized to the Sirius RF frequency for the beam injection process and other subsystems such as electron BPMs. The system is composed of Ethernet-configured standalone modules developed by SINAP through a collaboration with LNLS and remotely controlled by an EPICS soft IOC designed by LNLS [4].

The Sirius BPM and orbit feedback systems were developed as an open-source hardware platform [5] based on MicroTCA.4 crates, AMC and FMC modules, 1 Gigabit Ethernet and PCI Express connectivity. The digital back-end of these systems is the AMC FMC carrier (AFC) [6], a MicroTCA.4 AMC board partially based on Simple PCIe FMC carrier (SPEC) [7] design.

Thanks to the flexible clock circuits, the trigger and clock distribution options and the digital interfaces available in the AFC board, the same hardware platform was used to develop a timing receiver board to provide triggers and synchronized clocks for Sirius BPM electronics and other devices, upgrading the MicroTCA clock distribution board developed 3 years ago [3]. From now on, the timing receiver board shall be referred to as AFC timing.

HARDWARE

This section presents the AFC board focused on timing applications and the interface boards FMC 5 POF and MicroTCA RTM 8 SFP+.

* joao.brito@lnls.br

AFC

The AFC board was specified by LNLS and designed by WUT (Warsaw University of Technology) as a double-width AMC card with 2 fully populated high-pin count FMC mezzanine slots, 8 multigigabit links routed to the MicroTCA Rear Transition Module (uRTM) connector, 8 M-LVDS trigger and 2 clock lines available through the AMC backplane connector, connectivity to PCIe at Fat Pipe 1 (x4 link), redundant 1 Gb Ethernet ports, full hardware support for the White Rabbit [8] timing system and provision for standalone operation.

It has a Xilinx Artix-7 200T FFG1156 FPGA and the available clocking resources are: (*I*) a clock switch (Analog Devices ADN4604) allowing routing of MicroTCA.4 low-jitter clocks to any of the FMC slots or the AMC connector, (*II*) a 10-280 MHz I_2C programmable VCXO oscillator (Silicon Labs Si571, 571BJC000121G), (*III*) a 25 MHz VCTCXO (Mercury VM53S3-25.000) connected to a frequency synthesizer (Texas Instruments CDCM61004) configured to 125 MHz, (*IV*) a 20 MHz VCXO (IQD VCXO026156) and (*V*) 3 DACs (Analog Devices AD5662) for oscillators control.

Once inside a MicroTCA crate, an AFC timing board outputs triggers and a low-jitter synchronized clock to the other AFC boards running in the same crate through the MicroTCA crate backplane. This clock will be used as a reference clock to the BPM electronics ADCs.

Figure 1: AFC board with two FMC 5 POF mounted.

FMC 5 POF

The FMC 5 POF board [9] has 5 plastic optical fiber (POF) transceivers mapping the same number of trigger lines from the FPGA through a FMC connector on the AFC board. As the input and output transceivers are different components with the same footprint, the board can be manufactured with up to 5 POF inputs or outputs. In Sirius timing system, it will output synchronized triggers for varied devices

Content from this work may be used under the terms of the CC BY 3.0 licence (© 2018). Any distribution of this work must maintain attribution to the author(s), title of the work, publisher, and DOI.

ISBN: 978-3-95450-201-1 doi:10.18429/JACoW-IBIC2018-WEPA02

RECENT PROGRESS OF BUNCH RESOLVED BEAM DIAGNOSTICS FOR BESSY VSR *

J.-G. Hwang †, G. Schiwietz ‡, M. Koopmans, T. Atkinson,
A. Schälicke, P. Goslawski, T. Mertens, M. Ries, A. Jankowiak
Helmholtz-Zentrum Berlin für Materialien und Energie GmbH (HZB), Berlin, Germany

Abstract

BESSY VSR is an upgrade project of the existing storage ring BESSY II to create long and short photon pulses simultaneously for all beam lines by installing additional superconducting cavities with harmonic frequencies of 1.5 GHz and 1.75 GHz. The storage-ring operation will be influenced by a transient beam-loading effect of all cavities and by the complex filling pattern due to the disparity in the current of long and short bunches. This, in turn, could introduce a variation of beam trajectory, transverse profile, and length for the different bunches. This stimulates the development of bunch-resolved monitors for bunch length, beam size, filling pattern and beam trajectory displacement. In this paper, we show new developments of crucial beam diagnostics including measurements of the bunch-resolved temporal profile with a resolution of less than 1 ps FWHM and bunch-resolved profile with a resolution of less than 10 µm rms. The upgrade of the booster beam-diagnostics will be discussed as well.

INTRODUCTION

The BESSY Variable-pulse-length Storage Ring (BESSY VSR) project was launched at the Helmholtz-Zentrum Berlin to provide the capability of user accessible picosecond pulses at a high repetition rate, up to 250 MHz [1, 2]. The installation of additional harmonic-frequency superconducting radio-frequency (SRF) cavities generates a beating of the voltages of two SRF systems, thereby creating alternating buckets for long and short bunches [3]. BESSY VSR preserves the present average brilliance of BESSY II by filling more beam current in the long bunch buckets since the short bunch buckets have relatively low bunch charge to avoid the longitudinal microwave instability that occurs above a certain threshold current. This results in the disparity in 6-D phase space particle distribution such as spatial distribution, angular spread, and energy spread. The implementation of the 1.5 GHz and 1.75 GHz SRF cavities for BESSY VSR enhances a relative phase shift along multi-bunch train due to combined effects of a transient beam-loading in the cavities and complex filling pattern. The relative phase shift can cause a variation of beam trajectory, transverse profile, and length for the different bunches. This stimulates the development of bunch-resolved monitors for transverse and longitudinal electron distribution, relative arrival phase, filling pattern and central beam trajectory. We are in the process of carefully evaluating and define all feasible monitors for BESSY VSR [4].

BEAM DIAGNOSTICS PLATFORM REFURBISHMENT

Due to confined space of our present beam diagnostics platform and the installation of a new cryogenic system for BESSY VSR cryomodule near the platform in section 3 of BESSY II, we need to move diagnostics to a new platform in the section 12 of the ring. Several modifications are requested for the new platform, as shown in Fig. 1. The main modifications are the installation of the dedicated hutch for keeping a clean environment and constant temperature, and preparation of the second optical beam line for separating the ports of the profile monitor and bunch length monitor, respectively. The third beam line for THz-based diagnostics will be also prepared inside the accelerator bunker. During summer machine shutdown, the extension of the stage and preparation of new optical beam line such as drilling a hole into the accelerator bunker was conducted. The installation of the hutch is scheduled for next year for a smooth transition will allow time for commissioning of all devices at the new platform.

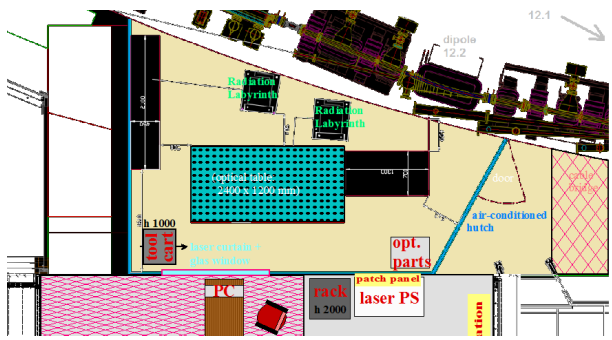

Figure 1: Schematic layout of new optical beam diagnostics platform for BESSY VSR with two beam lines and three separated optical tables.

In addition, we are putting in a great deal of effort into the evaluation and optimization of the optical transport system for timing experiments, which consists of a elliptical mirror with a hexapod 6-axis stage and toroidal mirror with a degree of freedom in angles. Based on a ray-tracing simulation and experimental results, we hope to improve the light output and the position sensitivity with less timing distortion. We are also preparing the isolation of optical tables from ambient vibration sources such as cryogenic compressors, vacuum

* Work supported by German Bundesministerium für Bildung und Forschung, Land Berlin, and grants of Helmholtz Association.
† ji-gwang.hwang@helmholtz-berlin.de
‡ schiwietz@helmholtz-berlin.de

Content from this work may be used under the terms of the CC BY 3.0 licence (© 2018). Any distribution of this work must maintain attribution to the author(s), title of the work, publisher, and DOI.

ISBN: 978-3-95450-201-1 doi:10.18429/JACoW-IBIC2018-WEPA06

THERMAL COEFFICIENT OF DELAY MEASUREMENT OF THE NEW PHASE STABLE OPTICAL FIBER *

Jiaji Liu†, Xinpeng Ma, Guoxi Pei, Institute of High Energy Physics Chinese Academy of Sciences, Beijing, China

Abstract

The Thermal Coefficient of Delay (TCD) is an essential parameter of optical fiber which determines a fiber's phase transfer stability due to temperature variation. The TCD of a new phase stable single mode optical fiber (YPSOC) from Yangtze Optical Fibre and Cable Company (YOFC) is measured. The radio frequency (RF) signal is modulated to optical wave by a laser module which is transmitted through the 400-meter long YPSOC to be measured. The returned optical wave is demodulated to RF signal by the photodetector. A phase detector and a data acquisition module (DAQ) are used to acquire the phase difference between the forward and returned signals. Two temperature-stabilized cabinets are designed to maintain and control the ambient temperature of the measurement system. The TCD of less than 10 ps/km/K at room temperature is obtained. YPSOC and the measurement platform can be applied on signal transmission or measurement system that need to compensate the temperature drift.

INTRODUCTION

In the long-distance optical wave transmission system, the optical path length will change due to the different temperatures on the transmission path, which will introduce phase drift to the RF/digital transmission system. The TCD range of most standard single mode fibers (SMFs) is from 33.4 to 42.7 ps/km/K.

But, The TCD of phase stable optical fiber (PSOF) by Furukawa is below 5 ps/km/K [1]. And the strong tether fiber optic cable (STFOC) from Linden Photonics is nearly as good as PSOF, its TCD is below 7 ps/km/K [2].

Using this kind of phase stable optical fiber instead of a conventional one will reduce the delay change of the stable RF transmission system.

TESTED CABLE

The phase stable optical fiber is generally composed of standard optical fiber and negative expansion coefficient materials, therefore it has a good temperature performance and tensile strength. YPSOC is coated with liquid crystal polymer (LCP). A purpose of LCP coating is to make the temperature dependence of transmission delay time small [1]. YPSOC has a 250 μm tight buffered cable core, followed by a tight buffered LCP coating and a soft outer jacket (Fig. 1) [3].

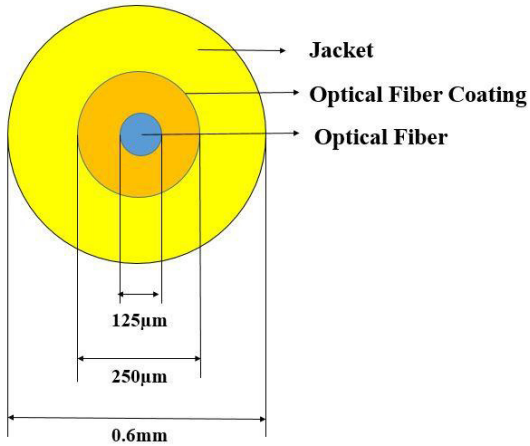

Figure 1: Cross sectional view of YPSOC.

MEASURE CONCEPT

There has several methods to measure the TCD of a fiber. For example, the TCD of a fiber which is coupled with jacket can be calculated by a formula. But it is complex and difficult to calculate TCD by using this formula [4].

On the other hand, an electronic and optical system can be used to measure the TCD by changing the ambient temperature of the fiber and detecting the time shift. This method is simple and operational. So, the TCD of a fiber can be calculated by the following formula.

$$\mathrm{TCD} = \frac{\text{Delay shift}}{\text{Temperature change} * \text{Fiber Path}} \quad (1)$$

A TCD measurement system based on the second method is designed. The layout of the fiber measurement system is shown in Fig. 2. The black lines are RF signal path and the green lines are optical wave path. The RF signal is sent to the power splitter from an analog signal generator, and transmitted to the laser module and the phase detector. The optical wave (1552 nm) from the laser module is propagated to the receiver through the optical circulator and the 400-meter long YPSOC, then retroreflected by a Faraday rotation mirror (FRM) at the end of the fiber. The round trip optical wave goes through the same fiber. The retroreflected optical wave is converted to RF signal by the photodetector, and transmitted to the phase detector through the amplifier, then compared with the local RF signal. Since the delay through fiber and other RF components is temperature dependent, RF and optical components are temperature stabilized to ±0.01 °C.

† liujj@ihep.ac.cn

Content from this work may be used under the terms of the CC BY 3.0 licence (© 2018). Any distribution of this work must maintain attribution to the author(s), title of the work, publisher, and DOI.

ISBN: 978-3-95450-201-1 doi:10.18429/JACoW-IBIC2018-WEPA07

BEAM PHASE MEASUREMENT SYSTEM IN CSNS LINAC

Peng Li#, [1], Wei Peng[2], Fang Li[1], Jun Peng[1], Ming Meng[1], Taoguang Xu[1]
[1] Institute of High Energy Physics (IHEP), Chinese Academy of Sciences (CAS), 523803, Dongguan, China
[2] 38th Institute of China Electronics Technology Group Corporation (CETC-38), 230088, Hefei, China

Abstract

We developed beam phase measurement system ourselves in CSNS (China Spallation Neutron Source). The resolution of the system is less than 0.1° and the accuracy is less than 1°. It played a key role in CSNS Linac commissioning especially in RFQ and DTL commissioning. Further we measured the beam energy by TOF (Time of Flight) method base on this system. The energy accuracy is less than 0.1 MeV.

INTRODUCTION

The CSNS accelerator consists of an 80MeV H- Linac, a 1.6 GeV Rapid Cycling Synchrotron (RCS) and related beam transport line. There are three beam transport line in Linac: Low Energy Beam Transport line (LEBT) after the 50 keV H- Ion Source, Medium Energy Beam Transport line (MEBT) after the 3MeV Radio Frequency Quadrupole (RFQ), Lianc to Ring Beam Transport line (LRBT) after Drift Tube Linac (DTL). Beam is transported to Target after it be accelerated to 1.6GeV in RCS [1]. The layout of the CSNS Linac is shown in Fig. 1.

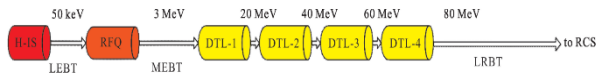

Figure 1. Layout of CSNS Linac.

The repeat period of H- beam macro-pulse is 40ms and pulse width is about 500μs. The radio frequency of beam is 324 MHz and the beam micro-pulse duty ratio is about 30%.

BEAM PHASE MEASUREMENT SYSTEM

FCT sensors are used as beam phase detectors [2] which were produced by Bergoz company. FCT sensor has a rapid signal rise time, which is shorter than 200 ps so it's good for 324 MHz signal's measurement. And the output of FCT sensor signal also has the 324 MHz time structure [3].

The electronics are researched and developed by IHEP and CETC-38 together in China. There are two sets beam phase measurement systems in CSNS Linac and each set has 8 channels for FCT output signals.

Sub-sampling technology has been adopted to realize the electronics. The ADC sample clock is just 100 MHz shown in Fig. 2. Each channel's phase output is the difference between FCT output signal phase and a reference signal phase. The reference signal is a 324 MHz sine wave signal which from the same RF frequency source with beam. Non-coherent digital IQ demodulation technology and CORDIC algorithm are used for phase calculation in FPGA. The schematic is shown in Fig. 3.

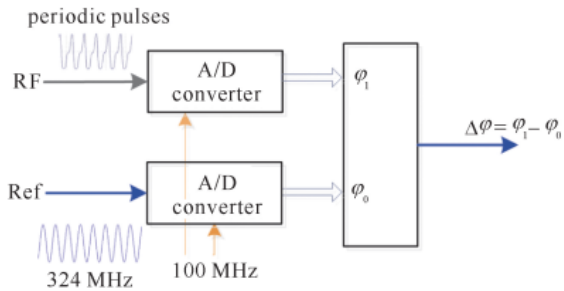

Figure 2. Principle of phase measurement.

The electronics phase resolution is less than 0.1° and the phase non-uniformity between channels limited in ±0.2°. The amplitude accuracy is better than 1% and the phase accuracy is better than 0.3°. We had test the whole system for more than 7 days online with a precise signal generator and find its accuracy is better than 1°.

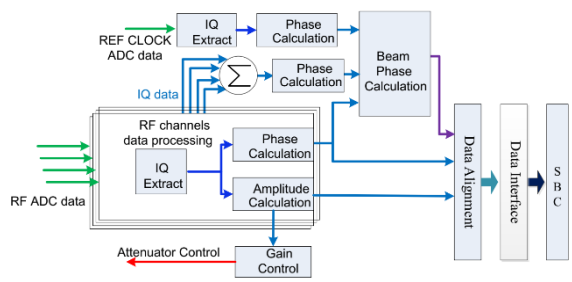

Figure 3: Schematic in FPGA.

The beam phase measurement system played a key role in CSNS Linac commissioning especially in RFQ and DTL commissioning. The RFQ and DTL cavity power phase varied after several days' shutdown or other accident problems. The beam phase measurement system would be running in such a situation.

BEAM ENERGY MEASUREMENT

Beam energy could be calculated by TOF method meanwhile [4]. The distance between FCT sensors are known after they were installed easily. The beam flight time between FCT sensors is computed by phase difference indirectly. Then the beam velocity and energy could be calculated.

There are 5 FCT sensors and 1 set electronics could be used to compute beam energy after beam pass through RFQ, Buncher-1, Buncher-2 in CSNS Linac MEBT. See Fig 4.

#lipeng@ihep.ac.cn

Content from this work may be used under the terms of the CC BY 3.0 licence (© 2018). Any distribution of this work must maintain attribution to the author(s), title of the work, publisher, and DOI.

ISBN: 978-3-95450-201-1 doi:10.18429/JACoW-IBIC2018-WEPA09

LONG TERM BEAM PHASE MONITORING BASED ON HOM SIGNALS IN SC CAVITIES AT FLASH

J. H. Wei†, NSRL, University of Science and Technology of China, 230026 Hefei, P. R. China
and Deutsches Elektronen-Synchrotron, 22607 Hamburg, Germany
L. Shi, Paul Scherrer Institut, 5232 Villigen PSI , Switzerland
N. Baboi, Deutsches Elektronen-Synchrotron, 22607 Hamburg, Germany

Abstract

The accelerating RF fields in superconducting cavities must be controlled precisely in FEL (Free Electron Laser) facilities to avoid beam energy spread and arrival time jitter. Otherwise the beam quality is degraded. The LLRF (Low Level Radio Frequency) system controls the RF field and provides a highly stable RF reference. A new type of beam phase determination technique based on beam-excited HOMs (Higher Order Modes) in cavities has been implemented. The two special couplers installed at both ends of each cavity, pick up the signals containing both the leakage of the accelerating field and the HOM signals. Therefore the signals can be used to calculate the beam phase directly with respect to the RF phase. We analysed the factors which may affect the result of the beam phase on a long-term based on an experimental platform at FLASH. Some phase drifts between the HOM-BPhM (Beam Phase Monitor) and the LLRF system phase measurement were observed and the reason will be further studied.

INTRODUCTION

Superconducting linac based FELs (Free Electron Lasers) require control of the main RF phase relative to beam arrival time at a very precise level. At FLASH [1] and the E-XFEL (European X-ray FEL) [2], the LLRF (Low Level Radio Frequency) system is responsible for regulation of the RF fields [3]. A "vector-sum" method is applied to control the beam phase. The field vector of each single cavity is measured and then the field vector-sum of up to 32 cavities is calculated. A klystron feeds up to 4 modules with high power 1.3 GHz fields. Each module contains eight superconducting nine cell cavities. Figure 1 shows a schematic view of the LLRF control system [4]. The vector-sum has to be stabilized in amplitude and phase to a given set point. [5]. The stability of the RF amplitude and phase is required to be below 0.01% and 0.01° RMS respectively for both FLASH and the E-XFEL. The control system acts onto the vector-sum and keeps it constant, while each single cavity field within the vector-sum can fluctuate.

A new method based on HOM (Higher Order Modes) to determine the beam phase was developed [6]. When an electron bunch transverses a superconducting cavity, HOMs are excited, which carry the beam phase information. Two couplers located at each side of the TESLA cavity were specially designed to damp and extract the HOM signals. The power leakage of the accelerating field is also picked up by the HOM couplers. These fields can be used to determine the beam phase with respect to the accelerating RF fields. The monopole modes are most suited for beam phase measurement since they are not affected by beam offset. In this paper, we choose the 2nd monopole mode in TM011 band and built a scope based setup. This HOM-BPhM system is an on-line direct beam phase measurement with respect to the RF.

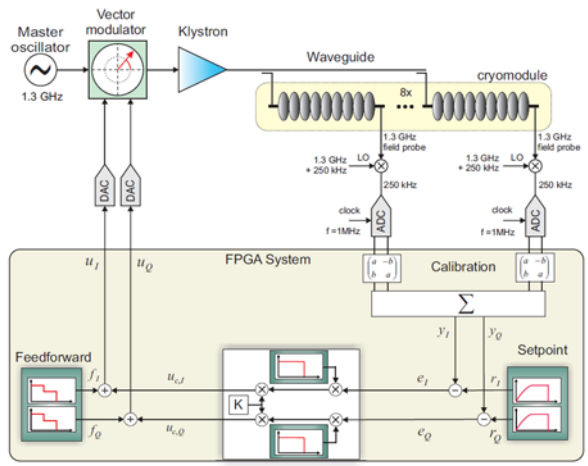

Figure 1: Schematic view of the current LLRF control system consists of analogue and digital sections [4].

In this paper, we first introduce the principle of the HOM-BPhM and then present the result of the long term measurements.

PRINCIPLE OF HOMBPHM

Beam Phase Concept

The electric field of each single cavity picked up with probe antennas give the vector-sum [7]. It is assumed that all cavities have the same physical behaviour, which means that the transient field induced by the beam has the same absolute value in each cavity [8]. The calibration is based on measuring this transient in amplitude and phase of each cavity and then calculating the ratio of the single cavity field to the vector-sum.

For maximum acceleration, the RF field should reach its maximum when the beam passes through the centre of the cavity. We define the beam phase according to the time difference between two instants: when the beam passes the cavity AND when the accelerating gradient in the cavity is maximum. The point of maximal accelerating voltage is called "on-crest", see Fig. 2 [8]. In ACC1 (the first accelerating module in FLASH), and similarly at the E-XFEL, the beam is accelerated "off-crest" to induce a bunch

† junhao.wei@desy.de.

Content from this work may be used under the terms of the CC BY 3.0 licence (© 2018). Any distribution of this work must maintain attribution to the author(s), title of the work, publisher, and DOI.

ISBN: 978-3-95450-201-1 doi:10.18429/JACoW-IBIC2018-WEPA12

DIFFERENTIAL EVOLUTION GENETIC ALGORITHM FOR BEAM BUNCH TEMPORAL RECONSTRUCTION*

D. Wu, D. X. Xiao, J. X. Wang†
Institute of Applied Electronics, China Academy of Engineering Physics, Mianyang, 621900, China

Abstract

Coherent radiation, such as coherent transition radiation, coherent diffraction radiation, coherent synchrotron radiation, etc, can be used to measure the longitudinal distribution of the electron beam bunch of any length, as long as the coherent radiation spectrum can be measured. In many cases, the Kramers-Krönig relationship is used to reconstruct the temporal distribution of the beam from the coherent radiation spectrum. However, the extrapolation of the low frequency will introduce the uncertainty of the reconstruction. In this paper, an algorithm of differential evolution (DE) for temporal reconstruction is discussed. The DE reconstruction works well for the complex and ultrashort distribution. It will be an effective tool to accurately measure the femtosecond bunch temporal structure.

INTRODUCTION

During the past decades, many methods were developed to measure ultrashort electron beam bunch length, such as streak camera [1], RF zero-phasing [2], deflecting cavity [3], electro-optic sampling [4] and coherent radiation [5–7]. Coherent radiation, such as coherent transition radiation, coherent diffraction radiation, coherent synchrotron radiation, etc, can be used to measure the longitudinal distribution of the electron beam bunch of any length, as long as the coherent radiation spectrum can be measured. When the electron bunch length become as short as a few femtosecond nowadays, the coherent radiation method method becomes the best length-measurement tool.

However, the coherent radiation measurement is to record the spectrum of the radiation, which looses the phase information. To reconstruct the longitudinal distribution, the phase information must be reconstructed first. For a long time, Kramers-Krönig (KK) relation was invited to retrieve the phase information. Unfortunately, there are at least three disadvantages of the KK relation. Firstly, extrapolation in the low frequency band will bring uncertainty to reconstruction. Secondly, KK relation is less accurate when time domain distribution is complicated. Thirdly, KK relation costs longer calculation time.

GrEedy Sparse PhAse Retrieval (GESPAR) method was presented by Y. Shechtman and Y. C. Eldar in 2014 [8, 9]. And then it has rapidly gained great applications in coherent imaging, signal processing, macromolecular imaging, and 5G communication[10–12]. GESPAR treats phase reconstruction as a nonlinear least squares problem, and assumes that the time domain signal is composed of a finite number of specific distributions.

In this paper, we invite the Differential evolution (DE) genetic algorithm to solve the nonlinear least squares problem. And the reconstruction with or with out the GESPAR assumption is presented, respectively. At last, a temporal reconstruction with DE algorithm is shown from the signal measured on the Chengdu THz FEL (CTFEL) [13] facility.

RECONSTRUCTION ALGORITHM

Phase Retrieval with Nonlinear Least Squares

Assumming $\rho(t)$ is the original time signal, whose frequency signal is $\widehat{\rho}(\nu) = F(\rho(t)) = |\widehat{g}(\nu)|e^{-\phi(\nu)}$, where F represents the Fourier transform, $|\widehat{g}(\nu)|$ is the amplitude and $\phi(\nu)$ is the phase.

Four the nonlinear least squares consideration, the objective is to minimize the function $f = ||\widehat{\rho}_G^2 - |\widehat{g}|^2||$, where $\widehat{\rho}_G$ is the G-th alternative signal. The flow-chart is shown in Fig. 1.

According to the Fourier transform relationship, we can normalize any segment of the time domain signal to the signal in the (0,1) time period. If the setting unit is 1 s, the corresponding frequency domain unit interval is 1 Hz, for example. And similarly, 1 ps in time domain corresponds 1 THz in frequency domain. This is the reasons why the coherent radiation can measure any shor bunch length as long as the frequency signal can be recorded correctly.

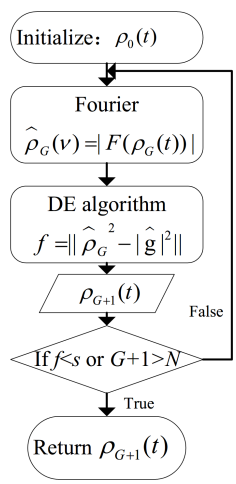

Figure 1: Phase retrieval flow chart with nonlinear least squares.

* Work supported by China National Key Scientific Instrument and Equipment Development Project (2011YQ130018), National Natural Science Foundation of China with grant (11475159, 11505173,11505174, 11575264, 11605190 and 11105019)
† jianxinwang1026@163.com

Content from this work may be used under the terms of the CC BY 3.0 licence (© 2018). Any distribution of this work must maintain attribution to the author(s), title of the work, publisher, and DOI.

ISBN: 978-3-95450-201-1 doi:10.18429/JACoW-IBIC2018-WEPA13

ELECTRO-OPTIC MODULATOR BASED BEAM ARRIVAL TIME MONITOR FOR SXFEL*

X.Q. Liu†, Y.B. Leng, R.X. Yuan, L.W. Lai, L.F. Hua, N. Zhang,
Shanghai Institute of Applied Physics,Chinese Academy of Sciences, Shanghai, China

Abstract

Beam arrival time monitor (BAM) is an important tool to investigate the temporal characteristic of electron bunch in free electron laser (FEL) like Shanghai soft X-ray Free Electron Laser (SXFEL). Since the timing jitter of electron bunch will affect the FEL's stability and the resolution of time-resolved experiment at FELs, it is necessary to precisely measure the electron bunch arrival time so as to reduce the timing jitter of the electron bunch with beam based feedback. The beam arrival time monitor based on electro-optic modulator (EOM) is already planned and will be developed and tested at SXFEL in the next three years. Here the design and preliminary results of the EOM based beam arrival time monitor will be introduced in this paper.

INTRODUCTION

As China's first X-ray free electron laser (FEL) facility, SXFEL has finished the infrastructure and installation, right now is under commissioning. The main parameters of SXFEL are listed in table 1.

Table 1: Main Parameters of SXFEL

parameter	value
Wavelength	3-9 nm
length	~300m
FEL principle	HGHG, EEHG
Beam energy	840 MeV
Peak current	500A
Normalized emittance	1.5mm.rad
Bunch length(FWHM)	500 fs

The SXFEL is a test facility for various external seeding modes, such as HGHG and EEHG. External seeding lasers are required for the generation of fully coherent radiation pulse. For seeded FEL, large timing jitter and drift of the electron bunch will affect the synchronization between the electron bunch and seed laser, then consequently reduce the stability of the output radiation. To reduce the timing jitter of the electron bunch with beam based feedback, it is necessary to precisely measure the electron bunch arrival time at different locations through the entire FEL facility. The Beam arrival time monitor (BAM) based on phase cavity and RF phase detecting technology has already been tested at SXFEL and obtained the 67.7 fs arrival time resolution [1], while efforts are ongoing to improve the resolution. Meanwhile, to achieve better bunch arrival time resolution, the electro-optic modulator (EOM) based beam arrival time monitor scheme originated from DESY [2-3] is also planned for SXFEL and will be developed and tested at SXFEL in the next three years. In this paper, we present the design of the EOM based beam arrival time monitor for SXFEL, as well some recent progress.

* Work supported by the National Key Research and Development Program of China (Grant No. 2016YFA0401990, 2016YFA0401903).
† liuxiaoqing@sinap.ac.cn

DESIGN OF THE BEAM ARRIVAL TIME MONITOR

Figure 1 shows the schematic diagram of the BAM for SXFEL. The BAM consists of three parts, the beam pick-up, the BAM frond-end and back-end. The beam pick-up is located in tunnel to extract the transient RF signal generated by the driving electron bunch. The BAM frond-end also placed in tunnel is used to transform the shifting of RF signal's first zero-crossing, which stands for the arrival time of the electron bunch, into intensity variation of a reference optical pulse. The BAM back-end placed outside the tunnel is used to detect the amplitude of the optical pulse and derive the electron bunch arrival time information.

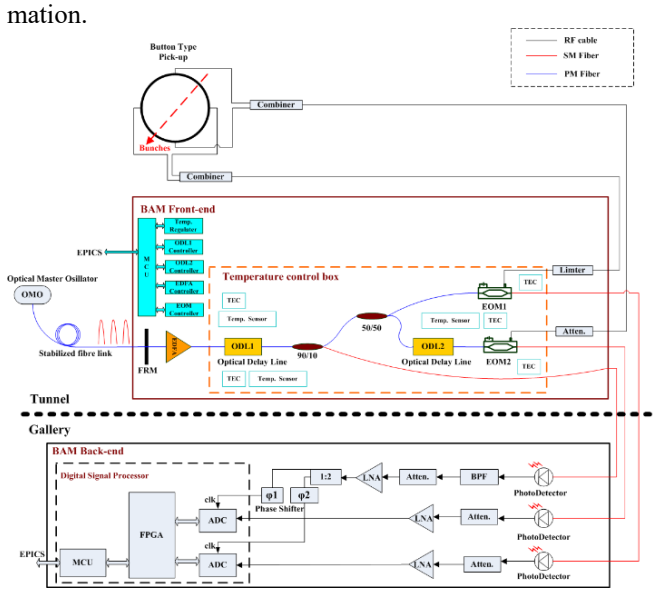

Figure 1: Schematic diagram of the BAM for SXFEL.

Operation Principle

As shown in Fig.1, the optical master oscillator (OMO) is a mode-locked fibre laser with 1550 nm wavelength and 238 MHz repetition rate. The ultra-stable femtosecond optical pulse emitted from OMO transmits over the stabilized fibre link to the remote BAM station and serves as the optical reference signal for BAM. The reference optical pulse enters the BAM front-end and a faraday rotator mirror (FRM) reflects part of it back to help stabilize the phase of the reference optical pulse. The rest optical pulse passes

Content from this work may be used under the terms of the CC BY 3.0 licence (© 2018). Any distribution of this work must maintain attribution to the author(s), title of the work, publisher, and DOI.

ISBN: 978-3-95450-201-1 doi:10.18429/JACoW-IBIC2018-WEPA15

DEVELOPMENT OF BAM ELECTRONICS IN PAL-XFEL

D.C. Shin*, C.-K. Min, G.J. Kim, C.B. Kim, H.-S. Kang, J. Hong†, PAL, Pohang, Korea

Abstract

We describe the electronics for electron bunch arrival time monitor (BAM) with a less than 10 femtosecond resolution, which was developed in 2017 and is currently in use at PAL-XFEL. When electron bunches go through an S-band monopole cavity, about 1 us long RF signal can be obtained to compare with a low phase noise RF reference. The differential phase jitter corresponds to the arrival time jitter of electron bunches. RF front-end (F/E) which converts the S-band pickup signal to intermediate frequency (IF) signal, is the essential part of a good time resolution. The digitizer and the signal processor of the BAM electronics are installed in an MTCA platform. This paper presents the design scheme, test results of the BAM electronics and future improvement plans.

INTRODUCTION

In the tunnel of PAL-XFEL, 10 BAM pickups are installed. The pickup is made of S-band monopole cavity type. The resonance frequency is 2826 MHz, which have the offset of ≈30 MHz from our reference, 2856 MHz to remove a dark contribution. More details on the BAM pickup are described in Ref. [1].

BAM electronics consists of RF F/E unit for the frequency conversion of the pickup signal to an IF signal and main IOC for digitizing and processing the signal. RF F/E was designed as non-platform type (e.g. pizza-box type) and main IOC was implemented on the MTCA.4 platform.

The prototype of the BAM electronics, which is developed in 2017, has been tested at both the injector and the main-dump sites.

Table 1 shows the main specifications of the BAM electronics.

Table 1: Specification of the BAM Electronics

Parameter	Value	Unit
Phase Measurement Resolution	≤ 10	fs
Repetition Rate for Operation	≥ 60	Hz
Input RF Frequency	2826	MHz
REF Frequency	2856	MHz
Sampling Frequency	238	MHz
Platform	MTCA.4	

ELECTRONICS

The block diagram of the BAM electronics is shown in Fig. 1.

The signals induced from the pickup are transmitted to the RF F/E via cables with good phase stability for temperature. The BAM pickup signals are converted to IF signals of about 30 MHz using a mixer.

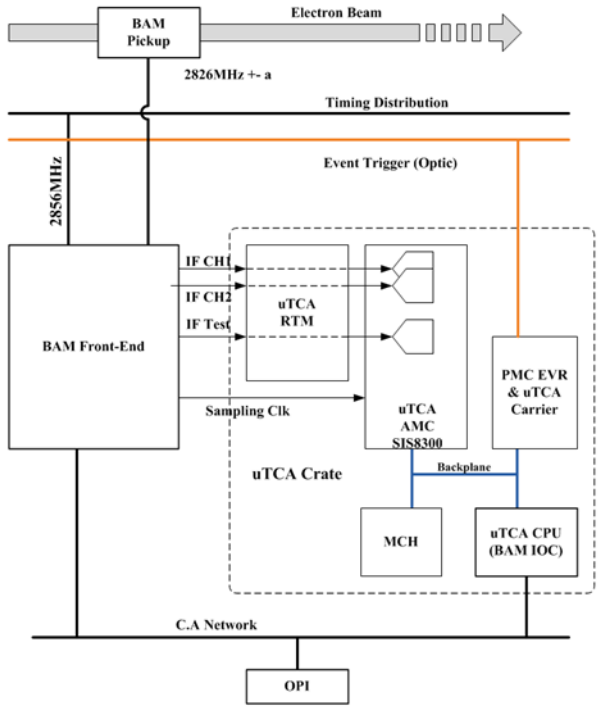

Figure 1: BAM electronics block diagram.

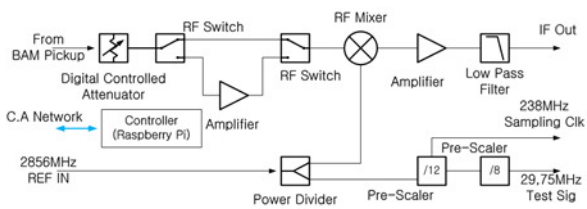

Figure 2: Block diagram of the RF F/E.

Figure 2 shows the RF F/E block diagram. A digital con-trolled attenuator is installed at the input, and is followed by a switch bank. In a high charge mode, the switch is bypassed and in a low charge mode, the signal is passed through the amplifier for power matching. The frequency down-converted signal using the reference in the mixer go through the IF amplifier and the low pass filter [2].

For the digitizer, a synchronized 238 MHz sampling clock, the 12th sub-harmonic of the reference, is generated in the RF F/E. The jitter of the sampling signal has to be small because it affects the signal noise ratio (SNR) of the system. We used HMC905LP3E and HMC794LP3E prescaler chips from Analog Device Inc. The total jitter of the 238 MHz sampling clock measured using a signal-

* dcshin@postech.ac.kr
† npwinner@postech.ac.kr.

Content from this work may be used under the terms of the CC BY 3.0 licence (© 2018). Any distribution of this work must maintain attribution to the author(s), title of the work, publisher, and DOI.

ISBN: 978-3-95450-201-1 doi:10.18429/JACoW-IBIC2018-WEPA16

MICROBUNCHING INSTABILITY MONITOR FOR X-RAY FREE ELECTRON LASER

C. Kim*, J.H. Ko, G. Kim, H.-S. Kang, and I.S. Ko
Pohang Accelerator Laboratory, POSTECH, Pohang 790-834, Korea

Abstract

A direct method was developed to measure the microbunching instability in the X-ray Free Electron Laser (XFEL). The microbunching instability comes from the interaction between the electron beam and the coherent synchrotron radiation (CSR), and the FEL intensity can be affected significantly by the microbunching instability. Until now, however, no effective method had been introduced to monitor the microbunching instability, and we tried to install a CCD camera to monitor the microbunching instability after the bunch compressor. The measurement result showed that the microbunching instability can be monitored by the CCD camera, and more interesting features of the microbunching instability were revealed from it.

INTRODUCTION

When an electron beam passes through an undulator, the spontaneous synchrotron radiation is generated and it can interact back with the electron beam again. The interaction makes the beam energy modulation on the scale of the resonant wavelength from the energy exchange between the radiation electric field and the oscillating motion of the electron beam to the transverse direction [1]. The undulator is a dispersive device and the energy modulation is changed into a longitudinal density modulation which is called a microbunching. The microbunching enhances the coherence of the radiation and increases the radiation intensity to develop a collective instability [2, 3]. The scale of the microbunching is much shorter than that of the bunch length and the microbunching instability grows up until the maximum bunching is achieved if the undulator length is long enough. In short, the microbunching instability is the working principle of Self-Amplified Spontaneous Emission (SASE) [4–6]

In the Free Electron Linac (FEL), bunch compressors are used to enhance the performance of the FEL by reducing the bunch length for high current and high brightness. A relativistic electron bunch can have an energy chirp while passing through the off crest of the linac RF phase before the bunch compressor, and lower energy electrons move to the front of the electron bunch and higher energy ones go back. Inside the bunch compressor, the electron beam passes through a strong dispersive section, and higher energy electrons follow a shorter trajectory and lower energy ones travel a longer trajectory. Because of the path length difference, the high energy electrons at the back of the electron bunch catch up with the lower energy ones in the front, and the bunch length decreases. In this process, it is important not to increase the energy spread or the transverse emittance beyond tolerances during the bunch compression.

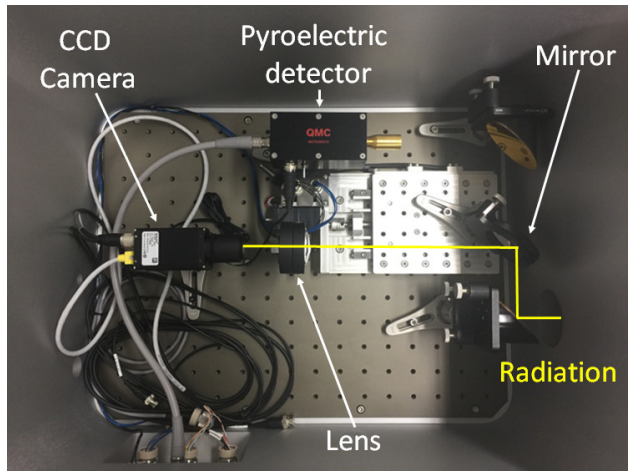

Figure 1: Experimental setup of the Coherent Radiation Monitor of PAL-XFEL.

Like an undulator, the bunch compressor is a dispersive device and synchrotron radiation can be generated from bending magnets. This means that the microbunching can be generated in the linac bunch compressor. Especially, Coherent Synchrotron Radiation (CSR) can be a source of the beam density modulation at wavelengths small compared to the bunch length. The effect of microbunching from CSR has been observed in computer simulations of the bunch compressor designed for the Linac Coherent Light Source (LCLS) [7], and in the bunch compressor simulation of the TESLA Test Facility [8]. Analytical studies of the CSR effects in bunch compressors also have been published in literature [9].

In this paper, we introduce a direct method to monitor the microbunching instability. A visible CCD camera is installed to measure the intensity of the coherent radiation after the bunch compressor. The measurement result shows that strong visible radiation is observed after the bunch compressor and the CCD camera can be used as a microbunching monitor without any beam interruption.

COHERENT RADIATION MONITOR

X-ray Free Electron Laser of Pohang Accelerator Laboratory (PAL-XFEL) is a hard X-ray FEL to produce 0.1 nm wavelength photon [10]. From a photo-cathode RF gun, an electron beam is generated with 5 MeV energy and 150 pC charge by using an Ultra-Violet (UV) laser pulse of 3 ps pulse width. The electron beam is accelerated to 10 GeV energy by using S-band (2856 MHz) RF structures in the

* chbkim@postech.ac.kr

Content from this work may be used under the terms of the CC BY 3.0 licence (© 2018). Any distribution of this work must maintain attribution to the author(s), title of the work, publisher, and DOI.

ISBN: 978-3-95450-201-1 doi:10.18429/JACoW-IBIC2018-WEPA17

DEVELOPMENT, FABRICATION AND LABORATORY TESTS OF BUNCH SHAPE MONITORS FOR ESS LINAC

S. Gavrilov†[1,2], A. Feschenko[1], D. Chermoshentsev[1,2]
[1]Institute for Nuclear Research of the Russian Academy of Sciences, Troitsk, Moscow, Russia
[2]Moscow Institute of Physics and Technology, Moscow, Russia

Abstract

Two Bunch Shape Monitors have been developed and fabricated in INR RAS for European Spallation Source linac. To fulfil the requirements of a 4 ps phase resolution the symmetric λ-type RF-deflector based on a parallel wire line with capacitive plates has been selected. Additional steering magnet to correct incline of the focused electron beam is also used. Limitations due to a space charge of the analysed beam and due to external magnetic fields are discussed. Laboratory tests of the monitors are described.

INTRODUCTION

Bunch Shape Monitors (BSMs) are intended for the measurements of a longitudinal distribution of particles in bunches of the accelerated proton beam in ESS: the first BSM will be installed in MEBT at 3.6 MeV, and the second one – between the normal conducting and the superconducting parts of the linac at 90 MeV.

The operation principle of BSM, developed in INR RAS, is based on the technique of a coherent transformation of a temporal bunch structure into a spatial charge distribution of low energy secondary electrons through a transverse RF-scanning [1] and is clear from Fig. 1.

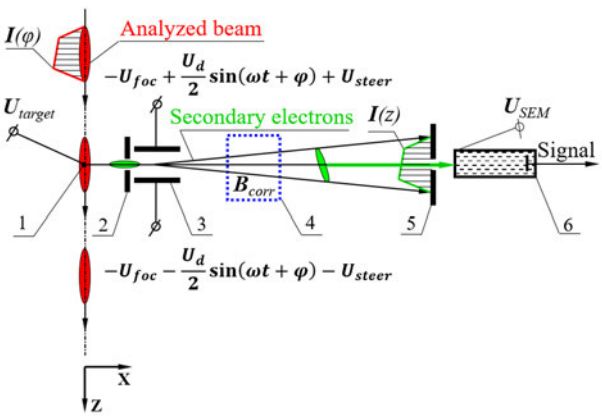

Figure 1: BSM scheme: 1 – tungsten wire target, 2 – inlet collimator, 3 – RF-deflector combined with electrostatic lens, 4 – correcting magnet, 5 – outlet collimator, 6 – secondary electron multiplier.

The series of the analysed beam bunches crosses the wire target 1 which is at a high negative potential about -10 kV. Interaction of the beam with the target results in emission of low energy secondary electrons, which characteristics of importance for bunch shape measurements are practically independent of beam energy, so the monitors are fabricated in practically the same design (Fig. 2), except for the beam aperture size.

† s.gavrilov@gmail.com

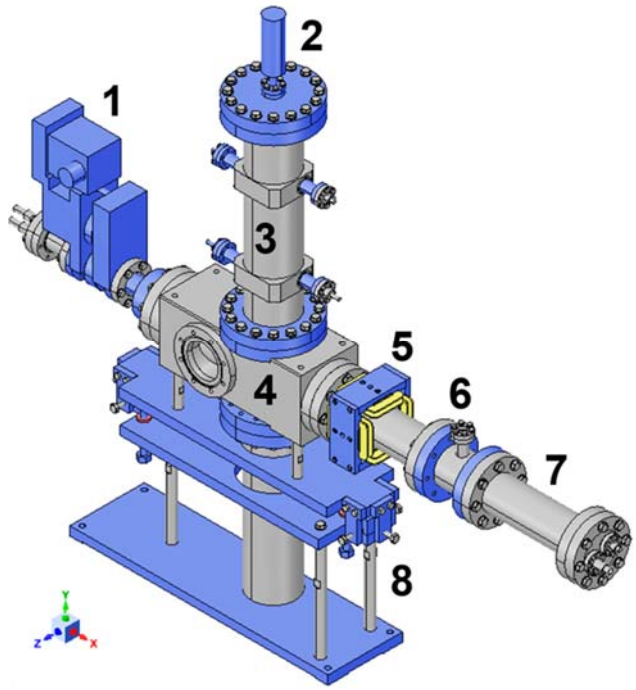

Figure 2: ESS BSM design: 1 – target actuator, 2 – tuner, 3 – RF-deflector, 4 – BSM box, 5 – quadrupole + dipole correcting magnet, 6 – viewport for optical control of e-beam, 7 – SEM-detector, 8 – support with 3D-adjustment.

The electrons are accelerated by electrostatic field and move almost radially away from the target. A fraction of the electrons passes through the inlet collimator 2 and enters the RF-deflector 3, where electric field is a superposition of electrostatic focusing and steering fields and RF-deflecting field with a frequency equal to the RF-field frequency in the linac: 352.2 MHz.

Passed electrons are scanned by the RF-field and an intensity of electrons passed through the outlet collimator 5 represents a fixed point of the longitudinal phase distribution of the primary beam. Other points can be obtained by changing the phase of the deflecting field with respect to the RF-reference. If the phase of the deflecting field is adjusted in a wide range, then the bunch can be observed twice per the period of the deflecting field.

By adjusting the steering voltage, one can change the measured phase position of the observed bunches and obtain the periodicity of bunches to be exactly equal to π. If the bunch duration is larger than π, the intensities corresponding the phase points differed by π are superimposes and the results of bunch shape measurements become wrong.

Content from this work may be used under the terms of the CC BY 3.0 licence (© 2018). Any distribution of this work must maintain attribution to the author(s), title of the work, publisher, and DOI.

ISBN: 978-3-95450-201-1 doi:10.18429/JACoW-IBIC2018-WEPA18

DEVELOPMENT OF LONGITUDINAL BEAM PROFILE DIAGNOSTICS FOR BEAM-BEAM EFFECTS STUDY AT VEPP-2000

M. Timoshenko*, V. Borin, V. Dorokhov, O. Meshkov, Yu. Rogovsky, D. Shwartz, Yu. Zharinov
BINP SB RAS, Novosibirsk, Russia

Abstract

The comprehensive development of beam longitudinal profile measurement systems based on stroboscopic optical dissector has started at VEPP-2000 electron-positron collider complex. The dissector was setted and commissioned at booster ring BEP that was deeply upgraded (2013-2015) to achieve top energy of 1 GeV. Bunch lengthening with current was studied at BEP with its new RF-cavity. In addition the method of synchrotron frequency measurement by dissector was applied. After dissector checkouts at BEP the similar studies were carried out with a single beam at VEPP-2000 storage ring in parallel with streak-camera measurements. Good agreement of results was observed. Series of single-turn longitudinal and vertical bunch profiles snapshots was made by streak-camera with respect to delay after counter beam injection. The unexpected longitudinal beam dynamics was observed for intensities above the beam-beam threshold. These studies together with beam-beam coherent oscillations spectra seen by pickups are of a great interest for understanding of flip-flop phenomenon which establish a fundamental luminosity limit at VEPP-2000 operating with round beams.

INTRODUCTION

The VEPP-2000 is a collider complex which mean parts are electron-positron booster BEP and collider VEPP-2000 with two detectors CMD-3 and SND [1]. After modernization BEP energy range began to be from 200 MeV to 1 GeV. It and BEP parameters are described in [2]. The experiments at the collider VEPP-2000 has become possible in this energy range without acceleration.

To achieve luminosity project value 10^{32} cm^{-1} s^{-1} the comprehensive beam monitoring system is required. There was no longitudinal beam distribution monitoring system. Its observation gave more full understanding of colliding beams nature.

MEASUREMENT SYSTEM AT BEP

Electron and positron booster BEP are needed for portioned storaging of particles supplied by Injection complex VEPP-5 [3] at 395 MeV energy. After storaging enough intensity of beams following accelerating (changing beam energy) and injection at collider VEPP-2000 occur. At the accelerating regime BEP work at the energy range from 200 MeV to 1 Gev. Operating with different sort of particle is possible due to polarity reverse of magnet systems.

* email address: tim94max@gmail.com

BEP synchrotron radiation spectrum contains optical range and its spectrum power maximum is around 30 nm. Beam motion is strictly periodical. These factors allow to use synchrotron radiation in optical diagnostic system. BEP have several outputs of synchrotron radiation but all are used. For these reason one of it was upgraded.

The system of longitudinal charge distribution of beam (dissector) was set and tested at BEP at first.

Optical Table Modernization

The task of modernization conclude in to save current beam transverse position monitor (CCD-camera) functional. For realization it and duplicating light of synchrotron radiation semitransparent mirror was setted in optical table tract. Yellow part of table and mirrors at the Fig. 1 is added in the modernization.

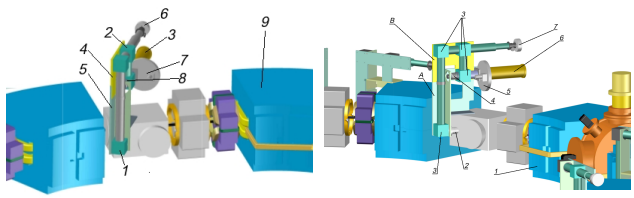

a) b)

Figure 1: Concept of modernization. Optical table before modernization a), and b) — after modernization.
1— bending magnet, 2— sync. rad. output, 3— cubes with moving mirrors, 4— calibration light source, 5— light filters, 6— dissector, 7— CCD-camera.

Alignment of Optical Table

After production necessary details and realization of optical table concept it was aligned outside BEP room with using portable CCD-cameras. The task was to pointing and focusing precisely simulation of synchrotron radiation light on the places where the real devices (CCD-camera and dissector) should be setted.

After preliminary alignment the optical table with both devices was installed to BEP synchrotron radiation output Fig. 2 and the final tuning was completed with very low intensity beam (around 100 μA) in the BEP.

DISSECTOR

Dissector is a optical stroboscopic device. One of the way of applying it is registration longitudinal distribution of beam charge in a circular accelerators where the beam motion is strictly periodical. The synchrotron radiation light

Content from this work may be used under the terms of the CC BY 3.0 licence (© 2018). Any distribution of this work must maintain attribution to the author(s), title of the work, publisher, and DOI.

ISBN: 978-3-95450-201-1 doi:10.18429/JACoW-IBIC2018-WEPA19

RESULTS FROM THE CERN LINAC4 LONGITUDINAL BUNCH SHAPE MONITOR

J. Tan†, G. Bellodi, CERN, Geneva, Switzerland
A. Feschenko, S. Gavrilov, Institute for Nuclear Research, Moscow, Russia

Abstract

The CERN Linac4 has been successfully commissioned to its nominal energy and will provide 160 MeV H⁻ ions for charge-exchange injection into the Proton Synchrotron Booster (PSB) from 2020. A complete set of beam diagnostic devices has been installed along the accelerating structures and the transfer line for safe and efficient operation. This includes two longitudinal Bunch Shape Monitors (BSM) developed by the Institute for Nuclear Research (INR, Moscow). Setting-up the RF cavities of Linac4 involves beam loading observations, time-of-flight measurements and reconstruction of the longitudinal emittance from phase profile measurements. In this paper the BSM is presented along with some results obtained during accelerator commissioning, including a comparison with phase measurements performed using the Beam Position Monitor (BPM) system.

INTRODUCTION

The Linac4 [1] is an 80 m-long, normal-conducting, pulsed, linear accelerator, providing a 160 MeV H⁻ ion beam every 1.2 s. A block diagram of the machine is shown in Figure 1. It will replace the ageing 50 MeV proton Linac2 as the injector of the PSB in 2020. The motivation for this upgrade is twofold: firstly to overcome the present space charge limitation at PSB injection, doubling the intensity within the same transverse emittance; secondly to minimise beam loss at PSB injection. The latter requirement is achieved with a charge exchange injection, an adequate chopping scheme and longitudinal phase space painting for high intensity beams.

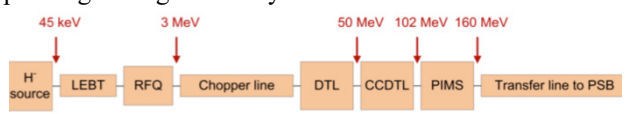

Figure 1: Linac4 schematic layout.

The beam instrumentation specifications [2, 3] along the accelerator and its transfer line must cover the challenging operational parameters summarized in Table 1.

Table 1: Linac4 Parameters and Achievements To Date

Parameters	Design target	Achieved
Peak current in the linac	40 mA	24 mA
Routine current in the linac	40 mA	20 mA
Transv. Emittance at 160 MeV	0.4 π.mm.mrad	0.3π.mm.mrad
Energy at PSB injection	160 MeV	160 MeV
Pulse length / rep. rate	400 μs / 1 Hz	up to 600 μs/1Hz

† jocelyn.tan@cern.ch

The achieved performance during the Linac4 commissioning stages from 45 keV to 160 MeV are presented in [4, 5, 6, 7]. Here we present results of longitudinal beam profile measurements performed with the BSMs located in the transfer line, including a comparison with phase measurements performed using the BPM system.

BEAM PHASE PROFILE DIAGNOSTICS

Bunch Shape Monitor

The BSM principle of operation is explained with Figure 2 and is described in detail elsewhere (see for example [8]). In brief, its operation is based on transforming the longitudinal structure of the beam under study into a transverse distribution of low energy secondary electrons.

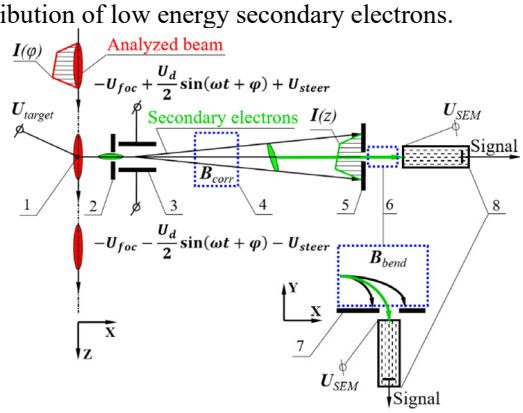

Figure 2: BSM principle: 1-wire target, 2-input collimator, 3- rf deflector combined with electrostatic lens, 4-corrector magnet, 5 and 7- collimators, 6-bending magnet, 8-electron multiplier.

This is achieved by placing a wire target in the beam, which emits secondary electrons in proportion to the instantaneous H⁻ intensity. These electrons are accelerated with a HV applied to the target and converted to a transverse distribution using an RF deflection, from which a specific slice is selected for detection using a collimator. The RF deflector operates at the accelerator frequency f_{RF} of 352.2 MHz. For a fixed setting of the RF deflecting phase with respect to the accelerator reference, the intensity of the secondary electrons passing the collimator and detected with the electron multiplier corresponds to the H⁻ intensity at a specific point of the longitudinal charge distribution of the beam under study. The whole distribution is obtained by scanning the phase of the RF deflecting field through a complete half period. The bending magnet is tuned to select only electrons with an energy corresponding to acceleration from the target potential, and is used to remove any influence from electrons detached from H⁻ ions

Content from this work may be used under the terms of the CC BY 3.0 licence (© 2018). Any distribution of this work must maintain attribution to the author(s), title of the work, publisher, and DOI.

ISBN: 978-3-95450-201-1 doi:10.18429/JACoW-IBIC2018-WEPA20

Content from this work may be used under the terms of the CC BY 3.0 licence (© 2018). Any distribution of this work must maintain attribution to the author(s), title of the work, publisher, and DOI.

FIRST RESULTS FROM THE BUNCH ARRIVAL-TIME MONITORS AT SwissFEL

V. Arsov†, P. Chevtsov, M. Dach, S. Hunziker, M. Kaiser, D. Llorente, A. Romann, V. Schlott, M. Stadler, D. M. Treyer, Paul Scherrer Institut, 5232 Villigen PSI, Switzerland

Abstract

Two Bunch Arrival-Time Monitors (BAMs) based on fiber optical Mach-Zehnder intensity modulators have been commissioned at SwissFEL. Both operate simultaneously up to 100 Hz with a resolution <5 fs at 200 pC. We have developed concepts and tested hardware, which enhance the BAM commissioning and user operation.

INTRODUCTION

Two Bunch Arrival-Time Monitors (BAMs) based on fiber optical Mach-Zehnder intensity modulators [1], operating simultaneously up to 100 Hz with a resolution <5 fs at 200 pC, have been commissioned at SwissFEL. They derive their high stability from a pulsed optical reference distribution system in which the length of the single-mode optical fibers is stabilized for drift and jitter. For commissioning, instead of using a balanced optical cross-correlator as a phase detector we use a technically less demanding approach based on low drift and jitter laser-to-RF direct conversion, which delivers few tens of fs stability [2, 3]. In order that all BAMs measure simultaneously, it is necessary that a reference laser (OMO) pulse overlaps with the bunch at the given location. In addition, an integer number of pulses should fit in the link. To meet the above two requirements during commissioning multiple timing scans of the OMO pulses should be made. A complete scan may require a time-shift over an entire pulse train period, i.e., 7 ns. To speed up commissioning and allow adding of further BAM stations we have developed a concept for fast OMO pulse timing scan.

BAM REFERENCE DISTRIBUTION AND READOUT

BAM Optical Master Oscillator (OMO2)

The core of the SwissFEL reference distribution is a mode-locked laser oscillator (Origami 15, NKT Photonics) with pulse repetition rate of 142.8 MHz, phase-locked to a stable microwave reference at 2998.8 MHz (SMA100A, Rohde & Schwarz), which is locked to a 10 MHz Rb standard (FS725, SRS) [4]. All machine relevant frequencies are derived via harmonic extraction and delivered to the remote locations by single-mode fiber optical links, stabilized according to the client's specific requirements. Among others, BAM has the most stringent stability requirements for sub-10 fs drift, which is achieved via balanced optical cross-correlation [1]. In the general case the fiber optical link length is arbitrary and does not necessarily provide an overlap of a reference OMO pulse with the electron bunch. To secure a timing overlap, it is necessary to phase shift the OMO pulses over a pulse train period. Since at SwissFEL the OMO is the source of the entire reference distribution, such shifting will not effectively result in an overlap with the bunch, because the effect is a common mode. The alternative is either to have an optical delay line for each individual pulsed link, or to use a second OMO dedicated only for BAM commissioning (OMO2). We chose the second approach (Fig. 1). As in the case of the machine OMO, the one for BAM is locked to the same stable microwave reference. In addition, there is a bucket synchronization at 1.9833 MHz (super period). The advantage is, that any machine component with corresponding bucket synchronization, e.g., the gun and the experimental lasers, have also a common timing origin. The bucket synchronization is obtained by phase locking of one of the 3 GHz slopes to the slope of the super period at the zero crossing. The overlap is achieved with an IQ modulator (aka. vector modulator, shortly VM), which has a 12 bit DAC.

BAM Pulsed Optical Front End

The pulsed link synchronization used for BAM commissioning is based on low drift stabilized phase detector [2, 3]. The set-up is all-fiber and the phase detection principle doesn't require a dispersion compensation. The good drift stability (~10 fs pk-pk) is achieved by temperature stabilization of the basic components within the package, proper choice of the working point of the two photo diodes (2651E, Emcore), as well as careful balance of the forward and backward branches and the corresponding optical pulse powers. Dispersion compensation to reduce the pulse width to ~250 fs is nevertheless made to preserve the BAM resolution. A combination of a piezo-stretcher (PZ2, Optiphase) and a delay stage (MDL-02, General Photonics) is used to compensate for jitter and drift (Fig. 1). The naked fibers are housed in a hermetic package to minimize the environmental influence. The system is located in the temperature and humidity regulated synchronization (T&S) room.

BAM Readout Electronics

The BAM photoreceiver, the 7-slot VME crate with the pulse-forming front-end and readout cards are located in a separate 19" rack in the technical gallery (Fig. 1).

Photoreceiver. The device is an in-house development with three channels - "fine" BAM, "coarse" BAM and ADC clock. The photodiodes (2651E, Emcore) have 3 GHz bandwidth. The optical pulses for the two BAM-

† vladimir.arsov@psi.ch

ISBN: 978-3-95450-201-1 doi:10.18429/JACoW-IBIC2018-WEPB01

PHOTON BEAM IMAGER AT SOLEIL

M. Labat*, J. Da Silva, N. Hubert, F. Lepage,
Synchrotron SOLEIL - L'Orme des Merisiers, [91 191] Gif-sur-Yvette, France

Abstract

In one of the long straight sections of SOLEIL is installed a pair of canted in-vacuum undulators for the ANATOMIX and NANOSCOPIUM beamlines. Since the upstream undulator radiation can potentially damage the downstream undulator magnets, an accurate survey of the respective alignment of the two devices is mandatory. An XBPM has been initially installed for this purpose in the beamline frontend. For redundancy and further analysis, an X-ray imager was then designed and added just downstream the XBPM. It is made of a diamond plate that can be inserted into the upstream beamline frontend at low current. We present the commissioning of this new device together with its first results in operation.

INTRODUCTION

The SOLEIL synchrotron light source is now in operation since 2006 [1]. The storage ring consists of 16 cells, with 24 straight sections of variable lengths, for undulator insertion. In one of the long straigth sections, the so-called SDL13, have been installed two horizontal canted undulators [2]. Both undulators are in-vacuum undulators with periods of 20 mm initially, and 18 mm since 2018. The upstream undulator delivers hard X-rays to the NANOSCOPIUM beamline, for nanoscale imaging experiments. The downstream undulator delivers hard X-rays too, to the ANATOMIX beamline dedicated to tomography experiments. The two beamlines are designed to be operated simultaneously.

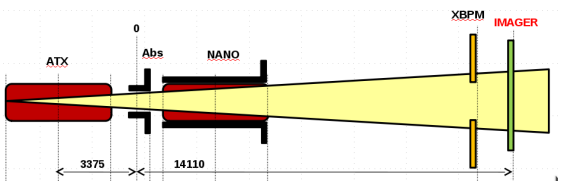

Figure 1: SDL13 (Long Straith Section in cell 13) layout. 0: middle of the straigth section. ATX: ANATOMIX and NANO: NANOSCOPIUM undulators. Distances given in mm.

The horizontal canting angle in between the undulators is 6.5 mrad while both insertion devices are separated by about 7 m. Therefore, as illustrated in Fig. 1, the upstream undulator radiation passes through the downstream undulator before reaching the beamline. In nominal operation, both upstream and downstream undulator gaps are set at 5.5 mm, which is found of the order of the vertical aperture of the upstream undulator radiation inside the downstream undulator. In this initial layout, the upstream undulator can seriously damage the downstream undulator magnets.

* marie.labat@synchrotron-soleil.fr

This is the reason why an absorber has been installed in 2016 in order to shadow the NANOSCOPIUM undulator magnets from the ANATOMIX undulator radiation. The schematic of this absorber, with respect to the electron and ANATOMIX photon beams is presented in Fig. 2. It is a piece of copper with an asymmetric 90 degrees U-shape. Its vertical aperture is 2.8 mm and its geometry was studied in detail in order not to jeopardize the performance of the storage ring in terms of collective effect induced instabilities, beam losses, injection efficiency and beam life time. It can be retracted when needed, thanks to a remote controlled pneumatic translation.

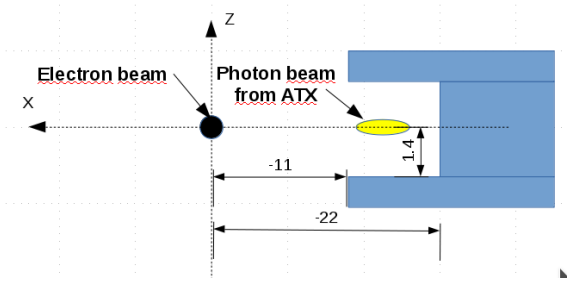

Figure 2: Schematic of the absorber installed in the middle of the SDL13.

If the upstream undulator, the absorber and the downstream undulator are properly aligned, the safety of all equipments is guranteed. But any drift from the nominal setting (slab distorsion, large temperature variations, human intervention, undulator offset adjustement, storage ring girders re-alignement, misteering of the beam, etc…) can have dramatic consequences. This is why a carefull survey of the relative alignment of those three critical equipements is required.

At the first stage of this two canted-undulators project, a double XBPM was installed in the double beamline front end [3]. It enables the simultaneous measurement of the NANOSCOPIUM and ANATOMIX photon beam positions at the exit of the straigth section. A couple of years later, it has been decided to give a redundancy to this diagnostic, using an X-ray imager. This paper presents the design, commissioning and operation of this imager.

IMAGER DESIGN

Specifications

The imager specifications were the following: (i) Image the ANATOMIX X-ray photon beam in the beamline frontend, (ii) Image the shadow created by the absorber on the ANATOMIX radiation pattern, (iii) Image the shadow (or its absence) created by the NANOSCOPIUM undulator on the

Content from this work may be used under the terms of the CC BY 3.0 licence (© 2018). Any distribution of this work must maintain attribution to the author(s), title of the work, publisher, and DOI.

ISBN: 978-3-95450-201-1 doi:10.18429/JACoW-IBIC2018-WEPB02

DEVELOPMENT OF A YAG/OTR MONITOR FOR BEAM HALO DIAGNOSTICS*

R. Yang†, P. Bambade, S. Wallon, LAL, CNRS/IN2P3, Université Paris-Saclay, Orsay, France
T. Naito, A. Aryshev, N. Terunuma, KEK, Tsukuba, Japan
M. Bergamaschi, CERN, Geneva, Switzerland

Abstract

To investigate the mechanisms of beam halo formation and its dynamics, a YAG/OTR monitor has been developed and tested at the KEK-ATF. The monitor has four ceramic Ce:YAG screens for the visualization of the beam core and beam halo and an OTR target to provide complementary beam core measurements. A high dynamic range (>10^5) and a high resolution (<10 μm) have been demonstrated experimentally. Measurements of beam halo using this monitor are consistent with previous results and theoretical modeling, and have allowed further progress in the characterization of the driving mechanisms.

INTRODUCTION

Beam halo is one of the critical issues limiting the performance and causing component damage and activation for the future linear or circular accelerator. Understanding halo formation and distribution is not only a crucial topic of accelerator physics but also of great importance for the mitigation of the unwanted background induced by halo particles, e.g., through an efficient collimation system. To uncover the physical origins of beam halo and how to suppress it, powerful diagnostics with extremely high dynamic range and sensitivity are required. Direct measurements of halo are considered for most accelerators, requiring a dynamic range of at least 10^5 and a capability to simultaneously measure core and halo, in order to appropriately probe theoretical predictions of beam halo [1–3].

As a successful test facility for the R&D of ILC, the Accelerator Test Facility (ATF) at KEK has provided an excellent opportunity to investigate the mechanisms of halo formation and demonstrate the necessary diagnostics [4,5]. Its nominal beam energy and beam intensity are 1.3 GeV and 0.1×10^{10}–1×10^{10} e/pulse, respectively. To achieve a sufficient dynamic range for halo measurements, a set of diamond sensor (DS) detectors have been developed and installed at ATF2 [6, 7], which is an extraction line built to address the feasibility of focusing electron beams to nanometer (nm) scale vertical size, and provide a beam orbit stability at the nm level at the virtual interaction point. After a reconstruction of measured profiles, the effective dynamic range of the DS detector has been found to be around 10^5. Furthermore, the transverse beam profile and its vacuum dependence observed using these DS detectors clearly indicate the correlation between vertical beam halo and beam-gas scattering (BGS) [8]. However, the saturation of charge collection inside the DS bulk and the deformations of DS waveforms have severely limited the performances and applications of the DS detectors [9]. To obtain a simultaneous diagnostics and confirm the observations given by the DS detector, a new YAG/OTR monitor has been developed and installed.

In this paper, the design of the YAG/OTR monitor toward the desired dynamic range and resolution are described, followed by performance tests with beam. Comparisons of beam halo measured by the DS detector and the YAG/OTR monitors are presented, which are in good agreement. Further foreseen applications and improvements of the YAG/OTR monitor are also discussed.

DEVICE CONFIGURATION

The favorable scintillating properties, mechanical rigidity and radiation hardness have made the scintillator material an excellent candidate for direct two-dimensional (2D) imaging devices, widely used for diagnostics of energetic particles and photons. Previous investigations have indicated that the Ce:YAG has a high photon yield (around 2×10^4 photons/MeV) and a fast decay time (<1 μs), which are suitable for halo diagnostics [10, 11]. Meanwhile, beam profile measurements using the OTR are saturation-free and can provide complementary diagnostics for dense beam core. Considering the practical beam parameters at ATF2, a YAG/OTR system has to satisfy two requirements: a dynamic range of more than 1×10^5 and a spatial resolution of less than 10 μm.

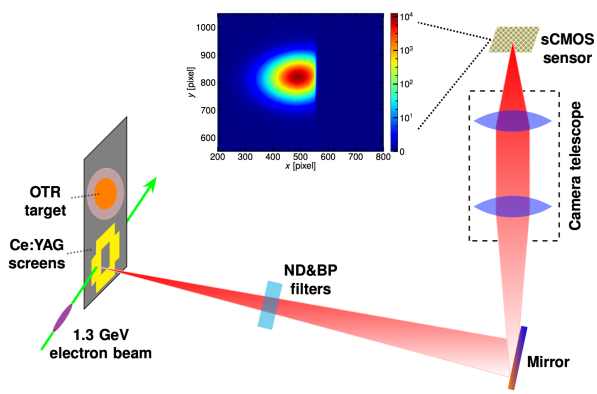

Figure 1: Schematic of the YAG/OTR monitor.

The YAG/OTR monitor mainly consists of four ceramic 0.5 mol% Ce:YAG screens and an OTR target on the same holder, a microscope lens (TS-93006/TS-93022 Sugito Co.), a 16-bit scientific Complementary Metal Oxide Semiconductor (sCMOS) camera (PCO.EDGE 4.2 L) with a low noise

* Work supported by MSCA-RISE E-JADE project (grant number 645479)
† ryang@lal.in2p3.fr

Content from this work may be used under the terms of the CC BY 3.0 licence (© 2018). Any distribution of this work must maintain attribution to the author(s), title of the work, publisher, and DOI.

ISBN: 978-3-95450-201-1 doi:10.18429/JACoW-IBIC2018-WEPB03

FIRST PROTOTYPE OF A CORONAGRAPH-BASED HALO MONITOR FOR bERLinPro*

Ji-Gwang Hwang † and Jens Kuszynski,
Helmholtz-Zentrum Berlin für Materialien und Energie GmbH (HZB), Berlin, Germany

Abstract

Since particle losses by beam halo induced by space charge force and scattering of trapped ions are critical issues for superconducting-linac based high power machines such as bERLinPro, a halo monitor is demanded to monitor and control particle distribution at the level of $10^{-4} \sim 10^{-5}$ of the core intensity. A coronagraph-based halo monitor was adopted and the first prototype has been designed as a demonstrator system aimed at resolving a halo-core contrast in the 10^{-3} to 10^{-4} range. This monitor was tested at BESSY II with various operation modes such as Transverse Resonance Island Buckets (TRIBs) and Pulse-Picking by Resonant Excitation (PPRE). We show our design parameters, experimental criterion, and experimental results.

INTRODUCTION

The Berlin Energy Recovery Linac Prototype (bERLinPro) project was launched at the Helmholtz-Zentrum Berlin (HZB) to demonstrate and establish technologies for energy recovery linac (ERL) based accelerators for a future light source [1, 2]. The bERLinPro will provide electron beams up to 50 MeV in the recirculation loop with several operation modes such as a single pulse mode with various repetition rates, bursting mode, and 50 MHz and 1.3 GHz continuous waves (CW) modes [3]. The bERLinPro injector, consisting of a photocathode 1.4-cell superconducting radio frequency (SRF) gun, followed by three 2-cell booster SRF cavities, generates high-quality electron beams with an energy of 6.5 MeV. The beam is transported to the main linac module and accelerated by three 7-cell SRF cavities up to 50 MeV energy [4]. The design layout is shown in Fig. 1.

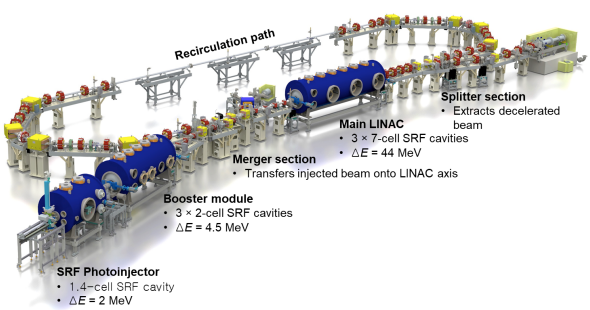

Figure 1: Layout of bERLinPro having accelerating structures of 1.4-cell SRF gun, three 2-cell SRF booster cavities, and three 7-cell SRF cavities for generation of high-quality and high-power electron beams [5].

* Work supported by German Bundesministerium für Bildung und Forschung, Land Berlin and grants of Helmholtz Association.
† ji-gwang.hwang@helmholtz-berlin.de

The construction of a building and basic infrastructure was completed in 2017 so that the installation of accelerator components has begun. As the first stage, the installation of the vacuum system of a "Banana" section, which includes the entire low energy beam path from the gun to the high power beam dump. The 5 mA SRF gun (Gun1) and the cryomodule of the booster cavities as well as a diagnostics line, is ongoing [6].

HALO MONITOR TEST SETUP

A total of five synchrotron light based electron beam diagnostics for measuring a beam halo distribution, and temporal and spatial distribution will be installed in the recirculator of the bERLinPro. Due to the heat capacity of a cryogenics, it is not allowed to provide an additional power load of more than 50 W on the cryomodule for main SRF cavities by small beam losses from halo particles, which corresponds to 10^{-5} level of maximum beam power. Since a halo monitor is a crucial diagnostic for minimizing uncontrolled beam losses by halo particles by adjusting the optics at the upstream of the first arc section, it stimulates the development of the beam halo monitor with the contrast ratio of 10^{-5}.

For the observation of the halo distribution with the contrast of 10^{-5} to the beam core, various monitors such as a wire-scanner monitor, diamond detector, the optical monitor based on a digital micromirror device (DMD), and coronagraph-based halo monitor were compared and analyzed. Finally, the coronagraph-based halo monitor is preferred since this technique can observe the full 2-D halo distribution without any disturbance to the beam and it has already been demonstrated at the KEK Photon Factory to achieve a 6×10^{-7} ratio for the background to peak intensity [7, 8]. The design study of the coronagraph-based halo monitor with a Lyot-stop technique, which produces the image of a entrance pupil using re-diffraction optics to remove the majority of diffraction fringes, is performed using a Fourier-optics interpretation which is equivalent to the classical optics approach using Fourier transforms, in which the waveform is regarded as made up of a superposition of plane waves [9].

The beam-halo monitor will be installed on the first dipole of the first arc section because this dipole has a relatively small dispersion, which does not disturb the horizontal beam distribution. Since the full energy operation of the bERLinPro is scheduled for 2020, a preliminary test is performed at a diagnostics beam line of BESSY II. The diagnostics beam line of BESSY II provides multi-platform for research and development of various synchrotron light based monitors [10, 11]. The beam line has a distance of 15.5 ± 0.5 m

Content from this work may be used under the terms of the CC BY 3.0 licence (© 2018). Any distribution of this work must maintain attribution to the author(s), title of the work, publisher, and DOI.

ISBN: 978-3-95450-201-1 doi:10.18429/JACoW-IBIC2018-WEPB04

COMPARISON OF YAG SCREENS AND LYSO SCREENS AT PITZ

R. Niemczyk*, P. Boonpornprasert, Y. Chen, J. Good, M. Gross, H. Huck, I. Isaev, D. Kalantaryan, C. Koschitzki, M. Krasilnikov, X. Li, O. Lishilin, G. Loisch, D. Melkumyan, A. Oppelt, H. Qian, Y. Renier, F. Stephan, Q. Zhao†,
Deutsches Elektronen-Synchrotron DESY, 15738 Zeuthen, Germany
W. Hillert, University Hamburg, 22761 Hamburg, Germany

Abstract

The Photo Injector Test facility at DESY in Zeuthen (PITZ) is dedicated to the development of high-brightness electron sources for free-electron lasers. At PITZ, to measure the emittance of space-charge-dominated beams, the slit scan technique is used. For slice emittance measurements a transverse deflecting structure (TDS) is employed. The electron beam distribution is measured by means of scintillator screens. Both the TDS and the slit mask reduce the signal strength, giving stringent requirements on the sensitivity of the screens. At PITZ, high-sensitivity Ce:LYSO screens have been installed at the same screen stations as the standard Ce:YAG screens to solve low-intensity issues. A comparison of both screens is presented.

INTRODUCTION

Scintillator screens are used to measure the beam distribution and position in particle accelerators. At the Photo-Injector Test Facility at DESY in Zeuthen (PITZ) cerium-doped ytterbium aluminium garnet (Ce:YAG) powder is used as standard screen material [1]. However, advanced electron beam diagnostics require precise measurements of the electron distribution with rather low charge density and, therefore, with low signal intensity from the detector.

Measurement of properties like the slice emittance, the longitudinal phase space [2] or the projected emittance of low-charged beams need a significant increase of the signal strength, especially during time-resolved measurements with the transverse deflecting structure (TDS). The TDS, developed by the Institute for Nuclear Research (INR RAS, Moscow, Russia) in collaboration with DESY, only allows to streak up to three consecutive electron bunches [3].

For a correct reconstruction of the beam distribution the screen and imaging system have to have a high homogeneity, a good signal linearity, a high spatial resolution and a high signal-to-noise ratio. In order to perform a cross-check with the existing system, several high-sensitivity cerium-doped lutetium yttrium orthosilicate (Ce:LYSO) screens were installed at the same screen station as Ce:YAG screens. The same TV read-out system was used for the image analysis.

In this paper, both the screen homogeneity and linearity in terms of light production are measured for both Ce:LYSO and Ce:YAG screens. Additionally, the beam size measurement uncertainty caused by screen non-uniformity is simulated.

* raffael.niemczyk@desy.de
† On leave from IMP/CAS, Lanzhou, China

At PITZ, the electron beam comes in bunch trains with a repetition rate of 10 Hz [4]. The number of electron pulses per train can be increased to up to 600 pulses at 1 µs bunch spacing [5]. For each measurement, ten beam images, i.e. images from ten consecutive bunch trains, and ten background images were taken. The images from the bunch trains were averaged in the postprocessing, after the averaged background was subtracted.

LARGE-SCALE SCREEN HOMOGENEITY

To estimate the screen homogeneity, the electron beam has been steered to nine different positions on the screen. At each beam position, the Ce:YAG and Ce:LYSO screen image was taken. At the screen station the two different screen types were inserted into the beam path and the screen image was taken by one single camera for both screens, i.e. camera gain and imaging from screen to camera was the same. Camera gain and exposure time were kept the same for both screen images. The sum of pixels[1] inside a squared frame with an edge length of 123 pixels around the beam centroid is calculated as measure for the beam intensity. The observation camera has 1024×1360 pixels [6]. It was used

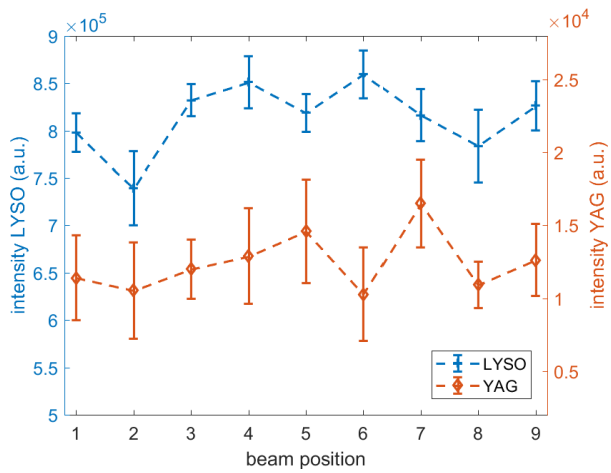

Figure 1: Intensity and rms intensity jitter for Ce:LYSO (blue) and Ce:YAG (orange) screens. The area of interest is square, with an edge length of 123 pixel (of the 512×680-wide images) for both screen materials. The AOI is centred around the beam centroid position, i.e. the AOI has a different position at each beam position.

[1] Sum of pixel fillings inside the area of interest

Content from this work may be used under the terms of the CC BY 3.0 licence (© 2018). Any distribution of this work must maintain attribution to the author(s), title of the work, publisher, and DOI.

ISBN: 978-3-95450-201-1 doi:10.18429/JACoW-IBIC2018-WEPB06

TIME-SYNCHRONOUS MEASUREMENTS OF TRANSIENT BEAM DYNAMICS AT SPEAR3*

Q. Lin† and Z. Sun, Donghua University, Shanghai, China
J. Corbett, D. Martin and K. Tian, SLAC, Menlo Park, CA

Abstract

Multi-bunch beam instabilities can often be controlled with high-speed digital bunch-by-bunch feedback systems. The detected motion is based on charge centroid measurements that, for short bunches, cannot resolve intrabunch charge dynamics. To compliment the BxB data, we installed a fast-gated camera with a rotating mirror to sweep visible-light synchrotron radiation across the camera CCD. The SR measurements present a complimentary view of the motion. For this work we generated transient beam events in SPEAR3 using the BxB feedback system and synchronously observed the motion on the camera. Results are presented for a high-order multibunch beam instability and for single bunch drive-damp experiments.

INTRODUCTION

SPEAR3 routinely uses a transverse bunch-by-bunch (BxB) feedback system [1] for high current User operations and to study storage ring beam dynamics [2]. The BxB system detects the dipole moment q•Δx for each bunch on each turn where q is the bunch charge and Δx is the displacement of the bunch centroid. The data is digitally processed with sufficient bandwidth to control the motion of each bunch independently. To date, the SPEAR3 BxB feedback system has been used to control multibunch instabilities, study beam dynamics during resonant drive events and for bunch cleaning. Although BxB feedback systems measure every bunch on every turn, for short bunches the measurement system cannot resolve coherent intrabunch motion or charge decoherence.

To compliment the BxB feedback system we synchronized a fast-gated camera equipped with a rotating mirror to sweep an image of the visible light synchrotron radiation (SR) across the camera CCD. The original idea to "streak" the optical SR beam using a deflecting mirror was developed at KEK [3], applied at PEP-II to measure fast-beam dump dynamics [4], and then used at both SPEAR3 [5] and ANKA [6] to diagnose the bunch bursting in low-alpha mode. For the applications reported here, we time-synchronized the optical SR measurements with the BxB acquisition system to provide complimentary diagnostics during transient beam motion.

At SPEAR3, a high-order multibunch instability can develop in the vertical plane due to resonances in an in-vacuum insertion chamber (IVUN) chamber [7]. The instability occurs at discrete gap settings where electromagnetic "pillbox" modes in the vacuum chamber couple to transverse beam modes. On a shot-to-shot basis, the motion of individual bunches evolves differently in time, often with complex profiles. Using the rotating mirror to streak the optical SR beam image, an integrated time profile containing the motion of all bunches can be captured.

Similarly, to diagnose single bunch motion, the BxB system or a standard turn-by-turn BPM processor can record driven betatron oscillations for dynamic aperture studies, bunch cleaning or resonant excitation tests for short-pulse x-ray production. Since the bunch charge can decohere in phase space it is important to measure the transverse beam profile using visible-light synchrotron radiation to identify (a) the onset of charge decoherence, and (b) the impact of decoherence on the physical process under investigation.

EXPERIMENTAL CONFIGURATION

For normal User operations SPEAR3 stores 500 mA beam current with charge distributed in 4 discrete bunch trains plus an isolated timing bunch for pump/probe experiments. Top-up injection occurs every 5 minutes with charge deposited at a 10 Hz rate into single, targeted bunches. A 10 Hz TTL pulse train triggers the injection kickers and provides a convenient signal to use for synchronized diagnostics.

In order to study transient beam dynamics, the timing system was configured to select solitary injection pulses from the 10 Hz pulse train to initiate grow/damp or drive/damp events. The same pulse is used to trigger multiple, synchronous diagnostics. The synchronized diagnostic systems include BxB data acquisition, turn-by-turn BPM processors and visible SR diagnostics.

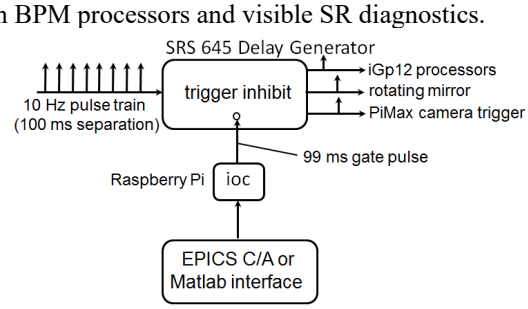

Figure 1: Schematic of the synchronous diagnostic timing system. A Raspberry Pi under EPICS control selects a single, time-isolated trigger.

*Work supported by the China Scholarship Council and the US Department of Energy Contract DE-AC03-76SF00515, Office of Basic Energy Sciences.
†linqi1207@sina.com, zhsun@dhu.edu.cn

Content from this work may be used under the terms of the CC BY 3.0 licence (© 2018). Any distribution of this work must maintain attribution to the author(s), title of the work, publisher, and DOI.

ISBN: 978-3-95450-201-1 doi:10.18429/JACoW-IBIC2018-WEPB09

WIRE SCANNER MEASUREMENTS AT THE PAL-XFEL*

G.J. Kim†, B. Oh, D.C. Shin, C.B. Kim, H.-S. Kang
Pohang Accelerator Laboratory, Gyeongbuk 37673, Korea

Abstract

The PAL-XFEL, an X-ray Free electron laser user facility based on a 10 GeV normal conducting linear accelerator, has been operational at Pohang, South Korea. The wire scanners are installed for transverse beam profile measurement at the Linac and the Hard X-ray undulator section. The wire scanner is a useful device for emittance measurements in the Hard X-ray undulator section. In this paper, we describe the details of the wire scanner and the results of the measurements.

INTRODUCTION

In order to operate an accelerator more stably and efficiently, it is necessary to adjust the operation conditions of the apparatus to the designed conditions. In order to perform this operation, it is important to obtain the accurate emittance of the electron beam by the transverse beam size measurement. At the PAL-XFEL are installed 54 screen monitors and 13 wire scanners for beam profile measurement. As shown in Fig. 1 the wire scanner is mainly located at the end of the linear accelerator and the undulator section. This is used to measure the emittance to optimize the FEL generation condition for the undulator section. The wire material is a 34 μm thick carbon wire suitable for the undulator line because it generates lower radiation when it is hit by electron beam [1]. This paper describes device configuration and beam commissioning results using wire scanner.

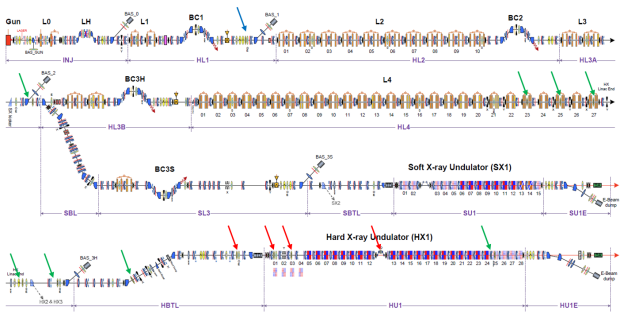

Figure 1: The layout of the PAL-XFEL. The arrows shows the location of the wire scanner. And the red arrow indicates the location of the device where the 34 μm carbon wire is installed.

HARDWARE FEATURES

The wire scanner measurement system consists of a motion stage and a radiation measuring device. The motion device is used to adjust the position of the wire causing the interference with the electron beam. The radiation measuring device measure the amount of energy loss caused by the interference of the electron beam with the wire.

Motion Stage

The wire scanner assembly is mounted on its 45° motion stage with linear motor. As shown in Fig. 2(a), the wire card is equipped with three wires (x, y, u) and an RF shielding tube. It has been reported that the position of the electron beam changes due to the changing of the magnetic field from the linear motor [1]. The linear motor is equipped with an ironless linear motor which is designed not to have attractive force. The wire material is based on the tungsten and carbon wire was selected to minimize the radiation damage to the undulator magnet. The wire scanner with carbon 34 μm wire is installed between after the dogleg section and the last undulator.

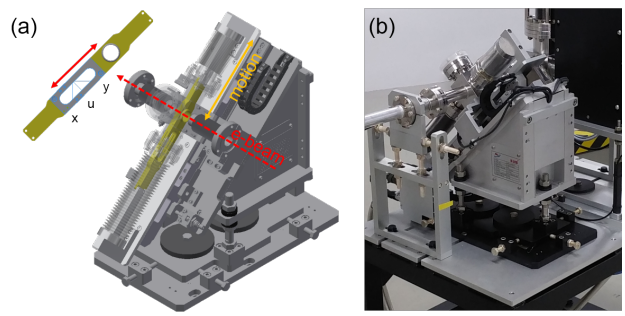

Figure 2: The wire scanner mounted on its motion stage. (a) The 3D modeling of the wire card and motion stage, (b) Installation of the wire scanner.

Beam Loss Monitor (BLM)

The Beam loss detectors are based on the idea of using optical fibers as a Cherenkov light radiator. The optical fiber used as the radiator is a plastic scintillating fiber of BCF-20 with 250 μm diameter which has 492 nm peak emission wavelength and 2.7 ns decay time [2]. The fiber is shielded from external light and connected directly to the PMT. It was installed by direct winding to the chamber as shown in Fig. 3(a) to measure the generated signal. The photomultiplier tubes (PMT) module uses the Hamamatsu H10722-110 as show in Fig. 3(b). It has 230 –700 nm spectral response range with voltage output. As shown in the figure, a certain space is required for installation of optical fiber-based BLM. Because of the limited installation space of the undulator section, the wire scanner was measured using the BLM for Undulators [3].

* Work supported by MSIP, Korea.
† gyujin_kim@postech.ac.kr

Content from this work may be used under the terms of the CC BY 3.0 licence (© 2018). Any distribution of this work must maintain attribution to the author(s), title of the work, publisher, and DOI.

ISBN: 978-3-95450-201-1 doi:10.18429/JACoW-IBIC2018-WEPB10

GRATING SCANNER FOR MEASUREMENT OF MICRON-SIZE BEAM PROFILES*

L. G. Sukhikh†, A. P. Potylitsyn, S. A. Strokov, Tomsk Polytechnic University, 634050, Tomsk, Russia
G. Kube, K. Wittenburg, Deutsches Elektronen Synchrotron DESY, 22607, Hamburg, Germany

Abstract

Wire scanners are widely used for transverse beam size diagnostics. The minimum detectable beam size is affected by the diameter of a single wire that is of about 4 microns. Sub-micron beam sizes have to be resolved due to development of modern electron accelerators and future linear electron-positron colliders. In this report we propose to use a set of of gold stripes with varying period (gap) on a Si substrate. By moving this scanner across the beam one could measure the Bremsstrahlung yield vs. the coordinate, resulting in an oscillating dependence. The visibility of the resulting image allows defining the beam sizes in the range of 0.5–1.5 μm for the proposed scanner parameters.

INTRODUCTION

Wire scanners are widely used for diagnostics of transverse beam size in the modern electron accelerators. The wire crosses the beam resulting in the bremsstrahlung generation and loss electrons generation. Measuring dependence of high energy photon or loss electron yield on wire coordinate one could obtain transverse beam profile projection. The minimal detectable beam size is affected by the diameter of a single wire. The smallest carbon or tungsten wires used so far have diameters of about 4 μm. If the beam size measured is comparable with the wire diameter is significantly affects the measured profile and should be taken into account. In case of smaller beam sizes one could meet the situation that measured "beam" profile contains only wire diameter. With the development of modern electron accelerators and the demands from future linear electron-positron colliders, micron and sub-micron beam sizes have to be resolved with sub-micron or better resolution. For this purpose a new generation of wire scanners should be developed and tested.

One of the possible methods to increase the resolution of the wire scanners is to decrease its size. The minimal diameter of single free-hanging wire (≈ 4 μm) is limited by the mechanical stress. However, one could consider wires with smaller size (units of microns or even sub-microns) on a substrate. In Ref. [1] authors proposed to use thin gold stripes of rectangular shape (1 μm or 2 μm width and 3 μm height) on Si_3N_4 membrane used as a substrate. In this case authors of Ref. [1] expect to increase beam size measurement resolution and to be able to resolve sub-micron beams. However, one of the paybacks while using small size wires is the limited dynamic range of the measurable beam sizes.

In this report we propose another arrangement of gold stripes on Si substrate. We propose to form a grating scanner from a set of gold stripes with variable distance between them. In this report we present the preliminary Geant4 simulations of such a grating scanner with varying gaps that show the possibility to measure beam sizes in the range of 0.5–1.5 μm.

GRATING SCANNER WITH VARYING GAPS

The scheme of the grating scanner with varying gap is shown in Fig. 1. The scanner considered in this report consists of eleven rectangular gold stripes on Si substrate of 50 μm thickness. The height of the gold stripes was equal to 10 μm. During the simulation we considered two stripe widths, namely $a = 1$ μm or $a = 3$ μm. The distance between stripes is non-equal and varies in the range of 0.25–3 μm.

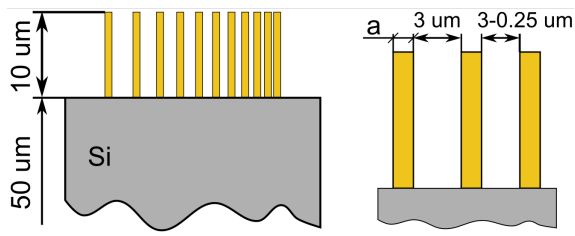

Figure 1: Schematic view of grating scanner with varying gaps.

The basic idea of beam size measurement using proposed scanner is the following. The electron beam interacts with the scanner while moving the scanner across the beam. Amount of the generated photons (or loss electrons) depends on which part of the scanner directly interacted with the beam. If the beam size is small comparing with the gap size the beam interacts either with a gold stripe and the substrate resulting in the maximal bremsstrahlung yield or with the substrate only resulting in the minimal (background) photon yield. In this case the dependence of the photon yield on the grating coordinate is oscillatory. When beam size is much larger than the gap size, the beam interacts with several stripes resulting in monotonic dependence of the photon yield on grating coordinate. The schematic view of beam interacting with the scanner is shown in Fig. 2.

The wire scanner with varying gaps was simulated using Geant4 [2]. The simulation scheme is shown in Fig. 3. The electron beam with electron energy $E_e = 1.25$ GeV and

* Work supported by Russian Ministry of Science and Higher Education, Program "Nauka" grant #3.1903.2017 and TPU Competitiveness enhancement Program
† sukhikh@tpu.ru

Content from this work may be used under the terms of the CC BY 3.0 licence (© 2018). Any distribution of this work must maintain attribution to the author(s), title of the work, publisher, and DOI.

ISBN: 978-3-95450-201-1 doi:10.18429/JACoW-IBIC2018-WEPB11

SPATIAL RESOLUTION IMPROVEMENT OF OTR MONITORS BY OFF-AXIS LIGHT COLLECTION

A. Potylitsyn[1,†], L. Sukhikh[1], G. Kube[2], A. Novokshonov[1,2]
[1]Tomsk Polytechnic University, 30, Lenin St., Tomsk, 634050, Russia
[2] Deutsches Elektronen-Synchrotron (DESY), Hamburg, Germany

Abstract

The spatial resolution of an OTR monitor, widely used for electron beam profile diagnostics, is determined by the resolution of the optical system and by the Point Spread Function (PSF) representing the single electron image. In the image plane, the PSF has a typical lobe-shape distribution with an inter-peak distance depending on wavelength and lens aperture ratio [1]. For a beam with a transverse rms size smaller than the distance, the reconstruction of the beam profile has several difficulties [2, 3]. We propose to reduce the PSF contribution and to improve the spatial resolution of an OTR monitor simply by rotating the lens optical axis with respect to the specular reflection direction. If the difference between the rotational angle and the lens aperture is much larger than the inverse Lorentz factor, the PSF has a Gaussian-like distribution which matches practically with the Airy distribution. Thus the resolution depends on wavelength and lens aperture. In principle, for lens apertures in the order of 0.1 rad such an approach should allow to measure beam sizes comparable to the wavelength of observation, using a simple deconvolution procedure for the measured image and the PSF.

INTRODUCTION

Transverse beam size measurements based on optical transition radiation (OTR) are a widely used technique and OTR monitor stations are operated at most modern electron linacs [4, 5]. For electron energies higher than 50 MeV the OTR intensity collected by a conventional optics system with numerical aperture of $\theta_m \sim 0.1$ rad achieves $N_{ph} \sim 10^{-3}$ photons per electron in the band width $\Delta\lambda/\lambda \sim 0.05$.

The spatial resolution of a transverse beam size monitor based on OTR is determined by the so-called Point Spread Function (PSF) or, in other words, by the response of the monitor optical system to a point charge crossing the target. With knowledge of the PSF, in principle it is possible to reconstruct beam size and beam shape from an electron bunch passing through the target applying a deconvolution algorithm to the measured OTR image.

The PSF has a double-lobe structure which is defined by the radiation wavelength λ, the acceptance angle or numerical aperture of the optical system θ_m, and the alignment accuracy. For the condition of ideal imaging the OTR monitor resolution determined by so-called diffraction limit can be expressed as

$$R = 1{,}12\frac{\lambda M}{\theta_m}. \quad (1)$$

Here M denotes the magnification factor of the optical system.

For beams with micrometer/submicrometer sizes such an optical system provides PSF dominated regime and one should applicate a spectral treatment of the data in order to extract a real beam size [6].

We propose optical schemes for OTR monitors with off-axis light collection in order to avoid a two-lobe structure of the PSF and improve its spatial resolution.

CALCULATIONS OF OTR PSF DISTRIBUTIONS

Under ultra-relativistic approximation the particle Coulomb field can be sufficiently described by its transverse components and it is possible to write down the OTR field in the lens plane in analogy with wave scattering at a finite size conducting screen:

$$E^L_{x,y}(\mathrm{X}_L,\mathrm{Y}_L) = \mathrm{const}\int_{S_T} d\mathrm{X}_T d\mathrm{Y}_T \begin{Bmatrix}\cos\varphi_T\\ \sin\varphi_T\end{Bmatrix} K_1\left(\frac{k}{\beta\gamma}R_T\right)\times \exp\left[i\frac{k}{2a}\left(\mathrm{X}_T^2+\mathrm{Y}_T^2\right)\right]\exp\left[-i\frac{k}{a}\left(\mathrm{X}_L\mathrm{X}_T+\mathrm{Y}_T\mathrm{Y}_L\right)\right]. \quad (2)$$

Here $R_T = \sqrt{\mathrm{X}_T^2+\mathrm{Y}_T^2}$, $(\mathrm{X}_T,\ \mathrm{Y}_T)$ and $(\mathrm{X}_L,\mathrm{Y}_L)$ are the coordinates of target surface and lens plane, a is the distance between target and lens, S_T is the target surface area, $\begin{Bmatrix}\cos\varphi_T\\ \sin\varphi_T\end{Bmatrix} = \frac{1}{\sqrt{\mathrm{X}_T^2+\mathrm{Y}_T^2}}\begin{Bmatrix}\mathrm{X}_T\\ \mathrm{Y}_T\end{Bmatrix}$, $K_1(x)$ is the MacDonald function of the first order, $k = 2\pi/\lambda$.

The OTR fields in the image plane using thin lens approximation can be written in the following way after integration over the lens aperture S_L:

$$E^D_{x,y}(\mathrm{X}_D,\mathrm{Y}_D) = \mathrm{const}\int_{S_L} d\mathrm{X}_L d\mathrm{Y}_L E^L_{X,Y}(\mathrm{X}_L,\mathrm{Y}_L)\times \exp\left[-i\frac{k}{b}\left(\mathrm{X}_L\mathrm{X}_D+\mathrm{Y}_L\mathrm{Y}_D\right)\right]. \quad (3)$$

b is the distance between lens and detector. Inserting Eq. (2) in the last expression and performing 4-fold

† email: potylitsyn@tpu.ru

Content from this work may be used under the terms of the CC BY 3.0 licence (© 2018). Any distribution of this work must maintain attribution to the author(s), title of the work, publisher, and DOI.

ISBN: 978-3-95450-201-1 doi:10.18429/JACoW-IBIC2018-WEPB12

DESIGN AND IMPLEMENTATION OF NON-INVASIVE PROFILE MONITORS FOR THE ESS LEBT

C.A. Thomas*, T. Grandsaert, H. Kocevar,
O. Midttun, N. Milas, R. Miyamoto, T. Shea,
European Spallation Source ERIC, Lund, Sweden

Abstract

Non-invasive Profile Monitors are designed and distributed along the ESS Linac. In the Low Energy Beam Transport (LEBT), a specific one has been designed to be primarily a beam position monitor. Its main requirement is to measure the beam position with 100 µm accuracy, and in addition it provides the beam profile and size. This performance have been shown to be possible and remains to be demonstrated experimentally. The instrument is also potentially capable of measuring the angle of the beam and its divergence. In this paper we will study the accuracy of such a measurement as function of the instrument image quality.

INTRODUCTION

Non-invasive Profile Monitors [1–3] (NPMs) have been designed at European Spallation Source for the measurement of the beam profile at high power [4]. They are distributed from the LEBT to the last section before the target. We call NPM a transverse profile monitor based on the interaction of the residual gas with the beam of charged particles. There are two principle which the NPMs are based on. One is performing an image of the beam induced gas fluorescence [1], and the other is performing a profile of the beam induced gas ionisation [3].

However, in the LEBT, the main role of the NPM is to measure the position of the beam with respect to the reference beam axis [5]. The required position accuracy is shown to be better than 50 µm, and it is assured by the alignment of the optical axis of the NPM in the general coordinate system in which the whole accelerator is defined. The measurement principle the NPM for the LEBT is based on imaging the gas fluorescence excited by the proton beam. The interaction of the beam with the vacuum residual gas has a same probability along the particle trajectory. Therefore, the fluorescence emission is uniform along the particle path. When projected on the image plane by an optic assembly, the image represents the trajectory of the particle, projected along the optical axis. As a result, the image from the NPM represents the beam profile along the beam trajectory, and projected along one of the transverse axis. Thus, it contains information on the beam position and angle, the size and divergence. Measurement on the image may retrieve this information, and it could be used for beam tuning applications.

In the following we will show how we model an NPM image, using beam parameters, and how the retrieval of these parameters from image processing and analysis can be affected by the image quality.

* cyrille.thomas@esss.se

BEAM PROPERTIES FROM NPM IMAGE

A typical NPM image can be modeled taking into account the beam parameters, the optics parameters and the noise of the camera. Such an image can be seen in Fig. 1.

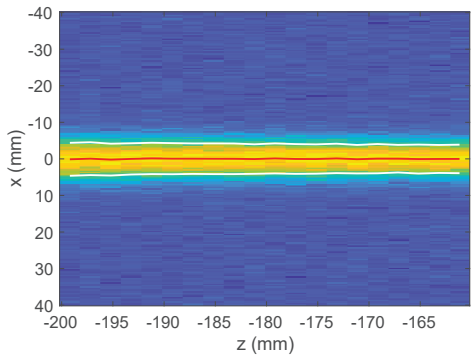

Figure 1: Model of an NPM image with ESS LEBT beam parameters. The white lines represents the beam size along the trajectory, and the red line the centre of mass, as retrieved by a Gaussian fitting algotrithm. SNR = 20.

To produce this image, we have used the beam transport model of the LEBT. The transport equations are given:

$$\beta_z = \beta_0 - 2\alpha_0 z + \gamma_0 z.^2 \quad (1)$$

$$\alpha_z = \alpha_0 - \gamma_0 z \quad (2)$$

$$\gamma_z = (1 + \alpha_z^2)/\beta_z \quad (3)$$

$$\sigma_x = \sqrt{\beta_z \varepsilon} \quad (4)$$

$$\sigma_x^{'} = \sqrt{\varepsilon \gamma_z} \quad (5)$$

$$c_x = a_1 z + a_0 \quad (6)$$

in which z is the beam longitudinal propagation coordinate; $\varepsilon = 16.8 \cdot 10^{-6}$ m.rad, the beam geometrical emittance; β_z, α_z, γ_z, the beam Twiss parameters at the coordinate z; $\beta_0 = 0.11$ m, $\alpha_0 = 1.02$, $\gamma_0 = 18.54$ m^{-1}, the Twiss parameter at the beamwaist at the exit of the LEBT; σ_x the beam size, and $\sigma_x^{'}$ the beam divergence; c_x is the beam centroid; a_i are the coefficient for the first order polynomial describing the kick angle of the beam.

Using Eqs. 5 and 6, one can compute the beam profile along the propagation axis, assuming for instance a Gaussian distribution.

Content from this work may be used under the terms of the CC BY 3.0 licence (© 2018). Any distribution of this work must maintain attribution to the author(s), title of the work, publisher, and DOI.

ISBN: 978-3-95450-201-1 doi:10.18429/JACoW-IBIC2018-WEPB13

BEAM-GAS IMAGING MEASUREMENTS AT LHCb

G. Coombs*, CERN, Geneva, Switzerland and University of Glasgow, Glasgow, United Kingdom
M. Ferro-Luzzi, R. Matev, CERN, Geneva, Switzerland
on behalf of the LHCb Collaboration

Abstract

The LHCb detector is one of the four large particle physics experiments situated around the LHC ring. The excellent spatial resolution of the experiment's vertex locator (VELO) and tracking system allows the accurate reconstruction of interactions between the LHC beam and either residual or injected gas molecules. These reconstructed beam-gas interactions gives LHCb the ability, unique among experiments, to measure the shape and the longitudinal distribution of the beams. Analysis methods were originally developed for the purpose of absolute luminosity calibration, achieving an unprecedented precision of 1.2% in Run I. They have since been extended and applied for online beam-profile monitoring that is continuously published to the LHC, for dedicated cross-calibration with other LHC beam profile monitors and for studies of the dynamic vacuum effects due to the proximity of the VELO subdetector to the beam. In this paper, we give an overview of the LHCb experience with beam-gas imaging techniques, we present recent results on the outlined topics and we summarise the developments that are being pursued for the ultimate understanding of the Run II measurements.

INTRODUCTION

The Beam-Gas Imaging technique in use at LHCb is unique among particle physics experiments in allowing the independent measurement of charged particle beam profiles of colliding beams. Its principal application is to provide measurements for the precise luminosity calibrations necessary for absolute cross-section determination [1] but it also permits a variety of additional beam diagnostic measurements. This technique was first developed and put to use during Run I of the LHC (from 2009–2013) when a record precision for the luminosity measurement at a bunched beam hadron collider was achieved [2]. This paper presents the technique's current use at LHCb and a set of additional applications developed during Run II.

THE LHCb DETECTOR

LHCb is a flavour physics experiment designed to observe the decays of b and c quarks produced in the high energy hadronic collisions taking place at the LHC [3]. The relatively long lifetimes of the decay products produced by these interactions necessitate a precise measurement of both primary and secondary decay vertices. This is achievable due to the excellent spatial resolution of the detector's tracking system, most notably the VELO subdetector. A schematic diagram of the full detector layout, including the various subdetectors, can be seen in Fig. 1.

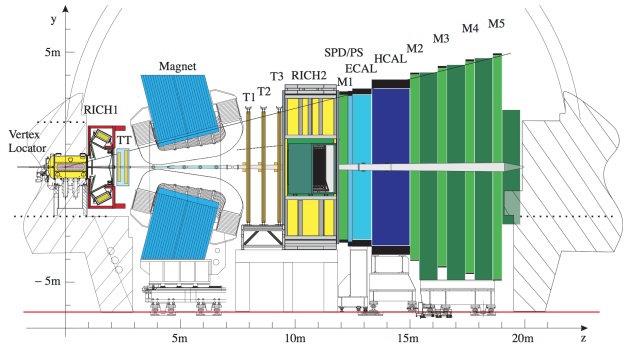

Figure 1: A side view of the LHCb detector showing the various subdetectors that make up the full experiment. The VELO is shown on the far left and the downstream tracking system is made up of the Trigger Tracker (TT), located before the magnet, and the tracking stations T1–T3, located after the magnet [3].

BEAM-GAS IMAGING

The VELO subdetector can also be used for the precise reconstruction of inelastic interactions between the high-energy proton beam and gas molecules within the LHCb interaction region. These reconstructed beam-gas vertices can then be used to measure the properties of the colliding beams such as their profiles, sizes or crossing angle.

Reconstruction

The reconstruction of these vertices uses hits in the VELO's 21 silicon strip r-ϕ sensor modules to form tracks which are then combined to find vertices using LHCb's pattern-matching algorithms [4]. A selection based on the vertex track multiplicity and spatial coordinates is applied in order to enhance the sample of beam-gas vertices. Vertices are required to have at least five constituent tracks and to fall within the longitudinal range of the VELO acceptance (±1500 mm). There is an additional radial cut of 4 mm to exclude any secondary interactions with the detector material. The directionality of the constituent tracks is then used to assign vertices to a given beam with a requirement that vertices assigned to beam 1(2) have all tracks in the forward(backward) direction. Forward tracks are defined as those tracks moving from the interaction point towards the LHCb magnet, i.e. from left to right in Fig. 1.

* george.rufus.coombs@cern.ch

Content from this work may be used under the terms of the CC BY 3.0 licence (© 2018). Any distribution of this work must maintain attribution to the author(s), title of the work, publisher, and DOI.

ISBN: 978-3-95450-201-1 doi:10.18429/JACoW-IBIC2018-WEPB14

Content from this work may be used under the terms of the CC BY 3.0 licence (© 2018). Any distribution of this work must maintain attribution to the author(s), title of the work, publisher, and DOI.

RECENT RESULTS ON NON-INVASIVE BEAM SIZE MEASUREMENT METHODS BASED ON POLARIZATION RADIATION

L. Bobb, Diamond Light Source, Oxfordshire, UK
M. Bergamaschi, R. Jones, R. Kieffer, T. Lefevre, S. Mazzoni†, F. Roncarolo, CERN, Geneva, CH
M. Billing, J. Conway, M. Forster, Y. Padilla Fuentes, J. Shanks, S. Wang, L. Ying, Cornell University, Ithaca, USA
P. Karataev, K. Lekomtsev, JAI at Royal Holloway University of London, Egham, UK
A. Aryshev, N. Terunuma, KEK, Tsukuba, Japan
V.V. Bleko, A. S. Konkov, A. P. Potylitsyn, Tomsk Polytechnic University, Tomsk, Russia

Abstract

We present recent results on non-invasive beam profile measurement techniques based on Diffraction Radiation (DR) and Cherenkov Diffraction Radiation (ChDR). Both methods exploit the analysis of broadband electromagnetic radiation resulting from polarization currents produced in, or at the boundary of, a medium in close proximity of a charged particle beam. To increase the resolution of DR, measurements were performed in the UV range at a wavelength of 250 nm. With such configurations, sensitivity to the beam size of a 1.2 GeV electron beam below 10 μm was observed at the Accelerator Test Facility (ATF) at KEK, Japan. In the case of the ChDR, a proof of principle study was carried out at the Cornell Electron Storage Ring (CESR) where beam profiles were measured in 2017 on a 5.3 GeV positron beam. At the time of writing an experiment to measure the resolution limit of ChDR has been launched at ATF where smaller beam sizes are available. We will present experimental results and discuss the application of such techniques for future accelerators.

INTRODUCTION

Non-invasive beam profile measurement techniques offer the advantage of providing beam size information without inserting an object in the beam path, as is required in more traditional methods such as profile measurement using wire scanners, Optical Transition Radiation (OTR) or scintillation screens. There are two main reasons for choosing such methods: being capable of measuring high intensity beams that would destroy any interceptive devices and avoiding any blow-up in emittance due to the interaction of the particles with material. Non interceptive methods can therefore allow a continuous monitoring of the transverse beam size during machine operation. This is the case of the proposed Compact Linear Collider (CLIC), where charge densities up to 10^8 nC/cm^2 can be reached in the main beam [1], a value that is approximately 100 times higher than the damage limit of the best thermal resistant materials such as Be or SiC.

We report here on the status of two projects that aim at studying Diffraction radiation (DR) and Cherenkov Diffraction Radiation (ChDR) as candidates for non-invasive beam profile measurement techniques. In DR, beam size information is obtained through the analysis of the far-field angular distribution of light produced when the beam passes through a narrow slit in a metallic screen [2]. In ChDR, light is produced at the boundary of a dielectric material (eg: fused silica) close to the beam path. Notwithstanding the differences in terms of geometry and properties of the emitted radiation, DR and ChDR are based on a similar physical mechanism, that of emission by polarisation currents induced at the surface of a medium [3] by the electromagnetic field of a relativistic particle. This electromagnetic field can be considered as quasi-transverse one, with an effective field radius given by

$$l = \gamma\lambda/2\pi \quad (1)$$

where γ is the Lorentz factor and λ the wavelength of observation. As a consequence, measurement methods based on DR / ChDR work when the impact parameter h of the target (the half aperture of a slit in the case of DR, the distance between beam path and crystal edge for ChDR) satisfies the condition $h \leq l$. If we consider the visible spectrum (e. g. $\lambda = 500$ nm) and relativistic electrons at 1 GeV ($\gamma \cong 2000$), we will obtain an appreciable DR/ChDR emission for $h \leq 160$ μm, a condition that can be attained and controlled experimentally.

While DR is a more established technique, the first proposal using it for beam diagnostics dating back to 1998 [4], ChDR can still be considered to be at a proof of concept stage. We will therefore report on these two separately throughout this paper.

STATUS OF DR EXPERIMENT AT ATF2

A DR setup was installed in 2016 in the extraction line of the Accelerator Test Facility 2 (ATF2) in KEK. A description of the instrument and target can be found in [5]. In the course of 2017, the instrument has been upgraded to its final configuration (see Fig. 1).

† email: stefano.mazzoni@cern.ch

ISBN: 978-3-95450-201-1 doi:10.18429/JACoW-IBIC2018-WEPB15

A MULTIPURPOSE SCINTILLATING FIBRE BEAM MONITOR FOR THE MEASUREMENT OF SECONDARY BEAMS AT CERN

I. Ortega Ruiz*, L. Fosse, J. Franchi, A. Frassier, J. Fullerton, J. Kral, J. Lauener, T. Schneider, J. Spanggaard, G. Tranquille, CERN, 1211 Geneva, Switzerland

Abstract

A scintillating fibre beam monitor has been developed at CERN for the measurement of low energy and low intensity secondary beams. This monitor can track the passage of individual particles up to intensities of 10^7 particles per second per mm^2, over an active area of ~ 20 cm × 20 cm, and with a spatial resolution of 1 mm. Thanks to an external trigger system, the achieved detection efficiency is ~ 95% and the noise level is kept below 10^{-4} events/second. The simple design of this monitor avoids the common production difficulties of scintillating fibre detectors and makes its maintenance easier, when compared to other tracking detectors, due to the absence of gas or cooling. Using special electronics, a version of the monitor can also be used for time-of-flight measurements, achieving a time resolution of 900 ps. Thanks to its versatility, the monitor will perform several functions when measuring the secondary beams of the CERN Neutrino Platform: beam profile measurement, magnetic momentum spectrometry, particle identification through time-of-flight, and trigger generation for the experiments.

INTRODUCTION

The Experimental Areas at CERN deliver beams of secondary particles that are used by many experiments related to high-energy physics research and R&D in particle detectors and accelerator technology. These beams are composed of hadrons and leptons that are delivered over a wide range of energies (1 GeV/c to 450 GeV/c), and intensities (10^2 to 10^7 particles per second per mm^2). The profile and position of these beams have been measured for decades with Multi-Wire Proportional Chambers and Delay Wire Chambers. However, these detectors are ageing, which compromises their performance, and they cannot fulfil the requirements of a new experimental area, the Neutrino Platform, since it requires large area monitors capable of detecting individual particles [1, 2].

For these reasons, the Beam Instrumentation group at CERN has investigated a new scintillating fibre beam monitor, whose first prototype was successfully tested with beam as reported in [3, 4]. This article describes the second prototype, which has the code name XBPF (eXperimental Beam Profile Fibre monitor), and the beam tests that have validated its production for the Neutrino Platform. Twelve monitors will be commissioned in this facility at the end of August 2018, at the same time as the new beam lines.

* inaki.ortega@cern.ch

XBPF AND XBTF

The XBPF for the Neutrino Platform is composed of 192 scintillating fibres Kuraray SCSF-78 of 1 mm thickness and square cross section. The fibres are packed together along one plane, forming the active area of the detector that stands in front of the beam (Fig. 1). The light from every fibre is read-out on one end by an individual Silicon Photomultiplier (SiPM) from Hamamatsu (model S13360-1350) that allows one to know which fibre has been activated and subsequently to reconstruct the track of the particle from multiple monitors. A mirror glued on the non read-out end of the fibre reflects back the light travelling in that direction along the fibre, thus increasing the total light signal reaching the photomultiplier.

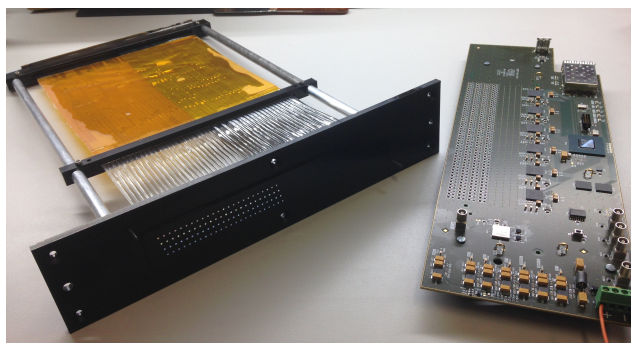

Figure 1: XBPF on the left, and front-end board with the 192 SiPMs on the right.

There exists a second version of the monitor, the XBTF (eXperimental Beam Trigger Fibre monitor), that is used to produce a fast trigger for the XBPF and for the neutrino experiments. In this monitor the fibres are grouped together into two bundles to be read-out by two Photo Multiplier Tubes (PMT) H11934-200 from Hamamatsu. These PMT have a very low dark count rate, at the level of a few Hz, and also have a low transit time spread (300 ps), which makes them suitable for Time-of-Flight applications.

Both the XBPF and XBTF have been designed to be vacuum compatible, which removes the need for vacuum windows, so helping to reduce the material budget of the beam line. The photo detectors are located outside vacuum, with the fibres exiting via a feed-through based on an innovative gluing technique that guarantees the necessary leak tightness. The vacuum tank of the new detectors has a modular design that allows it to host any desired combination of XBPF and XBTF, chosen to optimise the functionality of the beam line (Fig. 2).

Content from this work may be used under the terms of the CC BY 3.0 licence (© 2018). Any distribution of this work must maintain attribution to the author(s), title of the work, publisher, and DOI.

ISBN: 978-3-95450-201-1 doi:10.18429/JACoW-IBIC2018-WEPB16

Content from this work may be used under the terms of the CC BY 3.0 licence (© 2018). Any distribution of this work must maintain attribution to the author(s), title of the work, publisher, and DOI.

DEVELOPMENT OF A BEAM-GAS CURTAIN PROFILE MONITOR FOR THE HIGH LUMINOSITY UPGRADE OF THE LHC

R. Veness, M. Ady, N. S. Chritin, J. Glutting, T. Marriott-Dodington, O. R. Jones, R. Kersevan, S. Mazzoni, A. Rossi, G. Schneider, CERN, Geneva, Switzerland
P. Forck, S. Udrea, GSI, Darmstadt, Germany
A. Salehilashkajani, C. P. Welsch, H. D. Zhang, Cockcroft Institute and University of Liverpool, Warrington, UK
P. Smakulski, Wrocław University of Science and Technology, Wrocław, Poland

Abstract

High luminosity upgrades to the LHC at CERN and future high-energy frontier machines will require a new generation of minimally invasive profile measurement instruments.

Production of a dense, focussed gas target allows beam-gas fluorescence to be exploited as an observable, giving an instrument suitable for installation even in regions of high magnetic field.

This paper describes the development of a device based on these principles that would be suitable for operation in the LHC. It focusses on mechanisms for the production of a homogeneous gas curtain, the selection of an appropriate working gas and the optical fluorescence detection system.

INTRODUCTION

High-Luminosity LHC (HL-LHC) is under construction as an upgrade to the LHC at CERN [1], planned for commissioning from 2026. The upgrade to the LHC and its injectors will lead to a significant increase in beam intensity. Even the small amount expected to appear as a beam halo will contain significant energy, which must be constantly cleaned to avoid unacceptable losses on the collimation system. The principal technical solution under study for this purpose is a 'hollow electron lens' (HEL) [2] which uses a hollow cylindrical electron beam, constrained by a superconducting solenoid which is passed concentrically around the circulating proton beam over some 3 m of beamline.

Monitoring the concentricity of these two beams during operation will require simultaneous, minimally-invasive, transverse profile measurement of both proton and hollow electron beams. In addition, this measurement must be in close proximity to the solenoid field constraining the electron beam, preventing the collection of charged particles as an observable.

An instrument is being developed to image fluorescence generated by the interaction between these beams and a thin, supersonic, gas curtain [3,4,5]. By tilting this 'Beam Gas Curtain' (BGC) with respect to the beam axis, a 2-D image of both beams can be obtained in much the same way as for a traditional solid screen beam observation system.

The instrument consists of the following main components:

- a gas generation stage consisting of a supersonic gas nozzle followed by three skimmers which select and shape the gas jet.
- an interaction chamber where the 0.45-7 TeV proton beam and 10 keV electron beam interact with the gas jet.
- an optical system for image generation
- an exhaust chamber which pumps the residual gas jet and contains gas jet diagnostics.

There are a number of key developments required for this instrument. It is important to select a working gas that is compatible with the NEG-coated, LHC ultra-high vacuum system, whilst still producing an adequate fluorescence signal from the interaction of both keV electrons and TeV protons, preferably from the spectral line of a neutral atom or molecule to avoid image distortion from electric and magnetic fields. It is also necessary to study the production of a dense supersonic gas curtain whilst minimising the background gas load to the vacuum system, and to develop a radiation-hard imaging system that is efficient for both the electron and proton excited fluorescence signals.

WORKING GASES

As working gases, Nitrogen (N_2) and Neon (Ne) were initially considered [3,6], with estimations made on their cross-sections for relevant transitions at the energies of interest (see Table 2). However, recent considerations regarding vacuum compatibility at CERN lead to the conclusion that N_2 is less desirable than Neon and that a further alternative is Argon (Ar). A literature study was therefore conducted on the fluorescence of Ar and Ar^+ due to excitation by electrons and protons. Whilst a large amount of data is available for fluorescence cross-sections for relatively low-energy ($E_k \leq 1$ keV) electrons impinging on Ar, there is no relevant data for high-energy electrons or protons. According to measurements by [7] for excitation by ≤ 250 eV electrons, the most prominent lines are at 750.4 nm for Ar and 476.5 nm for Ar^+. However, high intensity lines at 751.5 nm (Ar) and 454.5 nm (Ar^+) can also be considered. For extrapolating to higher electron energies the model presented for Ne in [6] has been used for Ar, while for Ar^+ a

ISBN: 978-3-95450-201-1 doi:10.18429/JACoW-IBIC2018-WEPB18

PERFORMANCE OF A REFLECTIVE MICROSCOPE OBJECTIVE IN AN X-RAY PINHOLE CAMERA

L. Bobb *, G. Rehm, Diamond Light Source, Oxfordshire, U.K.

Abstract

X-ray pinhole cameras are used to measure the transverse beam profile of the electron beam in the storage ring from which the emittance is calculated. As improvements to the accelerator lattice reduce the beam emittance, e.g. with upgrades to fourth generation synchrotron light sources, likewise the beam size will be reduced such that micron and sub-micron scale resolution is required for beam size measurement. Therefore the spatial resolution of the pinhole camera imaging system must be improved accordingly. Here, the performance of a reflective microscope objective is compared to the high quality refractive lens which is currently in use to image the scintillator screen to the camera. The modulation transfer functions for each system have been assessed and will be discussed.

INTRODUCTION

There are three pinhole cameras in operation at Diamond Light Source: two of these systems continuously monitor the beam size [1] for vertical emittance feedback [2], whilst the third pinhole camera is installed on the Diagnostics X-ray beamline for research and development.

All of the pinhole cameras share a common layout in the storage ring as shown in Fig. 1. For each pinhole camera, synchrotron radiation from a bending magnet passes from vacuum to air through a 1 mm thick aluminium window. The spectrum has a photon energy range from 15 keV to approximately 60 keV and a peak at 25 keV. The X-rays then pass through the ≈24 µm pinhole aperture which is formed using a stacked arrangement of tungsten blades separated by chemically etched shims [3, 4]. The pinhole assembly is kept under nitrogen to prevent oxidation.

The first image plane is located at the scintillator screen which converts X-rays to visible photons. This image is relayed from the scintillator screen to the camera via a lens. The total path length is approximately 15 m.

The source-to-screen magnification is approximately 2.5. The horizontal beam size of the electron beam σ_x is ≈50 µm, therefore the horizontal beam size imaged at the scintillator screen is ≈125 µm. The electron beam profile which is approximated by a Gaussian extends much further than $\pm 1\sigma_x$, thus the field of view of the relay lens should be roughly an order of magnitude greater that the imaged beam size, in this case preferably 1 mm.

Rather than direct X-ray detection using an expensive detector, scintillator screens are incorporated to convert X-rays to visible photons which can be detected using machine vision CCD or CMOS cameras. In order to have a reasonable exposure time (< 100 ms), a sufficient intensity per pixel

* lorraine.bobb@diamond.ac.uk

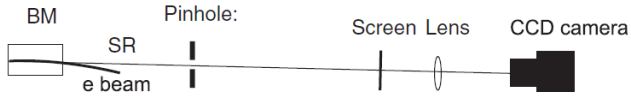

Figure 1: Schematic of the pinhole camera system [1]. A folding mirror is also typically included downstream of the scintillator such that the refractive lens and camera may be located away from the X-ray beam.

(i.e. light yield) to form an image above noise is required. This dictates the lower bound on the scintillator thickness for a given optical setup. The upper bound is determined by the spatial resolution that is required for imaging the electron beam. In some cases direct X-ray detection is necessary [5].

For pinhole cameras at third generation synchrotron light sources, the scintillator thickness is in the 100 to 500 µm range [1, 6]. Due to the limited information provided in the technical specifications from manufacturers, a series of experiments to compare and characterise different scintillator materials have been conducted largely by G. Kube *et al.* [7, 8]. These results have shown that although there is some variation of the spatial resolution for different materials, reducing the thickness of the scintillator provides the greatest improvement in spatial resolution [9].

The Point Spread Function (PSF) describes the spatial resolution of an imaging system. For pinhole cameras each optical element contributes to the overall PSF of the imaging system [3]. Using a Gaussian approximation the overall PSF may be represented as

$$\sigma^2_{\mathrm{PSF}} = \sigma^2_{\mathrm{pinhole}} + \sigma^2_{\mathrm{camera}} \quad (1)$$

with

$$\sigma^2_{\mathrm{pinhole}} = \sigma^2_{\mathrm{diffraction}} + \sigma^2_{\mathrm{aperture}} \quad (2)$$

and

$$\sigma^2_{\mathrm{camera}} = \sigma^2_{\mathrm{screen}} + \sigma^2_{\mathrm{lens}} + \sigma^2_{\mathrm{sensor}} \quad (3)$$

where the subscripts denote the sources of the PSF contributions [4]. The PSF contribution associated with imaging the scintillator screen denoted σ_{camera} may be measured using a knife-edge and uniform illumination. The PSF contribution from the pinhole denoted $\sigma_{\mathrm{pinhole}}$ may be calculated provided the aperture size is known [1].

The overall PSF is dominated by the contribution due to pinhole aperture size $\sigma_{\mathrm{pinhole}}$ and the contribution from the scintillator screen σ_{screen}. Investigations are under way to minimise $\sigma_{\mathrm{pinhole}}$ by improving the control of the pinhole aperture size using alternative fabrication methods such that the optimal size is used given the X-ray spectrum [4, 10].

Content from this work may be used under the terms of the CC BY 3.0 licence (© 2018). Any distribution of this work must maintain attribution to the author(s), title of the work, publisher, and DOI.

ISBN: 978-3-95450-201-1 doi:10.18429/JACoW-IBIC2018-WEPB20

EXPERIMENTAL SETUP OF APODIZATION TECHNIQUES FOR BEAM DIAGNOSTICS PERFORMED AT ELBE

B. Freeman, J. Gubeli, and K. Jordan, Jefferson Lab, Newport News, VA, USA
P. Evtushenko, HZDR, Dresden, Germany

Abstract

The ELBE (Electron Linac for beams with high Brilliance and low Emittance) facility in Dresden, Germany is a multi-purpose user facility, which is also used for accelerator R&D purposes. The beam line was setup for transverse beam profile measurements, where the imaging system includes a series of three apodizers and five circular apertures. Both of which could be changed remotely during beam operation, through automated LabVIEW routines. The bunch structure and charge were varied to collect a series of images that were acquired automatically, and then stored for later analysis. Over 12,000 images were captured and then analyzed using software written at Jefferson Lab that runs ImageJ as its main image processing library.

INTRODUCTION

Large Dynamic Range (LDR) diagnostics are becoming increasingly important for high current and high beam power accelerators. Machines where a transverse and longitudinal match must be computed to control the beam optics, a lower average beam current is tyically used. When setup is believed to be complete the beam current and duty cycle are usually increased. It has been the experience at the JLab machines, both CEBAF and the FEL [1], in its operation, that the best of setups are just not good enough initially to transport the beam at the requested beam power, without beam losses. The setup, either in the transverse or longitudinal plane must be revisited to sustain the beam power requested by the users. The reason for this, is the inability of the available diagnostics to detect beam tails and beam halo ahead of the machine protection system [1]. The operational impact of this can be significant and has caused some to investigate ways of improving the ability to setup, and to investigate diagnostics that could see the tails and halo during setup.

The smallest point that can be resolved in an optical system is defined by its point spread function (PSF). It is a function of the angular acceptance of the aperture. In the Fouier optics, it is the Fouier transform of the pupil function. When light is collected through the aperture, diffraction effects limit the smallest resolvable spot. To improve the dynamic range of the system, which is defined by *(Peak/Noise)*, apodizers have been suggested to decrease diffraction in the image plane and drive the noise level down even farther. Apodizers have been used in astronomy, when observing stars which are tiny point sources of light. An apodizer is a Gaussian spatial filter, which limits the amount of light that can enter the image plane by decreasing the transmission of light radial out from the center of the filter. The transmission profile of the filter is defined by

$$T(r,\sigma) = T_0 e^{-\left(\frac{r}{\sigma\sqrt{2}}\right)^2} \quad (1)$$

where $T_0 = 97\% \pm 1\%$ [2].

Three apodizers were ordered, all were made on a fused silica substrate. Two of the apodizers were made using a half tone dot method. Which means they were constructed with 10 µm pixels that have an increasing density radially by the relation Equation 1. The pixel density changes the amount of light that is transmitted through the filter. The two half tone gaussian profiles were made such that σ =6 mm ± 0.3 mm, and σ =12 mm ± 0.3 mm. The third apodizer was constructed using a reflective coating with increasing density radially outward from $r = 0$ at the center of the filter, with σ =12 mm ± 0.3 mm [2].

EXPERIMENTAL SETUP

The ELBE (Electron Linac for beams with high Brilliance and low Emittance) facility in Dresden, Germany was chosen because of the many configurations possible. The facility is a multipurpose user facility which can also be used for R&D applications. The electron beam at ELBE was setup to allow for several different bunch charges, at different micro-pulse frequencies. The overall purpose of the experiment was to put the Gaussian apodizers to the test, with a large range of various light intensities. The experimental setup was set up to automate the process of varying the apodizers, a series of 5 circular apertures, exposure times, and camera gains.

Mechanical Setup

A Large Dynamic Range Diagnostic Station (LDRDS) was used in this experiment to profile the electron beam. The LDRDS consists of a six inch cross with two beam intercepting devices and two six-inch conflat flange viewports. One device is a stepper motor driven linear shaft with a two wire fork (wire scanner). The fork is orientated at 45 degrees to the beam along two axes with the wires set horizontally and vertically along the beamline. This fork angle is set to allow any optical transition radiation from the wires, as they pass through the electron beam, to be directed out one of the viewports. This fork is electrically isolated from the chamber and connected to an SMA feedthrough. The lead-screw, gear box and stepper motor combination has a linear resolution of 127 nm (½ step) and a maximum linear speed of 1.27 mm/second.

The second device is a two-stage pneumatically driven linear stage. The center shaft is rigidly attached to a slide on two linear ball bushing bearings to produce a very repeatable insertion position. A ball bearing is used as a coupling

Content from this work may be used under the terms of the CC BY 3.0 licence (© 2018). Any distribution of this work must maintain attribution to the author(s), title of the work, publisher, and DOI.

ISBN: 978-3-95450-201-1 doi:10.18429/JACoW-IBIC2018-WEPB21

TRANSVERSE BEAM EMITTANCE MEASUREMENTS WITH MULTI-SLIT AND MOVING-SLIT DEVICES FOR LEREC*

C. Liu#, A. Fedotov, D. Gassner, X. Gu, D. Kayran, J. Kewisch, T. Miller, M. Minty, V. Ptitsyn, S. Seletskiy, A. Sukhanov, D. Weiss, Brookhaven National Laboratory, Upton, U.S.A.
A. Fuchs, Ward Melville High School, Setauket- East Setauket, U.S.A.

Abstract

Low Energy RHIC electron cooling (LEReC) is the first bunched electron cooler, designed to cool low energy ion beams at RHIC. The beam quality, including the transverse beam emittance, is critical for the success of cooling. The transverse electron beam emittance was characterized with a multi-slit and moving-slit device at various locations in the beamline. The beam emittance measurement and analysis are presented in this report.

INTRODUCTION

LEReC [1], a linear electron accelerator (Figure 1), is designed to cool RHIC ion beams and therefore improve luminosities at beam energies below 10 GeV/n [2]. Electron bunches are generated by a 400 kV DC electron photocathode gun; these bunches then go through a chain of cavities, which includes a 1.2/1.6 MeV 704 MHz superconducting booster cavity, a 2.1 GHz normal-conducting copper cavity to linearize beam energy chirp, a 704 MHz normal-conducting cavity to reduce energy spread of individual bunches and a 9 MHz normal-conducting cavity to reduce energy droop along bunch train due to beam loading. Each electron macro-bunch, consisting of 30 micro-bunches of 40 ps length at 704 MHz repetition frequency, will overlap with a RHIC ion bunch at 9 MHz frequency. The electron beam first propagates with the ion beam in one of the RHIC rings (Yellow) collinearly with the same speed, then turns around and propagates with the ion beam in the other RHIC ring (Blue). With extremely small energy spread (5E-4), the electron beam reduces the ion beam energy spread when interacting with it by coulomb friction force. The design electron beam current is 30-55 mA for beam energy 1.6-2.6 MeV, with bunch charge of 130-200 pC and normalized emittance <2.5 μm [1].

Matching the electron beam transverse emittance to that of the ion beam is crucial for cooling. With low energy and high bunch charge, the electron beam emittance is dominated by space charge effect. Therefore, emittance measurement devices made of slit/slits [3] were chosen in the LEReC accelerator to measure beam emittance along the beamline. The multi-slit and moving-slit sample several transverse slices of the beam which then project to downstream profile monitors. The space charge effect is substantially reduced due to reduction of charge density by the sampling of the slit/slits.

MATERIAL AND METHOD FOR BEAM EMITTANCE MEASUREMENT

A multi-slit device (Figure 2) [4], installed after the Booster cavity with a YAG profile monitor 2 m downstream, measures beam emittance in the DC gun test line. There are 10 horizontal and 10 vertical slits on the same mask, respectively for vertical and horizontal beam emittance measurement. The slit width is 150 μm, with slit spacing 1.346 mm. The mask was made of Tungsten plate of 1.5 mm thickness. The multi-slit mask is thick enough to stop most of the electrons at 1.6 MeV beam energy. This is designed to avoid background on the downstream profile monitor due to scattered electrons.

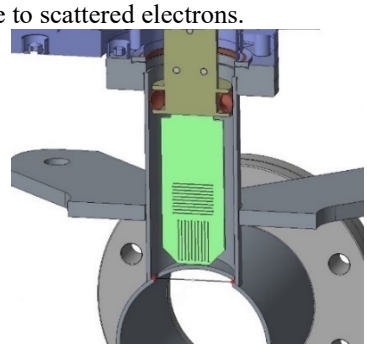

Figure 2: Drawing of multi-slit device at retracted position, with vertical slits at the bottom and horizontal slits at the top part of the mask.

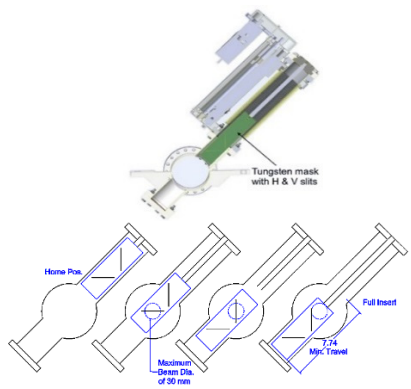

Figure 3: Schematics of moving-slit device. The image on top shows the assembly and the orientation, with a view along the beam path. The lower image illustrates the sampling process, first horizontal and then vertical with the mask driven in by a stepper motor.

*The work was performed under Contract No. DE-SC0012704 with the U.S. Department of Energy.
cliu1@bnl.gov

Content from this work may be used under the terms of the CC BY 3.0 licence (© 2018). Any distribution of this work must maintain attribution to the author(s), title of the work, publisher, and DOI.

ISBN: 978-3-95450-201-1 doi:10.18429/JACoW-IBIC2018-WEPC02

SYNCHROTRON EMITTANCE ANALYSIS PROCEDURE AT MedAustron

L. Adler*[1,2], A. De Franco[1], F. Farinon[1], N. Gambino[1], G. Guidoboni[1], C. Kurfürst[1], S. Myalski[1], M. Pivi[1], C. Schmitzer[1], I. Strasik[1], A. Wastl[1]
[1] EBG MedAustron, Wr. Neustadt, Austria
[2] Atominstitut TU Wien, Vienna, Austria

Abstract

MedAustron is a synchrotron based medical accelerator facility for particle therapy providing protons and carbon ions with clinical energies from 60 MeV to 250 MeV and 120 MeV/n to 400 MeV/n respectively. The facility features four irradiation rooms, three of which are dedicated to clinical operation and a fourth one to non-clinical research. Commissioning of all fixed lines has been completed for protons, while the commissioning for carbon ions and a proton gantry is ongoing.

For the commissioning of carbon ions, precise measurements of the transverse beam emittance in the synchrotron are of importance, to minimize beam losses and to correct for possible emittance variations due to the different clinically relevant beam intensities defined by a degrader at the end of the Linac.

The transverse beam emittance in the MedAustron synchrotron is measured via scraping at non-dispersive regions of the ring. The analysis procedure as well as emittance reconstruction accuracy for simulated data will be described in this paper, together with measurement results from the carbon commissioning.

INTRODUCTION

MedAustron is a synchrotron based ion therapy and research center located in Wr. Neustadt, Austria. Its design is based on PIMMS [1] and CNAO [2]. It features three ECR ion sources, a 400 keV/n RFQ and a 7 MeV/n IH Drift tube LINAC feeding the beam into a synchrotron with 77 m circumference. At the moment patient treatment with proton beams in the energy range of 62.4 MeV up to 252.7 MeV is taking place in two irradiation rooms featuring two fixed horizontal and a fixed vertical beamline [3].

During acceleration the beam is kept off-momentum and then extracted, using a betatron core slowly accelerating the beam onto a 3rd order resonance in the horizontal plane, which is generated using lattice quadrupoles and a dedicated sextupole magnet in a dispersion free region of the ring [4]. This allows a smooth extraction with spill-lengths between 0.1 s and 10 s. The off-momentum operation and the slow third order resonance extraction process require an accurate knowledge and precise measurements of the transverse emittance in the synchrotron.

The MedAustron accelerator features a so called *degrader* at the end of the Linac which is used to limit the number of particles being injected into the ring. It is a pepper pot like device allowing to reduce the intensity to 10, 20 or 50 % of the nominal intensity.

The current transformer in the synchrotron shows a Gaussian white noise, which is independent of the signal amplitude. This results in the signal to noise ratio being approximately 10 times worse for degrader 10 % compared to nominal intensity.

Parallel to patient treatment, commissioning of the first fixed horizontal beamline with carbon ion beam is ongoing. To facilitate the carbon commissioning, the transverse synchrotron emittance analysis procedure has been refined to obtain more accurate results , higher robustness of the analysis algorithms and allow for a completely automated measurement data analysis.

DESIGN EMITTANCES

In the following the design diluted ring emittances will be listed, since those values were chosen as simulation input to determine the stability and accuracy of the analysis procedure.

The numerical values of the design emittances can be seen in Table 1, they are the same for both planes.

Table 1: Design Emittances of the MedAustron Synchrotron in π mm mrad

Protons	60 MeV/n	250 MeV/n
RMS norm. emittance	0.519	0.519
RMS geom. emittance	1.4286	0.6679
Carbon ions	**120 MeV/n**	**400 MeV/n**
RMS norm. emittance	0.7482	0.7482
RMS geom. emittance	1.4286	0.7324

EMITTANCE ANALYSIS IN THE MEDAUSTRON FRAMEWORK

The automatic analysis program for the transverse synchrotron emittance has been coded in Python 3.4 [5] as a Level 3 tool in the MedAustron Measurement Data Analysis Framework *PACMAN* [6]. The measurements are taken via a so called *Operational Application*, a dedicated software tool in the MedAustron OpApp framework [7], which takes care of the provision of measurement configuration data to the accelerator and autonomously performs the resulting beam measurements.

* laurids.adler@medaustron.at

Content from this work may be used under the terms of the CC BY 3.0 licence (© 2018). Any distribution of this work must maintain attribution to the author(s), title of the work, publisher, and DOI.

ISBN: 978-3-95450-201-1 doi:10.18429/JACoW-IBIC2018-WEPC04

SETUP FOR BEAM PROFILE MEASUREMENTS USING OPTICAL TRANSITION RADIATION*

J. Pforr†, M. Arnold, T. Bahlo, L. Jürgensen, N. Pietralla, A. Rost,
TU Darmstadt, Darmstadt, Germany
F. Hug, Johannes Gutenberg-Universität Mainz, Mainz, Germany

Abstract

The S-DALINAC is a thrice-recirculating, superconducting linear electron accelerator at TU Darmstadt. It can provide beams of electrons with energies of up to 130 MeV and currents of up to 20 µA. The accelerator performance was improved by an extension of the beam diagnostics, as this increases the reproducibility of the machine settings. In addition, the installation of several beam profile measurement stations is planned, which should be operational down to a beam current of 100 nA, as this current is used for beam tuning. Combining these devices with a quadrupole scan also allows for emittance measurements. The beam profile measurements shall be done based on optical transition radiation (OTR), resulting from the penetration of relativistic electrons from vacuum into a metal target. The radiation can be detected using standard cameras that provide information on the two-dimensional particle distribution. This contribution will address the layout of the measurement stations and a first test measurement will be presented.

NEW DIAGNOSTIC STATIONS AT THE S-DALINAC

The current layout of the S-DALINAC is shown in Fig. 1. The electron beam coming from one of the two sources can be accelerated in the superconducting injector to up to 10 MeV beam energy [1]. After the injector the beam can be used at the DHIPS (Darmstadt High Intensity Photon Setup) experimental area [2] or be bent into the main linac. The electrons can pass the main linac up to four times due to the three existing recirculations [3] and are afterwards extracted to the experimental hall with a maximum energy of 130 MeV.

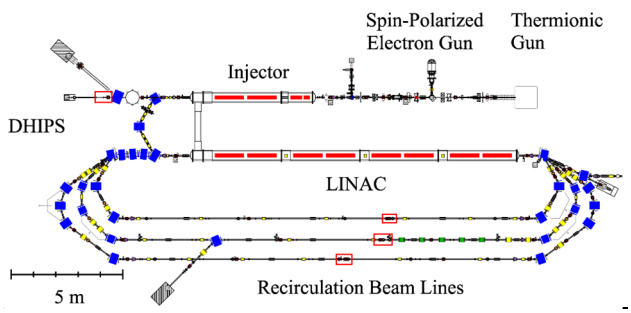

Figure 1: Layout of the S-DALINAC with three recirculation beam lines. The red boxes denote the positions of the planned diagnostic stations.

In order to enable an emittance measurement after each acceleration, there are several diagnostic stations necessary. One is located behind the superconducting injector and further diagnostic stations are planned in the straight sections of each recirculation beam line. The positions were chosen such that quadrupoles are available for an emittance measurement based on a quadrupole scan. In addition, the diagnostic stations consist of an OTR target and CMOS cameras (FLIR BFLY-PGE-31S4M-C) which detect the radiation. This type of camera was chosen for various reasons as a high resolution and framerate. Of special importance is the possibility to adjust many camera parameters, e.g. the exposure time and gain, remotely, which results in a high flexibility. As these cameras have to be protected from radiation damage, the target is supposed to be observed via a mirror in order to allow for better shielding.

OPTICAL TRANSITION RADIATION

Transition radiation is emitted when a relativistic charged particle crosses the boundary between two media with different permittivity, as the electric field has to rearrange at the boundary. This radiation was predicted in 1947 by Ginzburg and Frank [4], and after pioneering work by Wartski [5] it has been established as a tool for electron beam diagnostics. The emission of OTR is directed in two cones with opening angle of $1/\gamma$, as depicted in Fig. 2, where the metal target is inclined with 45° with respect to the electron beam. The radiated power for an electron with Lorentz factor $\gamma >> 1$ can be described by [6]

$$W_1(\theta) = \frac{e^2}{4\pi^3\epsilon_0 c}\frac{\beta^2\sin^2\theta}{(1-\beta^2\cos^2\theta)^2}$$

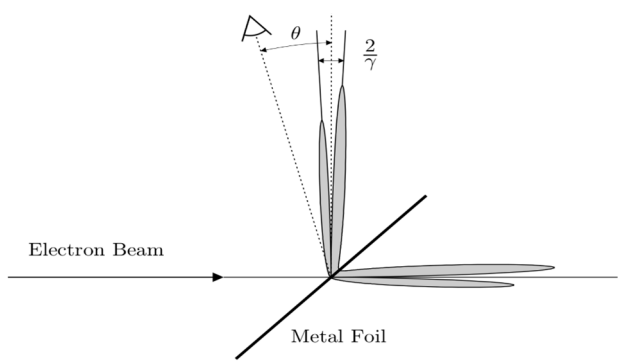

Figure 2: The directional dependence of the intensity of OTR light that is emitted by a metal foil with 45° angle to the electron beam [7].

* Work supported by DFG through GRK 2128.
† jpforr@ikp.tu-darmstadt.de

Content from this work may be used under the terms of the CC BY 3.0 licence (© 2018). Any distribution of this work must maintain attribution to the author(s), title of the work, publisher, and DOI.

ISBN: 978-3-95450-201-1 doi:10.18429/JACoW-IBIC2018-WEPC05

THE EUROPEAN XFEL WIRE SCANNER SYSTEM

T. Lensch*, S. Liu, M. Scholz, Deutsches Elektronen Synchrotron, DESY, Hamburg, Germany

Abstract

The European-XFEL (E-XFEL) is an X-ray Free Electron Laser facility located in Hamburg (Germany). The superconducting accelerator for up to 17.5 GeV electrons will provide photons simultaneously to several user stations. Currently 12 Wire Scanner units are used to image transverse beam profiles in the high energy sections. These scanners provide a slow scan mode which is currently used to measure beam emittance and beam halo distributions. When operating with long bunch trains (>100 bunches) also fast scans are planned to measure beam sizes in an almost nondestructive manner. Scattered electrons can be detected with regular Beam Loss Monitors (BLM) as well as dedicated wire scanner detectors. Latter are installed in different variants at certain positions in the machine. Further developments are ongoing to optimize the sensitivity of the detectors to be able to measure both, beam halo and beam cores within the same measurement with the same detector. This paper describes the current status of the system and examples of different slow scan measurements.

INTRODUCTION

At the E-XFEL there are about 60 screen stations installed. Twelve of these screen stations are additionally equipped with wire scanner motion units. These wire scanner units are placed in groups of three upstream of the collimation section and upstream of the three SASE undulator systems. Each wire scanner unit consists of two motorized forks (horizontal and vertical plane). Each fork is driven by a separate linear motor [1]. This 90° configuration of motors helps to avoid vibration influences. The wire position is measured with a linear ruler (Heidenhain) which has a resolution of 0.5 µm. The motion unit is integrated by a custom front end electronic into the MTCA.4 [2] environment. A set of three 90° tungsten wires (50, 30 and 20 µm) and two crossed 60° wires (10 µm) are mounted on each titanium fork (see Fig. 1).

Figure 2 shows a wire scanner motion unit installed upstream of the collimation section. Different detector setups as well as regular Beam Loss Monitors (BLM) downstream of the wire scanner motion units are used for detection of scattered particles. Figure 3 shows a simplified overview of installed wire scanner stations and detectors.

DETECTORS

Dedicated Wire Scanner Detectors

Several dedicated wire scanner detectors (WSD) for scattered electrons have been developed and installed downstream of each set of motion units. They are based on photomultipliers (PMTs) of type Philips XP2243B. These fast,

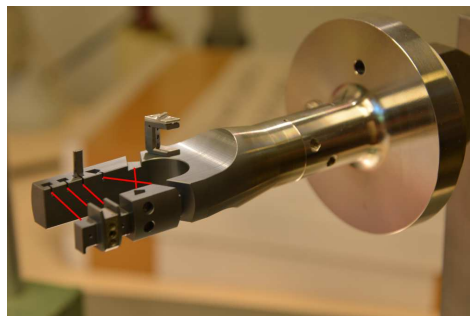

Figure 1: Titanium fork with tungsten wires which are indicated by red lines. From left to right: 50-30-20 µm, crossed wires 10 µm.

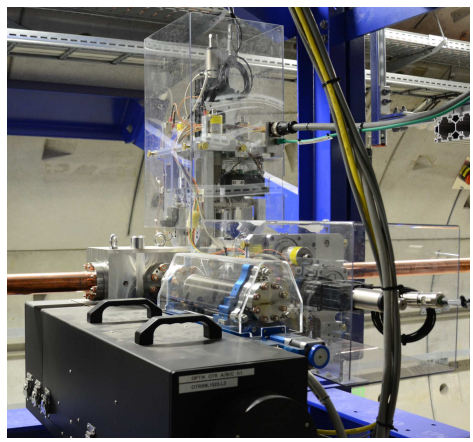

Figure 2: Wire scanner motion unit upstream SASE3 undulators. In the foreground a black optic box and a screen mover are visible.

red sensitive 6-stage tubes are well known from FLASH and HERA wire scanners for years. Currently two types of setups are installed. Plastic scintillating fibers (length: 4 m, diameter: 2 mm) optically coupled to the PMTs are wrapped around the beam pipe to be close to the beam showers. In order to gain more signal, paddles (made of NE110) with larger size compared to fiber detectors have been optically adapted to PMTs of the same type (Philips XP2243B). Measurements show that these paddle based detectors are much more sensitive and can be used better for measurements with low losses (i.e. study of beam halo distribution).

Regular BLMs

About 470 Beam Loss Monitors (BLM) are installed at the E-XFEL. They are used for machine protection and dark current measurement [3]. For detection of scattered electrons each of these BLMs can be used for the wire scanner analysis, too. Due to the non-linearity of these BLMs they cannot be used at a time for both beam halo and beam core

* timmy.lensch@desy.de

Content from this work may be used under the terms of the CC BY 3.0 licence (© 2018). Any distribution of this work must maintain attribution to the author(s), title of the work, publisher, and DOI.

ISBN: 978-3-95450-201-1 doi:10.18429/JACoW-IBIC2018-WEPC06

THE NEW DIAGNOSTIC SUITE FOR THE ECHO ENABLED HARMONIC GENERATION EXPERIMENT AT FERMI.

M. Veronese*, A. Abrami, E. Allaria, M. Bossi, I. Cudin, M. Danailov, R. De Monte, F. Giacuzzo, S. Grulja, G.Kurdi, P. Rebernik Ribic, R. Sauro, G. Strangolino and M.Ferianis, Elettra-Sincrotrone Trieste S.C.p.A., S.S. 14 km 163,5 in AREA Science Park, 34149 Trieste, Italy

Abstract

The Echo Enabled Harmonic Generation (EEHG) experiment has been implemented on the FEL2 line of the FERMI FEL at Elettra (Italy). The main purpose is to validate the expected performance improvements at short wavelengths before a dedicated major upgrade is deployed. This paper describes the new diagnostics and the operational experience with them during the EEHG experiment. By means of a multi position vacuum vertical manipulator, different optical components are positioned on the electron and seed laser path. Both transverse and longitudinal measurements are performed. A YAG:Ce screen (e beam) and a terbium doped UV scintillator (laser) are imaged on a dedicated CMOS camera. For the temporal alignment, an OTR screen and a scattering surface are used to steer radiation from the e-beam and laser, onto a fast photodetector. Also coherent OTR radiation, due to micro-bunching, is acquired by means of a PbSe photodetector. Finally, for the normal EEHG operation, the laser beam is injected on the electron beam axis by means of a UV reflecting mirror. The results of the installed diagnostics commissioning are here presented.

INTRODUCTION

One the most recent advances in Free Electron laser design is the so called Echo Enabled Harmonic Generation [1]. In this scheme the electron beam is modulated by two external lasers, compared to High Gain Harmonic Generation (HGHG) [2] where one seed laser is used and to Self Amplified Spontaneous Emission (SASE) [3] which has no external seeding and is based on amplification of shot noise microbunching, Recently microbunching at the 75th harmonic has been observed using a seed laser at 2400 nm [4]. In HGHG the external seed laser couples to electron beam in the modulator undulator to produce a bunched current distribution, then the electron beam pass through the radiator undulators and lasing occurs. The HGHG emission has a quicker built up compared to SASE. HGHG pulses have a high spectral purity and stability and can be fully coherent and transform limited [5] . The main limitation of HGHG at short wavelengths is its sensitivity to quality of the electron beam in terms of phase distortions [6]. EEHG can potentially decrease the sensitivity of the FEL to the electron beam quality and thus ease the operation of the FEL at short wavelengths. Moreover since in EEHG there is no FEL first stage, the beam does not undergo properties degradation due to first stage and so there is no need to use the fresh bunch technique [7] typical of HGHG multiple cascade FELs. This means that potentially the compression can be increased allowing for higher peak current. An EEHG experiment has been proposed [8] and installed in the FERMI FEL2, to validate the expected improvements. The experiment is aiming at comparing FEL operations in EEHG mode and in standard two stage HGHG with an electron beam energy ranging from 1.1 GeV to 1.5 GeV for wavelength in the 20 to 4 nm spectral range. Finally a new manipulator and diagnostics have been installed in the delay line and are the subject of this paper.

EEHG LAYOUT

The experiment has been setup in the FEL2 line of the FERMI FEL. FEL2 is a two stage cascade HGHG FEL usually operated in fresh bunch mode. The upgrade for the experiment involves the installation of a new modulator for the second stage of FEL2, a new laser line delivering up to 50 microJoules pulses at 260 nm with duration around 150 fs. The magnetic delay line magnet will be repositioned and a new power supply capable of 750 Amp has been installed allowing to reach R56 above 2 mm. The EEHG modulator undulator has variable gap, linear polarization and a period of 11 cm to fit the laser wavelength of 260nm. Figure 1 shows

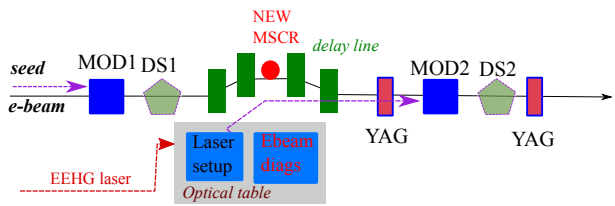

Figure 1: Layout of EEHG experiment at FERMI.

a pictorial layout of the EEHG experiment. The seed laser of the first stage is called 'seed1' and the first stage radiators are not depicted since they are not needed for EEHG and have been set at gaps fully open during the measurements. MOD1 is the first stage modulator and DS1 is the first dispersive section. The magnetic delay line is depicted as a series and green rectangles and is used as the main big R56 needed for EEHG. In the middle of it the new vacuum manipulator has been installed. On the lower part a gray rectangle depicts the optical table that houses all the laser setup that controls the steering, the compression and the third harmonic conversion to generate the 'seed2' UV laser. On the same table we also installed all the motorized actuators and detectors that compose the new diagnostics. Downstream this area we can see in Fig. 1 the YAG:Ce screens are depicted as red rectangles.

* marco.veronese@elettra.eu

Content from this work may be used under the terms of the CC BY 3.0 licence (© 2018). Any distribution of this work must maintain attribution to the author(s), title of the work, publisher, and DOI.

ISBN: 978-3-95450-201-1 doi:10.18429/JACoW-IBIC2018-WEPC08

OPTICAL SYSTEM OF BEAM INDUCED FLUORESCENCE MONITOR TOWARD MW BEAM POWER AT THE J-PARC NEUTRINO BEAMLINE

S. Cao*, M. Friend, K. Sakashita, High Energy Accelerator Research Organization (KEK), Tsukuba, Japan
M. Hartz[1], Kavli IPMU (WPI), University of Tokyo, Tokyo, Japan
[1]also at TRIUMF, Vancouver, Canada
A. Nakamura, Okayama University, Okayama, Japan

Abstract

A Beam Induced Fluorescence (BIF) monitor is being developed as an essential part of the monitor update toward MW beam power operation at the J-PARC neutrino beamline. By measuring the fluorescence light from proton-gas interactions, the BIF monitor will be used as a continuous and non-destructive diagnostic tool for monitoring the proton beam profile spill-by-spill, with position and width precision on the order of 200 µm. The main challenge lies in collecting a sufficient amount of fluorescence light for the beam profile reconstruction while controlling the beam-induced noise with the current beamline configuration. A study is presented with a particular focus on the optical system under development, which allows us to transport fluorescence light away from the high radiation environment near the proton beamline and detect the optical signal with a Multi-Pixel Photon-Counter-based fast readout.

J-PARC NEUTRINO BEAMLINE: TOWARD MW BEAM

The J-PARC complex [1] is serving as a producer of the most intense neutrino beam in the world to one of the world-leading neutrino oscillation experiment, Tokai-to-Kamioka (T2K) [2]. A J-PARC neutrino beamline is designed to guide protons extracted from Main Ring (MR), bend 80.7° toward the T2K far detector, Super-Kamiokande, before bombarding onto a graphite target in order to producing charged pions and kaons which are then decayed into ν_μ (or $\overline{\nu}_\mu$) in flight. Recent results from T2K experiment shows that the CP conserving values of CP violation phase, which is presented in the leptonic mixing matrix, fall outside of 2σ of confidence and credible intervals of measured range [3]. To further study CP violation in the leptonic sector, increasing the neutrino beam power is essential and play a role as the main driver for the neutrino intensity frontier. Since the start of user operation in 2010, the MR beam power has been increased steady and operated stably in 485 kW with an intensity of 2.5×10^{14} protons-per-pulse (ppp) at a repetition cycle of 2.48 s in 2018. Toward MW beam power, J-PARC aims to reduce the repetition cycle to 1.3 s and increase the beam intensity up to 3.2×10^{14} ppp by 2026.

To realize MW beam, beam loss handling and continuous monitoring the beam profile with high precision are crucial. Description of the beam loss and beam profile monitors in J-PARC neutrino beamline can be found elsewhere [2].

* cvson@post.kek.jp

Among these monitors, Segmented Secondary Emission Monitors (SSEM), which are used to monitor the beam profile including the beam center and beam width, are considered critically requiring an upgrade toward MW beam due to limitations discussed in the next section.

CURRENT BEAM PROFILE MONITOR AND THEIR LIMIT

In general, to measure the proton beam profile, material is inserted into the beamline. In J-PARC neutrino beamline, there is a suite of nineteen SSEMs, each of monitor consists of two 5-µm-thick Titanium (Ti) foils stripped vertically and horizontally along with a Ti foil of same thickness between thme. The strip withd is about from 2 cm to 5 cm, depending on the beam size at the installed position. Precision of the SSEM measurement on the beam width can be achieved up to 200 µm. However this method leads to 0.005% beam loss per SSEM. Due to this large amount of loss, only the most downstream SSEM is used continuously during normal operation, while others are inserted occasionally into the beamline for operation only during beam tuning periods. A Wire Secondary Emission Monitor (WSEM) has been developed with the same principle as the SSEM but using wires instead of strips to mitigate the beam loss. With WSEM, the beam loss can be reduced by factor of ten. However, continuous monitoring by a WSEM is still questionable, since even 0.0005% beam loss can cause serious problems, specifically the irradiation and damage of beamline components and a residual dose increase which makes maintenance become difficult. Thus, it is crucial to develop a non-destructive (or minimally destructive) beam profile monitor for the future operation of J-PARC at MW beam power.

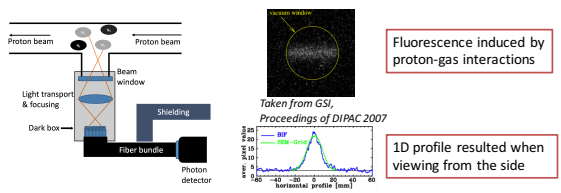

Figure 1: A BIF schematics has been built in the J-PARC neutrino beamline.

BIF MONITOR: PRINCIPLE AND A WORKABLE CONCEPT

In general, a BIF monitor makes uses of the fluorescence induced by proton beam interactions with gas in the beamline.

Content from this work may be used under the terms of the CC BY 3.0 licence (© 2018). Any distribution of this work must maintain attribution to the author(s), title of the work, publisher, and DOI.

ISBN: 978-3-95450-201-1 doi:10.18429/JACoW-IBIC2018-WEPC09

DESIGN AND TEST RESULTS OF A DOUBLE-SLIT EMITTANCE METER AT XiPAF

M. W. Wang[1], Q. Z. Xing, S. X. Zheng†, X. L. Guan, W. H. Huang, X. W. Wang
Key Laboratory of Particle & Radiation Imaging (Tsinghua University), Beijing 100084, China; Laboratory for Advanced Radiation Sources and Application, Tsinghua University, Beijing 100084, China; Department of Engineering Physics, Tsinghua University, Beijing 100084, China
Z. M. Wang, D. Wang, C. Y. Wei, M. T. Qiu,[1] also at State Key Laboratory of Intense Pulsed Radiation Simulation and Effect (Northwest Institute of Nuclear Technology), Xi'an 710024, China

Abstract

Xi'an 200 MeV Proton Application Facility (XiPAF) is composed of a linac injector, a 200-MeV synchrotron and a high energy transport line. To study the beam dynamics along the beam line, a double-slit emittance meter is used to measure the beam phase space in the linac. To have knowledge of the phase space upstream of the emittance meter, an inverse transport method is proposed in the presence of space charge. The design and preliminary test results of the emittance meter are presented in this paper.

INTRODUCTION

XiPAF (Xi'an 200 MeV Proton Application Facility), a proton radiation facility, consists of a linac injector, a medium energy transport line (MEBT), a synchrotron ring, a high energy transport line (HEBT) and a target [1]. The linac is composed of a low energy beam transport line (LEBT), a four-vane type RFQ and an alvarez-type DTL. During commissioning, knowledge of beam phase spaces at the LEBT output, RFQ output and DTL output are critical for beam matching. Especially at XiPAF, there is no matching section between RFQ and DTL [2]. The beam parameters of the linac are shown in Table 1. Due to the large energy range, the conventional electric scanner is not appliable. A double-slit type emittance meter is used to measure beam transverse phase spaces. Due to the small beam size and large divergence, it's usually hard to measure the beam phase spaces at the exit of the RFQ and DTL directly. Therefore, it's essential to deduce the beam phase spaces at the exits from the measured beam phase space downstream. The transportation is commonly achieved by transport matrix with assumption of linear particle motion. Whereas, the method is ineffective when the space charge effect is significant. A method, using the PIC code rather than transport matrix to simulate the particle motion, is proposed to transport the beam phase space from downstream to upstream with space charge effects. With this method, the knowledge of beam phase space distribution along the beam line can be obtained from the measured phase space at the position of the emittance meter. This paper shows the design and test results of the emittance meter.

†zhengsx@mail.tsinghua.edu.cn

Table 1: Main Beam Parameters of XiPAF Linac

Parameter	Value	Unit
Species	H^-	\
Beam energy	0.05~7	MeV
Peak current	3~10	mA
Pulse length	10~1000	μs
Repetition rate	0.5	Hz

DESIGN

Figure 1 shows the operation principle of the double-slit emittance meter. The emittance meter contains two slits: the position slit and angle slit. The width of the position slit determines the position resolution. The width of the angle slit and drift distance determine the angle resolution. The smaller the slits, the higher the resolution, but lower signal amplitude.

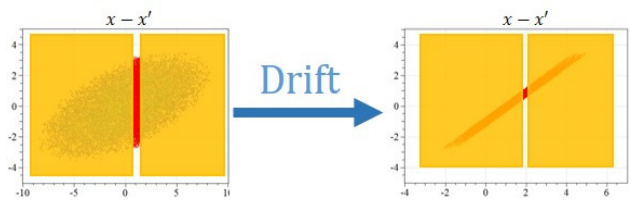

Figure 1: Operation principle of the double-slit emittance meter.

Due to the space limitation, the maximum drift distance is 247 mm. Figure 2 shows the signal amplitude as a function of slit widths. The widths of the two slits at XiPAF are 0.2 mm and 0.1 mm, respectively. Then the maximum current signal is 31.6 μA, and position and angle measurement resolution are 0.2 mm and 0.4 mrad, respectively. The current signal is measured by a Faraday cup mounted behind the angle slit.

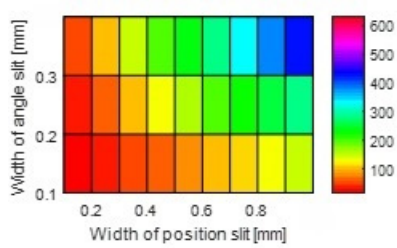

Figure 2: Signal amplitude as a function of slit widths.

Content from this work may be used under the terms of the CC BY 3.0 licence (© 2018). Any distribution of this work must maintain attribution to the author(s), title of the work, publisher, and DOI.

ISBN: 978-3-95450-201-1 doi:10.18429/JACoW-IBIC2018-WEPC15

Content from this work may be used under the terms of the CC BY 3.0 licence (© 2018). Any distribution of this work must maintain attribution to the author(s), title of the work, publisher, and DOI.

MACHINE LEARNING APPLIED TO PREDICT TRANSVERSE OSCILLATION AT SSRF *

B. Gao, Y.B.Leng †, Y.M. Zhou[1], J. Chen
Shanghai Institute of Applied Physics, Chinese Academy of Sciences, 201800 Shanghai, China
[1]also at University of Chinese Academy of Sciences, 100049 Beijing, China

Abstract

A fast beam size diagnostic system has been developed at SSRF storage ring for turn-by-turn and bunch-by-bunch beam transverse oscillation study. This system is based on visible synchrotron radiation direct imaging system. Currently, this system already has good experimental results. However, this system still has some limitations, the resolution is subject to the point spread function; and the speed of the online data processing is limited by the complex Gaussian fitting algorithm. In order to realize the online fast data processing, we present a technique that applied machine learning tools to predict transverse beam size. Using this technique at SSRF storage ring, we report mean squared errors below 4 µm for prediction of the horizontal beam size.

INTRODUCTION

Research of bunch-by-bunch beam diagnostics at the Beam Instrumentation (BI) group of SSRF (Shanghai Synchrotron Radiation Facility) has been started from the year of 2012 [1]. We also have focusing on the development of a six-dimensional bunch-by-bunch diagnostics system (published on this conference).

With the bunch-by-bunch diagnostics tool, further transverse and longitudinal instability information can be observed. Additionally, it is an excellent tool for machine impendence and wake-field investigations. Moreover, every bunch is the basic unit of the beam physics research, and the motion information of every bunch will be largely approximate to its natural properties.

The six-dimensional bunch-by-bunch diagnostics system consists of the beam position parameters (two dimensions), beam transverse size (two dimensions), beam longitudinal parameters (two dimensions). With this bunch-by-bunch diagnostics system, it is able to build a fast abnormal intelligent trigger system. The layout of the whole system is shown as Fig. 1: The bunch-by-bunch transeverse position was implemented with a resolution of 10 µm and was based on the bunch-by-bunch signal processor and delta over sum algorithm [4, 5]. A two-frequency system was employed for the bunch-by-bunch beam length measurement with large dynamic range of 30 pC–6 nC, and a resolution of less than 0.5 ps calibrated by the Streak Camera [6, 7]. For the bunch longitudinal phase measurement, we used the rise edge detection method to detect the button BPM signal, which could reach the resolution of approximately 1 ps [8]. The bunch-by-bunch beam size system is based on SR (syncrotron radition) light with a PMT (photomultiplier tubes) detector and Gaussian fitting algorithm [3].

Motivation

Previous section shows the whole six-dimension bunch-by-bunch diagnostics system and the fast intelligent trigger system. Fast trigger system relies on the online data processing.

In this paper, we will focus on the transverse oscillations. The transverse oscillations and transverse emittance enlargement will lead to machine instabilities. The precise bunch-by-bunch transverse position and size measurement is critical in machine abnormality studies and improvements.

A bunch-by-bunch beam size measurement system has been developed at SSRF. This system is capable of measuring bunches within a separation of 2 ns [2, 3]. However, this system still has some limitations, the speed of online data processing is limited by its complex algorithm. Fortunately, simple bunch-by-bunch diagnostics such as electron bunch monitors (beam position, beam current) can in principle work at the repetition rate. In order to estblish a fast abnormal intelligent trigger system, it is necessary to obtain the bunch-by-bunch data online.

Machine learning methods have been widely used in various fields. In this paper, the machine learning technique was applied to observe transverse oscillation. We prefer to use simple bunch-by-bunch diagnostics monitors to predict the result of complex bunch-by-bunch beam size monitors.

We have developed a machine learning tool to predict beam transverse size using beam position and charge as input. Using this technique at SSRF storage ring, we report mean squared errors below 4 µm for prediction of the horizontal beam size.

CORRELATION BETWEEN DIFFERENT PARAMETERS

Beam charge, positon, and size are the main parameters which can be used to characterise the transverse oscillation of the bunch. All of these parameters are related to the transverse oscillation. In order to realize the technique that using beam position and charge as input to predict beam size, correlation analysis between those parameters is indeed.

Correlation analysis between those bunch parameters has been started at SSRF.

In steady state of the storage ring, the transverse oscillation of the bunch is not obvious. Fortunately, the injection events can introduce obvious oscillation. Hence, we investigated the relationship between beam intensity and bunch

* Work supported by National Science Foundation of China (No.11375255)
† leng@sinap.ac.cn

ISBN: 978-3-95450-201-1 doi:10.18429/JACoW-IBIC2018-WEPC16

DESIGN AND RADIATION SIMULATION OF THE SCINTILLATING SCREEN DETECTOR FOR PROTON THERAPY FACILITY

P. Tian, Q.S. Chen, K.Tang, J.Q. Li, K.J. Fan†
State Key Laboratory of Advanced Electromagnetic Engineering and Technology,
Huazhong University of Science and Technology, Wuhan 430074, Hubei, China

Abstract

A proton therapy facility based on a superconducting cyclotron is under construction in Huazhong University of Science and Technology (HUST). In order to achieve precise treatment or dose distribution, the beam current would vary from 0.4 nA to 500 nA, in which case conventional non-intercepting instruments would fail due to their low sensitivity. So we propose to use a retractable scintillating screen to measure beam position and beam profile. In this paper, a comprehensive description of our new designed screen monitor is presented, including the choice of material of the screen, optical calibration and simulation of radiation protection. According to the off-line test, the resolution of the screen monitor can reach 0.13 mm/pixel.

INTRODUCTION

Huazhong University of Science and Technology (HUST) has planned to construct a proton therapy facility based on an isochronous superconducting cyclotron, from which 250 MeV proton beam is extracted. The layout of HUST proton therapy facility (HUST-PTF) is shown in Fig.1, with the basic specifications listed in Table 1.

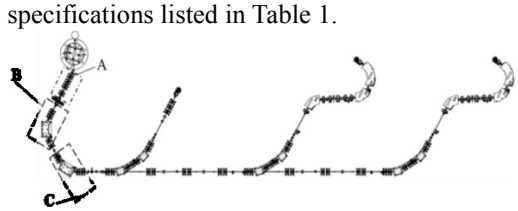

Figure 1: Layout of HUST proton therapy facility.

Table 1: Basic Beam Parameters of HUST-PTF

Phase	Energy/MeV	Current/nA
A	250	60-250
B	70-240	1-15
C	70-240	0.4-5

As the beam current is at the level of nanoampere, conventional non-intercepting instruments, such as inductive beam position monitors (BPMs), will fail to obtain effective beam signals without enough signal-to-noise ratio. Ionization chamber (IC) is popular for this kind of application, but it is too expensive to deploy IC all along the beamline. So we propose to use a relatively simple and economical instrument, scintillation screen, to measure beam position and profile.

The mechanical structure of the scintillation screen is shown in Fig.2. The CCD camera is located on the opposite side to the actuator, which is an air-driving type for the consideration of radiation damage.

* Work supported by national key R&D program, 2016YFC0105303.
† email address: kjfan@hust.edu.cn

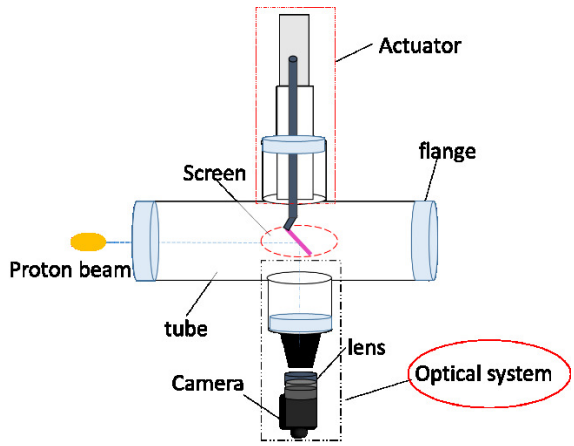

Figure 2: Scheme of retractable scintillator screen setup.

OPTIMIZATION OF SCREEN

Intercepting scintillation screens determine two-dimensional beam images and are frequently used for transverse profile measurements in beam transfer lines. High precision of profile and position measurements is important for controlling the spatial distribution of the beam [1]. For good luminescent screens, there are several key properties, including high efficiency of energy conversion, large dynamic range and good linearity between particles and light output, high radiation hardness and so on. Based on Refs. [2-4], the linearity of three common scintillators, separately YAG, P43, Al_2O_3:Cr are satisfied here when the current is 0.4nA. As for the photon yield related to energy deposition, P43 can produce higher number of photons. Figure 3 shows the different energy depositions of the three materials with thickness of 1 mm calculated by SRIM [5]. The luminescence intensity of the fluorescent screen with Al_2O_3:Cr was calculated by Eqs. (1) and (2) below

$$Y = \frac{\eta \times \Delta E \times n}{E_0} \quad (1)$$

with η the energy conversion efficiency, ΔE the energy loss of a particle，n the number of particles, E_0 the energy of the visible photon 3eV，thus yielding Y the number of the visible photons [6]. For particles of the beam, n is given by:

$$i = \frac{ne}{t} \quad (2)$$

with beam current i, e the charge of the proton, and t the width of the beam. Supposing the light output efficiency 0.2%, when beam current is 0.4 nA, the number of photon yield is 6.42×10^{11}/s, which is adequate for the CCD camera, with each pixel absorbing at least 1000-2000 photons [7].

Content from this work may be used under the terms of the CC BY 3.0 licence (© 2018). Any distribution of this work must maintain attribution to the author(s), title of the work, publisher, and DOI.

ISBN: 978-3-95450-201-1 doi:10.18429/JACoW-IBIC2018-WEPC17

X-RAY PINHOLE CAMERA IN THE DIAGNOSTICS BEAMLINE BL7B AT PLS-II

J. Ko[1†], J. Y. Huang[1], M. Yoon[2], K. Kim[1], B-H. Oh[1], D-T. Kim[1], D. Lee[1], J. Yu[1], and S. Shin[1]
[1]Pohang Accelerator Laboratory, POSTECH, Pohang, Gyungbuk 37673, KOREA
[2]Department of Physics, POSTECH, Pohang, Gyungbuk 37673, KOREA

Abstract

The beam diagnostics beamline BL7B using synchrotron radiation with 8.6 keV critical photon energy from bending magnet has been used to measure the electron-beam size and photon-beam profile on real-time basis. After the completion of the PLS-II, the Compound Refractive Lens (CRL) system was implemented in the optical hutch at BL7B to measure the electron-beam size from X-ray imaging. But we could not have a good image due to short available optical path caused by limited space of the optical hutch. To solve this problem a pinhole camera is implemented in the front-end of BL7B in return for the beamline extension. The progresses on the new x-ray imaging system are introduced in this paper.

INTRODUCTION

After the completion of the PLS-II project [1] to upgrade PLS [2] on March 21, 2012, Pohang Light Source II (PLS-II) is now in full operation. As a result of the upgrade, the PLS beam energy increased from 2.5 GeV to 3.0 GeV, and the stored beam current increased from 200 mA to 400 mA. The emittance is improved from 18.9 nm at 2.5 GeV to 5.8 nm at 3 GeV while the PLS storage ring tunnel structure remains unchanged. In addition, the top-up mode operation is used to stabilize the stored electron beam orbit and the synchrotron radiation flux.

Currently, a total of 31 beamlines including 18 insertion device beamlines are in PLS-II operation for user service. Figure 1 shows the beamline overview of PLS-II. Two multipole wiggler beamlines, three elliptically polarizing undulator beamlines, one planar undulator, twelve in-vacuum undulator beamlines and thirteen bending beamlines have been operated for surface science, magnetic spectroscope, material science, X-ray scattering, XAFS, MX, SAXS, imaging and lithography [3]. In addition to these beamlines, diagnostics beamline BL7B using bending radiation source have been used to measure photon beam stability, electron beam size and real time photon beam profile.

Beamline Overview

The specifications of bending radiation in PLS-II for beam diagnostics beamline BL7B are introduced in Table 1. Bending radiation source is the combined function dipole magnet with 1800 mm length. The central field is 1.46 T and is superposed with the focusing field gradient of -0.4 T/m [4]. The beam size at source point is 60 μm × 30 μm (H × V) and beam divergence at source point is 120 μrad × 2 μrad (H × V). With 3 GeV and 400 mA stored electron beam, photon flux at the critical energy of 8.7 keV is 1.28 $\times 10^{12}$ when measured at 15 m from the source point with 1 mm horizontal acceptance.

Unlike typical PLS-II beamline which consists of optical hutch and experimental hutch, beam diagnostics beamline BL7B have only optical hutch and share the optical hutch with the nearby insertion device beamline. Beam diagnostics beamline BL7B do not have the best situation for X-ray imaging due to short optical path length due to limited space, because all optical components are implemented within optical hutch.

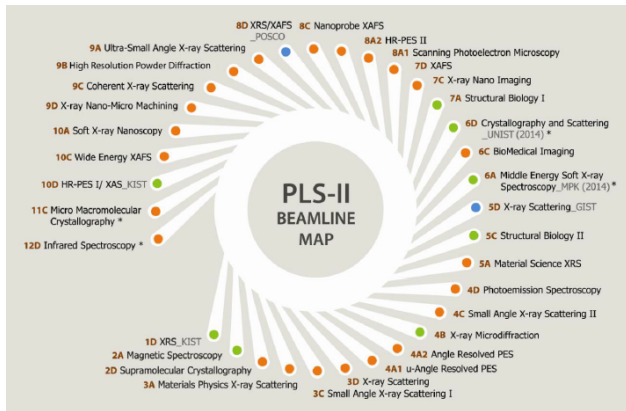

Figure 1: PLS-II beamline map. Here A and C are insertion device beamline, and B and D are bending beamline.

Table 1: The Specifications of Bending Radiation in PLS-II for Beam Diagnostics Beamline BL7B

Parameter	Value	Unit
Electron beam energy	3	GeV
Electron beam emittance	5.8	nm
# of bending magnets	24	
Length of bending magnet	1.8	M
Field / Gradient	1.46/-0.4	(T)/(T/m)
Crit. Photon energy	8.73	keV
Source size (H/V)	60 / 30	μm
Source divergence	120 / 2	μrad

Photon Beam Stability

In order to measure photon beam stability in beam diagnostics beamline BL7B, the most common PBPM [5], that is a simple structure equipped with two blades, is implemented before beam line optics. Figure 2 shows long term slow photon beam motion during 8 days user operation.

† kopearl@postech.ac.kr

Content from this work may be used under the terms of the CC BY 3.0 licence (© 2018). Any distribution of this work must maintain attribution to the author(s), title of the work, publisher, and DOI.

ISBN: 978-3-95450-201-1 doi:10.18429/JACoW-IBIC2018-WEPC19

SELECTION OF WIRES FOR THE NEW GENERATION OF FAST WIRE SCANNERS AT CERN

A. Mariet, R. Veness, CERN, 1211 Geneva, Switzerland

Abstract

A new generation of fast wire scanners is being produced as part of the LHC Injector Upgrade (LIU) project at CERN. The LIU beam parameters imply that these wire scanners will need to operate with significantly brighter beams. This requires wire scanner systems with micron level accuracy and wires with a considerably increased tolerance to beam damage. This paper presents the method of selection of such wires in terms of material choice and geometry. It also reports on studies with novel materials with a potential to further extend the reach of wire scanners for high brightness beams.

INTRODUCTION

Instrument Principle

Wire-scanners are devices used to measure the transverse beam density profile by moving a thin wire across the particle beam. The interaction between the beam and the wire creates secondary particle showers with an intensity proportional to the number of particles crossing the wire.

These secondary particles are intercepted by a scintillator, positioned downstream of the wire, coupled to a photomultiplier which amplifies the resulting signal. The acquisition of the wire position and the signal intensity are combined to reconstruct the transverse beam density profile.

The LHC Injector Upgrade (LIU) project at CERN [1] is increasing beam brightness across the LHC injector chain (Proton Synchrotron Booster (PSB), Proton Synchrotron (PS) and Super Proton Synchrotron (SPS)), to produce smaller, higher intensity beams.

Due to this higher brightness, the principal wire failure mode is expected to be due to the fast increase of temperature leading to melting or surface sublimation. The loss of matter weakens the wire until failure occurs [2].

In order to minimise this issue, the new fast beam wire-scanner (BWS) developed at CERN for LIU (see Fig. 1) has increased the linear velocity of the wire to 20 $m.s^{-1}$, such that the wire remains in the beam for much less time [3]. The downside to this, however, is that for very small beams a signal is only produced for a few points along the profile.

Wire Research Development

Wire-scanners were first used in 1964 in Oxford and Heidelberg [4], as robust and direct profile measurement instruments. They have since evolved along with accelerator technology, and remain one of the fundamental instruments for measuring the beam profile in most particle accelerators.

Different wire materials and geometries have been used throughout this time. Among the first were steel, tantalum and beryllium, followed later by carbon, quartz, tungsten and titanium, as well as copper-beryllium alloys and silicon carbide. The advantages and disadvantages of some of these materials will be investigated in this paper. In addition, the geometry of the wire has an important role to play. Existing wires used at CERN have diameters from 7 to 34 µm, and are either single or multi strand (see Table 1).

Table 1: Rotational Wire-scanner Configuration

Ring	PSB	PS	SPS
Wire configuration	12x 7	12x 7	1x 34
Equivalent diameter [µm]	24	24	34
Wire length [mm]	120	153	153
Forks length [mm]	150	183	183

The other important parameter in wire scanner design is the scan speed. This parameter defines the time needed by the wire to cross the beam and is directly related to the number of useful data points taken per scan. This combination of material, geometry and scanning speed must satisfy three main criteria:

- Maximal measurement resolution
- Sufficient interaction to generate a signal
- Maximal lifetime of the wire

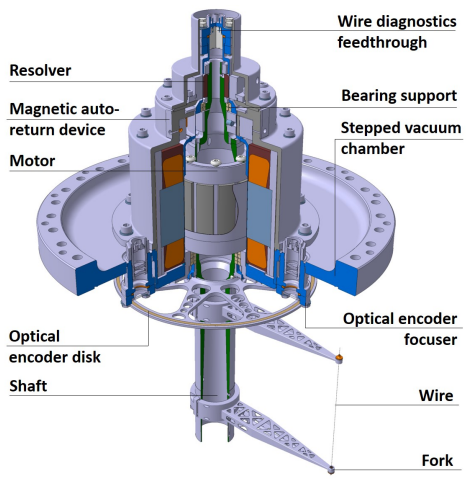

Figure 1: New Fast Beam Wire Scanner for LIU

MATERIAL SELECTION FOR MECHANICAL PROPERTIES

Wire Pre-Load

The pre-tension load is a key factor to determine the maximal wire deflection during movement of the scanner movement and hence the limiting resolution of the measurement. Table 2 compiles parameters, the ultimate tensile strength

Content from this work may be used under the terms of the CC BY 3.0 licence (© 2018). Any distribution of this work must maintain attribution to the author(s), title of the work, publisher, and DOI.

ISBN: 978-3-95450-201-1 doi:10.18429/JACoW-IBIC2018-THOA01

LOW VS HIGH LEVEL PROGRAMMING FOR FPGA

Jan Marjanovic*, Deutsches Elektronen-Synchrotron DESY, Hamburg, Germany

Abstract

From their introduction in the eighties, Field-Programmable Gate Arrays (FPGAs) have grown in size and performance for several orders of magnitude. As the FPGA capabilities have grown, so have the designs. It seems that current tools and languages (VHDL and (System)Verilog) do not match the complexity required for advanced digital signal processing (DSP) systems usually found in experimental physics applications. In the last couple of years several commercial High-Level Synthesis (HLS) tools have emerged, providing a new method to implement FPGA designs, or at least some parts of it. By providing a higher level of abstraction, new tools offer a possibility to express algorithms in a way which is closer to the mathematical description. Such implementation is understood by a broader range of people, and thus minimizes the documentation and communication issues. Several examples of DSP algorithms relevant for beam instrumentation will be presented. Implementations of these algorithms with different HLS tools and traditional implementation in VHDL will be compared.

INTRODUCTION

According to [1], FPGAs have reached its fourth age. After the "Age of Invention", "Age of Expansion" and "Age of Accumulation" there are devices with enough capacity to include the entire system on a single chip [2]. Although the need to efficiently use the resources provided by the FPGA is still present, the main challenges are managing the complexity of the design and integration of 3rd party IP cores (e.g. DDR3/4 memory controllers, PCIe blocks, DMAs, 1 and 10 Gigabit Ethernet MAC, processors, DSP blocks...).

Numerous approaches to provide a higher level of abstraction were and are presented, mostly by academia, but also by the commercial vendors. One tool which successfully made a transition from an academic tool [3] to a tool in FPGA engineer's toolbox is Xilinx Vivado HLS.

Several studies of HLS vs RTL can be found in the literature. Vendors of the tools are compelled to present their tools in the nicest way [4] or with usually simplified examples. Some of the studies are also quite general [5] or the examples are simplified versions of the problems from experimental physics [6]. In some cases comparison is valuable but only partially relevant for experimental physics applications [7–9].

The framework described in [10] provides a method to develop applications in Matlab for certain MicroTCA boards. Vivado HLS is also used in 10G and 40G Ethernet accelerators, described in [11], and for two real-time data acquisition applications (crystal identification and timestamp sorting), described in [12]. Recently, Vivado HLS was used for the development of `hls4ml` [13], a machine learning framework for particle physics.

In the rest of the paper, three examples of modules relevant for experimental physics will be presented. Implementations in VHDL and C++ targeting Vivado HLS are presented side-by-side. Interesting snippets of the code are presented to highlight the differences in the two languages, and to give the reader a possibility to compare the readability of the code for himself or herself. Number of lines of code (reported by cloc[14]), resource usage and minimal clock period (= $1/f_{max}$) for both implementations are also reported.

There are several reasons to base the evaluation on Vivado HLS:

- Author has considerable experience both with Xilinx FPGAs in general and with related tools (Vivado, Vivado HLS)
- Xilinx FPGAs are heavily used at DESY and on MicroTCA AMC boards
- The created IP integrates nicely with the rest of the IPs in Xilinx ecosystem
- Vivado HLS is significantly cheaper than other HLS software suites; therefore it is very likely that industrial partners will have access to it

The latest version available at the time of the writing, Vivado HLS 2018.2, was used for the examples in this paper.

Several other High-Level Synthesis software suites exists, such as Intel HLS Compiler, LabVIEW FPGA, Mathworks HDL Coder, Cadence Status, Mentor Graphics Catapult, and Synopsys Synphony C Compiler. Some open-source tools, such as Panda Bamboo and LegUp are also available. These tools were not considered for this paper.

EXAMPLES

To better illustrate the differences, the advantages and the shortcomings of both methods, three examples will be compared. The examples are presented in the order of complexity, simplest first.

The first example, linearization function, requires high throughput, but it is in its core quite simple - each sample is processed on its own; there are no dependencies between the samples. The scheduler has an easy task pipelining the operations.

The second example, two-dimensional mean and standard deviation is slightly more complex; because the samples need to be accumulated together, scheduler needs some help from the designer to be able to pipeline the operations.

The third example, IIR filter is a well studied topic in digital signal processing [15]. In the case presented here,

* jan.marjanovic@desy.de

Content from this work may be used under the terms of the CC BY 3.0 licence (© 2018). Any distribution of this work must maintain attribution to the author(s), title of the work, publisher, and DOI.

ISBN: 978-3-95450-201-1 doi:10.18429/JACoW-IBIC2018-THOA02

HIGH-SPEED DIRECT SAMPLING FMC FOR BEAM DIAGNOSTIC AND ACCELERATOR PROTECTION APPLICATIONS

J. Zink*, M. K. Czwalinna, M. Fenner, S. Jablonski, J. Marjanovic, H. Schlarb
DESY, Hamburg, Germany

Abstract

The rapid development, in the field of digitizers is leading to *Analog-to-Digital Converters* (ADC) with ever higher sampling rates. Nowadays many high-speed digitizers for RF applications and radio communication are available, which can sample broadband signals, without the need of down converters. These ADCs fit perfectly into beam instrumentation and diagnostic applications, e.g. Bunch Arrival time Monitor (BAM), klystron life-time management or continuous wave synchronization. To cover all these high-frequency diagnostic applications, DESY has developed a direct sampling FMC digitizer board based on a high-speed ADC with an analog input bandwidth of 2.4 GHz. A high-speed data acquisition system capable of acquiring 2 channels at 500 MS/s will be presented. As first model application of the versatile digitizer board is the coarse bunch arrival time diagnostics in the free electron laser FLASH at DESY.

INTRODUCTION

Modern linear accelerators require a very high precision *Low-Level-RF* (LLRF) control system. In the *European X-Ray Free Electron Laser* (XFEL) and *Free-Electron-Laser in Hamburg* (FLASH) the LLRF-systems are realized in *Micro Telecommunication Computing Architecture* (MTCA.4). In addition to the control system the accelerators need very high accuracy diagnostic systems to measure, e.g. the beam position, the bunch arrival time , klystron failures, and other accelerator parameters. To reduce the board space and the number of components in the system, the authors designed a digitizer board based on an ADC with a maximum sampling rate of 1 GS/s. The new digitizer board (see Fig. 1) in ANSI/VITA 57.1 2010 [1] FMC form factor will be used in different diagnostic applications. It is integrated in the existing MTCA infrastructure and installed on a DESY *Advanced Mezzanine Card* [2] DAMC-FMC25 [3] carrier board. Due to the high input bandwidth of the digitizer, there is no need for a down converter stage in front of the ADC.

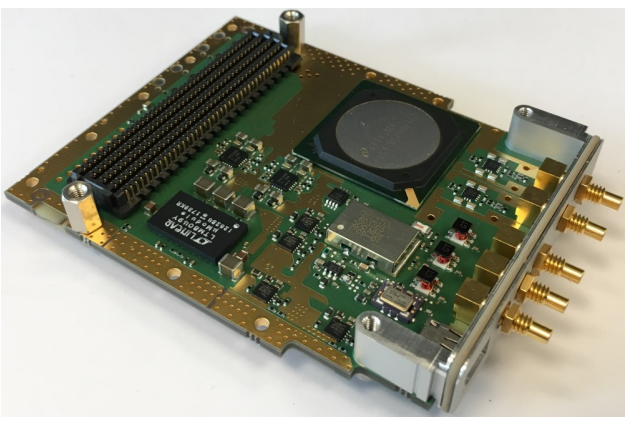

Figure 1: New DFMC-DS500 digitizer board.

FMC DIGITIZER DFMC-DS500

The core component of the converter board is a dual channel 12-bit RF sampling ADC from Texas Instruments with a sampling rate of 500 MS/s per channel. In *dual edge sampling* (DES) mode the two channels are combined together and the ADC is sampling at 1 GS/s. The minimum guaranteed single channel analog bandwidth is 2.4 GHz. In DES mode the bandwidth is decreased down to 1.2 GHz. Since the manufacturer offers a whole family of compatible ADCs, different variants can be fitted onto the FMC [4].

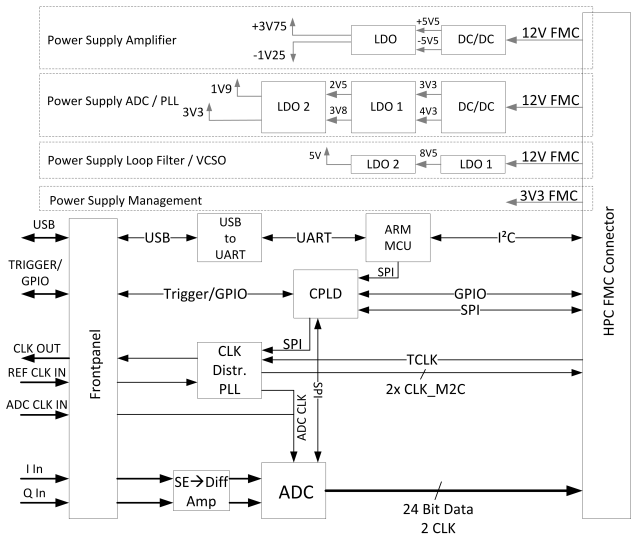

Figure 2: Block diagram of the DFMC-DS500 digitizer.

Figure 2 depicts the block diagram of the digitizer board. The inputs of the ADC are driven by fully differential amplifiers (FDA) [5, 6] with a large-signal bandwidth of 4.8 GHz. These amplifiers act as active baluns and replace the transformers which are normally converting single ended input signals to differential signals. The ADC has two 12-bit wide *low voltage differential signaling* (LVDS) data connections to the carrier card to achieve minimal latency. These lines can be driven with well defined voltage levels independent from the level of the adjust voltage (V_{ADJ}) [1].

Clock Tree

Clocking the ADC can be done in different ways. In addition to a direct clock feed via a front panel connector,

* johannes.zink@desy.de

Content from this work may be used under the terms of the CC BY 3.0 licence (© 2018). Any distribution of this work must maintain attribution to the author(s), title of the work, publisher, and DOI.

ISBN: 978-3-95450-201-1 doi:10.18429/JACoW-IBIC2018-THOA03

PROGRESS ON TRANSVERSE BEAM PROFILE MEASUREMENT USING THE HETERODYNE NEAR FIELD SPECKLES METHOD AT ALBA

S. Mazzoni, F. Roncarolo, G. Trad, CERN, Geneva, Switzerland
B. Paroli, M. Potenza, M. Siano, Università degli Studi di Milano, Milan, Italy
U. Iriso, C. S. Kamma-Lorger, A. A. Nosych, ALBA, Barcelona, Spain

Content from this work may be used under the terms of the CC BY 3.0 licence (© 2018). Any distribution of this work must maintain attribution to the author(s), title of the work, publisher, and DOI.

Abstract

We present the recent developments of a study aimed at measuring the transverse beam profile using the Heterodyne Near Field Speckles (HNFS) method. The HNFS technique works by illuminating a suspension of Brownian nanoparticles with synchrotron radiation and studying the resulting interference pattern. The transverse coherence of the source, and therefore, under the conditions of validity of the Van Cittert and Zernike theorem, the transverse electron beam size is retrieved from the interference between the transmitted beam and the spherical waves scattered by each nanoparticle. We here describe the fundamentals of this technique, as well as the recent experimental results obtained with 12 keV undulator radiation at the NCD beamline at the ALBA synchrotron. The applicability of such a technique for future accelerators (e.g. CLIC or FCC) is also discussed.

INTRODUCTION

The HNFS method is a powerful, yet conceptually simple and inexpensive method to measure the transverse coherence properties of a light source. It is described mathematically by the Complex Coherence Factor (CCF):

$$\boldsymbol{\mu}(\boldsymbol{x_1}, \boldsymbol{x_2}) = \frac{\langle \boldsymbol{E}(\boldsymbol{x_1}, t)\boldsymbol{E}^*(\boldsymbol{x_2}, t)\rangle}{[I_1 I_2]^{1/2}} \qquad (1)$$

where $\boldsymbol{E}(\boldsymbol{x_i}, t)$ is the electric field at a given point in space and time, $I_i = \langle \boldsymbol{E}(\boldsymbol{x_i}, t)\boldsymbol{E}^*(\boldsymbol{x_i}, t)\rangle$ is the intensity of the electric field and $\langle \dots \rangle$ denotes time averaging. The ability to measure the CCF of a light source is of interest for beam diagnostics as, under the conditions of validity of the Van Cittert and Zernike (VCZ) theorem [1], the CCF is the Fourier transform of the source intensity distribution. As a consequence, when Synchrotron Radiation (SR) is used as the light source, a measurement of its transverse coherence allows the transverse profile of the beam at the emission plane to be retrieved.

The traditional method for measuring the beam size through the CCF is Young's two slit interferometer [2], where SR impinges on a pair of narrow slits forming an interference pattern. In this case, the CCF is retrieved from the *visibility* V of the fringes:

$$V \overset{\text{def}}{=} \frac{I_{max} - I_{min}}{I_{max} + I_{min}} = \frac{2\sqrt{I_1 I_2}}{I_1 + I_2} |\boldsymbol{\mu_{12}}| \qquad (2)$$

where I_i is the time averaged intensity at slit i and $\boldsymbol{\mu_{12}}$is a short form for the CCF as defined in Eq. 1. The HNFS method is an alternative to Young's double slit method that offers some potential advantages. HNFS does not require the almost completely blocking of SR radiation as in the Young's slits configuration, and it does not require the challenging fabrication of narrow slits in a medium that must be opaque to X-rays. While HNFS is known a well-known particle sizing technique, it has never, to our knowledge, been used for beam size monitoring in particle accelerators. We will report of the status of a proof of concept experiment at ALBA to measure beam size using X-ray radiation.

THE HNFS TECHNIQUE

A typical HNFS setup using X-ray radiation (see Fig. 1) is composed of a suspension of nanoparticles in water positioned at a distance z_1 from the source, which can be a dipole or insertion device. The transmitted and scattered fields propagate for a distance z_2 where they impinge on a YAG scintillator that produces visible light at 550 nm with the same intensity modulations as the incident X-ray radiation. The visible signal is extracted from the X-ray beam path by means of a mirror at 45º. A highly magnified image of the YAG screen is then produced on a sensor by means of a microscope objective.

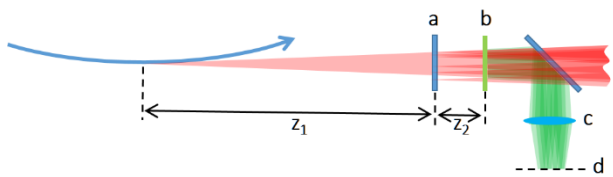

Figure 1: A typical HNFS setup for X-rays (shown in red). a) target composed of a suspension of nanoparticles in water. b) YAG screen with visible light shown in green. c) microscope objective. d) sensor

Heterodyne Near Field Scattering (HNFS) is an interferometric technique where the incident light beam $\boldsymbol{E_0}$ impinging on the target generates a large number of weak spherical waves ($\boldsymbol{E_s}, |\boldsymbol{E_s}| \ll |\boldsymbol{E_0}|$) that interfere with the transmitted field. The resulting intensity distribution is known as a speckle field and it is recorded onto the scintillator plane at a distance z_2 downstream the scattering sample. The coherence properties of the source are determined from analysis of the stochastic interferogram formed at the scintillator plane with the resulting light intensity distribution given by:

$$I = |\boldsymbol{E_0} + \boldsymbol{E_s}|^2 = |\boldsymbol{E_0}|^2 + 2Re|\boldsymbol{E_0}^* E_s| \qquad (3)$$

ISBN: 978-3-95450-201-1 doi:10.18429/JACoW-IBIC2018-THOB01

INJECTION TRANSIENT STUDY USING 6-DIMENSIONAL BUNCH-BY-BUNCH DIAGNOSTIC SYSTEM AT SSRF *

Y.M. Zhou †, B. Gao, N. Zhang, Y.B. Leng#
SSRF, SINAP, Shanghai, China

Abstract

Beam instability often occurs in the accelerator and even causes beam loss. The beam injection transient process provides an important window for the study of beam instability. Measurement of the bunch-by-bunch dynamic parameters of the storage ring is useful for accelerator optimization. A 6-dimensional bunch-by-bunch diagnostic system has been successfully implemented at SSRF. The measurements of transverse position and size and longitudinal phase and length are all completed by the system. Button BPM is used to measure beam position, phase and length, and the synchrotron radiation light is used to beam size measurement. Signals are sampled simultaneously by a multi-channel acquisition system with the same clock and trigger. Different data processing methods are used to extract the 6-dimensional information, where delta-over-sum algorithm for beam position extraction, Gaussian fitting algorithm for beam size extraction, zero-crossing detection algorithm for beam phase extraction and the two-frequency method for bunch length extraction. The system set up and performance will be discussed in more detail in this paper. The application of the injection transient study brings a lot of interesting phenomena and results, which will be discussed as well.

INTRODUCTION

The Shanghai synchrotron radiation facility (SSRF) is the third synchrotron radiation light source facility in Shanghai China, which can produce broad rates of X-rays for primary scientific research and applications in other domains. The SSRF consists of a 150MeV linear accelerator, a 3.5GeV booster synchrotron and a 3.5GeV storage ring. In the user operation mode, about 500 bunches are stored with 2ns spacing in the storage ring. The harmonic number is 720 with the RF frequency of 499.654MHz [1]. In order to take full advantage of the SSRF, phase-II project is under construction since 2011, 16 beam lines would be built and the electron storage ring would be upgraded. More insertion devices (IDs) with small gaps will be added, which will cause beam instability problems.

For the construction and operation of the machine, if the distribution of high energy particles in three dimensions and the evolution over time can be measured, almost all other parameters can be derived from the above measurements. Therefore, bunch-by-bunch diagnostics is necessary for the bunching beams. Once the diagnostics is realized, it can be used to online monitor the steady or unsteady beam parameters during the user operation mode, which is of great importance for the operation mode optimization and the capture of transient process. At the same time, it is also a useful tool for further analysis of instability, such as the tremendous change of betatron amplitude and beam size or phase.

In the injection system of the SSRF storage ring, there is a set of beam kickers, which is used to change the momentum of a bunch to meet the injected one [2]. Then, it can change back to the original orbit with the injected bunch. However, due to the imperfect mount, align and configure of the kickers, residual betatron oscillations occurred in the injection system. Therefore, bunches would be affected by the kicker field or the wake-fields from preceding bunches. The bunch-by-bunch diagnostics is a machine research tool for wake field and impedance study.

In recent years, Beam Instrumentation (BI) group at SSRF has also been focusing on the development of bunch-by-bunch diagnostics since 2012. If the bunching beam is assumed to be Gaussian in the three-dimensional space, six spatial parameters ((x, y) in the transverse position, $(\sigma x, \sigma y)$ in the transverse size, $(z, \sigma z)$ in the longitudinal phase and length) can fully describe an independent bunch with the bunch charge. A 6-dimensional (6D) bunch-by-bunch diagnostic system has been set up to measure the parameters simultaneously at SSRF.

PRINCIPLES

In the acquisition of beam signals, the synchrotron radiation (SR) light is the most ideal signal because it contains all beam information, whereas the button-type beam position monitor (BPM) cannot get the transverse size information. However, it is easy to condition and capture signal for the button BPM signal, and the SR light signal is limited by the bandwidth of the signal conditioning and data acquisition system. So, to realize the 6-dimensional diagnostic system, we use the SR light to obtain the transverse position and size information and use the button BPM to obtain the longitudinal phase and length information or transverse position as well.

Optical Imaging System

Figure 1 shows the optical direct imaging system in the bunch-by-bunch size system. The concave lens (Lens 1) and convex lens (Lens 2) are used to focus and magnify the light spot, and to adopt the pixel size to the photoelectric detector. The visible light from the SSRF storage ring was separated into two paths through a reflecting mirror: one path was toward the interferometer system for spread function (PSF) calibration, and the other one was toward the bunch-by-bunch size measurement. A diaphragm was used to correct the deformation of the Be mirror. Since the Be mirror deformation mainly occurred in the vertical direction, the measurement of beam vertical size was destroyed. Therefore, we were more concerned with the measurement of beam horizontal size, and the horizontal size result was

Content from this work may be used under the terms of the CC BY 3.0 licence (© 2018). Any distribution of this work must maintain attribution to the author(s), title of the work, publisher, and DOI.

ISBN: 978-3-95450-201-1 doi:10.18429/JACoW-IBIC2018-THOB02

ENERGY LOSS MEASUREMENTS WITH STREAK CAMERA AT ALBA

A. A. Nosych, B. Bravo, U. Iriso
ALBA-CELLS, Cerdanyola de Vallés, Spain

Abstract

Analyzing streak camera images of the beam injected into a Storage Ring with no RF voltage allows calculating several parameters, like the energy loss per turn and the energy mismatch between injected and stored beams. These measurements are based on the analysis of the centroid drift path of a bunch as it spirals inwards, changing its rotation period. This drift is clear and measurable in single and multi-bunch modes in several horizontal sweep speeds of the streak. With this technique we also measure the momentum compaction factor and observe its change with respect to the insertion devices' open/closed states. The obtained values are comparable with theoretical expectations, as well as with values measured by other means.

INTRODUCTION

Since its commissioning in 2011 the beam diagnostics beamline at ALBA is using the visible part of the synchrotron radiation for dedicated longitudinal studies of the Storage Ring (SR) beam. Among the tools on the optical table is the Optronis SC-10 streak camera (SC), whose details can be checked at Refs. [1,2]. In short, the SC uses two sweep units to distinguish the bunches spaced by 2 ns: the fast (vertical) unit with the synchroscan frequency of 250 MHz at different amplitudes, allowing deflection speeds of 15, 25 and 50 ps/mm (equivalent to full scales of 215, 360 and 720 ps respectively), and the slow (horizontal) unit at some trigger frequency allowing sweep speeds from 660 ps to 5 ms/mm (equivalent to full scales of 9 ns and 72ms respectively). For a proper visualization of the beam bunch, the slow sweep unit is synchronized with both the SR revolution frequency and the injection repetition rate of 3 Hz.

Measurements to characterize the bunch length and the longitudinal beam dynamics at ALBA are shown in Ref. [2], where a proper injection phase and energy matching is performed between the Booster (Bo) and the SR and how to measure it with the RF system on.

In this work we study the dynamics of a bunched beam which is injected into a machine with its RF system off. The beam revolution period changes and it starts to spiral inwards until it is eventually lost. This was described in Ref. [3] for a beam, whose injected energy was exactly the same as the equilibrium energy of the SR. In our case, we consider the possibility to have a small Bo to SR energy offset, and show that it still is possible to calculate the energy loss per turn and the energy mismatch, having the SR RF system off. Furthermore, provided that the energy loss per turn is inferred with other means, we also show how this method can be used to measure the momentum compaction factor.

For reference, we list the main parameters of the longitudinal plane of the ALBA SR in Table 1.

Table 1: Machine parameters of the ALBA Storage Ring. The energy loss per turn below corresponds to losses only due to synchrotron radiation produced by the dipoles.

beam energy, GeV	2.979
bunch spacing, ns	2
RF frequency, MHz	500
revolution time, ns	896
energy spread, %	0.105
momentum compaction factor	$0.88 \cdot 10^{-3}$
energy loss/turn, keV	990
RF voltage, MV	[2.1 - 3.1]
bunch length, σ_z	[21 - 17] ps

INJECTION MATCHING WITH RF ON

Studies with the streak camera allow to match the injection process longitudinally. First, we overview the RF phase match between the Bo and the SR, and secondly, the energy match.

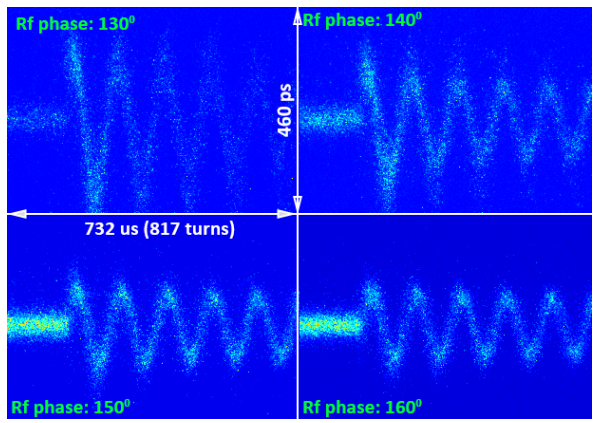

Figure 1: Injection oscillations as seen by the SC for various RF phase mismatch of the Bo and the SR.

RF Phase Matching

Despite some phase and energy mismatch between the injected and stored beam, the injected bunch eventually gets damped to the proper synchronous phase and its natural bunch length. The injection RF phase match can be checked by looking at the injection time interval with the SC, which requires a precise work with the timing and SC triggers.

Injection into the ALBA SR uses a conventional local injection bump with four dipole kickers [4]. For our studies, the best way to properly visualize this injection process is to delay kicker-1 trigger such that the Bo beam is injected but not accumulated.

Content from this work may be used under the terms of the CC BY 3.0 licence (© 2018). Any distribution of this work must maintain attribution to the author(s), title of the work, publisher, and DOI.

ISBN: 978-3-95450-201-1 doi:10.18429/JACoW-IBIC2018-THOB03

LONG TERM INVESTIGATION OF THE DEGRADATION OF COAXIAL CABLES

M. Kuntzsch*, R. Schurig, Helmholtz-Zentrum Dresden-Rossendorf, Dresden, Germany
S. Burger, T. Weber, el-spec GmbH, Geretsried, Germany

Abstract

Coaxial cables are important components for the control and diagnostics of any accelerator facility. Their electrical and mechanical properties have major impact on the quality of the acquired analogue signals and in turn on the performance of the whole machine.

Cables installed in immediate vicinity to the beam line are exposed to ionizing radiation that is mainly generated by beam-loss. In this environment cables change their electrical properties which directly affects the signal on the receiver side and in turn the measured beam parameters. For the transport of broadband signals in the multi-GHz range cables using PTFE ("Teflon") as dielectric medium are used most frequently. Optimized products offer low insertion loss, small phase drift and large spectral bandwidth at a moderate price level. At the same time PTFE commonly known to be prone to radiation induced degradation. This statement holds for a qualitative discussion but real measurement data are rarely published. At the ELBE accelerator at Helmholtz-Zentrum Dresden-Rossendorf (HZDR) 40 GHz-bunch arrival time monitors (BAMs) are used to measure the arrival time of the electron bunches with high accuracy [1]. In order to improve the sensitivity of the setup it has been considered to replace the SiO2 cables connecting the beam line pickup and the electro-optical modulator (EOM) by low-loss and low-drift PTFE-based cables. Since these cables are exposed to the activated environment a long-term test has been performed to characterize the degradation of the sample cables under real conditions. A maximum accumulated dose of 93.85 kGy has been applied to the test samples.

MEASUREMENT SETUP

Preliminary Dose Mapping Setup

For the irradiation of cable samples a place had to be found which allowed to accumulate a dose corresponding to multiple years of normal operation within a much shorter time frame. At the same time the distribution of the gamma radiation should be as homogeneous as possible to avoid effects triggered by a local maximum. Since no dedicated beam time could be spend on this investigations it has been decided to mount two cable samples on an aluminum plate that was place behind the beam dump of ELBE's undulator U100. The dump is used routinely during user operation in the free electron laser (FEL) cave. The beam energy and therefore the emitted spectrum of Bremsstrahlung-photons is defined by the user's demand for the FEL operation. The characteristic spectrum of Bremsstrahlung is a broadband distribution were the maximum energy is defined by the electrons incident energy. Before the final setup was installed, a coarse field map using five alanine dosimeter [2] has been created. One sensor was put directly on the interpolated beam axis and four with a defined distance from the center. The sensor distribution can be seen in Figure 1 and the aquired data in Table 1.

Figure 1: Dose mapping setup.

Table 1: Preliminary Dose Mapping Behind U100 Beam Dump

Position	Name	Accumulated Dose
Top-Left	B1C2	780 Gy
Top-Right	B2C2	850 Gy
Bottom-Left	B3C2	2520 Gy
Bottom-right	B4C2	3330 Gy
Center	A4C1	19 260 Gy

Final Measurement Setup

For the final setup two types of cable have been installed concentrically around the imaginary beam axis on the base plate. In the following sections the two cable types are always referred as cable under test 1 (CUT1), and cable under test 2 (CUT2). Both samples were connected to a patch panel that was accessible by RF measurement equipment using 5 m patch cables made of the same cable type like CUT2. Before the installation of the base plate at the back of the beam dump, ten alanine dosimeters have been attached to the cable spools in order to give a good spatial resolution of

* m.kuntzsch@hzdr.de

Content from this work may be used under the terms of the CC BY 3.0 licence (© 2018). Any distribution of this work must maintain attribution to the author(s), title of the work, publisher, and DOI.